ANALYTICA CHIMICA ACTA

International monthly devoted to all branches of analytical chemistry
Revue mensuelle internationale consacrée à tous les domaines de la chimie analytique
Internationale Monatsschrift für alle Gebiete der analytischen Chemie

ELSEVIER PUBLISHING COMPANY
AMSTERDAM

✓*Anal. Chim. Acta*, Vol. 36, No. 4, 413–548, December 1966
Completing Volume 36

ANALYTICA CHIMICA ACTA

GENERAL INFORMATION

Languages

Papers will be published in English, French or German.

Submission of papers

Papers should be sent to: Prof. PHILIP W. WEST, Coates Chemical Laboratories, College of Chemistry and Physics, Louisiana State University, Baton Rouge 3, La. 70803 (U.S.A.) or to

DR. A. M. G. MACDONALD, Department of Chemistry, The University, P.O. Box 363, Birmingham 15 (Great Britain)

Manuscripts

Authors should submit two copies in double-spaced type with adequate margins on pages of uniform size. Acknowledgements, summary and references should be placed at the end of the paper.

Tables should be typed on separate pages and numbered in Roman numerals in the order in which they are mentioned in the text. All Tables should have descriptive titles. The use of chemical formulae and conventional abbreviations is encouraged in Tables and Figures but chemical formulae should not be used in the text unless they are necessary for clarity. Units of weight, volume, etc., when used with numerals should be abbreviated and unpunctuated (*e.g.*, 2%, 2 ml, 2 g, 2 μl, 2 μg, 2 ng, 2 cm, 200 mμ).

Figures should be drawn in Indian ink on drawing or tracing paper with all lettering in **thin** pencil. Standard symbols should be used in line drawings; the following are available to the printers:

▼ ▽ ■ □ ● ◎ ■ ◘ ⊖ ▣ ▪ + ×

Photographs should be submitted as clear black and white glossy prints. Figures and photographs should be of the same size as the typed pages. Legends for figures should be **typed on a separate page**. Figures should be numbered in Arabic numerals in the order in which they are mentioned in the text.

References should be given at the end of the paper and should be numbered in the order of their appearance in the text (**not** arranged alphabetically). Abbreviations of journal titles should conform to those adopted by the *Chemical Abstracts List of Periodicals*, 1961 Edition and supplements. The recommended form for references to journal papers and books is as follows:

1. J. J. LINGANE AND A. M. HARTLEY, *Anal. Chim. Acta*, 11 (1954) 475.
2. F. FEIGL, *Spot Tests in Organic Analysis*, 7th Ed., Elsevier, Amsterdam, 1966, p. 516.

For multi-author references, **all** authors must be named, and initials given, in the reference list, although the use of, for example, SMITH *et al.*, is desirable in the text.

Summaries are published in English, French and German; authors must always provide a summary in the language of the paper, and are encouraged to supply translations where convenient. No summaries are needed for Short Communications.

Reprints

Fifty reprints will be supplied free of charge. Additional reprints (minimum 100) can be ordered at quoted prices. They must be ordered on order forms which are sent together with the proofs.

Publication

Analytica Chimica Acta has four issues to the volume, and three volumes appear per year. Subscription prices: $ 17.50 or £ 6.6.— or Dfl. 63.— per volume; $ 52.50 or £ 18.18.— or Dfl. 189.— per year, plus postage. Additional cost for copies by airmail available on request. For advertising rates apply to the publishers.

Subscriptions

Subscriptions should be sent to:

ELSEVIER PUBLISHING COMPANY, P.O. Box 211, Amsterdam, The Netherlands

SUMMARIES OF PAPERS PUBLISHED IN ANALYTICA CHIMICA ACTA

VOL. 36, No. 4, December 1966

COMPLEX FORMATION OF ZIRCONIUM AND HAFNIUM WITH XYLENOL ORANGE

The factors affecting the formation of zirconium and hafnium complexes of xylenol orange (XO) in perchloric acid have been examined. The optimum acid concentration for both systems is in the range 0.2–0.5 *M* $HClO_4$. When excess of metal is present, an initial complex with XO:metal ratio of 1:1 is formed; this complex then undergoes an acid-dependent reaction, taking approximately 2 h to reach completion. Rate constants for this reaction have been determined. When excess of xylenol orange is present (*i.e.* XO:metal $\geqslant 2$) a 2:1 complex is formed which does not undergo further reaction. Extinction coefficients are given for the various complexes.

PH. M. CHAMPION, P. CROWTHER AND D. M. KEMP,
Anal. Chim. Acta, 36 (1966) 413–421

THEORY OF COMPLEXIMETRIC TITRATIONS WITH REDOX INDICATORS

EDTA TITRATION OF IRON(III) USING VARIAMINE BLUE AS INDICATOR

Theoretical expressions are derived for the color transition of variamine blue B base used as a redox indicator in the compleximetric titration of iron(III) with EDTA, and photometric and visual methods of end-point location are discussed. The addition of iron(II) favored the elimination of the interference of some metals. The effect of added iron(II) is illustrated and quantitatively accounted for.

N. NAKASUKA AND M. TANAKA,
Anal. Chim. Acta, 36 (1966) 422–430

DIMERIZATION AND ASSOCIATION OF AN ORGANOPHOSPHORIC ACID IN VARIOUS ORGANIC SOLVENTS

The association of bis(*p*-chlorophenyl)phosphoric acid with various organic solvents as well as its dimerization in these solvents was investigated. In inert solvents like kerosene, carbon tetrachloride and benzene, dimerization is very high and decreases with increasing polarity of the solvent. In polar solvents like alcohols and ketones, a strong association between HA and solvent molecules exists. The association constants were determined; the values may be regarded as a measure for the basicity of the solvents in question. The following order of the increasing basicity of the solvents was established: hydrocarbons and chlorinated hydrocarbons < ethers < ketones < alcohols.

F. KRAŠOVEC, M. OSTANEK AND C. KLOFUTAR,
Anal. Chim. Acta, 36 (1966) 431–438

AN ION-EXCHANGE SCHEME FOR THE DETERMINATION OF THE MAJOR CATIONS IN SEA WATER

A cation-exchange scheme is described for the determination of the principal cations in sea water. The cations are adsorbed onto a column of Amberlite CG 120. Sodium and potassium are eluted together using 0.15 M ammonium chloride and determined gravimetrically as sulphates; potassium is then determined gravimetrically as potassium tetraphenylboron and sodium is determined by difference. Magnesium and calcium are eluted by means of 0.35 M ammonium chloride and 1 M ammonium acetylacetonate (pH 9.6) respectively, and titrated with EDTA. Finally, strontium is eluted with 2 M nitric acid and determined by flame photometry. Tests made using an artificial sea water showed that the method had coefficients of variation of 0.02, 0.22, 0.04, 0.08 and 0.8% for sodium, potassium, magnesium, calcium and strontium respectively.

R. Greenhalgh, J. P. Riley and M. Tongudai,
Anal. Chim. Acta, 36 (1966) 439–448

TITRIMETRIC DETERMINATION OF HYDRAZINES WITH SULFATOCERIC ACID

Titrimetric methods for the determination of hydrazine and some simple alkyl and aryl derivatives are described. Iodine monochloride serves as pre-oxidant and indicator, and sulfatoceric acid as the titrant. Mercury(II) is added to ensure complete oxidation of some compounds.

S. Singh and J. R. Siefker,
Anal. Chim. Acta, 36 (1966) 449–453

SOME NEW AROMATIC HYDROXYLAMINES AS SPECTROPHOTOMETRIC REAGENTS FOR VANADIUM

A comparative study is described of the use of N-benzoyl-*o*-tolyl-, N-benzoyl-*m*-tolyl-, N-benzoyl-*p*-tolyl-, N-benzoyl-*p*-chlorophenyl- and N-phenylacetylphenylhydroxylamines, as spectrophotometric reagents for the determination of vanadium, after extraction with chloroform. All the reagents form 1:2 (metal:reagent) complexes in hydrochloric acid media or at pH 4.8–6.0; the dissociation constants of the complexes are of the order of 10^{-9} and 10^{-8}, respectively, except those of N-benzoyl-*p*-chlorophenylhydroxylamine which are of the order of 10^{-8} in both media. The reactions in hydrochloric acid media are more selective and sensitive than those at pH 4.8–6.0. In presence of alcohol, the wavelengths of maximum absorption decrease. The pK_a values of the hydroxylamines were determined in water and in alcohol–water (1:1) solutions.

A. K. Majumdar and G. Das,
Anal. Chim. Acta, 36 (1966) 454–459

STABILITY OF SOME STATIONARY PHASES IN THE SEPARATION OF POLYPHENYL MIXTURES BY GAS CHROMATOGRAPHY

Some liquid phases utilized in the analysis of polyphenyl mixtures show variations in their chromatographic properties when used in packed columns; a study was therefore made of methods of increasing its stability, the influence of the solid support and the conditioning process. Reproducibility in the column preparation was checked by means of conditioning curves. Stable columns were obtained by using stationary mixed phases at 5% on chromosorb P, of silicone oil DC-710:UCON 50 LB in the proportion 3:1 and with silicone oil DC-710:carbowax 20 M in the proportions 3:1 and 1:1.

L. Gascó-Sánchez and F. Burriel-Martí,
Anal. Chim. Acta, 36 (1966) 460–468

MULTICHANNEL INTEGRATING FLAME PHOTOMETER

A new high-speed optical chopping and demodulation system is described for use in flame photometry. Methods are described which allow integration of signal and noise over many optical pulses of flame energy. The method has been used to develop a direct-reading instrument for sodium, potassium and calcium. With this method, 4 signal channels are integrated simultaneously. With the integration technique, ordinary flame noise is significantly reduced. By using an internal standard, all signal channels are referenced to known energy levels regardless of flame variations.

J. W. Haagen-Smit and J. Ramírez-Muñoz,
Anal. Chim. Acta, 36 (1966) 469–477

THE DETERMINATION OF TRACE SILVER IN HIGH-PURITY ZINC BY NEUTRON ACTIVATION

(in French)

Below the p.p.m. level, the determination of silver in zinc by non-destructive γ spectrometry is no longer feasible due to the activation of the matrix element. The activated zinc is dissolved in nitric acid, sulfamic acid and silver carrier are added, and ^{110m}Ag (253 d) is obtained in a radiochemically pure state after two successive electrolyses on gold cathodes.

After two days of irradiation in a thermal neutron flux of the order of $3 \cdot 10^{13}$ n/cm^2/sec (BR2-Mol), 30 ng of silver can easily be evaluated with an error of 5%. Data obtained by integral γ-counting or by γ-spectrometry are compared.

F. Mousty, J. Fouarge and G. Duyckaerts,
Anal. Chim. Acta, 36 (1966) 478–488

EMISSION SPECTRA OF ORGANIC LIQUIDS IN OXY–HYDROGEN FLAMES

Organic compounds were aspirated into an oxy–hydrogen flame and the emission spectra studied. Spectra from terminal combustion products were observed and some emission in the infrared may be attributed to larger molecular fragments. Qualitative analysis of combustion processes may be feasible using this process, but numerous problems made quantitative analysis difficult.

J. W. Robinson and V. Smith,
Anal. Chim. Acta, 36 (1966) 489–498

THE EXTRACTION OF LANTHANIDES AND ACTINIDES WITH ALKYLPHOSPHINE OXIDES

PART I. THE EXTRACTION OF NITRIC ACID WITH TRI-*n*-BUTYLPHOSPHINE OXIDE

(in French)

The distribution of TBPO, water and nitric acid has been measured between an aqueous phase and various inert diluents at 25°. This study allowed the determination of the apparent stability constants for two molecular complexes, TBPO . HNO$_3$ ($K_1' = 17.5 \pm 1.3$ $(M/\mathrm{l})^{-2}$ (benzene); 20.1 ± 0.8 (M/l)$^{-2}$ (toluene); 11 ± 2 $(M/\mathrm{l})^{-2}$ (*n*-hexane)) and TBPO . 2 HNO$_3$. H$_2$O ($K_2' = (2.9 \pm 0.3)\ 10^{-3}$ $(M/\mathrm{l})^{-2}$ (benzene)).

J. Goffart and G. Duyckaerts,
Anal. Chim. Acta, 36 (1966) 499–507

SECOND-ORDER INTERFERENCE IN THE NEUTRON ACTIVATION ANALYSIS OF ARSENIC IN A GERMANIUM MATRIX

The second-order interference $^{74}\mathrm{Ge}(n,\gamma;\beta^-;n,\gamma)\ ^{76}\mathrm{As}$ can occur in the activation analysis of arsenic in a germanium matrix, using thermal neutrons. As the literature data show poor agreement, this interference was determined experimentally. A practical formula was derived, for irradiation times longer than 2 h, which showed that the interference, expressed as an apparent arsenic concentration, is proportional to the neutron flux. Experiments were performed for irradiation times of 10, 15 and 20 h at a neturon flux of 10^{14} n/cm^2/sec, yielding apparent arsenic concentrations in the germanium matrix of respectively 223, 408 and 597 p.p.b. From these results a value of 0.48 ± 0.06 barn could be calculated for the activation cross-section of ^{74}Ge for neutron capture.

R. De Neve, D. De Soete and J. Hoste,
Anal. Chim. Acta, 36 (1966) 508–514

DIRECT EDTA TITRATION OF VANADIUM(V) USING VARIAMINE BLUE B BASE AS INDICATOR IN THE PRESENCE OF EXCESS IRON(II)

Continuous expressions are derived for the titration of vanadium(V) with iron(II) in the presence of excess EDTA and for the titration of vanadium(V) with EDTA in presence of excess iron(II). A new method of EDTA titration of vanadium(V) is developed based on the theoretical consideration of these expressions. The method is simple, selective and reliable.

M. Tanaka and A. Ishida,
Anal. Chim. Acta, 36 (1966) 515–521

EFFECT OF REAGENT CONCENTRATION IN THE PHOTOMETRIC DETERMINATION OF VANADIUM(V) WITH 8-QUINOLINOL

(Short Communication)

M. Tanaka and I. Kojima,
Anal. Chim. Acta, 36 (1966) 522–525

CONDUCTOMETRIC END-POINT DETECTION IN THE TITRATION OF FLUORIDE AND FLUOSILICIC ACID WITH THORIUM NITRATE

(Short Communication)

Y. Israel, B. Bernas and A. Yahalom,

Anal. Chim. Acta, 36 (1966) 526–529

A COMMENT ON THE MASS SPECTROMETRY OF MATERIALS PRODUCING SULFUR TRIOXIDE

(Short Communication)

R. S. Gohlke and H. G. Langer,
Anal. Chim. Acta, 36 (1966) 530–532

A COAXIAL NMR CELL

(Short Communication)

J. F. Hinton and E. S. Amis,
Anal. Chim. Acta, 36 (1966) 532–536

EXTRACTION AND STABILITY CONSTANTS OF COPPER COMPLEXES OF 1,5-DIPHENYLCARBAZONE

(Short Communication)

H. R. Geering and J. F. Hodgson,
Anal. Chim. Acta, 36 (1966) 537–540

COMPLEX FORMATION OF ZIRCONIUM AND HAFNIUM WITH XYLENOL ORANGE

PHYLLIS M. CHAMPION, P. CROWTHER AND D. M. KEMP
National Nuclear Research Centre, Pelindaba, Pretoria (South Africa)

(Received May 3rd, 1966)

The published data on the complexes of zirconium with the aminopolycarboxylic acid, xylenol orange (XO), give conflicting evidence as to their composition. BABKO AND SHTOKALO[1] report a 1:1 XO–zirconium complex in 1 *N* hydrochloric acid, and a 2:1 complex at pH 2. BABKO AND GRIDCHINA[2] describe the presence of a polyion, in 0.01–2.0 *N* hydrochloric acid media, with the structure $-Zr(OH)_2-O-Zr(OH)_2-O-$ which undergoes decomposition to form complexes with XO. BUDESINSKY[3] postulates a complex with 2 moles of zirconium per 1 mole of XO. CHENG[4–6] reports 1:1 complexes for both zirconium and hafnium in 0.2–1.0 *N* perchloric acid media, but also suggests that the complexes may have some other composition when excess of XO is present. No experimental evidence is offered to support this latter suggestion.

EXPERIMENTAL

Apparatus and reagents

Absorption measurements were carried out on a Zeiss Model RPQ 20AV double-beam recording spectrophotometer using 1-cm quartz cells.

Standard Zr solution. 10^{-3} *M* solution in 1 *N* perchloric acid prepared from Merck analytical grade $ZrOCl_2 \cdot 8H_2O$.

Standard Hf solution. 10^{-3} *M* solution in 1 *N* perchloric acid prepared from Johnson, Matthey & Co. spectroscopically standardised $HfOCl_2 \cdot 8H_2O$ containing 0.47% Zr.

Xylenol orange. 10^{-3} *M* solution prepared from B.D.H. laboratory reagent.

Perchloric acid. B.D.H. AnalaR product was used.

Absorption spectra

The wavelength of the maximum absorption of both the zirconium and the hafnium complexes was found to vary with time and with the ratio of metal to XO present in the solution under examination. For both the complexes the wavelength varied from 530 to 550 nm. All measurements were made at the peak maximum.

Under certain conditions, periods of several hours were necessary for the attainment of final and constant values of the absorbance.

RESULTS

Rate of formation of the complexes

The development of the complexes was followed with time. Depending upon the ratio of metal to XO present, different curves were obtained as shown in Fig. 1. Curves of type a were obtained when the mole ratio XO/metal was less than or equal to 1. In the case shown, with 1.2 μmole Hf and 0.8 μmole XO per 50 ml of solution, the absorbance increased smoothly from 0.45 to 0.685 over 1.5 h. The initial and final wavelengths were 546 nm and 549 nm respectively.

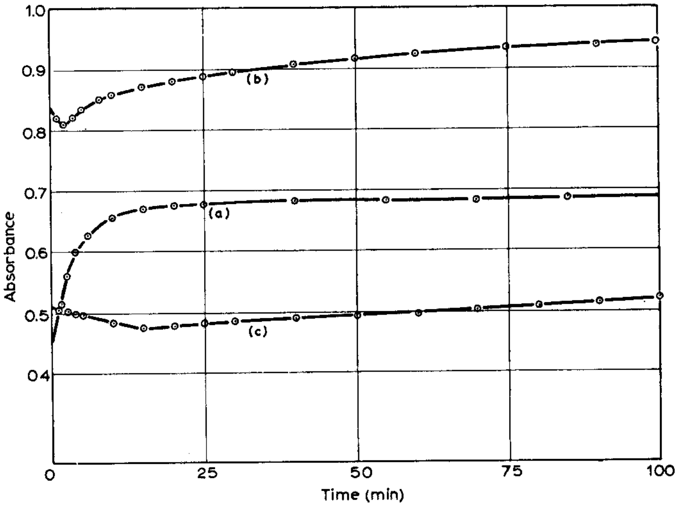

Fig. 1. Time development of Hf–XO complex in 0.25 *N* $HClO_4$. (a) 1.2 μmole Hf, 0.8 μmole XO/50 ml; (b) 1.0 μmole Hf, 1.8 μmole XO/50 ml; (c) 0.5 μmole Hf, 2.0 μmoles XO/50 ml.

Curves of type b were obtained when the mole ratio XO/metal was just less than 2. In the case shown with 1 μmole Hf and 1.8 μmole XO per 50 ml of solution, the initial absorbance of 0.835 decreased to 0.81 over 2 min, and then increased to 0.94 over 1.5 h. In this case the initial and final wavelengths were 542 nm and 545 nm respectively.

When XO was present in large excess as in curve c, where XO/metal = 4, with 0.5 μmole Hf and 2 μmoles XO per 50 ml of solution, the absorbance decreased from 0.51 to 0.475 over 15 min, and then increased slightly over 2 h to 0.52. The wavelength remained unchanged at 540 nm.

No explanation can at this stage be advanced for the initial decrease in absorbance in cases b and c.

Composition of the complexes

JOB'S *method of continuous variation*[7]. Absorbances were measured for a series of solutions containing varying mole fractions of metal and XO, their sum remaining constant. The results obtained are shown in Fig. 2.

The initial curve, a, shows a maximum corresponding to a mole ratio XO/XO + metal of 0.62, this being an intermediate between 0.5 (1:1 complex) and 0.67 (2:1 complex). The final curve, b, shows a maximum at 0.5 and there is an indication of a discontinuity at 0.67.

Mole ratio method of YOE AND JONES[8]. The absorbances were measured for a series of solutions which contained varying amounts of one constituent with a constant amount of the other. Figure 3 represents the absorbances of solutions containing a constant amount of the metal (0.5 μmole) and varying amounts of XO. Curve a was plotted, using the initial absorbance obtained by extrapolation to zero time, while curve b shows the absorbance after 20 h.

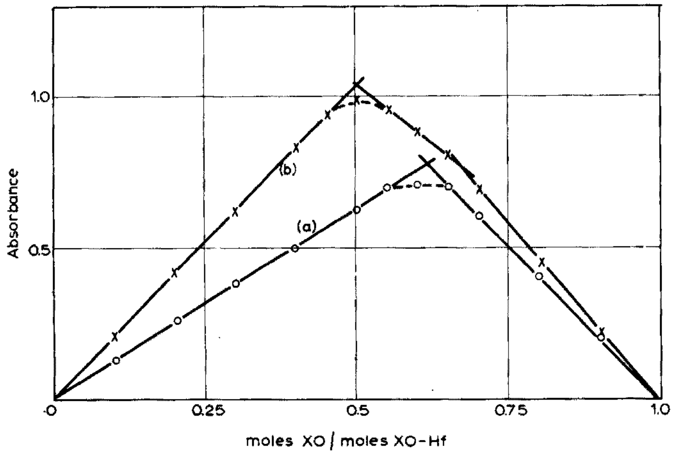

Fig. 2. Job curve for Hf–XO complex in 0.25 N $HClO_4$. Total of 2 μmoles/50 ml. (a) Absorbance at time $t = 0$; (b) absorbance at time $t = 20$ h.

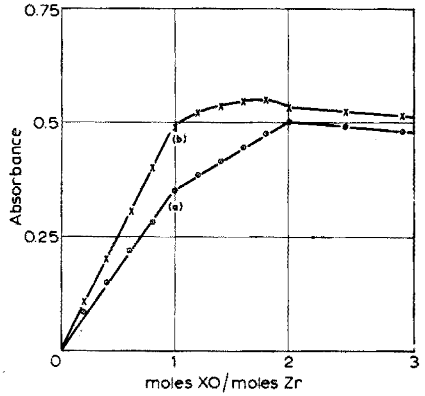

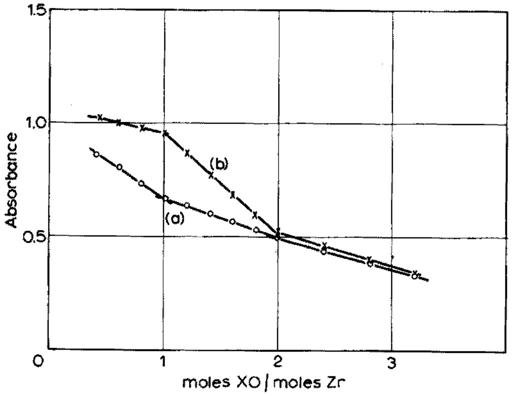

Fig. 3. Mole ratio curve for Zr–XO complex in 0.25 N $HClO_4$. 0.5 μmole Zr/50 ml. (a) Absorbance at time $t = 0$; (b) absorbance at time $t = 20$ h.

Fig. 4. Mole ratio curve for Zr–XO complex in 0.25 N $HClO_4$. 1 μmole XO/50 ml. (a) Absorbance at time $t = 0$; (b) absorbance at time $t = 20$ h.

The initial curve a shows straight lines intersecting at the points corresponding to mole ratios of 1 and 2, demonstrating the existence of complexes containing XO: metal in the ratios 1:1 and 2:1. In the final curve b, the initial straight line has become slightly curved between mole ratio values of 1 and 2, but still shows discontinuity.

Figure 4 was obtained similarly to Fig. 3, except that in this case the XO was kept constant at 1 μmole and varying additions of the metal were made. Again intersections demonstrate the existence of 1:1 and 2:1 XO-metal complexes.

Extinction coefficients

The extinction coefficients of the above complexes were measured and are listed in Table I.

TABLE I

EXTINCTION COEFFICIENTS

Complex	*l/mole/cm*	
	XO/metal $\leqslant 1$	*XO/metal* $\geqslant 2$
Initial Zr	$1.88 \cdot 10^4$	$2.30 \cdot 10^4$
Final Zr	$2.52 \cdot 10^4$	$2.65 \cdot 10^4$
Initial Hf	$1.55 \cdot 10^4$	$2.50 \cdot 10^4$
Final Hf	$2.52 \cdot 10^4$	$2.72 \cdot 10^4$

Effect of acid concentration

The effect of the perchloric acid concentration is shown in Fig. 5 for solutions containing different ratios of XO and metal ion. It is apparent that the optimum acid concentration for the hafnium complexes is 0.1–0.4 *N* in perchloric acid, and 0.1–0.5 *N* for the zirconium complexes.

Figure 5b shows the difference in initial absorbance depending on the age of the standard hafnium solution. Curve (i) represents the initial absorbances of the XO

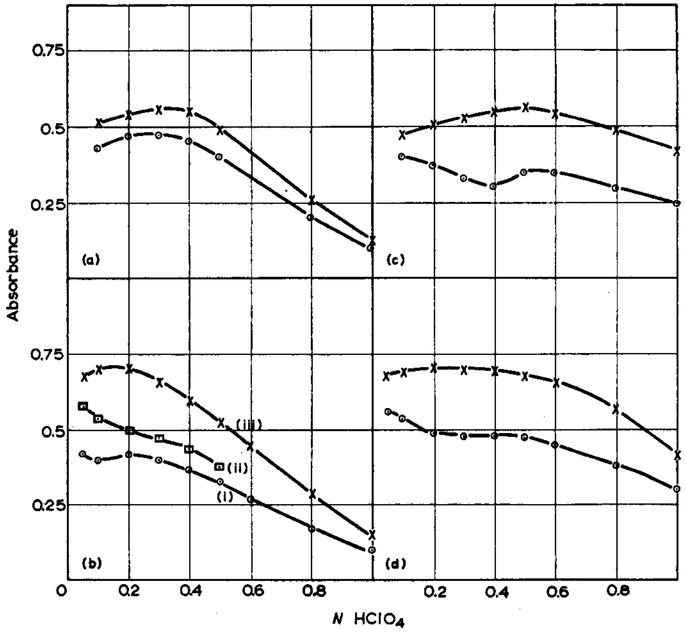

Fig. 5. Effect of acid concentration. ⊙ = absorbance at time t = 0 (standard metal solution freshly prepared); ⊡ = absorbance at time t = 0 (standard metal solution aged for 24 h); × = absorbance at time t = 4 h. (a) 0.5 μmole Hf, 1.0 μmole XO/50 ml; (b) 1.0 μmole Hf, 0.6 μmole XO/50 ml; (c) 0.5 μmole Zr, 1.0 μmole XO/50 ml; (d) 1.0 μmole Zr, 0.6 μmole XO/50 ml.

complexes of a freshly prepared hafnium solution. Curve (ii) represents the initial absorbances of XO complexes of the same hafnium solution aged for 24 h. Curve (iii) represents the final absorbances of the complexes of both solutions.

Formation of stable 1:1 complexes

Order of reaction. It is assumed that in the case of the 1:1 complex the initial absorbance is due to an intermediate complex which then undergoes reaction by either rearrangement or hydrolysis in acidic solution to form a final stable complex. The order of this reaction was determined as previously described by CROWTHER AND KEMP[9].

The absorbance E_A of the initial complex formed is given by

$$E_A = E_0 \left\{\frac{E_\infty - E_t}{E_\infty - E_0}\right\} \qquad (1)$$

where E_0 = absorbance at time $t = 0$, E_∞ = absorbance at completion of reaction, and E_t = absorbance at any time t.

The reaction was followed for solutions containing 0.8 μmole of XO and 1 μmole of zirconium per 50 ml in (*a*) 0.2 *N* perchloric acid, and (*b*) 0.4 *N* perchloric acid. The absorbance *vs.* time curves are shown in Fig. 6.

For curve a: $E_0 = 0.550$, and $E_\infty = 0.895$.

A fractional order of 3/2 with respect to the initial zirconium complex was obtained (see Fig. 7).

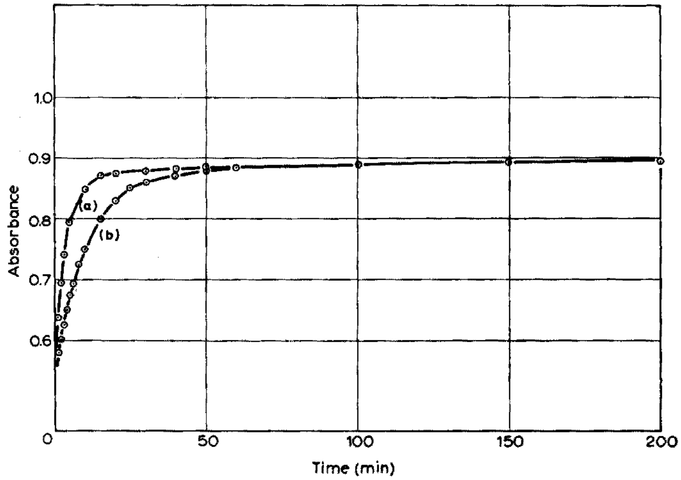

Fig. 6. Time development of Zr–XO complex. 1 μmole Zr, 0.8 μmole XO/50 ml. (a) 0.2 *N* $HClO_4$; (b) 0.4 *N* $HClO_4$.

Rate of reaction. In a system with 2 reacting species, the rate constant *k* of the reaction is defined by

$$\frac{-\mathrm{d}c}{\mathrm{d}t} = kC_A{}^nC_B{}^m \qquad (2)$$

where C_A is the concentration of initial complex, C_B is the concentration of hydrogen ion, n is the order of reaction with respect to A, and m is the order of reaction with respect to B.

If $C_B \gg C_A$, C_B remains effectively constant and $-dc/dt = k'C_A^n$.
Integrating:

$$(n-1)C_0^{n-1}k't = \frac{C_0}{C_A} - 1 \tag{3}$$

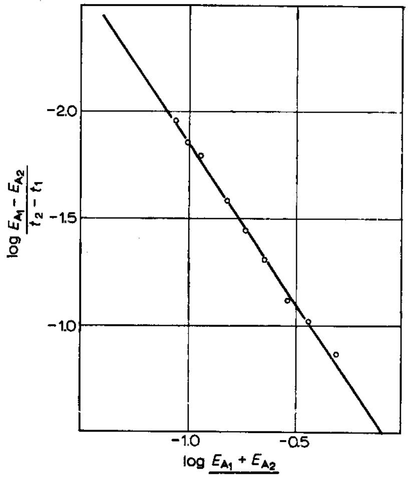

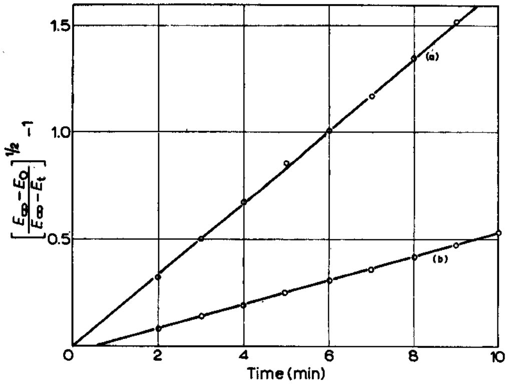

Fig. 7. Determination of order of reaction. E_{A1} is value of E_A at time t_1; E_{A2} is value of E_A at time t_2. Slope of line = 1.5.

Fig. 8. Determination of rate constant k'. (a) 0.2 N $HClO_4$; slope 0.1685/min; (b) 0.4 N $HClO_4$; slope 0.057/min.

where C_0 is the initial value of C_A.

Since the solution is dilute with respect to A, and the concentrations of the other components do not change appreciably, it is assumed that the absorbance of A is a linear function of its concentration, *i.e.* $C_0 \propto E_0$, and $C_A \propto E_A$.

Substituting from eqn. (1) and using $n = 3/2$

$$\tfrac{1}{2}C_0^{\frac{1}{2}}k't = \left[\frac{E_\infty-E_0}{E_\infty-E_t}\right]^{\frac{1}{2}} - 1 \tag{4}$$

A plot of the right-hand side of eqn. (4) *vs.* t should give a straight line with slope $\frac{1}{2}C_0^{\frac{1}{2}}k'$.

Using the results of Fig. 6 the rate constants for the 2 systems were determined from Fig. 8.

Now $C_0 = 1.6 \cdot 10^{-5}$ moles/l

$C_0^{\frac{1}{2}} = 4.0 \cdot 10^{-3}$ moles/l

Thus k' (0.2 N $HClO_4$) = 84.3 l/mole/min.

and k' (0.4 N $HClO_4$) = 28.5 l/mole/min.

DISCUSSION

Table II gives a comparison of reported data with the present observed results.

TABLE II

COMPARISON OF REPORTED LITERATURE DATA WITH PRESENT OBSERVATION

Previous data	*Present observations*
1. XO forms 1:1 complexes with Zr and/or Hf[1,6]; 2:1 complex with Zr[1]; 1:2 complex with Zr[3].	1:1 and 2:1 complexes with Zr and Hf indicated.
2. Formation of the complexes is immediate[6]; complex development is time-dependent[2].	Time-dependent and competing reactions observed.
3. Zr–XO has maximum absorbance at 535 nm[6]; 555 nm[1].	Maxima vary between 530–550 nm.
4. Hf–XO has maximum absorbance at 530 nm[6].	Maxima vary between 530–550 nm.
5. $\varepsilon = 3.38 \cdot 10^4$ l/mole/cm[4] $\varepsilon = 2.42 \cdot 10^4$ l/mole/cm[6] for Zr–XO in 0.8 *N* $HClO_4$[4].	$\varepsilon = 1.88 \cdot 10^4$ l/mole/cm for initial Zr complex; $2.52 \cdot 10^4$ l/mole/cm for final complex in 0.2 *N* $HClO_4$, lower values in 0.8 *N* $HClO_4$.
6. $\varepsilon = 1.57 \cdot 10^4$ l/mole/cm for Hf–XO in 0.2 *N* $HClO_4$[6].	$\varepsilon = 1.55 \cdot 10^4$ l/mole/cm for initial Hf complex; $2.52 \cdot 10^4$ l/mole/cm for final complex.
7. Zr–XO has maximum absorbance in 0.5–1.0 *N* $HClO_4$[6].	0.1–0.5 *N* $HClO_4$.

Two major differences are apparent between the perchloric acid system and the hydrochloric acid system described by BABKO AND GRIDCHINA[2]:

(*a*) Whereas the latter reported continuous increasing absorbance with increasing hydrochloric acid concentration, it was observed in the present work that absorbance maxima are obtained depending on the perchloric acid concentration, as shown in Fig. 5.

(*b*) BABKO AND GRIDCHINA observed increasing rate of formation of the complexes with increasing hydrochloric acid concentration, while in perchloric acid media the inverse is true (Fig. 6).

It appears that the polymeric species of zirconium or hafnium, $-M(OH)_2-O-M(OH)_2-O-$ is present in both systems, but to a lesser extent in the perchloric acid system. Pre-heating of zirconium or hafnium solutions, 0.1 *N* in perchloric acid, before the addition of XO, reduces the final absorbance, while this effect is apparent in hydrochloric acid up to 2 *N*[2].

At 0.02 *N* perchloric acid, the metal species is rendered almost completely inactive to complex formation by pre-heating.

BABKO has proposed that complexing with XO proceeds via the decomposition of the polymer, which explains his observation of increasing rate of reaction with increasing acid concentration. However, the present observed decrease in the rate with increasing acid concentration indicates an hydrolysis reaction in the perchloric acid system.

The following reactions are proposed for the formation of the 1:1 XO complexes in the perchloric acid system:

$$Hf^{4+} + H_2O \rightleftarrows HfO^{2+} + 2\,H^+ \qquad (5)$$

the equilibrium being dependent upon the hydrogen ion concentration.

$$HfO^{2+} + XO \rightleftarrows [HfO(XO)] + 2\ H^{+} \quad (6)$$

$$Hf^{4+} + XO \rightleftarrows [Hf(XO)]^{2+} + 2\ H^{+} \quad (7)$$

$$[Hf(XO)]^{2+} + H_2O \rightleftarrows [HfO(XO)] + 2\ H^{+} \quad (8)$$

Both eqns. (6) and (8) describe the formation of the same final complex.

The initial absorbance E_0 may be attributed to either $[Hf(XO)]^{2+}$ formed from the initial Hf^{4+}, or to $[HfO(XO)]$ resulting from the initial HfO^{2+} present.

The increase in absorbance with time could be due to either

(*a*) the hydrolysis of $[Hf(XO)]^{2+}$ (eqn. (8)), or

(*b*) the shift of the hydrolysis equilibrium in eqn. (5) as one or other of the reacting species is used up. The setting up of this equilibrium is a slow reaction as shown by curves (i) and (ii) of Fig. 5b.

SUMMARY

The factors affecting the formation of zirconium and hafnium complexes of xylenol orange (XO) in perchloric acid have been examined. The optimum acid concentration for both systems is in the range 0.2–0.5 *M* $HClO_4$. When excess of metal is present, an initial complex with XO : metal ratio of 1:1 is formed; this complex then undergoes an acid-dependent reaction, taking approximately 2 h to reach completion. Rate constants for this reaction have been determined. When excess of xylenol orange is present (*i.e.* XO : metal $\geqslant$ 2) a 2:1 complex is formed which does not undergo further reaction. Extinction coefficients are given for the various complexes.

RÉSUMÉ

Les auteurs ont examiné les facteurs affectant la formation des complexes zirconium et hafnium–xylénol orange (XO), en milieu perchlorique. En présence d'un excès de métal, il se forme un complexe XO: métal dans le rapport 1:1; si le xylénol orange est en excès, on a un complexe XO : métal, 2:1. Les coefficients d'extinction sont donnés pour divers complexes.

ZUSAMMENFASSUNG

Die Faktoren, welche die Bildung des Zirkonium- und Hafnium-Komplexes mit Xylenolorange (XO) in Perchlorsäure beeinflussen, wurden geprüft. Die optimale Säurekonzentration für beide Systeme liegt im Bereich von 0.2 bis 0.5 *M* $HClO_4$. Bei einem Metallüberschuss wird anfangs ein Komplex mit dem Verhältnis XO : Metall von 1:1 gebildet. Dieser unterliegt dann einer säureabhängigen Reaktion, welche annähernd 2 h für ihren vollständigen Ablauf benötigt. Für diese Reaktion wurden die Geschwindigkeitskonstanten bestimmt. Bei einem Überschuss von Xylenolorange (XO : Metall $\geqslant$ 2) wird ein 2:1-Komplex gebildet, welcher keiner weiteren Reaktion unterworfen ist. Für die verschiedenen Komplexe werden die Extinktionskoeffizienten angegeben.

REFERENCES

1 A. K. Babko and M. I. Shtokalo, *Ukr. Khim. Zh.*, 27 (1961) 566.
2 A. K. Babko and G. I. Gridchina, *Russ. J. Inorg. Chem. (Engl. Transl.)*, 7 (1962) 889.
3 B. Budesinsky, *Collection Czech. Chem. Commun.*, 28 (7) (1963) 1956.
4 K. L. Cheng, *Talanta*, 2 (1959) 61.
5 K. L. Cheng, *Talanta*, 3 (1959) 81.
6 K. L. Cheng, *Anal. Chim. Acta*, 28 (1963) 41.
7 W. C. Vosburgh and G. R. Cooper, *J. Am. Chem. Soc.*, 63 (1941) 437.
8 J. H. Yoe and A. L. Jones, *Ind. Eng. Chem., Anal. Ed.*, 16 (1944) 11.
9 P. Crowther and D. M. Kemp, *Anal. Chim. Acta*, 29 (1963) 97.

THEORY OF COMPLEXIMETRIC TITRATIONS WITH REDOX INDICATORS

EDTA TITRATION OF IRON(III) USING VARIAMINE BLUE AS INDICATOR

NORIYUKI NAKASUKA AND MOTOHARU TANAKA

Laboratory of Analytical Chemistry, Faculty of Science, Nagoya University, Chikusa-ku, Nagoya (Japan)

(Received March 10th, 1966)

Variamine blue B base, a redox indicator, has been studied several times for the compleximetric titration of iron(III) with EDTA[1-4]. Although the color transition of metal indicators in compleximetric titrations has been fully discussed by many authors[5-11], no quantitative account has been attempted for the color transition of redox indicators used in compleximetric titrations.

In the present paper, expressions are derived for the color transition of variamine blue B in the compleximetric titration of iron(III) with EDTA, and photometric and visual methods of end-point location are discussed. The addition of iron(II) favored the elimination of the interference of some metals; this effect is illustrated and quantitatively accounted for.

THEORETICAL CONSIDERATIONS

The oxidation–reduction reaction of 4-amino-4'-methoxy-diphenylamine (the leuco-base of variamine blue B) has been described as follows:

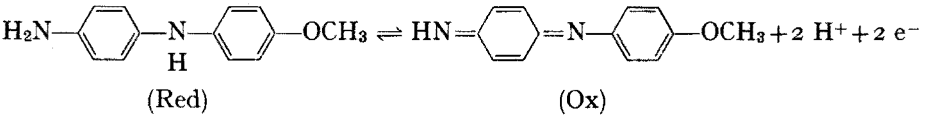

(1)

in which 2 electrons and 2 protons are involved[1,12-14]. The participation of two electrons was also confirmed by the present authors by the photometric method.

The following reactions are involved in the compleximetric titration of iron(III) ion using this indicator:

$$2\ \mathrm{Fe(III)}' + \mathrm{Red}' = 2\ \mathrm{Fe(II)}' + \mathrm{Ox}' + 2\ \mathrm{H}^+ \tag{2}$$

$$\mathrm{Fe(III)}' + \mathrm{Y}' = (\mathrm{Fe(III)Y})' \tag{3}$$

where Red and Ox denote the reduced and oxidized forms of the indicator. The formation of Fe(II)Y may be neglected under the experimental conditions (pH 2–3). The conditional constants of redox equilibrium (2) and complex formation (3) are given respectively by:

$$K'_{\mathrm{Fe-I}} \equiv \frac{[\mathrm{Fe(II)}]'^2[\mathrm{Ox}]'[\mathrm{H}]^2}{[\mathrm{Fe(III)}]'^2[\mathrm{Red}]'} \tag{4}$$

$$K'_{\mathrm{FeY}} \equiv K_{\mathrm{Fe(III)'Y'(Fe(III)Y)'}} \equiv \frac{[\mathrm{Fe(III)Y}]'}{[\mathrm{Fe(III)}]'[\mathrm{Y}]'} \tag{5*}$$

where $[\mathrm{Fe(II)}]'$ and $[\mathrm{Fe(III)}]'$ refer to the total concentration of the relevant species not combined with Y and:

$$[\mathrm{Red}]' = [\mathrm{Red}] + [\mathrm{HRed}] \equiv [\mathrm{Red}]\alpha_{\mathrm{H(Red)}} \tag{6}$$

$$[\mathrm{Ox}]' = [\mathrm{Ox}] + [\mathrm{HOx}] \equiv [\mathrm{Ox}]\alpha_{\mathrm{H(Ox)}} \tag{7}$$

$$[\mathrm{Y}]' \equiv [\mathrm{Y}]\alpha_{\mathrm{H(Y)}} \tag{8}$$

$$\begin{aligned}[\mathrm{Fe(III)Y}]' &= [\mathrm{Fe(III)Y}] + [\mathrm{Fe(III)HY}] + [\mathrm{Fe(III)OHY}] \\ &\equiv [\mathrm{Fe(III)Y}]\alpha_{\mathrm{H,OH(Fe(III)Y)}}\end{aligned} \tag{9}$$

Here α's denote the side-reaction coefficients which are dependent only upon pH.

Stoichiometric relationships (10), (11) and (12) hold throughout the titration:

$$C_{\mathrm{Fe(III)}} = [\mathrm{Fe(III)}]' + [\mathrm{Fe(III)Y}]' + 2[\mathrm{Ox}]' \tag{10}$$

$$C_{\mathrm{Y}} = [\mathrm{Y}]' + [\mathrm{Fe(III)Y}]' \tag{11}$$

$$C_{\mathrm{I}} = [\mathrm{Red}]' + [\mathrm{Ox}]' \tag{12}$$

where $C_{\mathrm{Fe(III)}}$, C_{Y} and C_{I} represent the total concentrations of iron(III), EDTA and indicator respectively.

Then combining eqns. (10) and (11), we have:

$$C_{\mathrm{Y}} = C_{\mathrm{Fe(III)}} - [\mathrm{Fe(III)}]' - 2[\mathrm{Ox}]' + [\mathrm{Y}]' \tag{13}$$

From eqns. (5) and (10):

$$[\mathrm{Y}]' = \frac{C_{\mathrm{Fe(III)}}}{K'_{\mathrm{FeY}}[\mathrm{Fe(III)}]'} - \frac{1}{K'_{\mathrm{FeY}}} - \frac{2[\mathrm{Ox}]'}{K'_{\mathrm{FeY}}[\mathrm{Fe(III)}]'} \tag{14}$$

Substituting eqn. (14) into eqn. (13), we have an expression for the fraction titrated, a:

$$\begin{aligned} a \equiv \frac{C_{\mathrm{Y}}}{C_{\mathrm{Fe(III)}}} &= 1 - \frac{[\mathrm{Fe(III)}]'}{C_{\mathrm{Fe(III)}}} - \frac{2[\mathrm{Ox}]'}{C_{\mathrm{Fe(III)}}} + \frac{1}{K'_{\mathrm{FeY}}[\mathrm{Fe(III)}]'} \\ &- \frac{2[\mathrm{Ox}]'}{K'_{\mathrm{FeY}}C_{\mathrm{Fe(III)}}[\mathrm{Fe(III)}]'} - \frac{1}{K'_{\mathrm{FeY}}C_{\mathrm{Fe(III)}}} \end{aligned} \tag{15}$$

Designating $[\mathrm{Ox}]'/C_{\mathrm{I}}$ as the indicator transition, ϕ, we get:

$$[\mathrm{Red}]' = C_{\mathrm{I}} - [\mathrm{Ox}]' = C_{\mathrm{I}}(1 - \phi) \tag{16}$$

No prior addition of iron(II) to the titration system

In this case the following relationship holds:

$$[\mathrm{Fe(II)}]' = 2[\mathrm{Ox}]' \tag{17}$$

Then from eqns. (4), (16) and (17):

$$[\mathrm{Fe(III)}]'^2 = \frac{4[\mathrm{H}]^2[\mathrm{Ox}]'^3}{K'_{\mathrm{Fe-I}}[\mathrm{Red}]'} = \frac{4C_{\mathrm{I}}^2[\mathrm{H}]^2\phi^3}{K'_{\mathrm{Fe-I}}(1-\phi)} \tag{18}$$

---

* The notation $\gamma_{\mathrm{M',Y'}}$ previously used[11] is equivalent to $K_{\mathrm{M'Y'(MY)'}}$[9]. K'_{FeY} is used hereafter for $K_{\mathrm{Fe(III)'Y'(Fe(III)Y)'}}$ for simplicity.

Substituting eqn. (18) into eqn. (15) we have:

$$a = 1 - \frac{2C_{\mathrm{I}}[\mathrm{H}]}{K'_{\mathrm{Fe-I}}{}^{\frac{1}{2}}C_{\mathrm{Fe(III)}}}\left(\frac{\phi^3}{1-\phi}\right)^{\frac{1}{2}} - \frac{2C_{\mathrm{I}}}{C_{\mathrm{Fe(III)}}}\phi + \frac{K'_{\mathrm{Fe-I}}{}^{\frac{1}{2}}}{2K'_{\mathrm{FeY}}C_{\mathrm{I}}[\mathrm{H}]}\left(\frac{1-\phi}{\phi^3}\right)^{\frac{1}{2}} - \frac{K'_{\mathrm{Fe-I}}{}^{\frac{1}{2}}}{K'_{\mathrm{FeY}}C_{\mathrm{Fe(III)}}[\mathrm{H}]}\left(\frac{1-\phi}{\phi}\right)^{\frac{1}{2}} - \frac{1}{K'_{\mathrm{FeY}}C_{\mathrm{Fe(III)}}} \tag{19}$$

In eqn. (19) the last two terms may be practically neglected because of their extremely small contribution to a. Each coefficient is substituted by f_1 for simplicity:

$$a = 1 - f_2\left(\frac{\phi^3}{1-\phi}\right)^{\frac{1}{2}} - f_3\phi + f_4\left(\frac{1-\phi}{\phi^3}\right)^{\frac{1}{2}} \tag{19'}$$

where the second and third terms are concerned mainly with the indicator transition before the equivalence point and the last term is concerned mainly with that after the equivalence point. Moreover, the second term is negligible in the vicinity of the equivalence point ($\phi < 0.99$).

If only one electron and one proton were involved in the reaction, the corresponding expression would be:

$$a = 1 - \frac{[\mathrm{H}]C_{\mathrm{I}}}{k'_{\mathrm{Fe-I}}C_{\mathrm{Fe(III)}}}\frac{\phi^2}{1-\phi} - \frac{C_{\mathrm{I}}}{C_{\mathrm{Fe(III)}}}\phi + \frac{k'_{\mathrm{Fe-I}}}{K'_{\mathrm{FeY}}C_{\mathrm{I}}[\mathrm{H}]}\frac{1-\phi}{\phi^2} - \frac{k'_{\mathrm{Fe-I}}}{K'_{\mathrm{FeY}}C_{\mathrm{Fe(III)}}[\mathrm{H}]}\frac{1-\phi}{\phi} - \frac{1}{K'_{\mathrm{FeY}}C_{\mathrm{Fe(III)}}} \tag{20}$$

where the corresponding conditional constant of redox equilibrium, $k'_{\mathrm{Fe-I}}$, is defined as:

$$k'_{\mathrm{Fe-I}} \equiv \frac{[\mathrm{Fe(II)}]'[\mathrm{Ox}]'[\mathrm{H}]}{[\mathrm{Fe(III)}]'[\mathrm{Red}]'}$$

Prior addition of iron(II)

If an excess amount of iron(II) is added, *viz.* $C_{\mathrm{Fe(II)}} \gg 2C_{\mathrm{I}}$:

$$[\mathrm{Fe(II)}]' = C_{\mathrm{Fe(II)}} + 2[\mathrm{Ox}]' \doteqdot C_{\mathrm{Fe(II)}} \tag{21}$$

where $C_{\mathrm{Fe(II)}}$ represents the total concentration of iron(II) added. This approximation is rational, especially near the equivalence point. Then from eqns. (4), (16) and (21):

$$[\mathrm{Fe(II)}]'^2 = \frac{C_{\mathrm{Fe(II)}}{}^2[\mathrm{H}]^2}{K'_{\mathrm{Fe-I}}(1-\phi)} \tag{22}$$

Substituting eqn. (22) into eqn. (15):

$$\begin{aligned} a = 1 &- \frac{C_{\mathrm{Fe(II)}}[\mathrm{H}]}{K'_{\mathrm{Fe-I}}{}^{\frac{1}{2}} C_{\mathrm{Fe(III)}}} \left(\frac{\phi}{1-\phi}\right)^{\frac{1}{2}} - \frac{2C_{\mathrm{I}}}{C_{\mathrm{Fe(III)}}}\phi \\ &+ \frac{K'_{\mathrm{Fe-I}}{}^{\frac{1}{2}}}{K'_{\mathrm{FeY}} C_{\mathrm{Fe(II)}}[\mathrm{H}]} \left(\frac{1-\phi}{\phi}\right)^{\frac{1}{2}} \\ &- \frac{2K'_{\mathrm{Fe-I}}{}^{\frac{1}{2}} C_{\mathrm{I}}}{K'_{\mathrm{FeY}} C_{\mathrm{Fe(II)}} C_{\mathrm{Fe(III)}}[\mathrm{H}]} \left(\phi-\phi^2\right)^{\frac{1}{2}} \\ &- \frac{1}{K'_{\mathrm{FeY}} C_{\mathrm{Fe(III)}}} \end{aligned} \tag{23}$$

The last two terms may be neglected as in the preceding case and each coefficient being substituted by f'_1:

$$a = 1 - f'_2 \left(\frac{\phi}{1-\phi}\right)^{\frac{1}{2}} - f'_3\phi + f'_4 \left(\frac{1-\phi}{\phi}\right)^{\frac{1}{2}} \tag{23'}$$

In eqns. (23) and (23′), the second and third terms are concerned mainly with the indicator transition before the equivalence point and the last term is concerned mainly with that after the equivalence point. As in the preceding case, the second term can be neglected when $\phi < 0.99$.

Effect of the presence of a second metal

The effect of a second metal can be easily considered quantitatively in terms of conditional constant $K_{\mathrm{Fe(III)'Y'(Fe(III)Y)'}}$, where the following side-reaction coefficient $\alpha_{\mathrm{H,M(Y)}}$ is used instead of $\alpha_{\mathrm{H(Y)}}$:

$$\begin{aligned} [\mathrm{Y}]' &= [\mathrm{Y}]\alpha_{\mathrm{H(Y)}} + [\mathrm{MY}]' \\ &= [\mathrm{Y}]\left(\alpha_{\mathrm{H(Y)}} + [\mathrm{M}]' K_{\mathrm{M'Y(MY)'}}\right) \equiv [\mathrm{Y}]\alpha_{\mathrm{H,M(Y)}} \end{aligned} \tag{24}$$

Thus in the presence of a second metal M, we have:

$$\begin{aligned} K_{\mathrm{Fe(III)'Y'(Fe(III)Y)'}} &= \frac{[\mathrm{Fe(III)Y}]'}{[\mathrm{Fe(III)}]'[\mathrm{Y}]'} \\ &= K_{\mathrm{Fe(III)Y}} \frac{\alpha_{\mathrm{H,OH(Fe(III)Y)}}}{\alpha_{\mathrm{Fe(III)}}\alpha_{\mathrm{H\ M(Y)}}} \end{aligned} \tag{25}$$

Then the use of the conditional constant given by eqn. (25) allows the construction of potentiometric and photometric titration curves in the same way as in the absence of a second metal (see Figs. 2–4).

RESULTS AND DISCUSSION

No prior addition of iron(II) to the titration system

As shown in Fig. 1, a sharp break-point occurs at the equivalence point, and the theory agrees well with the experiment. The slope of the linear portion in the titration curve is connected with the third term of eqn. (19). The observed $\Delta a/\Delta\phi$ values of the linear portion are:

Curve A in Fig. 1: $(\Delta a/\Delta\phi)_{\text{obs.}} = 0.136$ for the theoretical value $2C_{\text{I}}/C_{\text{Fe(III)}} = 0.130$ and

Curve B in Fig. 1: $(\Delta a/\Delta\phi)_{\text{obs.}} = 0.067$ for the theoretical value $2C_{\text{I}}/C_{\text{Fe(III)}} = 0.064$.

Thus the slope does not correspond to $C_{\text{I}}/C_{\text{Fe(III)}}$, but to $2C_{\text{I}}/C_{\text{Fe(III)}}$. This gives further evidence of the participation of 2 electrons and 2 protons (*cf.* eqns. (19) and (20)). A cursory glance at Fig. 1 shows that the end-point may be determined graphically as the point of intersection of 2 straight lines before and after the equivalence point.

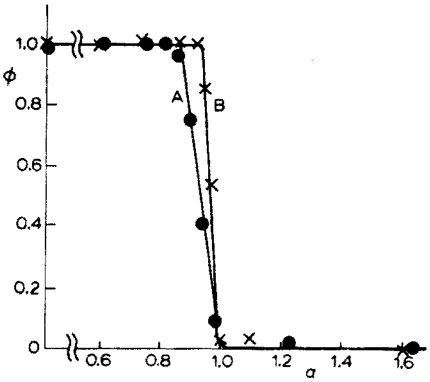

Fig. 1. Titration of iron(III) with EDTA (no prior addition of iron(II)). ● = Experimental results under the following conditions (theoretical curve A): $C_{\text{Fe(III)}} = 8.03 \cdot 10^{-4}\,M$, $C_{\text{I}} = 5.21 \cdot 10^{-5}\,M$; pH = 2.36, $\mu = 0.01$, at 25°. × = Experimental results under the following conditions (theoretical curve B): $C_{\text{Fe(III)}} = 8.19 \cdot 10^{-4}\,M$, $C_{\text{I}} = 2.61 \cdot 10^{-5}\,M$; pH = 2.34, $\mu = 0.01$, at 25°. For the constants used, see APPENDIX.

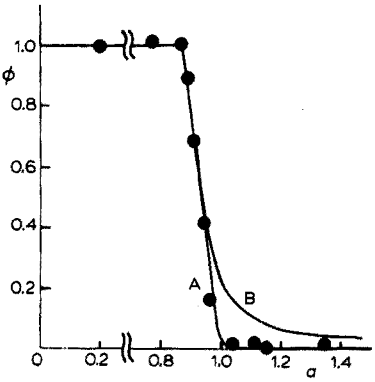

Fig. 2. Titration of iron(III) with EDTA in the presence of cadmium. ● = Experimental results under the following conditions (theoretical curve A): $C_{\text{Fe(III)}} = 8.45 \cdot 10^{-4}\,M$, $C_{\text{I}} = 5.21 \cdot 10^{-5}\,M$, $C_{\text{Fe(II)}} = 1.00 \cdot 10^{-3}\,M$, $C_{\text{Cd}} = 1.00 \cdot 10^{-2}\,M$; pH = 2.31, $\mu = 0.04$, at 25°. Curve B: Theoretical curve under the above conditions but in the absence of iron(II). For the constants used, see APPENDIX.

If, for instance, the point of intersection of the horizontal line at $\phi = 0$ with the straight line through $\phi = 0.1$ and $\phi = 0.6$ is taken as an end-point, the theoretical titration error is calculated as:

$$\text{Titration error} \equiv a - 1 = 24 f_4 = \frac{12 K'_{\text{Fe-I}}{}^{\frac{1}{2}}}{K'_{\text{FeY}} C_{\text{I}} [\text{H}]} \tag{26}$$

The error is less than 0.1% and always positive.

It may be noted that the experimental values given in Fig. 1 are corrected for the decomposition of the indicator (see EXPERIMENTAL). It should be emphasized, however, that in practice the decomposition of the indicator would not make the titration error much larger (*cf.* Fig. 3).

It was found that the value of a is unity when $\phi = 0.02 - 0.04$. Therefore the end-point in a visual titration should be assigned to a point where the blue-violet color of the indicator can hardly be recognized. This is just as recommended by the previous authors[2,3].

*Prior addition of iron(II) to the titration system**

Although the presence of a second metal makes an end-point obscure, the addition of iron(II) was found very effective in obtaining an improved end-point (Figs. 2, 3 and 4). The observed $\Delta a/\Delta\phi$ value of the linear portion is 0.12 for the theoretical value of $2C_I/C_{Fe(III)} = 0.123$ (Fig. 2). The agreement of the theoretical titration curve with the experimental curve in Fig. 2 may be considered to substantiate eqn. (23) and the assumption in eqn. (21). The favorable effect of the added iron(II), particularly in the presence of a second metal, *e.g.* aluminum or cadmium, is demonstrated in Fig. 3, where percent transmittance is recorded on the ordinate instead of absorbance.

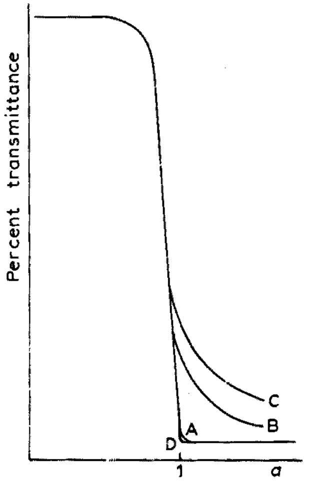

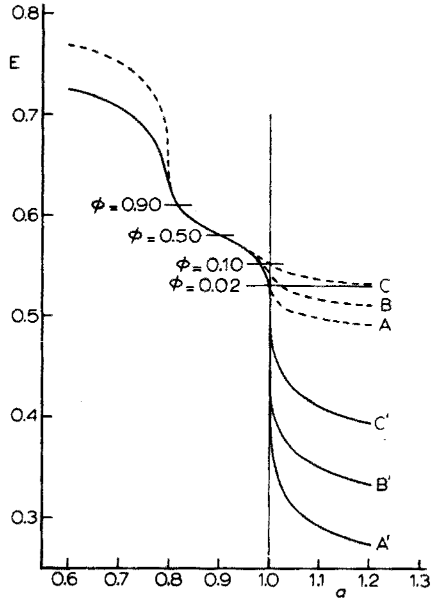

Fig. 3. Effect of iron(II) on the titration of iron(III) in the presence of aluminum or cadmium. Experimental conditions: $C_{Fe(III)} = 7.70 \cdot 10^{-4}\ M$, $C_I = 5.2 \cdot 10^{-5}\ M$, at 20°. Curve A: $C_{Fe(II)} = 0\ M$, $C_M = 0\ M$; pH $= 2.28$, $\mu = 0.01$. Curve B: $C_{Fe(II)} = 0\ M$, $C_{Al} = 1.7 \cdot 10^{-1}\ M$; pH $= 1.90$, $\mu = 1$. Curve C: $C_{Fe(II)} = 0\ M$, $C_{Cd} = 8.3 \cdot 10^{-3}\ M$; pH $= 2.20$, $\mu = 0.04$. Curve D: $C_{Fe(II)} = 7.1 \cdot 10^{-4}\ M$, $C_{Al} = 1.7 \cdot 10^{-1}\ M$; pH $= 1.91$, $\mu = 1$; or $C_{Fe(II)} = 7.1 \cdot 10^{-4}\ M$, $C_{Cd} = 8.3 \cdot 10^{-3}\ M$; pH$=2.27$, $\mu = 0.04$. Titration speed of the automatic titrator: 0.5–1 ml/min.

Fig. 4. Potential variation during the titration of iron(III) in the presence of a second metal. $C_{Fe(III)} = 10^{-3}\ M$, $C_I = 10^{-4}\ M$; pH $= 2$. - - - - - - $C_{Fe(II)} = 0\ M$, ——— $C_{Fe(II)} = 10^{-3}\ M$. Curves A and A′: $\log K'_{FeY} = 12$ ($\log C_M K_{M'Y(MY)'} = 13$). Curves B and B′: $\log K'_{FeY} = 11$ ($\log C_M K_{M'Y(MY)'} = 14$). Curves C and C′: $\log K'_{FeY} = 10$ ($\log C_M K_{M'Y(MY)'} = 15$). For the constants used, see APPENDIX.

Another illustration of the effects of a second metal and added iron(II) is given in Fig. 4, where the potential (E) of the system is correlated with a.

In the presence of a second metal M ($K_{M'Y(MY)'} < K_{Fe(III)'Y(Fe(III)Y)'}$), the titration system after the equivalence point may be regarded as a ligand buffer containing

---

* It has been recommended that the titration of iron(III) with EDTA be carried out in the presence of added iron(II) using cacotheline as a redox indicator[15]. But no account has been given of the favorable effect of the added iron(II) on the indicator transition in the presence of a second metal.

the second metal in excess[16]. Then after the equivalence point pY is buffered more or less at a higher level than in the absence of M. Because of pFe(III) being buffered at a lower level, the potential break becomes less pronounced in the presence of a second metal (see Fig. 4). Correspondingly, the end-point in the photometric or visual titration becomes more or less sluggish, and the end-point location becomes difficult (see Figs. 2 and 3). This difficulty is easily overcome, however, by the addition of iron(II), which restores a normal or even greater potential break in the vicinity of the equivalence point. As is evident from Fig. 4, the presence of a second metal which modifies $\log K'_{\mathrm{FeY}}$ down to 9 seems to be tolerable for the quantitative determination of iron(III) in the presence of an excess amount of iron(II). In other words, *to be successful in the determination of iron(III)* $\log \alpha_{\mathrm{H,M(Y)}}$ *should be smaller than 16.* This statement can be expressed in a simpler form: $\log C_{\mathrm{M}}K_{\mathrm{M'Y(MY)'}}$ should be smaller than 16, $[\mathrm{M}]'$ being replaced by C_{M} in the vicinity of the equivalence point (*cf.* eqn. (24)). Thus for example, 10^{-3} *M* iron(III) can be determined with EDTA in the presence of $2 \cdot 10^{-1}$ *M* aluminum or $3 \cdot 10^{-2}$ *M* cadmium by the prior addition of 10^{-3} *M* iron(II) (*cf.* Figs. 2 and 3).

EXPERIMENTAL

Reagents

1.004 · 10^{-2} M EDTA solution. EDTA disodium dihydrate salt (G.R., Kanto Chemical Co., Inc., Tokyo, Japan) was purified by precipitation with methanol; the precipitate was washed with acetone and ethyl ether, and finally air-dried. The aqueous solution of purified reagent was standardized compleximetrically with 10^{-2} *M* zinc standard solution using eriochrome black T as indicator.

10^{-3} M iron(III) solution. Iron(III) chloride (G.R., Wako Pure Chemical Industries, Ltd., Osaka, Japan) was converted to iron(III) perchlorate by repeated evaporation with perchloric acid. The solution contained no detectable chloride and was 0.01 *M* in perchloric acid. The solution was standardized gravimetrically by the 8-hydroxyquinoline method.

Variamine blue B base hydrochloride solution. This was freshly prepared by dissolving 39.3 mg of N-(*p*-methoxyphenyl)phenylenediamine hydrochloride (Dojindo Chemical Co., Kumamoto, Japan) in 250 ml of distilled water. The purity, determined by acid–base titration with $2 \cdot 10^{-2}$ *M* sodium hydroxide solution, was 100 ±1%.

1 M aluminum solution. Aluminum chloride (G.R., Wako Pure Chemical Industries, Ltd., Osaka, Japan) was dissolved in distilled water, and the absence of iron(II) and iron(III) was assured with *o*-phenanthroline and variamine blue B base.

All other reagents were of general reagent grade and used without further purification.

Apparatus

Beckman DU Spectrophotometer. Automatic Recording Titrator (Hirama Rika Kenkyujo, Kawasaki, Japan). Horiba pH Meter Model P (Horiba Instruments Inc., Kyoto, Japan).

Procedures

For comparison of the theory with the experimental results given in Figs. 1

and 2, Procedure 1 was followed where the irreversible oxidation of the indicator was taken into account. In the other experiments (Fig. 3) Procedure 2 was followed using the automatic recording titrator.

Procedure 1. The iron(III) solution was diluted to about 10^{-3} M and the pH was adjusted to 2.35 with $1.0 \cdot 10^{-2}$ M potassium hydrogen phthalate buffer solution (pH 4). This solution may contain a second metal and/or iron(II). Various amounts of the EDTA solution were added to 50 ml of this solution, and then 5 ml of the indicator solution was added with stirring. The absorbance was measured at 560 nm after different time intervals. The absorbance increased first and then decreased. Then by extrapolation the absorbance at time zero was easily obtained assuming that the indicator was oxidized instantaneously and that the oxidized indicator began to fade at time zero.

Procedure 2. Titrations were carried out by means of the automatic recording titrator with an optical filter of 562 nm. It may be noted that in this procedure *transmittance* is recorded against ml of added EDTA solution.

Recommended procedure

To about 50 ml of acidic sample solution, add 1 ml of 10^{-2} M iron(II) solution in 10^{-2} M sulfuric acid and adjust the pH to 2.2 ± 0.3. After addition of 5 ml of the indicator solution, titrate with EDTA solution either visually or by means of an automatic titrator.

The authors wish to express their grateful appreciation to Dr. GENKICHI NAKAGAWA, Nagoya Institute of Technology, for helpful discussions, particularly with regard to the addition of iron(II) to the titration system.

APPENDIX

The values of the equilibrium constants used for calculation in the present paper were:

Log $K_{\mathrm{Fe(III)Y}} = 25.1$, log $K^{\mathrm{H}}_{\mathrm{Fe(III)HY}} = 1.4$, log $K^{\mathrm{OH}}_{\mathrm{Fe(III)OHY}} = 6.51$; log $K_{\mathrm{Fe(II)Y}} = 14.26$, log $K^{\mathrm{H}}_{\mathrm{Fe(II)HY}} = 2.75$[17].

Log $K_{\mathrm{CdY}} = 14.46$, log $K^{\mathrm{H}}_{\mathrm{CdHY}} = 2.9$[18].

Log $K^{\mathrm{H}}_{\mathrm{RedH}} = 5.70$ (at 20°)[19], log $K^{\mathrm{H}}_{\mathrm{OxH}} = 6.6$[14].

Log $K_{\mathrm{Fe\text{-}I}} = 2.44$, calculated from the values of standard potential $E° = 0.700$[14] for variamine blue B base and $E° = 0.771$ for iron.

SUMMARY

Theoretical expressions are derived for the color transition of variamine blue B base used as a redox indicator in the compleximetric titration of iron(III) with EDTA, and photometric and visual methods of end-point location are discussed. The addition of iron(II) favored the elimination of the interference of some metals. The effect of added iron(II) is illustrated and quantitatively accounted for.

RÉSUMÉ

Des expressions théoriques sont dérivées pour la variation de couleur de la base bleu variamine B, utilisée comme indicateur, lors du titrage complexométrique du fer(III) au moyen d'EDTA et lors des méthodes de détermination photométriques et visuelles du point final. L'addition de fer(II) favorise la suppression d'interférences de certains métaux.

ZUSAMMENFASSUNG

Es werden theoretische Ausdrücke für den Farbübergang der Variaminblau-B Base abgeleitet, die als Redoxindikator bei der komplexometrischen Titration von Eisen(III) mit AeDTE verwendet wird. Photometrische und visuelle Methoden der Endpunktsbestimmung werden diskutiert. Die Zugabe von Eisen(II) verringert die Störung einiger Metalle. Der Einfluss des zugegebenen Eisen(II) wird dargestellt und quantitativ erklärt.

REFERENCES

1 L. Erdey and A. Bodor, *Z. Anal. Chem.*, 137 (1953) 410.
2 H. Flaschka, *Mikrochim. Acta*, (1954) 361.
3 L. Erdey and G. Rády, *Z. Anal. Chem.*, 149 (1956) 250.
4 P. Wehber, *Mikrochim. Acta*, (1955) 812.
5 G. Schwarzenbach and H. Flaschka, *Die Komplexometrische Titration*, 5. Auflage, F. Enke Verlag, Stuttgart, 1965.
6 J. M. H. Fortuin, P. Karsten and H. L. Kies, *Anal. Chim. Acta*, 10 (1954) 356.
7 H. Flaschka and S. Khalafallah, *Z. Anal. Chem.*, 156 (1957) 401.
8 H. Flaschka, *Talanta*, 1 (1958) 60.
9 A. Ringbom, *Complexation in Analytical Chemistry*, Interscience, New York, 1963, p. 38, 75.
10 R. W. Schmid and C. N. Reilley, *Anal. Chem.*, 31 (1959) 887.
11 M. Tanaka and G. Nakagawa, *Anal. Chim. Acta*, 32 (1965) 123, and their preceding papers cited therein.
12 L. Erdey, E. Zalay and E. Bodor, *Acta Chim. Acad. Sci. Hung.*, 12 (1957) 251.
13 L. Erdey, I. Buzás and L. Vigh, *Talanta*, 1 (1958) 377.
14 É. Bányai and P. Zuman, *Collection Czech. Chem. Commun.*, 24 (1959) 522.
15 G. G. Rao, V. N. Rao and G. Somidevamma, *Z. Anal. Chem.*, 152 (1956) 346.
16 M. Tanaka, *Anal. Chim. Acta*, 29 (1963) 193.
17 G. Schwarzenbach and J. Heller, *Helv. Chim. Acta*, 34 (1951) 576.
18 G. Schwarzenbach, R. Gut and G. Anderegg, *Helv. Chim. Acta*, 37 (1954) 937.
19 N. Nakasuka, unpublished data.

DIMERIZATION AND ASSOCIATION OF AN ORGANOPHOSPHORIC ACID IN VARIOUS ORGANIC SOLVENTS

F. KRAŠOVEC, M. OSTANEK AND C. KLOFUTAR
Institute "J. Stefan", Ljubljana (Yugoslavia)
(Received June 6th, 1966)

The influence of organic solvents on the extraction of metal ions with chelating reagents has been very extensively investigated. It is generally assumed that the organic solvent affects the value of the distribution constant of the extracting reagents K_d as well as the value of the distribution constant of the extracting chelate[1]. Organophosphoric acids, which are a very important group of extracting reagents, are in addition more or less dimerized in the organic solvents[2-7], sometimes even polymerized[6] and again the solvent affects the degree of dimerization. Moreover, it has been reported that polar organic solvents interact with organophosphoric acids forming water-insoluble complex compounds[6].

In the present work, the association of bis(*p*-chlorophenyl)phosphoric acid (HD-*p*Cl-PP, HA) with several organic diluents was investigated as well as its dimerization in the same solvents. The more detailed knowledge of its association and dimerization should throw more light on the processes occurring during the extraction of metal ions with solutions of phosphoric acid diesters in different organic solvents and should give further information concerning the influence of the solvents on the extraction efficiency.

EXPERIMENTAL

The method applied for the determination of the dimerization constant has been described previously[2,5]. A similar procedure was also applied for the determination of the association constants. In the latter case the distribution of the acid was measured as a function of the investigated solvent concentration in an inert diluent. The distribution of the HD-*p*Cl-PP between the organic and the water phase was measured radiometrically using with ^{32}P-labeled organophosphoric acid.

The radioactive HD-*p*Cl-PP was prepared by the procedure given by WELCHER[8] using $POCl_3$ labeled with ^{32}P. The latter was prepared[9] by the reaction between $H_3{}^{32}PO_4$ and PCl_5. The product had a constant melting point after several recrystallizations (132°).

The organic solvents used were of analytical grade. Chloroform was washed with water before use while ketones and ethers were successively washed with dilute solutions of sodium bicarbonate and perchloric acid and with water. Kerosene was treated with concentrated sulfuric acid and then washed with water. Other solvents were not further purified.

All distribution experiments were carried out at room temperature.

RESULTS

Determination of the association constants K_{B_1} and K_{B_2}

The association constants K_{B_1} and K_{B_2} are defined as the equilibrium constants of the reactions

$$\mathrm{HA\ (org) + B\ (org) \rightleftharpoons HAB\ (org)}$$

and

$$\mathrm{H_2A_2\ (org) + B\ (org) \rightleftharpoons H_2A_2B\ (org)}$$

Thus K_{B_1} and K_{B_2} are equal to

$$K_{B_1} = [\mathrm{HAB}]_{\mathrm{org}}[\mathrm{HA}]_{\mathrm{org}}^{-1}[\mathrm{B}]_{\mathrm{org}}^{-1} \qquad (1)$$

and

$$K_{B_2} = [\mathrm{H_2A_2B}]_{\mathrm{org}}[\mathrm{H_2A_2}]_{\mathrm{org}}^{-1}[\mathrm{B}]_{\mathrm{org}}^{-1} \qquad (2)$$

The association between HD-*p*Cl-PP and various organic solvents was measured by

TABLE I

DISTRIBUTION OF $3.5 \cdot 10^{-4}$ *M* HD-*p*Cl-PP BETWEEN CARBON TETRACHLORIDE AND 0.1 *M* $\mathrm{HClO_4}$ AS A FUNCTION OF AN ORGANIC BASE CONCENTRATION C_B IN THE ORGANIC PHASE
(Data are given as log D and log C_B)

Octyl alcohol: log D (log C_B): 2.14 (−0.09), 1.96 (−0.22), 1.70 (−0.40), 1.55 (−0.53), 1.31 (−0.70), 1.19 (−0.82), 0.68 (−1.09), 0.50 (−1.22), 0.30 (−1.40), −0.15 (−1.60), −0.05 (−1.70), −0.45 (−1.82), −0.60 (−2.00), −0.17 (−2.00).

Hexol (methyl isobutyl carbinol): 1.97 (−0.09), 1.89 (−0.22), 1.65 (−0.40), 1.43 (−0.53), 1.11 (−0.70), 0.63 (−1.00), 0.46 (−1.09), 0.27 (−1.22), 0.06 (−1.40), −0.08 (−1.53), −0.23 (−1.70), −0.44 (−2.00).

Cyclohexanol: 1.87 (0.00), 1.89 (−0.20), 1.68 (−0.34), 1.42 (−0.57), 1.13 (−0.74), 0.65 (−1.00), 0.33 (−1.20), 0.14 (−1.34), −0.09 (−1.57), −0.25 (−1.74), −0.43 (−2.04).

Benzyl alcohol: 1.47 (−0.09), 1.37 (−0.22), 1.08 (−0.40), 0.87 (−0.53), 0.56 (−0.70), 0.08 (−1.00), 0.04 (−1.09), −0.25 (−1.22), −0.32 (−1.40), −0.45 (−1.53), −0.60 (−1.70), −0.70 (−2.00).

Cyclohexanone: 0.56 (−0.01), 0.48 (−0.10), 0.11 (−0.40), −0.21 (−0.70), −0.42 (−1.00), −0.53 (−1.22), −0.62 (−1.52), −0.69 (−1.70).

Hexone (methyl isobutyl ketone): 1.10 (0.60), 0.69 (0.38), 0.37 (0.20), 0.20 (0.00), −0.15 (−0.34), −0.42 (−0.64), −0.60 (−1.00), −0.70 (−1.20), −0.82 (−1.57), −0.79 (−2.04).

Isopropyl ether: 0.70 (0.51), 0.46 (0.29), 0.30 (0.11), 0.28 (0.00), −0.05 (−0.34), −0.26 (−0.64), −0.49 (−1.00), −0.55 (−1.20), −0.70 (−1.64), −0.78 (−2.04).

Dibutyl ether: −0.04 (−0.10), −0.17 (−0.22), −0.20 (−0.40), −0.30 (−0.52), −0.36 (−0.70), −0.52 (−1.00), −0.54 (−1.10), −0.60 (−1.22), 0.64 (−1.40), −0.72 (−1.52), −0.79 (−1.70), −0.76 (−2.00), +0.21 (+0.25), +0.06 (+0.07).

Butyl acetate: 0.08 (0.00), −0.15 (−0.20), −0.28 (−0.34), −0.48 (−0.57), −0.60 (−0.74), −0.74 (−1.00), −0.79 (−1.20), −0.86 (−1.34), −0.92 (−1.57), −0.94 (−1.74), −0.95 (−2.04).

Chloroform: −0.28 (0.80), −0.40 (0.53), −0.48 (0.40), −0.60 (0.20), −0.72 (−0.10), −0.75 (−0.22), −0.75 (−0.40).

determining the net distribution ratio D of the investigated organophosphoric acid as a function of the concentration of an organic base C_B (acceptor for HA through hydrogen bonding) in an inert diluent. Carbon tetrachloride was used as the inert solvent while the water phase was 0.1 M perchloric acid. The total acid concentration in the system, C_A, was kept as low as possible and amounted to $3.5 \cdot 10^{-4}$ M. Thus, $C_B \approx [B]_{org}$, the free concentration of B, if no self-association of B occurs which may be the case with alcohols.

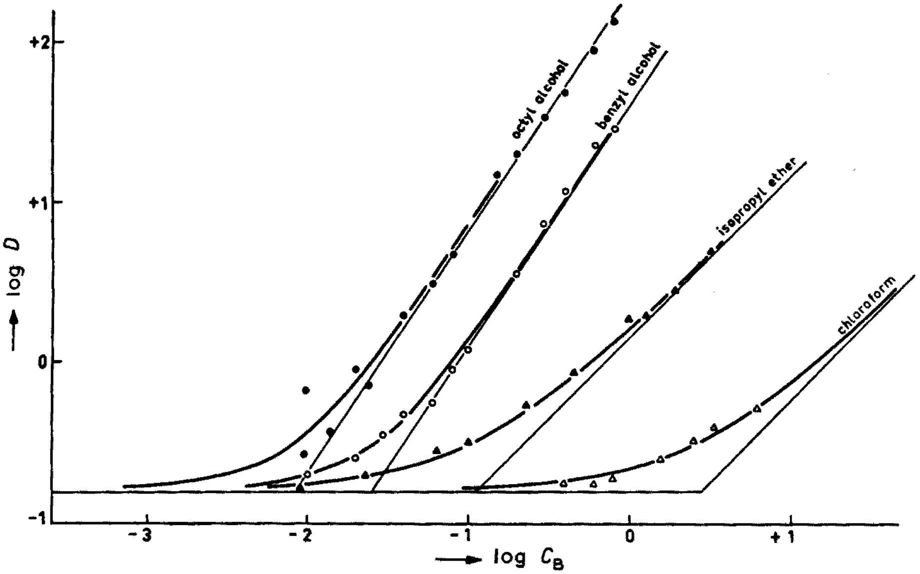

Fig. 1. Distribution of HD-pCl-PP between carbon tetrachloride and 0.1 M $HClO_4$ as a function of an organic base concentration C_B in the organic phase. The normalized curves $Y = \log(1+v^{1.5})$ and $Y = \log(1+v)$, $X = \log v$, are fitted to the data.

The experimental data are given in Table I as log D and log C_B. In Fig. 1 some of the data are also plotted graphically. It is interesting to note that the graphs do not have the same shape. In the case of alcohols the experimental points fit the normalized curve $Y = \log(1+v^{1.5})$, $X = \log v$, fairly well while it seems that with ethers, ketones, butyl acetate and chloroform the points fit much better the normalized curve $Y = \log(1+v)$, $X = \log v$. In the latter case the whole curve cannot be constructed from the experimental points and therefore an extrapolation must be made. This is due to the fact that the base concentration in the system can be varied only in a definite concentration range which is limited by the molarity of the undiluted base and by the concentration of the HD-pCl-PP in the system. The applied method thus requires that C_B be much higher than C_A. It was not possible to use a lower concentration of HA than $3.5 \cdot 10^{-4}$ M due to the specific activity of the HA that was available.

The curves in Fig. 1 may be divided into 3 parts. The first one is that with a constant log D corresponding to the horizontal asymptote to the curve. Log D of this part should be identical with log D for $3.5 \cdot 10^{-4}$ M HD-pCl-PP in pure carbon tetrachloride although a slightly higher value was obtained as may be seen from comparing

Figs. 1 and 2. In this part only monomeric and dimeric HA molecules exist in the organic phase and there is no evidence for a large amount of HAB or H_2A_2B. At high C_B in the organic phase the experimental points fit the straight lines which are identical with the second asymptote to the normalized curve. The slope of these lines was 1.5 for alcohols and 1.0 for the other solvents investigated. This suggests that in the former case a $HAB_{1.5}$ complex is formed while with ethers, ketones, butylacetate and chloroform a 1:1 complex is produced, *i.e.* HAB. In the part of the curves between both asymptotes all reagent species in the organic phase exist, *i.e.* HA, H_2A_2 and HAB or $HAB_{1.5}$ respectively. Thus, in any case the existence of H_2A_2B complex was observed, which may be due to a high C_B/C_A ratio. Consequently, only K_{B_1} could be calculated from these experiments.

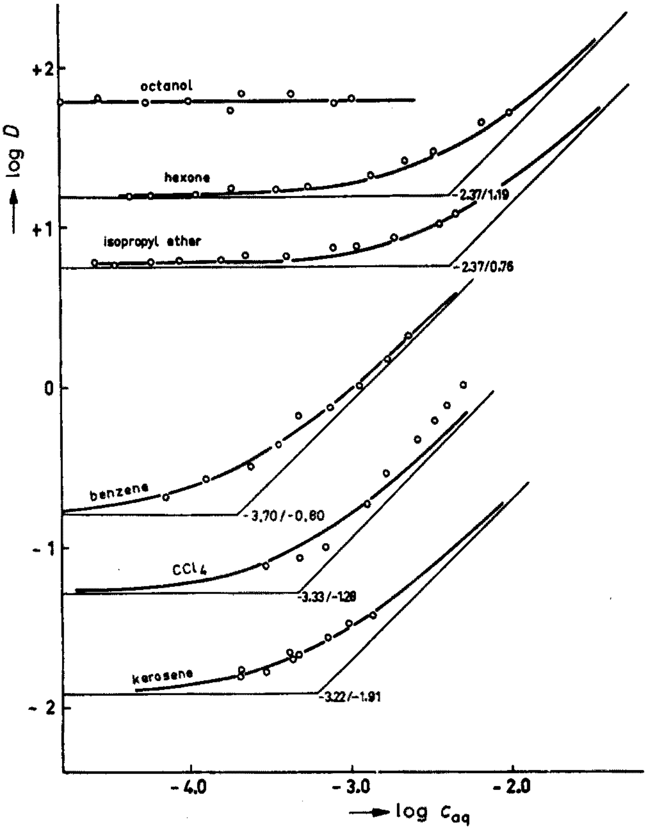

Fig. 2. Distribution of HD-*p*Cl-PP between various organic solvents and 0.1 *M* $HClO_4$ as a function of the HD-*p*Cl-PP concentration in the aqueous phase. The normalized curve Y = log (1+v), X = log v, is fitted to the data.

For the determination of the association constant K_{B_1} only the straight part of the curves, in which HAB is the only acid species in the organic phase, is useful. In this case the net distribution ratio *D* which was experimentally determined can be written as

$$D = C_{org}/C_{aq} = [HAB]_{org}([HA] + [A^-])^{-1} \qquad (3)$$

On the other hand, the equation of the straight part of the curves in Fig. 1 is equal to

$$D = 10^{a} \cdot [\mathrm{B}]_{\mathrm{org}} \tag{4a}$$

or

$$D = 10^{a} \cdot [\mathrm{B}]_{\mathrm{org}}^{1.5} \quad \text{for alcohols} \tag{4b}$$

where a is the value of log D at $C_B = 1$ M.

From eqns. (3) and (4a) and the definitions for the association constant K_{B_1} and for the distribution constant $K_d = [\mathrm{HA}]_{\mathrm{org}}[\mathrm{HA}]^{-1}$, the following equation may be derived when $C_B \approx [\mathrm{B}]_{\mathrm{org}}$

$$K_{B_1} = 10^{a} \cdot \varphi \cdot K_d^{-1} \tag{5}$$

where φ is a constant and defined as $\varphi = 1 + K_a[\mathrm{H}^+]^{-1}$. As shown previously[5], the acid dissociation constant K_a for HD-pCl-PP is equal to 0.63, which for an aqueous phase containing 0.1 M perchloric acid gives $\varphi = 7.3$. K_d for carbon tetrachloride is 0.383 (see Table III). Inserting these values in eqn. (5) K_{B_1} can easily be calculated. The K_{B_1} values obtained by this method are given in Table III. For comparison, eqn. (4b) was also used to obtain K_{B_1} values for alcohols, even though the alcohols are somewhat polymerized at 1 M in carbon tetrachloride[10]. The K_{B_1} values for alcohols are therefore given in parentheses.

Determination of the dimerization constant K_2

The dimerization constant K_2 which is defined as the equilibrium constant of the reaction

$$\mathrm{HA\ (org)} + \mathrm{HA\ (org)} \rightleftharpoons \mathrm{H_2A_2\ (org)}$$

was determined by measuring the distribution of HA between both phases as a function of the initial concentration of the acid, C_A, in the system. The aqueous phase was always kept constant and contained 0.1 M perchloric acid. Dimerization in the following solvents was studied: benzene, carbon tetrachloride, kerosene, isopropyl ether, methyl isobutyl ketone (hexone) and octyl alcohol. Experimental data are

TABLE II

DISTRIBUTION OF HD-pCl-PP BETWEEN VARIOUS ORGANIC SOLVENTS AND 0.1 M $HClO_4$ AS A FUNCTION OF THE INITIAL HD-pCl-PP CONCENTRATION IN THE ORGANIC PHASE
(Data are given as log D and log C_{aq}, where $C_{aq} = C_A (D+1)^{-1}$)

Octyl alcohol: log D (log C_{aq}): 1.81 (−2.97), 1.78 (−3.08), 1.83 (−3.35), 1.84 (−3.66), 1.73 (−3.73), 1.79 (−3.99), 1.78 (−4.26), 1.79 (−4.79), 1.81 (−4.56).

Hexone (methyl isobutyl ketone): 1.69 (−2.01), 1.64 (−2.17), 1.46 (−2.47), 1.41 (−2.64), 1.32 (−2.86), 1.25 (−3.25), 1.23 (−3.45), 1.24 (−3.73), 1.21 (−3.95), 1.20 (−4.22), 1.19 (−4.36).

Isopropyl ether: 1.07 (−2.33), 1.01 (−2.44), 0.94 (−2.72), 0.87 (−2.95), 0.87 (−3.09), 0.82 (−3.39), 0.82 (−3.64), 0.79 (−3.79), 0.79 (−4.05), 0.78 (−4.23), 0.77 (−4.45), 0.78 (−4.56).

Benzene: 0.32 (−2.63), 0.17 (−2.76), 0.01 (−2.94), −0.17 (−3.31), −0.13 (−3.12), −0.36 (−3.44), −0.49 (−3.62), −0.56 (−3.90), −0.67 (−4.15).

Carbon tetrachloride: 0.01 (−2.28), −0.12 (−2.39), −0.21 (−2.46), −0.33 (−2.58), −0.54 (−2.77), −0.73 (−2.89), −1.01 (−3.14), −1.07 (−3.31), −1.12 (−3.53).

Kerosene: −1.42 (−2.86), −1.48 (−3.01), −1.56 (−3.16), −1.67 (−3.33), −1.64 (−3.39), −1.78 (−3.53), −1.79 (−3.68), −1.76 (−3.68), −1.68 (−3.36).

given in Table II as logarithms of the net distribution ratio log D and logarithms of the equilibrium HA concentration in the aqueous phase. The volumes of both phases were equal and consequently $C_A = C_{org} + C_{aq}$.

Figure 2 shows the plots log D against log C_{aq}, where C_{aq} was calculated as $C_A(D + 1)^{-1}$. From these plots the values of K_2 and K_d were calculated as before[2,5-7]. The values K_2 and K_d are given in Table III.

According to DYRSSEN AND LIEM[11], the difference in K_2 and K_d for HA in various organic solvents can be explained by assuming that HA and H_2A_2 form HAB and H_2A_2B complexes with the organic diluents exhibiting basic properties. They assumed that for an inert solvent like *n*-hexane there is no complex formation with HA and H_2A_2 and that for *n*-hexane $K_d = K_d^*$ and $K_2 = K_2^*$, where K_d^* and K_2^* are the distribution and dimerization constants for free HA and H_2A_2 species respectively. They found that

$$K_d = K_d^*(1 + K_{B_1} \cdot [B]_{org}) \qquad (6)$$

and

$$K_2 K_d^2 = K_2^* K_d^{*2}(1 + K_{B_2} \cdot [B]_{org}) \qquad (7)$$

Using eqns. (6) and (7) the values K_{B_1} and K_{B_2} can be calculated from the K_d and K_2 values obtained above. In our calculations, it was assumed that for kerosene there is no complex formation with HA and H_2A_2. The K_{B_1} and K_{B_2} values obtained by this treatment are also given in Table III.

TABLE III

DISTRIBUTION CONSTANT K_d, DIMERIZATION CONSTANT K_2 AND ASSOCIATION CONSTANTS K_{B_1} AND K_{B_2} OF HD-*p*Cl-PP IN VARIOUS ORGANIC SOLVENTS CALCULATED FROM DISTRIBUTION MEASUREMENTS
(The aqueous phase was always 0.1 M $HClO_4$)

	K_d	K_2	K_{B_1}		K_{B_2}
			From eqn. (5)	*From eqn. (6)*	*From eqn. (7)*
Kerosene	0.089	64500	—	0.00	0.00
Carbon tetrachloride	0.383	20400	0.00	0.31	0.46
Benzene	1.15	15800	—	1.06	3.52
Chloroform[a]	3.8	2750	1.38	3.31	6.11
Butyl acetate	—	—	18.20	—	—
Dibutyl ether	—	—	17.40	—	—
Isopropyl ether	42.60	20.40	30.20	65.77	9.57
Methyl isobutyl ketone	112	7.60	28.80	157	23.13
Cyclohexanone	—	—	57.54	—	—
Benzyl alcohol	—	—	(725)	—	—
Cyclohexanol	—	—	(2880)	—	—
Methyl isobutyl carbinol	—	—	(2880)	—	—
n-Octyl alcohol	435	Very low	(4000)	774	—

[a] Values taken from ref. 5.

DISCUSSION

The results of the dimerization constant determinations for HD-*p*Cl-PP in various organic solvents are quite consistent with those obtained for dibutylphosphoric acid by HARDY AND SCARGILL[4] and for diethyl- and dibutylphosphoric acid by Dyrssen and Liem[6,7]. In inert organic solvents like kerosene and carbon tetrachloride dimerization is very high and it decreases with increasing polarity of the solvent. In polar solvents like alcohols, ketones and ethers, these is a strong interaction between HD-*p*Cl-PP and the solvent molecules. In these solvents the oxygen atom acts as an acceptor in hydrogen bonding and consequently exhibits the property of a base. The basicity of the investigated organic solvents differs considerably and from this aspect they can be divided into several groups. The alcohols with the highest association constants are the most basic group; among them octyl alcohol is the strongest, cyclohexanol and hexol are weaker and benzyl alcohol is the weakest. The alkyl group releases electrons while the phenyl group withdraws electrons, hence the basicity of the aliphatic alcohols is higher. Thus the values of the association constants may be taken as a relative measure for the basicity of the investigated organic solvents.

It is surprising that the plots log D against log C_B in Fig. 1 for different alcohols do not fit a straight line with a slope equal to 1 but with a slope 1.5. This would suggest that 1:1.5 complexes are formed between alcohols and HD-*p*Cl-PP. However, the odd function for alcohols may be due to the fact that alcohols show extensive self-association in carbon tetrachloride[10]. Consequently, the concentration of the monomeric alcohol molecules is much lower than the total alcohol concentration and therefore it is questionable if the above method ought to be used for the determination of the association constant for the alcohols.

The second group of the investigated solvents contains ethers, esters and ketones with association constants K_{B_1} ranging between 10 and 50. With these solvents the complex HAB has been observed. From the results it may be concluded that ketones are more basic than ethers and esters.

In the third group are solvents with very low association constant. Here only chloroform was investigated. It can be assumed that only very weak interaction between chloroform and HD-*p*Cl-PP molecules exists which can be due to hydrogen bonding, chloroform acting as proton donor. However the values of the association constants K_{B_1} and K_{B_2} calculated by means of eqns. (6) and (7) show that a weak interaction between HA and the solvents like carbon tetrachloride and benzene also exists. In this study, carbon tetrachloride was assumed to be a completely inert solvent. This is probably the reason for significant differences between the experimental and calculated K_{B_1} values. However, the order of increasing interaction is in both cases identical and consistent with that obtained by Dyrssen and Liem[11], *i.e.* kerosene $<$ CCl_4 $<$ benzene $<$ $CHCl_3$ $<$ ethers $<$ ketones $<$ alcohols.

It should be noted that under the conditions given above, in no case was the presence of the H_2A_2B observed. The existence of complexes like H_2A_2B and HAB_2 has recently been discussed by Dyrssen and Liem[11].

The authors wish to thank Professor D. Dyrssen for valuable suggestions and helpful discussion.

SUMMARY

The association of bis(*p*-chlorophenyl)phosphoric acid with various organic solvents as well as its dimerization in these solvents was investigated. In inert solvents like kerosene, carbon tetrachloride and benzene, dimerization is very high and decreases with increasing polarity of the solvent. In polar solvents like alcohols and ketones, a strong association between HA and solvent molecules exists. The association constants were determined; the values may be regarded as a measure for the basicity of the solvents in question. The following order of the increasing basicity of the solvents was established: hydrocarbons and chlorinated hydrocarbons < ethers < ketones < alcohols.

RÉSUMÉ

On a examiné l'association de l'acide bis(*p*-chlorophényl) phosphorique avec divers solvants organiques, de même que la dimérisation de ces solvants. Dans les solvants inertes, tels que kérosène, tétrachlorure de carbone et benzène, la dimérisation est très élevée et diminue avec l'augmentation de polarité du solvant. Dans des solvants polaires comme alcools et cétones, il existe une forte association entre HA et molécules de solvants. Les constantes d'association sont déterminées; leurs valeurs peuvent être considérées comme une mesure de basicité des solvants en question. On a établi l'ordre suivant de basicité croissante: hydrocarbures, hydrocarbures chlorés < éthers < cétones < alcools.

ZUSAMMENFASSUNG

Die Assoziation von Bis(*p*-chlorophenyl)phosphorsäure mit verschiedenen organischen Lösungsmitteln und seine Dimerisation in diesen Lösungsmitteln wurde untersucht. In inerten Lösungsmitteln wie Kerosin, Tetrachlorkohlenstoff und Benzol ist die Dimerisation sehr hoch und verringert sich mit wachsender Polarität des Lösungsmittels. In polaren Lösungsmitteln wie Alkohole und Ketone besteht eine starke Assoziation zwischen HA und den Lösungsmittelmolekülen. Die Assoziationskonstanten wurden bestimmt; ihre Werte können als ein Mass für die Basizität des betreffenden Lösungsmittels angesehen werden. Es wurde die folgende Reihenfolge für die ansteigende Basizität der Lösungsmittel gefunden: Kohlenwasserstoffe und chlorierte Kohlenwasserstoffe < Äther < Ketone < Alkohole.

REFERENCES

1 D. Dyrssen, *Svensk Kem. Tidskr.*, 68 (1956) 212.
2 D. Dyrssen, *Acta Chem. Scand.*, 11 (1957) 1771.
3 Ph. Dreze, *Bull. Soc. Chim. Belges*, 68 (1959) 674.
4 C. J. Hardy and D. J. Scargill, *J. Inorg. & Nucl. Chem.*, 11 (1959) 128.
5 F. Krasovec and J. Jan, *Croat. Chem. Acta*, 35 (1963) 183.
6 D. Dyrssen and D. H. Liem, *Acta Chem. Scand.*, 14 (1960) 1091.
7 D. Dyrssen, S. Ekberg and H. D. Liem, *Acta Chem. Scand.*, 18 (1964) 135.
8 F. J. Welcher, *Organic Analytical Reagents*, Vol. 4, D. Van Nostrand Co., New York, 1953, p. 315.
9 J. L. Kalinsky and A. Weinstein, *J. Am. Chem. Soc.*, 76 (1954) 5882.
10 W. C. Coburn, Jr. and E. Grunwald, *J. Am. Chem. Soc.*, 80 (1958) 1318.
11 D. Dyrssen and D. H. Liem, *Acta Chem. Scand.*, 18 (1964) 224.

AN ION-EXCHANGE SCHEME FOR THE DETERMINATION OF THE MAJOR CATIONS IN SEA WATER

R. GREENHALGH, J.P. RILEY AND M. TONGUDAI
Department of Oceanography, The University, Liverpool 3 (Great Britain)
(Received May 30th, 1966)

The theory that the relative ionic composition of sea water is constant, first propounded in 1819 by MARCET[1], appears to have become generally accepted, at least so far as the major components are concerned. However, CARPENTER AND CARRITT[2] have pointed out that there is some evidence that variations do occur which cannot be accounted for by analytical errors. Thus, DITTMAR[3] during his classical work on the samples collected during the Challenger Expedition (1873–1876) found variations in the concentration ratios of certain of the major ions to chloride which were greater than the experimental error. An appreciable variation was found for calcium, about which DITTMAR wrote: "It really appears as if the deep waters did contain more lime than the shallow, on account of their coming from greater depth". Although many subsequent workers have studied the ratios of individual constituents to chlorinity, variations produced by differences in analytical procedures make the intercorrelation of the results difficult and tend to obscure significant effects. Since the publication of the paper by CARPENTER AND CARRITT[2] interest in the problem of the constancy of the relative ionic composition of sea water has revived, particularly with respect to its bearing on the relationships between the chlorinity, electrical conductivity and density of sea water.

Since the time of DITTMAR few complete analyses of sea water for its major component ions have been published and workers have generally concentrated on the determination of individual ions. CULKIN[4] has reviewed the literature on the determination of the major cations in sea water. In most of these procedures the cations were determined gravimetrically, frequently after separations carried out by repeated precipitation. Such processes are often highly inaccurate owing to coprecipitation of other ions and to mechanical and solubility losses.

Ion-exchange separations are inherently free from these defects but seem to have been applied to sea water only for the determination of calcium and magnesium[5]. The present paper gives an account of the use of ion exchange for the separation of the individual major cations in sea water prior to their determination.

COX AND CULKIN[6] have recently described a system for the determination of the major cations in sea water. Potassium is determined gravimetrically as its tetraphenylboron derivative; calcium is determined titrimetrically with 1,2-bis-2-di-(carboxymethyl)-aminoethoxy-ethane (EGTA); strontium is determined by flame spectrophotometry. Titration with EDTA gives the total equivalents of magnesium + calcium + strontium, from which magnesium can be estimated by difference. Total cations are determined by passing the sample through a cation-exchange column in its hydrogen form and determining hydrogen ion thus liberated. Sodium is determined by difference from the total cations after making allowance for the other major cations. The same workers have used this analytical scheme in a world-wide survey of the composition of sea water[6].

Development of ion-exchange separation scheme

Amberlite CG 120, a sulphonated resin based on styrene crosslinked with 8% of divinylbenzene, was used in the development of the method. It was found that a column of this resin 18.5 cm in length and 7 mm in diameter would retain the cations from 30 ml of sea water of chlorinity 19.5‰ and allow sufficient excess exchange capacity for bringing about the separation of the cations during elution. Preliminary attempts at the elution of the adsorbed cations from this volume of sea water showed that sharper elution curves were obtained by using ammonium chloride solution than by use of the same molarity of hydrochloric acid. Sodium together with potassium could be completely eluted by means of 200 ml of 0.15 *M* ammonium chloride solution; at least a further 50 ml of this reagent had to be passed through the column before any traces of magnesium began to appear. Sodium was eluted slightly more readily than potassium (see Fig. 1), but to achieve a separation of these 2 elements it would be necessary to use a much longer column than would have been feasible in the present work.

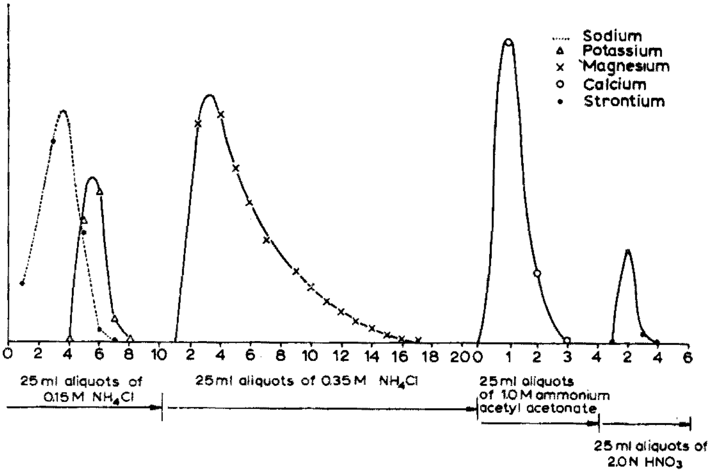

Fig. 1. Curves for successive elution of sodium, potassium, calcium and magnesium from an Amberlite CG 120 column (18 cm × 0.7 cm).

When the elution was continued with 0.15 *M* ammonium chloride, magnesium was the next element to be eluted. However, a very large volume of this strength of eluant was required to remove magnesium completely. It was found that magnesium could be eluted completely, without contamination from calcium, by means of 450 ml of 0.35 *M* ammonium chloride solution. This eluant has the advantage that magnesium can be titrated in it directly using EDTA, unlike the ammonium acetylacetonate reagent, used for the same purpose by CARPENTER[5], which must be destroyed since it interferes in the titration. Attempts were made to elute calcium with 0.35–1.0 *M* ammonium chloride solution; even after 250 ml of the 1.0 *M* eluant had been passed through the column, the elution was not complete and strontium had begun to appear. Similar results were obtained when 0.25 *M* and 0.5 *M* ammonium formate buffer (at pH 4) were used for the elution; with 1.0 *M* ammonium formate buffer, strontium was eluted with the bulk of the calcium. Calcium forms a much more stable complex with acetylacetone than does strontium and CARPENTER[5] has used a 1 *M* solution of ammonium acetylacetonate (pH 9.6) for the elution of calcium in a method for its determination in sea water. It was found that calcium could be eluted completely from the Amberlite CG 120 column by means of 80 ml of CARPENTER's reagent without eluting any detectable amount of strontium. After calcium had been eluted in this way, strontium could be removed completely from the column by the use of 100 ml of 2 *M* nitric acid.

Determination of the separated elements

After the elements have been separated by ion-exchange they can be determined accurately without risk of inter-element interferences.

Determination of sodium and potassium

No direct methods are available for the determination of sodium which have sufficient precision to reveal the existence of small variations in the Na/Cl ratio in sea water. It was therefore decided to determine sodium and potassium together gravimetrically as their sulphates, to determine potassium in the mixed sulphates and to determine sodium by difference. It was found that evaporation of the 0.15 *M* ammonium chloride eluate to dryness after acidification with 0.6 ml of concentrated sulphuric acid, followed by gradual heating to 800° and ignition at this temperature for at least an hour, yielded a neutral residue of the pure alkali sulphates. Since this residue was slightly hygroscopic, precautions such as cooling *in vacuo*, were necessary to avoid uptake of water before weighing. If these precautions were taken, the total alkali sulphates could be determined with a coefficient of variation of 0.02%; the results were *ca.* 0.02% lower than the theoretical values (see Table I).

In contrast to sodium, potassium can be determined gravimetrically in a number of forms. However, many of these are not suitable for accurate work, owing for example either to their non-stoichiometric composition or to their relatively high solubilities. Methods in which potassium is precipitated with sodium tetraphenylboron, are free from these difficulties and have been used by SPOREK[7] and by COX AND CULKIN[6] for the direct determination of potassium in sea water. The application of this procedure to the determination of potassium in the mixed alkali sulphates was therefore investigated. It was observed, in agreement with the findings of COX AND CULKIN[6] that the acidity (0.2 *M*) used by SPOREK[7] for the precipitation was too high. Results in better agreement with theory (see Table I) were obtained by carrying out the precipitation at 0° from 40 ml of solution, at an acidity of 0.055 *M*, using 20 ml of 1.13 % sodium tetraphenylboron solution. Attempts were also made to complete the determination by potentiometric titration of either the excess of reagent or the redissolved potassium precipitate with silver nitrate, but the results were very much inferior in both precision and accuracy to those found gravimetrically.

TABLE I

ANALYSIS OF ARTIFICIAL SEA WATER

(Expressed as weights in g/30 ml of artificial sea water)

	Mixed alkali sulphates	*Potassium*	*Sodium*	*Magnesium*	*Calcium*	*Strontium* $\cdot 10^4$
Theoretical	1.05450	0.011836[a]	0.33281	0.044176	0.012645	3.00
Found	1.05427	0.011810	0.33276	0.044167	0.012656	—
	1.05444	0.011858	0.33278	0.044176	0.012622	—
	1.05422	0.011867	0.33270	0.044154	0.012642	2.99
	1.05455	0.011841	0.33283	0.044167	0.012640	2.98
	1.05444	0.011799	0.33282	0.044167	0.012658	2.99
	1.05391	0.011816	0.33264	0.044154	0.012631	2.98
Average	1.05431	0.011832	0.33275	0.044164	0.012649	2.98
Coefficient of variation (%)	0.02	0.22	0.02	0.04	0.08	0.8
Average difference from theoretical	0.00019	0.000004	0.00006	0.000012	0.000004	0.2
% difference from theoretical	0.02	0.004	0.02	0.03	0.03	0.7

[a] Corrected for potassium present in sodium chloride.

Determination of calcium and magnesium

In most of the earlier work on the determination of calcium and magnesium in sea water[4] calcium was determined gravimetrically after precipitation of its oxalate; magnesium was subsequently precipitated from the filtrate as its ammonium phosphate and weighed as the pyrophosphate. Coprecipitation causes considerable interference in both determinations and it is necessary to carry out multiple precipitations in order to purify the precipitates. A further source of uncertainty in the determination is the incompleteness of coprecipitation of strontium with the calcium oxalate. The advent of compleximetric methods for the titrations of calcium and magnesium has revolutionized the determination of these elements in sea water. In the first applications of the method[8-10] calcium was determined by titration with EDTA after precipitation of magnesium as hydroxide at pH 12. Calcium and magnesium were determined together by titration with EDTA at pH 10 and magnesium was estimated by difference. However, the precipitate of magnesium hydroxide carries down *ca.* 1% of the calcium present in the sample and the results for calcium therefore tend to be low. Cox and Culkin[6] have surmounted this difficulty by determining calcium using EGTA which forms a strong complex with calcium and a much weaker complex with magnesium. Since in the present work, as in the method of Carpenter[5], calcium and magnesium are separated from one another, both elements can be determined directly by EDTA titration.

Experiments were carried out to find the optimum conditions for the titration of the eluate with EDTA. It proved satisfactory to titrate the magnesium directly in the 0.35 *M* ammonium chloride eluate after bringing to pH 10.0 with ammonia solution. Eriochrome black T proved the best of a number of indicators tested for this purpose. With this indicator, photometric titration with EDTA (added from a Knudsen burette) gave a coefficient of variation of 0.03% in the determination of magnesium. Preliminary tests showed that calcium could be titrated photometrically with EDTA with a coefficient of variation of 0.06% at pH 10 using eriochrome black T as indicator provided that some magnesium was present in the solution. However, it was not possible to determine calcium directly in the ammonium acetylacetonate eluate by EDTA titration owing to interference by the eluting agent. Although CARPENTER[5] claimed that they were able to destroy the latter by boiling, it was found that the solution remaining after boiling was brownish in colour and did not give a sharp end-point when titrated with EDTA. Experiments showed that the acetylacetone could be destroyed by digestion with nitric acid; since nitrate ion oxidizes the EBT indicator it was found to be essential to remove all traces of it by evaporation to dryness several times with hydrochloric acid.

Determination of strontium

Flame photometric techniques offer a relatively simple way of determining strontium at low concentration. They have been used both by CHOW AND THOMPSON[11] and by COX AND CULKIN[6] for the direct determination of strontium in sea water. Owing to the enhancing and depressing effects of other ions on the emission of strontium it was necessary to calibrate the method by measuring the emission of sea water alone, and after addition of known increments of strontium. The problem in the present method is considerably simpler since strontium is separated from the other cations in the water. It is however present in the 2 *M* nitric acid eluate at a rather low concentration in the presence of somewhat variable amounts of ammonium nitrate. When the eluate was evaporated to dryness a residue remained containing considerable amounts of organic matter (arising perhaps from decomposition of the ion-exchange resin) which interfered with the flame photometric determination of strontium. If this residue was heated at 800° in order to burn off the organic matter, the strontium became insoluble in dilute acid, owing perhaps to reaction with traces of silica. It could, however, be brought into solution by evaporating to dryness with a mixture of hydrofluoric and perchloric acids. Flame photometry was carried out with a coal gas–air burner using a solution in 0.5 *N* hydrochloric acid enriched with 10% of acetone to enhance the strontium emission. The calibration of the flame photometer was carried out using solutions of known amounts of strontium in the same medium and yielded a linear calibration between strontium concentration and photometer reading. The photometric method showed a coefficient of variation of 0.8% at a strontium concentration of *ca.* 30 μg/ml.

EXPERIMENTAL

Apparatus

An EEL Quantitrator fitted with an Ilford No. 607 filter (orange-red) was used in the titration of calcium and magnesium.

An EEL flame photometer fitted with interference filter having its maximum transmission at 670 nm was used for the determination of strontium.

Eluting agents

Ammonium acetylacetonate solution, 1 M. Mix 45 ml of freshly distilled acetylacetone, 218 ml of 2 *M* ammonia solution and 195 ml of water. This reagent, which has a pH value of 9.6, should be prepared immediately before use since it is very unstable.

Other reagents used were 0.15 and 0.35 *M* ammonium chloride and 2 *M* nitric acid.

Ion exchanger

Purify Amberlite CG 120 (100–200 mesh) by heating on a water bath with 3 *M* hydrochloric acid. After 1 h decant the acid and pour the resin into an ion-exchange column (internal diameter 7 mm). Wash the resin with 3 *M* hydrochloric acid until all traces of sodium have been removed and then with distilled water until free from acid. Adjust the length of the resin column to 18.5 cm.

Reagents for the determination of potassium

Sodium tetraphenylboron reagent. Dissolve 1.7 g of sodium tetraphenylboron in 150 ml of water and stir in 0.5 g of aluminium hydroxide gel. Filter the solution, which has a pH of *ca.* 5 through a Whatman No. 42 paper. The reagent is stable for about 1 week.

Wash solution. Saturate 250 ml of water by shaking with *ca.* 25 mg of potassium tetraphenylboron. After 30 min add 1 g of aluminium hydroxide gel and shake for a further 1–2 min. Filter the solution through a Whatman No. 42 paper.

Reagents for the determination of calcium and magnesium

Buffer. Dissolve 70 g of ammonium chloride in 600 ml of ammonia solution (s.g. 0.880) and dilute to 1 l with water.

EDTA solution. Dissolve 2.6 g of the disodium salt of ethylenediamine tetraacetic acid in *ca.* 750 ml of water, add 10 ml of standard magnesium solution (see below) and 2–3 drops of toluene and dilute to 1 l.

EBT indicator. Dissolve 0.1 g of EBT in *ca.* 20 ml of ethyl alcohol. Keep the solution in a dark glass bottle and discard after 2 days.

Standard magnesium solution. Dissolve 0.300 g of spectrographic grade magnesium rod in dilute hydrochloric acid in a silica flask. When dissolution is complete, evaporate to dryness on the water bath to remove excess hydrochloric acid. Take up the residue in 25 ml of distilled water containing a few drops of 2 *M* hydrochloric acid and dilute to 1 l. This solution contains 300 mg/ml.

Standard calcium solution. Dissolve 0.49945 g of spectrographic grade calcium carbonate (dried at 250°) in a slight excess of dilute hydrochloric acid and dilute to 500 ml with water. This solution contains 400 μg Ca/ml.

Reagents for determination of strontium

Standard strontium solution. Dissolve 50.6 mg of spectrographic grade strontium carbonate (dried at 130°) in a mixture of 200 ml of water and 50 ml of concentrated hydrochloric acid, add 100 ml of acetone and dilute to 1 l. This solution contains 30 μg Sr/ml.

METHOD

Ion-exchange separation

Weigh out accurately about 30 ml of sea water in a covered conical flask. This is an appropriate volume for water with a chlorinity of *ca.* 19‰; with waters having chlorinities differing from this by more than *ca.* 2‰ the volume of sample taken should be increased or decreased proportionately. Transfer the weighed sample quantitatively to the top of the ion-exchange column, and allow it to flow through; the flow rate is *ca.* 20 ml/h. Rinse the upper chamber of the column with *ca.* 5 ml of water and allow the liquid to pass through. Elute sodium and potassium with 200 ml of 0.15 *M* ammonium chloride solution and combine the eluate with the percolate and washings from the column. Test the completeness of removal of these elements by passing a further 20 ml of this eluant through the column and examining the eluate for sodium and potassium by means of a flame photometer, and for magnesium colorimetrically with EBT at pH 10. It should contain less than 0.05 p.p.m. of these elements. If appreciable concentrations of sodium and potassium are present add this solution to the combined eluate (Solution A), which is retained for the determination of these elements (see below).

Elute magnesium from the column with 450 ml of 0.35 *M* ammonium chloride solution and collect the eluate in a 500-ml graduated flask. To ensure that magnesium has been completely eluted, pass a further 25 ml of 0.35 *M* ammonium chloride solution through the column, collect the eluate separately and test a small portion of it for magnesium using EBT at pH 10. In the unlikely event of its containing detectable amounts of magnesium, add the remainder to the graduated flask containing the main 0.35 *M* ammonium chloride eluate. Dilute to 500 ml and retain for the titrimetric determination of magnesium (Solution B).

Pass 100 ml of ammonium acetylacetonate reagent through the column in order to elute calcium. Collect the eluate in a 250-ml conical flask and use it for the determination of calcium (Solution C). Wash the column free from acetylacetone by passing 100 ml of water through it, and reject the washings. Elute strontium with 100 ml of 2 *M* nitric acid and collect the eluate in a 150-ml conical flask (Solution D).

Determination of sodium and potassium

Evaporate Solution A to dryness in a 250-ml beaker on the water bath. Transfer the residue quantitatively to a tared platinum crucible (dried at 120° and cooled *in vacuo*) using a jet of water. Add 0.5 ml of concentrated sulphuric acid and heat the crucible on the water bath. When most of the water has been removed, place the crucible under a Vitreosil infrared heater and heat the paste gently to prevent loss by spattering. When the residue is dry, lower the heater until it is *ca.* 10 cm above the crucible and continue heating until no more fumes are evolved. At this stage the residue is slightly brown because of charring of traces of organic matter. Stand the crucible in a large silica crucible, three-quarters cover it with its lid and place in a cold muffle furnace. Over a period of about 2 h raise the temperature to 500° and maintain at this temperature for 1 h to remove the bulk of the volatile material. Raise the temperature to 800° and heat at this temperature for a further hour. Allow the crucible to cool in the air for 2 min, transfer it to a vacuum desiccator containing no desiccant and evacuate to *ca.* 0.1 mm Hg. After not less than 1 h admit air to the desiccator *via* a magnesium perchlorate drying tube and weigh the covered crucible immediately.

Dissolve the mixed sulphates in water and transfer the solution quantitatively to a 100-ml beaker. Dilute the solution to *ca.* 40 ml with water and add 2.2 ml of 1 *M* sulphuric acid. Cool the covered beaker in a ice-salt mixture; when the temperature of the solution is *ca.* 0°, add 20 ml of sodium tetraphenylboron reagent gradually with stirring. Allow the beaker to stand in the ice-bath for 10 min and then filter the solution rapidly through a tared sintered glass filter crucible (porosity 4) using suction. Rinse the beaker with a few ml of water and add the washings to the filter. Wash the precipitate with 2 successive 5-ml aliquots of the saturated solution of potassium tetraphenylboron. Dry the filter crucible at 120° for at least 3 h and allow it to cool *in vacuo* for 1 h before weighing.

Calculate the weight of potassium present by multiplying the weight of potassium tetraphenylboron by 0.1091. Calculate the weight of sodium present in the sample from the weight of the combined sodium and potassium sulphates, after making allowance for the amount of potassium present.

Determination of magnesium

Pipette 80 ml of Solution B into a 300-ml titration beaker, add 1 ml of ammonia solution (s.g. 0.880) and 1 ml of aqueous 50% (v/v) triethanolamine solution and stir for 2 min, before adding 0.3 ml of EBT indicator solution. While stirring vigorously, add EDTA solution rapidly from a Knudsen burette until the pink colour begins to disappear. Continue the titration more slowly by adding 0.1-ml increments of EDTA and reading the galvanometer of the photoelectric titrimeter after each addition. Plot the burette readings against the galvanometer percent transmission readings; determine the end-point by extrapolation.

To standardize the EDTA solution treat 20 ml of the standard magnesium solution with 60 ml of distilled water, 2 ml of buffer solution, 1 ml of 50% (v/v) triethanolamine solution and 0.3 ml of EBT indicator, and titrate with EDTA as described above.

Determination of calcium

Evaporate the ammonium acetylacetonate eluate (Solution C) almost to dryness on a hotplate. Cool, and add 15 ml of concentrated nitric acid. Close the top of the flask with a bulb stopper and heat it on a cool hotplate in order to destroy organic matter. When the solution becomes almost colourless (2–3 h) remove and rinse the stopper and evaporate to small volume. After cooling, add concentrated hydrochloric acid and again evaporate to small volume. Repeat the evaporation with hydrochloric acid until no more oxides of nitrogen are evolved and finally evaporate almost to dryness on the water bath. Take up the residue in a few ml of 2 *N* hydrochloric acid, add 40 ml of water and quantitatively transfer the solution to a titration beaker, filtering if necessary through a 9-cm Whatman No. 41 paper. Add 1 ml of 50% (v/v) triethanolamine solution and sufficient of the ammonia–ammonium chloride buffer to bring the solution to *ca.* pH 10. Titrate the solution with EDTA as described above for magnesium. Standardize the EDTA solution by titrating 25 ml of the standard calcium solution after adding 1 ml of 50% (v/v) triethanolamine and 1 ml of buffer.

Determination of strontium

Evaporate the 2 *M* nitric acid eluate (Solution D) to dryness in a 30-ml platinum crucible under an infrared heater. When all the ammonium nitrate present has decomposed and only a dark brown residue remains, ignite the crucible at 850° in a muffle furnace for 1 h. Remove traces of silica from the residue by evaporating to dryness on the water bath with 1 ml of hydrofluoric acid and 2 ml of 60% (w/w) perchloric acid. Evaporate under an infrared lamp until all traces of perchloric acid are removed. Rinse the walls of the crucible with 1 ml of concentrated hydrochloric acid and evaporate to dryness. Dissolve the residue in 0.5 ml of concentrated hydrochloric acid and, using water, transfer the solution to a 10-ml graduated flask containing 1 ml of acetone. Dilute to volume with water. Determine strontium by means of its emission at 6710 or 4607 Å, using a flame photometer set to read 100% transmission with a standard solution of strontium (30 µg/ml) containing 5% (v/v) of concentrated hydrochloric acid and 10% (v/v) of acetone.

Reagent blanks

Although the reagent blank for each element is normally extremely small it is advisable to carry a blank run through the whole procedure whenever fresh batches of reagents are used.

RESULTS

In order to check the accuracy and precision of the method an artificial sea water of accurately known composition was analyzed. This water was prepared by dissolving 28.2022 g of A.R. sodium chloride and 0.74695 g of "specpure" potassium chloride (both previously ignited at 600° and cooled *in vacuo*) in *ca.* 500 ml of redistilled water in a N.P.L. certified 1-l graduated flask. To this solution were added solutions prepared by dissolving 1.3253 g of "specpure" magnesium, 1.0526 g of "specpure" calcium carbonate (dried at 120°) and 0.01687 g of "specpure" strontium carbonate (dried at 120°) in the minimum feasible quantity of hydrochloric acid, evaporating to dryness, and taking up in 0.01 *N* hydrochloric acid. After mixing, the pH of the solution was adjusted to *ca.* 8.0 by addition of ammonia solution; it was then diluted to 1 l with water. Aliquots (30 ml) of this artificial sea water were passed through ion-exchange columns and the cations were separated and determined as described in the experimental section.

In order to ascertain the amounts of impurities present in the chemicals used in the preparation of the artificial sea water, blank runs were carried out using solutions of the individual salts. These tests showed that the sodium chloride contained 0.010% of potassium and negligible amounts of calcium, magnesium and strontium. No traces of impurities were detected in the solutions of the other cations. The results of these experiments (Table I) indicate that both the precision and accuracy of the procedure are satisfactory.

As a further test of the method duplicate analyses were carried out on 6 different sea waters taken from widely different localities. These analyses gave coefficients of variation of 0.03%, 0.2%, 0.04%, 0.08%, and 1.0% for sodium, potassium, magnesium, calcium and strontium determinations respectively.

SUMMARY

A cation-exchange scheme is described for the determination of the principal cations in sea water. The cations are adsorbed onto a column of Amberlite CG 120. Sodium and potassium are eluted together using 0.15 *M* ammonium chloride and determined gravimetrically as sulphates; potassium is then determined gravimetrically as potassium tetraphenylboron and sodium is determined by difference. Magnesium and calcium are eluted by means of 0.35 *M* ammonium chloride and 1 *M* ammonium acetylacetonate (pH 9.6) respectively, and titrated with EDTA. Finally, strontium is eluted with 2 *M* nitric acid and determined by flame photometry. Tests made using an artificial sea water showed that the method had coefficients of variation of 0.02, 0.22, 0.04, 0.08 and 0.8% for sodium, potassium, magnesium, calcium and strontium respectively.

RÉSUMÉ

On décrit un procédé avec échangeur de cations pour le dosage des principaux cations dans l'eau de mer. On utilise une colonne d'Amberlite CG 120. Sodium et potassium sont élués simultanément au moyen de chlorure d'ammonium 0.15 *M* et dosés gravimétriquement comme sulfates. On dose ensuite le potassium gravimétriquement comme potassium tétraphénylbore et le sodium par différence. Magnésium et calcium sont élués au moyen de chlorure d'ammonium 0.35 *M* et acétylacétonate d'ammonium *M* (pH 9.6) respectivement et titrés avec EDTA. Enfin, le strontium est élué avec acide nitrique 2 *M* et dosé par photométrie de flamme.

ZUSAMMENFASSUNG

Für die Bestimmung der wichtigsten Kationen in Seewasser wird ein Kationenaustauscher-Schema beschrieben. Die Kationen werden auf einer Kolonne mit Amberlite CG 120 adsorbiert. Natrium und Kalium werden zusammen mit 0.15 *M* Ammoniumchlorid eluiert und gravimetrisch als Sulfat bestimmt. Kalium wird darauf gravimetrisch mit Tetraphenylborat bestimmt; Natrium ergibt sich aus der Differenz. Magnesium und Calcium werden mit 0.35 *M* Ammoniumchlorid bzw. 1 *M* Ammoniumacetylacetonat (pH 9.6) eluiert und mit AEDTE titriert. Zum Schluss wird Strontium mit 2 *M* Salpetersäure eluiert und flammenphotometrisch bestimmt. Versuche mit künstlichem Seewasser zeigten, dass die Methode einen Variationskoeffizienten von 0.02, 0.22, 0.04, 0.08 und 0.8% für Natrium, Kalium, Magnesium, Calcium bzw. Strontium besitzt.

REFERENCES

1 A. MARCET, *Phil. Trans. Roy. Soc. London*, 109 (1819) 161.
2 J. H. CARPENTER AND D. E. CARRITT, *Nat. Acad. Sci. Natl. Res. Council Publ.*, 600 (1958) 67.
3 W. DITTMAR, Report on the Scientific Results of the Exploring Voyage of H.M.S. Challenger, *Physics and Chemistry*, Vol. 1, H.M. Stationery Office, London.
4 F. CULKIN, The Major Constituents of Sea Water, in J. P. RILEY AND G. SKIRROW, *Chemical Oceanography*, Academic Press, London, 1965.
5 J. H. CARPENTER, *Limnol. Oceanog.*, 2 (1957) 271.
6 R. A. COX AND F. CULKIN, *Deep Sea Res.*, in press.
7 K. F. SPOREK, *Analyst*, 81 (1956) 540.
8 A. VOIPIO, *Suomen Kemistilehti*, B32 (1959) 61.
9 J. B. PATE AND R. J. ROBINSON, *J. Marine Res. (Sears Found. Marine Res.)*, 17 (1958) 390.
10 J. B. PRICE AND R. R. PRIDDY, *Bull. Marine Sci. Gulf Caribbean*, 11 (1961) 198.
11 T. J. CHOW AND T. G. THOMPSON, *Anal. Chem.*, 27 (1955) 18

TITRIMETRIC DETERMINATION OF HYDRAZINES WITH SULFATOCERIC ACID

SURJIT SINGH* AND JOSEPH R. SIEFKER**
St. Louis University, St. Louis, Mo. (U.S.A.)
(Received February 14th, 1966)

Aqueous solutions of hydrazine reduce strong oxidizing agents in dilute acid medium to give nitrogen, ammonia and hydrazoic acid. The nature and relative abundance of the oxidation products depend upon reaction conditions and the oxidant[1]. KIRK AND BROWNE[2] have classified different oxidants as mono-electron removers or di-electron removers and stated that nitrogen is the main oxidation product when oxidants of the second type are employed. Some of the redox processes involve both types of electron removal simultaneously. HIGGINSON *et al.*[3] suggested that a further distinction be made between those oxidants which could form a complex of the type

$$\text{Oxidant} + NH_2\text{–}NH_2 = \text{Oxidant} \leftarrow NH_2\text{–}NH_2$$

before the reaction and those which could not. The theory is only partially satisfactory as some reagents are known[1] to behave differently under different experimental conditions, such as varying acidity, temperature or even the manner of mixing the reagents. The suggestion that two 2-electron transfers should quantitatively oxidize hydrazine to N_2 is substantiated by its oxidation with thallium(III) in dilute acid solution[3], with co-ordination complex formation preceding the electron transfer.

Iodine monochloride is about 8% ionized[4] and the equilibrium is instantaneously adjusted if some I^+ ions are removed in complex formation. Since I^+ is much stronger acid than H_3O^+, the reaction of iodine monochloride with hydrazine in acid medium could be represented as

$$H_4N_2{:}H^+ + ICl_2^- = H_4N_2{:}I^+ + H^+(aq) + 2\ Cl^-$$

which will oxidize hydrazine to H_2N_2

$$H_4N_2{:}I^+ = H_2N_2 + 2\ H^+ + I^- \qquad \text{(slow)}$$

H_2N_2 is then oxidized to nitrogen by more iodine monochloride or free iodine present in solution

$$H_2N_2 + ICl_2^- = N_2 + 2\ H^+(aq) + I^- + 2\ Cl^-$$

$$H_2N_2 + I_2 = N_2 + 2\ H^+(aq) + 2\ I^-$$

The last two reactions are apparently fast because of the relative instability of H_2N_2.

---

* Present address: Waynesburg College, Waynesburg, Pa.
** Present address: Indiana State University, Terre Haute, Ind.

A titrimetric method for the oxidative determination of hydrazine and its common derivatives is proposed using iodine monochloride as a pre-oxidant and indicator. The iodine monochloride is regenerated in solution by sulfatoceric acid.

EXPERIMENTAL

Reagents

Iodine monochloride. This was prepared by titrating potassium iodide solutions of suitable concentration with a potassium iodate solution in a 6 N hydrochloric acid medium, using a potentiometric method to indicate the end-point. The solution was stored in a dark bottle (containing a few ml of chloroform also).

Hydrazine sulfate, phenylhydrazine hydrochloride and 2,4-dinitrophenylhydrazine. The samples were recrystallized twice from suitable solvents and then dried in a vacuum desiccator.

Methylhydrazine and dimethylhydrazine. These chemicals were purchased from the Mathieson Chemical Company and were repeatedly distilled until sharp boiling points within ±0.5° of the literature values were observed.

Procedure

Weigh a known amount of substance or transfer an accurately measured aliquot of standard solution to a 250-ml iodine titration flask. Add sufficient distilled water to give a final volume of 25 ml, followed by concentrated hydrochloric acid to give an initial concentration of about 6 N. Before commencing the titration add 5–10 ml of iodine monochloride solution. The concentration of iodine monochloride solution ranged from 0.005 M to 0.1 M depending on the nature of the reductant. Titrate the mixture with standard sulfatoceric acid solution until each addition of oxidant is accompanied by effervescence due to evolution of nitrogen. When a distinct iodine color appears, add 6–10 ml of carbon tetrachloride and continue the titration. Near the end-point, replace the stopper after each small addition of titrant and shake the flask vigorously. Repeat this process until a single drop of the titrant decolorizes the carbon tetrachloride layer (or changes it from light purple to pale yellow with higher concentrations of ICl).

Modified experimental conditions are needed for semicarbazide and aryl hydrazines. Treat the semicarbazide solution with dilute alkali solution and warm to expel ammonia before titration. In the case of 2,4-dinitrophenylhydrazine the use of high acid concentrations causes low results: start the titrations in 2 N acid solution without any iodine monochloride; when the color of the solution changes from orange to pale brown, adjust the acid concentration to 3.0–3.5 N and add 5 ml of 0.05 M ICl and about 10 ml of carbon tetrachloride before continuing the titration until the color of the organic layer changes from orange-red to pale yellow. For substituted hydrazines with aliphatic groups, pre-oxidation with basic ICl solution gave very good results. Addition of about 2 g of $HgCl_2$ improves the end-point and facilitates the oxidation in earlier stages. Presence of Cr(III), VO(II) and Mn(II) in the solution also seems to give better results.

Several titrations were performed for each of the reagents and results of some of the determinations picked at random are listed in Table I.

TABLE I

DETERMINATION OF VARIOUS COMPOUNDS BY THE PROPOSED METHOD

Compound taken (g)	*Volume of sulfatoceric acid used (ml)*	*Compound found (g)*
Hydrazine sulfate[a]		
0.1523	37.48	0.1525
0.1679	41.23	0.1678
0.1481	36.54	0.1487
0.1213	29.97	0.1210
0.1285	31.35	0.1276
Semicarbazide hydrochloride[b]		
0.1635	45.92	0.1605
0.1326	37.86	0.1324
0.1221	34.48	0.1206
0.1454	41.35	0.1446
0.1370	39.27	0.1373
Phenylhydrazine HCl[c]		
0.1395	31.45	0.1388
0.1690	37.98	0.1677
0.1920	43.21	0.1907
0.1629	36.50	0.1611
0.1750	39.62	0.1749
2,4-Dinitrophenylhydrazine[d]		
0.1339	26.05	0.1325
0.0680	13.03	0.0663
0.1816	35.95/36.00	0.1829
0.1226	23.90	0.1216
0.1601	31.20	0.1587
Methylhydrazine[e,f]		
0.1857	35.53	0.1851
0.1761	33.54	0.1752
0.1974	37.78	0.1974
0.1584	30.20	0.1578
0.2219	42.25	0.2217
Dimethylhydrazine[c,f]		
0.3157	42.37	0.3109
0.3010	39.92	0.2929
0.2710	35.43	0.2600
0.3400	45.89	0.3361
0.3081	41.22	0.3025

[a] Concentration of sulfatoceric acid: 0.1251 *N*.
[b] Concentration of sulfatoceric acid: 0.1254 *N*.
[c] Concentration of sulfatoceric acid: 0.1221 *N*.
[d] Concentration of sulfatoceric acid: 0.1027 *N*.
[e] Concentration of sulfatoceric acid: 0.1134 *N*.
[f] Compound taken in 100 ml of water.

DISCUSSION

The results are within ±0.2% when hydrazine is determined by the above method, indicating that quantitative oxidation to nitrogen is accomplished. A set of determinations for semicarbazide and phenylhydrazine were 2.2% low. This could result from incomplete oxidation of these compounds because of possible stabilization of the intermediates, $NH_2{:}CO{:}N{::}NH$ and $C_6H_5{:}N{::}NH$. Formation of hydrazoic acid or its derivatives is of no consequence as sulfatoceric acid oxidizes it quantitatively to nitrogen. Elimination of ammonia is expected to be a source of error because it will lead to much larger errors. Hydrolysis of semicarbazide is, therefore, deemed necessary before titration. Experimentally the results improved to within 0.7% of the known value when hydrolysis was employed. Since diazobenzene is fairly stable in acid solution, slow addition of titrant and vigorous shaking of the solution are necessary. A complete pre-oxidation in basic solution also causes low results, partly because of the formation of iodo-derivatives of benzene. Mercury(II) forms a complex with iodide ions and enhances the redox potential for the redox couple $I^- \rightleftharpoons I^+ + 2\,e$ considerably thus making the reaction conditions more drastic and facilitating the oxidation. The role of mercury(II) may well be more complex since other ions also seem to catalyse this reaction. The results are not very accurate and involve negative errors to the extent of 1.5 to 2.0%.

The oxidation of 1,1-dimethylhydrazine is slow at low concentrations and a negative error of the order of 2.9% is observed. A slow rate of reaction could be attributed to steric hindrance of methyl groups to redox complex formation. Possible elimination of some methylamine may also partly contribute to the negative error.

Similar factors seem to influence the determination of methylhydrazine.

Oxidation of 2,4-dinitrophenylhydrazine is very fast even though the nitro groups at the 2,4-positions should decrease the electron density at the azo group thus making the electron loss more difficult; a feasible explanation is the elimination of electrons at the oxygen atoms of the nitro groups. In this determination the original acid and ICl concentrations are not very critical, which somewhat confirms this view. Addition of ICl in the case of 2,4-dinitrophenylhydrazine and addition of carbon tetrachloride in the case of substituted hydrazines is delayed; this is done to avoid the solubility of the addition product in the nonpolar solvent, which would decrease the rate of reaction making it unsuitable for a fast titration. Foam formation at the junction of the water and carbon tetrachloride layers also takes place as the organic component on the hydrazine group becomes bulky. In such a case the results have an entirely random error with a maximum of 5%.

Although comparatively large sources of errors arise, the method is especially useful when common inorganic ions like iron(III) and rare earths are present along with the hydrazines. The presence of these ions makes the spectrophotometric titration with nitrite solution difficult and the accuracy of the above method for simple hydrazines is greater.

SUMMARY

Titrimetric methods for the determination of hydrazine and some simple alkyl and aryl derivatives are described. Iodine monochloride serves as pre-oxidant and indicator, and sulfatoceric acid as the titrant. Mercury(II) is added to ensure complete oxidation of some compounds.

RÉSUMÉ

Les auteurs décrivent des méthodes titrimétriques pour le dosage de l'hydrazine et de ses dérivés. On utilise le monochlorure d'iode comme pré-oxydant et indicateur, l'acide sulfatocérique comme titrant. On ajoute du mercure(II) pour permettre une oxydation complète de certains composés.

ZUSAMMENFASSUNG

Es werden massanalytische Methoden zur Bestimmung von Hydrazin und einigen einfachen Alkyl- und Arylderivaten mit Sulfatocersäure beschrieben. Jodmonochlorid dient als Oxydationsmittel und Indikator. Quecksilber(II) wird zugegeben, um die vollständige Oxydation einiger Verbindungen zu sichern.

REFERENCES

1 L. F. AUDRIETH AND B. A. OGG, *The Chemistry of Hydrazine*, John Wiley, New York, 1951.
2 R. E. KIRK AND A. W. BROWNE, *J. Am. Chem. Soc.*, 51 (1928) 337.
3 W. C. E. HIGGINSON, D. SUTTON AND P. WRIGHT, *J. Chem. Soc.*, (1953) 1380, 1402; (1955) 1551.
4 J. AROSTKY AND M. C. R. SYMONS, Halogen Cations, *Quart. Rev.*, Vol. XVI, No. 3 (1962).

SOME NEW AROMATIC HYDROXYLAMINES AS SPECTROPHOTOMETRIC REAGENTS FOR VANADIUM

A. K. MAJUMDAR AND GAYATRI DAS
Department of Inorganic and Analytical Chemistry, Jadavpur University, Calcutta-32 (India)
(Received March 25th, 1966)

Recently, N-benzoyl-*o*-tolylhydroxylamine[1] (I) and N-benzoyl-*p*-chlorophenylhydroxylamine[2] (II) have been proposed as spectrophotometric reagents for the determination of vanadium. Of these reagents, the former under suitable experimental conditions behaves as a specific reagent for vanadium and the latter is highly selective in its reaction.

Further investigation under the same conditions has shown that N-phenylacetylphenylhydroxylamine (III), N-benzoyl-*m*-tolylhydroxylamine (IV) and N-benzoyl-*p*-tolylhydroxylamine (V) have similar characteristics to the *o*-tolyl derivative. The former forms a reddish violet complex while the latter two form violet complexes with the vanadate ion. These coloured complexes on extraction with chloroform from strong hydrochloric acid solutions, form the basis of highly sensitive and specific methods for the determination of vanadium (Table I). The colour intensities of the complexes formed under these conditions are greatly reduced, and can even be changed to different hues, in the presence of even traces of alcohol; the chloroform used for extraction must therefore be free from alcohol.

However, in the presence of alcohol, all the 5 reagents were found to form yellow coloured complexes at a pH of 4.8–6.0. These complexes on extraction with chloroform from a buffered acetic acid–sodium acetate solution show absorption maxima at 440 mμ. These coloured systems obey Beer's law from 1–12 μg of vanadium with optimum ranges from 3–12 μg of vanadium. The percent relative errors in these regions are 2.736 with the reagents (I), (IV) and (V), and 2.715 and 2.726 with the reagents (III) and (II) respectively.

EXPERIMENTAL

Preparation of the reagents

The reagents IV and V were prepared in the same way as proposed for the *o*-tolyl derivative[1]. These colourless reagents were purified by recrystallisation from aqueous alcohol (m.p. 70° and 108°, respectively. Found: C, 73.96; H, 5.84; N, 6.22% for (IV) and C, 74.02; H, 5.70; N, 6.13% for (V); calculated: C, 74.08; H, 5.72; N, 6.16%).

Reagent III was prepared from nitrobenzene and phenylacetyl chloride. First the nitrobenzene was reduced by zinc dust to phenylhydroxylamine, which was then coupled with phenylacetyl chloride as described previously[3]. The product was recrystallized from ethanol (m.p. 90°. Found: C, 73.98; H, 5.78; N, 6.12%; calculated: C, 74.08; H, 5.72; N, 6.16%).

Solutions (0.5%, w/v) of the reagents in purified chloroform were used for the spectrophotometric studies of vanadium from hydrochloric acid solution.

For studies at pH 4.8–6.0, 0.5% solutions of the reagents in ethanol were used.

Apparatus and solutions

A Unicam SP 600 spectrophotometer and a Cambridge pH meter were used respectively for absorbance and pH measurements.

Solutions of different ions including that of vanadate and other chemicals were the same as used previously[1,2].

Buffer solutions of different pH were prepared by mixing in varying proportions 0.2 *M* solutions of acetic acid and sodium acetate.

Studies at a high acid concentration

The general procedure followed for the determination of vanadium, studies of the effect of time, temperature, acidity and reagents on the colour systems and also investigations of absorption curves, Beer's law, optimum ranges, relative errors, composition and instability constants of the complexes were made in the same way as described in previous papers[1,2]. Results are given in Table I.

Interferences. In hydrochloric acid solutions of optimum concentration (Table I), even 4 µg of vanadium could be determined in the presence of a large excess of the foreign ions by extraction with a chloroform solution of reagents (I), (III), (IV) or (V). No interference was found from the following ions: Al^{3+} (20 mg), Fe^{3+} (30 mg), Mn^{2+} (20 mg), UO^{2+} (20 mg), Cr^{3+} (20 mg), Zr^{4+} (20 mg), Cu^{2+} (20 mg), Mo^{6+} (20 mg), Ti^{4+} (10 mg), W^{6+} (15 mg), Th^{4+} (20 mg), Co^{2+} (15 mg), Cd^{2+} (15 mg), Hg^{2+} (15 mg), Pb^{2+} (20 mg), As^{3+} (10 mg), As^{5+} (15 mg), Be^{2+} (20 mg), Mg^{2+} (15 mg), Ba^{2+} (20 mg), Sn^{4+} (15 mg), Bi^{3+} (20 mg), Ni^{2+} (20 mg), Zn^{2+} (10 mg), Sb^{3+} (15 mg), Ca^{2+} (15 mg), Sr^{2+} (10 mg), rare earths (20 mg), Os^{8+} (12 µg), Ir^{4+} (1.8 mg), Rh^{3+} (27.5 µg), Ru^{3+} (25 µg), Pd^{2+} (1.22 mg), Pt^{4+} (2.3 mg), EDTA (20 mg), fluoride (10 mg), oxalate (15 mg), tartrate (15 mg), phosphate (20 mg), citrate (10 mg), acetate (15 mg) or borate (10 mg).

In the case of Ti^{4+}, NaF was used as a masking agent. The addition of hydrogen peroxide (1 ml 20 vol.) did not interfere with reagent (I); with reagents (III), (IV) and (V), the presence of only 0.2 ml of 20 vol. hydrogen peroxide made it necessary to extract several times with excess of reagent for complete recovery of vanadium. In the presence of molybdate, with reagent (V), 5 extractions of vanadium with a chloroform solution of the reagent were necessary. For separation from iron with reagent (III), the procedure followed was the same as that described previously[2]. For separation from molybdate, with this reagent (III), 8 extractions, each with 3 ml of the reagent, were required.

Studies at pH 4.8–6.0

An aliquot portion of the vanadium(V) solution was transferred to a separating funnel and 15 ml of the required sodium acetate–acetic acid buffer solution were added to maintain the pH anywhere between 4.8 and 6.0. After the addition of 2 ml of any of the reagent solutions in alcohol, the coloured complex of vanadium was extracted into

TABLE I

COMPARISON OF REAGENTS STUDIED IN HYDROCHLORIC ACID MEDIA

	N-benzoyl-o-tolylhydroxylamine[a]	*N-benzoyl-m-tolylhydroxylamine*	*N-benzoyl-p-tolylhydroxylamine*	*N-phenylacetyl-N-phenylhydroxylamine*
Maxima (mμ)	510	530	530	510
Sensitivity (μg/cm^2)	0.0108	0.0108	0.0108	0.0121
Beer's law range (μg)	0.5–10	0.5–10	0.5–10	0.5–10
Optimum range[4] (μg)	2–10	2–10	2–10	2–8
Optimum acid concentration	4–8 *N* HCl	2.7–8 *N* HCl	2.7–7.5 *N* HCl	2.8–7 *N* HCl
Composition[5-7]	Metal:reagent 1:2	Metal:reagent 1:2	Metal:reagent 1:2	Metal:reagent 1:2
Average dissociation constant at room temp.[7,8]	$8 \cdot 10^{-9}$	$6.4 \cdot 10^{-9}$	$4.0 \cdot 10^{-9}$	$3.8 \cdot 10^{-9}$
% Relative error[9]	2.730	2.729	2.717	2.722

[a] The values for N-benzoyl-*o*-tolylhydroxylamine are given for comparison.

TABLE II

COMPARISON OF REAGENTS STUDIED AT pH 4.8–6.0

	N-benzoyl-o-tolylhydroxylamine	*N-benzoyl-m-tolylhydroxylamine*	*N-benzoyl-p-tolylhydroxylamine*	*N-phenylacetyl-N-phenylhydroxylamine*	*N-benzoyl-N-p-chlorophenylhydroxylamine*
Sensitivity (μg/cm^2)	0.0129	0.0129	0.0129	0.0145	0.0137
Composition[5-7]	Metal:reagent 1:2	Metal:reagent 1:2	Metal:reagent 1:2	Metal:reagent 1:2	Metal:reagent 1:2
Average dissociation constant[7,8] at room temp.	$2.40 \cdot 10^{-8}$	$2.33 \cdot 10^{-8}$	$2.46 \cdot 10^{-8}$	$2.92 \cdot 10^{-8}$	$3.1 \cdot 10^{-8}$
% Relative error[9] at the optimum range 3–12 μg of vanadium	2.736	2.736	2.736	2.715	2.726

chloroform and made up to 25 ml by addition of more chloroform. The optical density of the colour system so prepared was measured at different wavelengths.

Under these conditions the colour systems formed with all the reagents gave maxima at 440 mμ. Moreover, all these systems were found to obey Beer's law over the range 1–12 μg of vanadium with optimum ranges of 3–12 μg of vanadium. The percent relative errors over the above range, the compositions and the dissociation constants of the complexes and the sensitivities of the reactions are given in Table II.

Studies of the effect of acidity, time and reagent suggested that the colour intensity of the systems was highest at a pH 4.8–6.0, where only 2 ml of any of the reagent solutions was sufficient for 8 μg of vanadium. The colour systems under these conditions were stable for 48 h at room temperature.

Interferences. At pH 4.8 to 6.0, with all these reagents, 8 μg of vanadium could be determined in the presence of a large excess of various foreign ions. No interference was found from Ba^{2+} (15 mg), Ca^{2+} (15 mg), Mg^{2+} (15 mg), Sr^{2+} (15 mg), Be^{2+} (20 mg), Cr^{3+} (20 mg), Mn^{2+} (10 mg), Co^{2+} (15 mg), Ni^{2+} (15 mg), Zn^{2+} (10 mg), Cd^{2+} (20 mg), Hg^{2+} (10 mg), As^{3+} (15 mg), As^{5+} (15 mg), fluoride (15 mg), tartrate (10 mg), borate (15 mg) or phosphate (15 mg).

pK_a values

The pK_a values for these reagents in 1:1 alcohol–water mixture and also in water were determined by pH titration of 0.025 *M* solutions of the reagents in the respective solvents with 0.025 *M* sodium hydroxide solution (Table III).

TABLE III

pK_a VALUES FOR THE REAGENTS[a]

	In 1:1 alcohol–water at 22.5°	*In water at 25°*
N-Benzoyl-*o*-tolylhydroxylamine	9.92 ±0.04	8.40 ± 0.04
N-Benzoyl-*m*-tolylhydroxylamine	9.92 ±0.04	Insoluble
N-Benzoyl-*p*-tolylhydroxylamine	9.92 ±0.04	8.40 ±0.04
N-Phenylacetyl-N-phenylhydroxylamine	10.08 ±0.04	8.60 ±0.04
N-Benzoyl-*p*-chlorophenylhydroxylamine	9.60 ±0.04	Insoluble
N-Benzoyl-N-phenylhydroxylamine	9.80 ±0.04	8.30 ±0.04

[a] pK_a values of N-benzoyl-N-phenylhydroxylamine were determined for comparison.

DISCUSSION

The pK_a values of the reagents as found above show the acid dissociation constants to be in the order II > I $\simeq$ IV $\simeq$ V > III. Reagents with such small differences in pK_a values cannot be expected to show any great differences in the formation of complexes under the conditions stated above. However, as the basicity of the reagent increases, the sensitivity of the reaction towards vanadium increases, except with reagent III which has a somewhat different structure from the others. Here the $-CH_2-$ group bound to phenyl is attached to the $\overset{}{\underset{|}{-C=O}}$ group, while in the other reagents, substitution is on the phenyl ring attached to the $-\overset{|}{N}-OH$ group. This also explains the low acid dissociation constant of reagent III.

In the pH range 4.8–6.0, the reagents are not very selective and they behave alike towards interfering ions with which they probably form complexes of rather similar stability.

In solutions containing free hydrochloric acid, the reagents behave somewhat differently towards one or two ions. Such differences are probably due to steric effects. The methyl group at the 2-position usually imparts steric strain and thereby reduces the stability of the complexes. This explains why reagent I is so selective in its reaction. Reagents IV and V show similar behaviour, perhaps because the basic geometry needed for the overlap of the orbitals of the ligands and metals is absent. The same can be said of reagent III where the phenyl group attached to $-CH_2-$ has free rotation.

As the groups responsible move further apart, less steric strain is experienced by the reactive atomic groupings; hence reagent III is less selective than reagent V. Again in the latter reagent, if the methyl group with directed bonds is replaced by a chlorine atom, the reagent becomes still less selective as is found with reagent II[2].

During the study of the composition of the complexes it was observed that with the progressive addition of alcohol to the chloroform extract, the absorption maxima of the complexes formed in hydrochloric acid solutions, shifted gradually from 510/530 mμ to 490 mμ and thence to 440 mμ, which is the maximum absorption region of the complexes formed in sodium acetate–acetic acid buffer.

SUMMARY

A comparative study is described of the use of N-benzoyl-*o*-tolyl-, N-benzoyl-*m*-tolyl, N-benzoyl-*p*-tolyl-, N-benzoyl-*p*-chlorophenyl- and N-phenylacetylphenylhydroxylamines, as spectrophotometric reagents for the determination of vanadium, after extraction with chloroform. All the reagents form 1:2 (metal:reagent) complexes in hydrochloric acid media or at pH 4.8–6.0; the dissociation constants of the complexes are of the order of 10^{-9} and 10^{-8}, respectively, except those of N-benzoyl-*p*-chlorophenylhydroxylamine which are of the order of 10^{-8} in both media. The reactions in hydrochloric acid media are more selective and sensitive than those at pH 4.8–6.0. In presence of alcohol, the wavelengths of maximum absorption decrease. The pK_a values of the hydroxylamines were determined in water and in alcohol–water (1:1) solutions.

RÉSUMÉ

On a effectué une étude comparative sur l'emploi des N-benzoyl-*o*, -*p* or -*m*-tolyl-, N-benzoyl-*p*-chlorophényl- et N-phénylacétylphénylhydroxylamines comme réactifs spectrophotométriques pour le dosage du vanadium, après extraction au moyen de chloroforme. Tous ces réactifs forment des complexes 1:2 (métal:réactif) en milieu acide chlorhydrique ou à pH 4.8–6.0; les constantes de dissociation des complexes sont de l'ordre de 10^{-9} et 10^{-8} respectivement, à l'exception de celles de la N-benzoyl-*p*-chlorophénylhydroxylamine qui sont de l'ordre de 10^{-8} dans les deux milieux. Les réactions en milieu acide chlorhydrique sont plus sélectives et plus sensibles que celles obtenues à pH 4.8–6.0. On a déterminé les valeurs pK_a des hydroxylamines dans l'eau et dans les solutions alcool–eau (1:1).

ZUSAMMENFASSUNG

Es werden vergleichende Untersuchungen beschrieben über die Verwendung von N-Benzoyl-*o*-tolyl-, N-Benzoyl-*m*-tolyl-, N-Benzoyl-*p*-tolyl-, N-Benzoyl-*p*-chlorophenyl- und N-Phenylacetylphenyl-hydroxylamin als spektralphotometrische Reagentien zur Bestimmung von Vanadin nach Extraktion mit Chloroform. Alle diese Reagentien bilden in salzsaurem Medium oder beim pH 4.8–6.0 1:2-Komplexe (Metall: Reagenz). Die Dissoziationskonstanten der Komplexe liegen in der Grössenordnung von 10^{-9} bzw. 10^{-8}, ausser der von N-Benzoyl-*p*-chlorophenylhydroxylamin, mit 10^{-8} in beiden Medien. Die Reaktionen in stark salzsaurem Medium sind selektiver und empfindlicher als beim pH 4.8–6.0. In Gegenwart von Alkohol verschiebt sich das Absorptionsmaximum nach kleineren Wellenlängen. Die pK_a-Werte der Hydroxylamine wurden in Wasser und in Alkohol–Wasser-Lösungen bestimmt.

REFERENCES

1 A. K. Majumdar and Gayatri Das, *Anal. Chim. Acta*, 31 (1964) 147.
2 A. K. Majumdar and Gayatri Das, *J. Indian Chem. Soc.*, 42(3) (1965) 189.
3 A. K. Majumdar and A. K. Mukherjee, *Anal. Chim. Acta*, 19 (1958) 23.
4 A. Ringbom, *Z. Anal. Chem.*, 115 (1938) 332.
5 P. Job, *Compt. Rend.*, 180 (1925) 928; *Ann. Chim. (Paris)*, 9 (1928) 113.
6 J. H. Yoe and A. L. Jones, *Ind. Eng. Chem., Anal. Ed.*, 16 (1944) 111.
7 A. E. Harvey and D. L. Manning, *J. Am. Chem. Soc.*, 72 (1950) 4488.
8 A. K. Majumdar and B. Sen, *Anal. Chim. Acta*, 8 (1953) 369.
9 G. H. Ayres, *Anal. Chem.*, 21 (1949) 652.

STABILITY OF SOME STATIONARY PHASES IN THE SEPARATION OF POLYPHENYL MIXTURES BY GAS CHROMATOGRAPHY

L. GASCÓ-SÁNCHEZ AND F. BURRIEL-MARTÍ
"Junta de Energía Nuclear", Division of Chemistry and Isotopes, Department of Analytical Chemistry, C.S.I.C. and Faculty of Sciences, Madrid (Spain)

(Received May 8th, 1966)

During recent years it has been noted that the stationary phases in gas chromatography, during the lifetime of the columns, are subject to transformations which affect the results of quantitative analyses or the retention volumes in qualitative analyses. KELLER *et al.*[1-3] have reviewed in detail the investigations carried out on this particular subject and have pointed out that during the conditioning process or the production of the chromatograms, the stationary phase undergoes transformations which may be caused by: impurities in the carrier gas, non-volatile impurities in the stationary phase, catalytic reactions with the solid support, catalytic reactions with degradation products originating from the liquid phase, or polymerization of polymeric materials in the stationary phase.

The above-mentioned phenomena may be responsible for the introduction of material to the effluent or for the change in column behaviour. The anomalous behaviours are mainly found in stationary phases made of polymers, *i.e.* polyesters and polysiloxanes; anomalies in polyester columns have been mentioned[4], and CHEN AND GACKE[5] have studied the change in structure of some polysiloxanes and its effect on the retention volumes of polar and non-polar compounds.

In some previous investigations[6,7], various stationary phases made of poly siloxanes were selected for the analysis of polyphenyl mixtures; later it was proved that columns prepared from these stationary phases undergo a change in behaviour as a function of time as regards the separation of polyphenyl mixtures.

In this paper, a number of factors that influence these variations in behaviour is described, and some experimental conditions minimizing the instability phenomena of the columns are established.

EXPERIMENTAL AND RESULTS

Instruments

Gas Chromatograph F.M., Model 500 equipped with a flame-ionization device, Model 1609. Perkin-Elmer Gas Chromatograph, Model 116E.

Stationary phases

Silicone oils DC-703, DC-704, DC-710, F-50, SF-96, L-45. Silicone rubbers SE-30, SE-33, W-96, W-950, W-960. Carbowax 20 M, UCON 50 LB (Applied Science

Laboratories). Silicone oils MS-200, MS-510, MS-550, MS-555, MS-710 (Hopkins Williams). Embaphase Silicone Oil (May and Baker).

Columns

Prepared according to the conventional method with chromosorb, 80–100 mesh. Length 2.00 m, internal diameter 4.8 mm.

Chromatograms

Described by the following variables in accordance with standard usage[8,9]:

t'_R = adjusted retention time of the component that appears last.
n = column efficiency expressed in theoretical plates.
R = resolving power in accordance with IUPAC standard[8].
δ = resolving power in accordance with KAISER.
As = peak asymmetry.
r = relative retention referred to triphenylmethane in separations of terphenyls and to naphthalene in the separation of biphenyl–biphenyl oxide.

In order to simplify the methods of calculating the dead volume of the column (gas hold-up)[10] with the flame-ionization detector, the retention time of city gas was determined; it was established that under the same experimental conditions the retention time was the same as for air.

Stability of some silicones as stationary phases

In previous investigations a series of stationary phases was selected for the separation of mixtures of biphenyl and biphenyl oxide[6], and of diphenyl and triphenyl[7], and the best separation conditions were determined for columns that had been conditioned following the conventional method (heating for some 12 h, and passing carrier gas through at a temperature 25–50° higher than the column working temperature, without reaching its maximum utilization temperature). When chromatograms were made with the same columns after some time, it was observed that the values of the descriptive magnitudes differed in some cases from those originally obtained.

In Table I, the values of n, δ and As for the separation of mixtures of biphenyl and biphenyl oxide are shown, and in Table II those for the separation of triphenyl isomers. Both Tables show the results corresponding to recently prepared columns as well as those obtained after the elapse of a certain time during which the columns were not utilized. The experimental conditions were chosen as the best possible for the separation selected on the basis of other work[6,7].

Table I shows that with regard to the separation of biphenyl from biphenyl oxide, the stationary phases may be classified in 3 groups:

(*a*) Silicone oils which according to specifications may be utilized up to 200°: Embaphase, DC-703, DC-710, MS-220, MS-510, MS-550, MS-555 and MS-710. After a certain period of time had elapsed following their preparation, the columns prepared with these stationary phases showed a considerable decrease in efficiency and resolving power, and the chromatograms showed greater asymmetry (tailing) of the biphenyl oxide peak. In spite of its higher utilization temperature, the stationary phase F-50, behaved similarly.

(*b*) Silicone oils SF-96 and L-45 that have a longer linear chain and may be utilized at higher temperatures (250°). The chromatograms obtained with these

TABLE I

SEPARATION OF BIPHENYL AND BIPHENYL OXIDE

(Variation of the efficiency of columns prepared with silicones as a function of time)

Stationary phase	*Column temp.*	*t (months)*	*n*		*δ*		*As*	
			Initial	*Later*	*Initial*	*Later*	*Initial*	*Later*
Embaphase	125	4.9	1792	347	87	39.8	+1.30	+1.56
DC-703	143	3.5	2829	624	100	74.5	−1.03	+1.16
DC-710	150	2.6	2044	200	96	40.0	+1.02	+1.48
MS-200	120	4.1	1673	415	89	58.8	+1.11	+1.55
MS-510	119	4.0	946	249	89	38.1	+1.07	+1.38
MS-550	125	4.6	964	520	88	63.1	+1.01	+1.15
MS-555	108	4.0	805	93	—	61.2	—	+2.02
MS-710	140	4.1	1049	711	96	76.1	−1.06	+1.25
F-50	110	4.9	942	312	76	28.3	+1.24	+1.28
SF-96	129	2.0	2111	1402	84	59.6	−1.16	−1.02
L-45	123	4.0	3435	2856	84	84.4	+2.51	+1.24
SE-30	132	2.0	2102	3148	78	88.0	+1.16	+1.04
SE-33	117	2.1	1466	2635	74	86.1	−1.09	+1.00
W-96	122	2.0	2218	2645	87	94.6	−1.06	+1.19
Carbowax 20 M	150	3.2	1382	888	75.7	54.2	+1.16	+1.05
UCON 50 LB	156	3.2	2058	1644	87.4	82.4	+1.16	+1.08

TABLE II

SEPARATION OF *m*-TRIPHENYL AND *p*-TRIPHENYL

(Variation of the efficiency of columns prepared with silicones as a function of time)

Stationary phase	*Column temp.*	*t (months)*	*n*		*δ*		*As*	
			Initial	*Later*	*Initial*	*Later*	*Initial*	*Later*
SF-96	212	2.0	2344	1444	96	81	−1.10	−1.05
L-45	217	3.1	3400	3004	93	90	+1.14	+1.14
SE-30	235	2.0	2667	2323	96	93	+1.06	+1.02
SE-33	235	2.1	1929	2921	92	97	−1.06	−1.04
W-96	232	2.0	2076	2570	93	95	−1.09	−1.08
W-950	221	4.2	1483	1880	83	86	−1.02	+1.03
W-960	245	3.5	2297	3931	78	84	−1.02	+1.05

products showed decreased efficiency and improved asymmetry of biphenyl oxide.

(*c*) Polysiloxanes with bidimensional chain, silicone rubbers. The chromatograms exhibited improved efficiency and asymmetry.

The UCON 50 LB and the Carbowax 20 M behaved in a manner similar to that of the silicone oils included in the first group.

The relative retention values, not indicated in the Table, with respect to naphthalene, showed no significant variation.

The results collected in Table II on the efficiency and the separation of *m*- and *p*-triphenyl, indicate that stationary phases made of silicone oils utilizable at temperatures up to 250°, and those made of silicone rubbers, are more stable in general than silicone oils usable at lower temperatures, in spite of the fact that the separation temperature is higher. A not very pronounced correlation may be established between efficiency of separation and chemical composition; the methyl-polysiloxanes, SF-96, L-45 and SE-30, showed decreased efficiency and separation, whereas the methyl-vinyl-polysiloxanes, SE-33, W-96 and W-960, showed an increase in these magnitudes. The methyl-polysiloxane, W-950, did not follow the indicated correlation. The variations in the values of the asymmetries were not significant.

In general, a greater stability of the stationary phase is evident with respect to the separation of the *m*- and *p*-triphenyls, even though the working temperature is higher.

Influence of the solid support and conditioning on column stability

In most of the experiments carried out in order to obtain packed columns with high stability, the stationary phase DC-710 was used at a level of 5% on solid support; DC-710 offers a better efficiency for the separation of biphenyl and biphenyl oxide as well as a well-defined interaction with the support. Some experiments were also made with the DC-704 silicone oil stationary phase, which showed certain peculiarities in its conditioning. The maximum temperature at which this stationary phase may be used is 200°; however, when the columns were conditioned with chromosorb P or chromosorb W as solid support at this temperature, they did not separate biphenyl from biphenyl oxide. With sterchamol support, the results obtained were not reproducible or controllable; at 175° the conditioning curves depended on the manner in which the heating was effected. When the column was heated for 2.5 h at 175°, and then the oven was cooled and afterwards brought back to the same temperature, a resolution of $R = 0.96$ was obtained; but if the column was conditioned by keeping the temperature constant at 175°, the resolving power became zero ($R = 0.0$). Fairly acceptable conditioning could be achieved by heating at 100° and by letting a stream of carrier gas flow through until a stable baseline was obtained, and subsequently carrying out the chromatograms at 160°.

With the stationary phase DC-710, reproducible conditioning of the columns can be attained, where the respective curves depend on the type of support utilized.

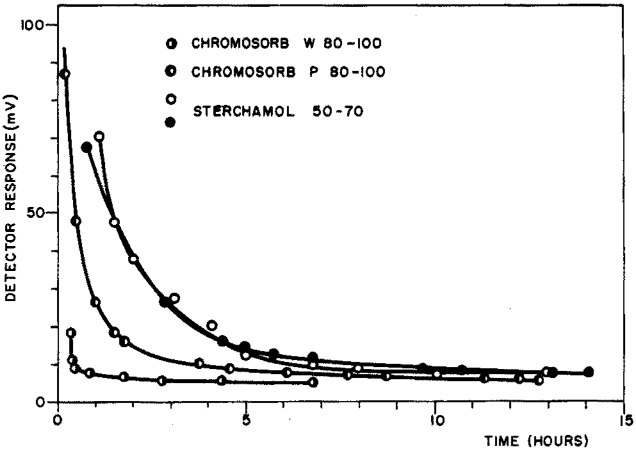

Fig. 1. Conditioning curves of packed columns of DC-710 silicone oil at 200°.

Figure 1 shows the curves that have been obtained[9] with the solid supports chromosorb W, chromosorb P and sterchamol (containing 5% of stationary phase), recorded at 200° with an argon flow of 41.3 ml/min, 21.7 ml hydrogen/min and 183 ml air/min. (All the conditioning curves mentioned below were obtained under these conditions.) A stable baseline is reached after 3 h with chromosorb W, after 6 h with chromosorb P and after 8 h with sterchamol. As can be seen from the 2 curves obtained with sterchamol, the conditioning curves are reproducible.

Table III shows the variations in the descriptive magnitudes as a function of time (without utilizing the columns), of the chromatograms obtained in columns conditioned as for the curves indicated in Fig. 1 (argon flow 58.4 ml/min, hydrogen flow 21.7 ml/min, air flow 183 ml/min). A significant improvement may be observed compared to the values indicated in Table I. It is also evident that more stable columns are obtained with chromosorb W. Unsatisfactory results were obtained with other solid supports used in freshly prepared columns. Table IV shows that the best characteristics were obtained with chromosorb P for the separation of biphenyl and biphenyl oxide, when silicone oil DC-710 was used. Chromosorb P, when treated with hexamethyldisilazane in order to reduce its surface activity, showed both poorer

TABLE III

DESCRIPTIVE MAGNITUDES OF COLUMNS PREPARED WITH SILICONE OIL DC-710 AS A FUNCTION OF TIME

Solid support	*Chromosorb W*			*Chromosorb P*		
Temperature	*136°*			*148°*		
Time (months)	0	3.5	6.8	0	3.5	6.6
t'_R(OD) (min)	37.7	39.8	41.1	37.4	39.5	39.8
n(OD)	1301	976	1002	1319	819	7.34
R	1.29	1.12	1.15	1.20	0.94	0.88
δ	89.3	83.3	82.1	86.4	72.5	69.2
As(OD)	1.08	1.07	1.02	1.18	1.10	1.10
r_D	3.01	3.02	3.00	2.81	2.82	2.82
r_{OD}	3.51	3.52	3.50	3.22	3.24	3.24

TABLE IV

DESCRIPTIVE MAGNITUDES OF VARIOUS SOLID SUPPORTS IN SILICONE OIL DC-710

(Argon flow 58.4 ml/min)

	Chromosorb P[a]		*Glass beads*[b]	*Sterchamol*[a]
	with HMDS	*without HMDS*		
temperature	150°	148°	92°	136°
n	580	1319	147	814
R	0.78	1.20	0.57	0.86
As(OD)	1.15	1.18	1.26	1.66
r_D	2.82	2.81	4.81	3.06
r_{OD}	3.23	3.22	5.82	3.46

[a] 5% Stationary phase.
[b] 0.2% Stationary phase.

resolving power and poorer efficiency than the untreated product; there was an insignificant improvement in peak asymmetry, while the relative retentions of the biphenyl and biphenyl oxide towards naphthalene remained unchanged. Unsatisfactory results were also obtained when glass beads and sterchamol were utilized.

The curves shown in Fig. 2 correspond to experiments carried out in order to prove whether transformations of the stationary phase, which might give rise to a greater bleeding rate, would be obtained if the conditioning was effected in accordance with the experimental conditions described above. These curves were obtained with columns containing 5% silicone oil DC-710 on chromosorb W, and they represent the performance of the detector as a function of the temperature and carrier gas flow (hydrogen 217 ml/min, air 183 ml/min). Curves obtained under the same experimental conditions with columns prepared from chromosorb P or sterchamol were similar to those described in Fig. 2. This means that there is no difference in the release of volatile substances arising from the stationary phase with the different solid supports tested. Furthermore, it was established that the columns in which the bleeding curves were carried out, did not lose their efficiency after they had been heated to 220°.

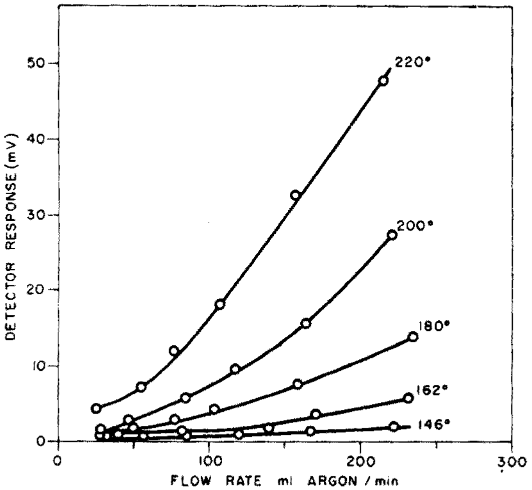

Fig. 2. "Bleeding" curves of columns of DC-710 silicone oil on 80–100 mesh chromosorb W.

The chromatograms obtained in columns conditioned in a controlled manner, proved to be more reproducible than those obtained from columns conditioned conventionally. This is shown by the results in Table V, in which the precision between duplicate chromatograms carried out on the same day in the same column are used for comparative purposes.

The performance of the column was checked in order to detect possible modifications in its behaviour caused by keeping it at the temperature at which the separation was made and at constant flow, *i.e.*, maintaining the chromatograph in operation day and night. A column of silicone oil DC-710 (5%) on chromosorb P at 150° with a nitrogen flow of 58.4 ml/min (optimum conditions for the separation of biphenyl and biphenyl oxide), during a period of 300 h showed no significant efficiency loss, and the values of $t'_R(OD)$, R, δ and r_D and r_{OD} remained practically unchanged; however, the precisions of these magnitudes, as calculated from day to day, differed considerably from those calculated on the same day. When the experiment was repeated keeping the chromatograph in operation during the day only, the precision of the descriptive magnitudes from day to day was essentially the same as that obtained in the same day.

TABLE V

REPRODUCIBILITY OF COLUMNS PREPARED WITH STATIONARY PHASE DC-710

(Expressed in terms of standard deviation)

Type of test	*a*	*b*	*c*
t'_R(OD) (min)	4.3	4.0	0.64
n(OD)	480	48	128
R	0.22	0.06	0.06
δ	5.3	1.8	1.8
As(OD)	0.08	0.023	0.055
r_D	0.03	0.011	0.014
r_{OD}	0.04	0.017	

a = Duplicate tests carried out in different, non-stabilized columns.
b = Duplicate tests carried out in different, conditioned and stabilized columns.
c = Average value of duplicate tests carried out on the same day in the same column.

Stability of columns prepared with mixed stationary phases

In an effort to improve the stability referring to the separations of biphenyl and biphenyl oxide, columns were prepared containing 5% mixed stationary phases of DC-710 silicone oil with carbowax 20 M, both with chromosorb P as solid support. The columns were conditioned in the same way as those mentioned in Table III (41.3 ml argon/min, 21.7 ml hydrogen/min and 183 ml air/min flows). The respective conditioning curves did not show any peculiarity, resembling one another closely when one of the components was carbowax; however, when UCON 50 LB was used as the mixed component, the curves shifted towards the abscissae axis as the silicone oil concentration increased.

Tables VI and VII show the values of the descriptive magnitudes of chromatograms obtained in columns with the mixed phase after their conditioning as mentioned

TABLE VI

STABILITY OF COLUMNS PREPARED WITH SILICONE OIL DC-710: CARBOWAX 20 M MIXED STATIONARY PHASES

DC-710	*25%*		*50%*		*75%*	
Time (months)	0	3.3	0	3.5	0	3.4
t'_R(OD) (min)	44.7	47.2	39.8	41.9	35.3	36.7
n(OD)	2228	2168	2164	1942	2001	1144
R	1.30	1.28	1.26	1.28	1.38	1.02
δ	88.6	88.4	88.6	88.4	90.0	77.2
As(OD)	1.06	1.05	1.08	1.02	1.06	1.06
r_D	2.69	2.73	2.72	2.73	2.73	2.77
r_{OD}	3.02	3.07	3.07	3.08	3.11	3.16

above and again after a period of 3–6 months had elapsed without utilizing the columns. When these values are compared with those obtained with the stationary phases of silicone oil DC-710 (Table III) and of UCON 50 LB and carbowax (Table I), it may be observed that the mixed stationary phases did not present much better characteristics than those of their components taken separately, the efficiencies being somewhat higher and the asymmetries lower. The relative retentions were intermediate between those of the pure components.

TABLE VII

STABILITY OF COLUMNS PREPARED WITH SILICONE OIL DC-710:UCON 50 LB-1200× MIXED STATIONARY PHASES

DC-710	*25%*		*50%*		*75%*	
Time (months)	0	3.4	0	3.6	0	3.5
t'_R(OD) (min)	42.5	—	40.7	41.6	38.8	41.3
n(OD)	2098	1012	1844	801	2036	1710
R	1.30	0.91	1.26	0.80	1.37	1.26
δ	89.4	70.3	88.1	60.8	90.6	88.5
As(OD)	1.09	1.02	1.06	1.02	1.06	1.02
r_D	2.78	2.79	2.78	2.81	2.79	2.79
r_{OD}	3.13	3.16	3.14	3.17	3.17	3.18

With regard to the stability as a function of time, the variations in behaviour were significant. The stationary phases containing 25% UCON 50 LB were the most stable; after 6 months they showed a better efficiency rate and resolving power than either of the two stationary phases taken separately.

The stationary phases containing 25 and 50% carbowax also exhibited a better stability, and after 3.5 months showed better characteristics than any of the other two phases. Consequently, the use of mixed stationary phases causes the phenomenon of variation in behaviour of the columns as a function of time to be reduced.

SUMMARY

Some liquid phases utilized in the analysis of polyphenyl mixtures show variations in their chromatographic properties when used in packed columns; a study was therefore made of methods of increasing its stability, the influence of the solid support and the conditioning process. Reproducibility in the column preparation was checked by means of conditioning curves. Stable columns were obtained by using stationary mixed phases at 5% on chromosorb P, of silicone oil DC-710:UCON 50 LB in the proportion 3:1 and with silicone oil DC-710:carbowax 20 M in the proportions 3:1 and 1:1.

RÉSUMÉ

Les auteurs ont examiné la stabilité de quelques phases lors de l'analyse de mélanges polyphényls par chromatographie gazeuse. Des colonnes stables sont obtenues avec des phases mixtes stationnaires sur chromosorb P avec huiles de silicone DC-710 : UCON 50 LB et DC-710 : carbowax 20 M.

ZUSAMMENFASSUNG

Einige flüssige Phasen, die bei der Analyse von Polyphenyl-Mischungen verwendet werden, zeigen Veränderungen in ihren chromatographischen Eigenschaften, wenn sie in Füllkörpersäulen benutzt werden. Es wurde deshalb deren Stabilität untersucht. Stabile Kolonnen wurden erhalten durch Verwendung stationärer, gemischter Phasen auf chromosorb P mit 5% Silikonöl DC-710 : UCON 50 LB im Verhältnis 3 : 1 und mit Silikonöl DC-710 : Carbowax 20 M in Verhältnis von 3 : 1 und 1 : 1.

REFERENCES

1 R. A. Keller, R. Bate, B. Costa and P. Forman, *J. Chromatog.*, 8 (1962) 157.
2 R. A. Keller and G. H. Steward, *J. Chromatog.*, 9 (1962) 1.
3 G. H. Steward and R. A. Keller, *J. Chromatog.*, 12 (1963) 150.
4 W. Gerrard, S. J. Hawkes and E. F. Money, in R. P. W. Scott, *Gas Chromatography 1960*, Butterworths, Washington, 1960, p. 199.
5 Ch. Chen and D. Gacke, *Anal. Chem.*, 36 (1964) 72.
6 L. Gascó, *Anales Real Soc. Espan. Fis. Quim. (Madrid)*, to be published.
7 L. Gascó, *Anales Real Soc. Espan. Fis. Quim. (Madrid)*, to be published.
8 D. Ambrose, A. T. James, A. I. M. Keulemans, E. Kovats, H. Rock, C. Rouit and F. H. Stross, *Pure Appl. Chem.*, 1 (1960) 177.
9 L. S. Ettre, *J. Gas Chromatog.*, 1 (1963) 36.
10 R. A. Hively, *Anal. Chem.*, 35 (1963) 1921.

Further Volumes Planned
in the Series
**REACTION MECHANISMS
IN ORGANIC CHEMISTRY**

NUCLEOPHILIC AROMATIC SUBSTITUTION
By **J. Miller**

MECHANISMS OF REACTIONS OF STEROIDS
By **M. P. Hartshorne** and **D. N. Kirk**

REACTION MECHANISMS IN FLUORINE CHEMISTRY
By **J. Burdon**

FREE RADICAL POLYMERIZATION
By **A. D. Jenkins**

EVIER PUBLISHING COMPANY
STERDAM LONDON NEW YORK

REACTION MECHANISMS IN ORGANIC CHEMISTRY

A SERIES OF MONOGRAPHS

Edited by C. EABORN
Professor of Chemistry, University of Sussex, Brighton

and N. B. CHAPMAN
Professor of Chemistry, University of Hull

(former Editor: the late
E. D. HUGHES, F. R. S.
Professor of Chemistry, University College, London)

ELSEVIER PUBLISHING COMPANY
Amsterdam London New York

ORDER FORM:

To your regular bookseller or, in case of difficulty, to the publisher

ELSEVIER PUBLISHING COMPANY
P.O. Box, 211, Amsterdam

I wish to order:
(please indicate requirement below)

............copy/copies of: (title)

....

............copy/copies of: (title)

....

............copy/copies of: (title)

....

............copy/copies of: (title)

....

Name (please print)

....

Address

....

....

....

....

....

MONOGRAPH 1

NUCLEOPHILIC SUBSTITUTION AT A SATURATED CARBON ATOM

By **C. A. Bunton**
Reader in Chemistry, University
London

FROM REVIEWS...

"... sets an excellent standard for the serie
whole... All students of physical organic ch
will wish to study carefully the volume as a
and the greater part of it will be valuable to
chemists generally, especially to third-year h
and first year Ph. D. students."

N

"... it will be valuable to all students of
chemistry, whether at the H.N.C., graduate o
graduate level. Its value will be increased wh
in conjunction with its announced companion vol
elimination reactions, and with other works
series.'

JOURNAL OF THE ROYAL INS
OF CHEM

The general subject of physical organic chemistr
of age when organic chemists began to rati
their observations in terms of physical chemis
This approach was particularly fruitful in the s
reaction mechanisms, because so many
reactions are accessible to precise kinetic investi
One of the fields to be studied first was nucle
substitution, and progress here has been extraor
rapid. Whereas twenty years ago one general
was sufficient to cover most of the field, the
monograph can attempt to discuss only one
part of the subject — that which deals with subs
at a saturated carbon atom.
The first chapter is concerned with general prin
whilst the second considers the relation b
structure and reaction rate. The remaining ch
deal with the stereochemistry of the reaction
effects of changes in the reaction medium, a
role of electrophilic catalysts.

CONTENTS: 1. Nucleophilic substitution an
duality of mechanism. 2. Structural effects upo
of substitution. 3. Stereochemistry. 4. Solvent
5. Salt effects. 6. Electrophilic catalysis. Add
Subject index.

5½ x 8½ ix + 172 pages 4 figs. 9 tables 341
1963 Dfl. 20.00 or 40s. or $7.00
Paperback edition Dfl. 12.00 or 24s. or $4.00

MONOGRAPH 2

LIMINATION REACTIONS

By **D. V. Banthorpe**
Lecturer in Chemistry, University College, London

OM REVIEWS.

> . . It is well-nigh impossible to find a better presenta- n of this subject matter . . . highly recommended to vanced students and to anyone interested in reaction echanisms."
>
> *ANGEWANDTE CHEMIE* (International Edition)

e various kinds of elimination reactions form one of largest of the groups into which organic processes n be divided, and they are exceptionally important th from the synthetic aspects and from the point of w of the general theory of reaction mechanism.

is is the first detailed and unified account of these actions, with the main emphasis on the best studied d most important sub-class — the heterolytic elimi- tions which form olefins. The approach is to relate oducts and stereochemistry to the mechanism and ucture of the transition state of the reaction. Early rk is only briefly discussed, but the advances of the t decade and recent theories and speculations are ated in detail, and several novel points of view are opted.

ree chapters deal respectively with general aspects the fundamental mechanisms and stereochemistry, th the influence of environmental factors on rate and chanism, and with pyrolytic reactions in the gas ase. The remainder of the book considers more ecialized topics. A special attempt has been made correlate and interpret those reactions which occur der unusual conditions, to delineate the scope of isting theories and to point the way for future devel- ments.

NTENTS: Preface. 1. The fundamental mechanisms elimination. 2. The influence of environmental factors rate and mechanism. 3. Orientation rules and their erpretation. 4. Less usual elimination mechanisms. Elimination in cyclic systems. 6. Other elimination cesses. 7. Pyrolytic eliminations. Subject index.

x 8½" viii + 215 pages 18 tables 482 lit.refs. 1963 Dfl. 22.50 or 45s. or $8.00

perback edition Dfl. 12.00 or 24s. or $4.50

MONOGRAPH 3

ELECTROPHILIC SUBSTITUTION IN BENZENOID COMPOUNDS

By **R. O. C. Norman**
Professor of Chemistry, University of York
and **R. Taylor**
Lecturer in Chemistry, University of Sussex, Brighton

Electrophilic substitution of benzene has proved one of the most rewarding areas for research within the confines of organic chemistry, particularly as in recent years the newer developments in physicochemical techniques have contributed to our knowledge of aromatic reactivities. This timely volume reviews the subject.

After first describing the principles of the mechanistic processes of electrophilic substitution the authors deal with individual reactions with reference to current theory of mechanism. A separate chapter is devoted to the most recent theoretical developments. Synthetic applications of the reactions are described and it is demonstrated how the choice of a suitable preparative method is influenced by an understanding of the principles of mechanism. A deliberate attempt is made to relate theoretical studies to practical work.

The text is expressly designed as a stimulating and comprehensive introduction for the student while simultaneously providing the research worker with a timely review of up-to-date theory and practice which, it is hoped, will serve as the basis for future research into the many problematic areas of this subject.

CONTENTS: 1. Introduction. 2. The mechanism of electrophilic substitution. 3. Reactions involving electrophilic nitrogen. 4. Reactions involving electrophilic sulphur and oxygen. 5. Electrophilic halogen. 6. Reactions involving electrophilic carbon. 7. Electrophilic metallation. 8. Hydrogen-exchange. 9. The replacement of a substituent by hydrogen. 10. The replacement of a substituent X by a substituent Y. 11. Recent developments in the theory of electrophilic aromatic substitution. 12. Preparative aspects of electrophilic aromatic substitution. Subject index.

5½ x 8½" ix + 343 pages 8 tables 62 illus. 1965 Dfl. 35.00 or 70s. or $12.75

Paperback edition Dfl. 21.00 or 42s. or $7.00

MONOGRAPH 4

ELECTROPHILIC ADDITIONS TO UNSATURATED SYSTEMS

By **P. B. D. de la Mare**
Professor of Chemistry and Head of the Department of Chemistry, Bedford College, University of London
and **Roger Bolton**
Lecturer in Chemistry, Bedford College, University of London

This volume is the first to provide a comprehensive comparison of electrophilic additions. To achieve this, the authors have, as far as possible, presented the chemical facts, the evidence for electrophilic attack, the stereochemistry and the nature of the reaction paths available for each individual reaction as it is dealt with.

The opening chapter discusses the classification of addition reactions and the mechanisms by which they may proceed. The important subsequent chapter directs the reader's attention to the properties and the reactions of carbonium ions, setting the scene for a systematic account of additions which, because they are initiated by electrophiles, necessarily involve the development of carbonium ionic character at an intermediate stage in the reaction.

There are also chapters on addition across other unsaturated systems than mono-olefins: dienes and acetylenes are discussed in some detail, and additions to benzenoid systems are discussed to bring out the inter-relations between substitution and addition in conjugated systems. The final chapter considers addition across carbon-oxygen, carbon-nitrogen and other multiple bonds as far as they are known to be initiated by electrophilic attack.

CONTENTS: 1. Introduction. 2. The chemistry of carbonium ions. 3. Electrophilic hydrogen: addition of water to olefinic compounds. 4. Electrophilic hydrogen: addition of weak acids to olefinic compounds. 5. Electrophilic hydrogen: addition of mineral acids to olefinic compounds. 6. Halogen additions: electrophilic chlorine. 7. Additions involving electrophilic bromine and iodine. 8. Additions involving electrophilic oxygen and sulphur. 9. Additions involving electrophilic nitrogen, phosphorus and arsenic. 10. Electrophiles involving elements of groups IV, III, II and I. 11. Additions to acetylenes and allenes. 12. Additions to conjugated double bonds and to aromatic hydrocarbons. 13. Additions to other multiple bonds. Subject index.

5½ x 8½" x + 284 pages 56 schemes 24 tables
3 illus. 1966 Dfl. 40.00 or 80s. or $14.50

In Production:

THE ORGANIC CHEMISTRY OF PHOSPHORUS

By **A. J. Kirby** and **S. G. Warren**

CONTENTS: 1. Electronic structure. 2. Structi and reactivity. 3. Nucleophilic attack by valent phosphorus. 4. Elimination of trival phosphorus. 5. Free radical reactions at ph phorus. 6. Four centred rearrangements. 7. I actions not involving a central phosphorus atc 8. Nucleophilic attack on trivalent phospho compounds. 9. Nucleophilic attack on ph phonium salts and pentavalent phosphorus co pounds. 10. Nucleophilic attack on tetrahed P^V compounds. 11. Phosphorylation.

AROMATIC REARRANGEMENTS

By **H. J. Shine**

CONTENTS: 1. The acid-catalyzed rearran ments of alkyl- and halogenoaromatic co pounds. 2. The rearrangement of esters a ethers. 3. The rearrangement of N-substitut aminoaromatic compounds. 4. The rearrangem of N-oxides. 5. Base-catalyzed rearrangeme accompanying nucleophilic substitution. 6. Pho chemical rearrangements.

MULTICHANNEL INTEGRATING FLAME PHOTOMETER

J. W. HAAGEN-SMIT AND J. RAMÍREZ-MUÑOZ
Scientific and Process Instruments Division, Beckman Instruments, Inc., Fullerton, Calif. 92634 (U.S.A.)

(Received April 4th, 1966)

A newly-developed concept in flame photometry, primarily designed for rapid analysis of such routine samples as biological fluids and tissues, waters and many fluids in which sodium, potassium and calcium determinations are involved at low, medium and high concentrations, is described. The instrument developed is fitted with an automatic sample changer, so that 60 samples may be analyzed per hour (24 samples/run) without operator attendance. The capabilities of the instrument in the analysis of blood serum are summarized in Table I.

TABLE I

ANALYSIS OF BLOOD SERUM

Range, blood serum:
from 100 to 200 meq/l Na (sample at 1:200 dilutions)
0 to 10 meq/l K (sample at 1:200 dilutions)
0 to 10 meq/l Ca (sample at 1:25 dilutions)
other samples may be measured at appropriate dilution.
Instrument range, fullscale without dilutions:
from 0.5 to 1.0 meq/l Na; 0–0.05 meq/l K; 0–0.4 meq/l Ca
Repeatability:
±0.5% of fullscale standard deviations (±1 meq/l, 1:200 dilutions) for sodium
±1% of fullscale standard deviations (±0.1 meq/l, 1:200 dilutions) for potassium
±1% of fullscale standard deviations (±0.1 meq/l, 1:25 dilutions) for calcium
Aspiration rate: approximately 1 ml/min.
Aspiration time: approximately 30 sec.
Practical minimum blood serum sample: 0.01 ml.
Cycle time (automatic sampling attachment): 1 min/sample.

As is well known, emissions from flames are subject to variations, due, principally, to known factors such as flame temperature, sample flow and unknown factors that arise mainly in the spray chamber and atomizer. In order to minimize variations in readings due to various changes, a fixed concentration of lithium as a soluble lithium salt is added to each sample as an internal standard. The instrument readout, therefore, is actually the ratio of the ion of interest to lithium ion. Several investigators have proved the usefulness of the internal standard technique[1]. For the internal standard to be of any value, the emission characteristics of the standard and the ion to be measured must, of course, be very similar, and in the present case where 3 ions were to be measured simultaneously, matching of 3 emission characteristics under the same flame conditions became rather difficult. However, a reasonable match was achieved for K, Na and Ca. Even so, sodium is not perfectly compensated for large changes in flame temperature, so that pressure regulation of fuel and air is still an important factor. Figure 1 illustrates stability of readings as a function of fuel pressure.

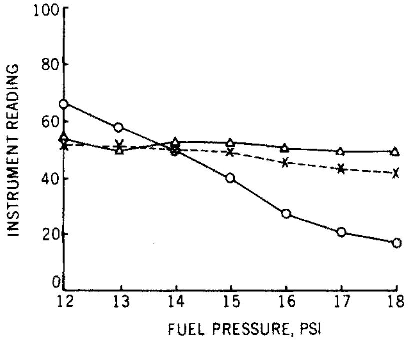

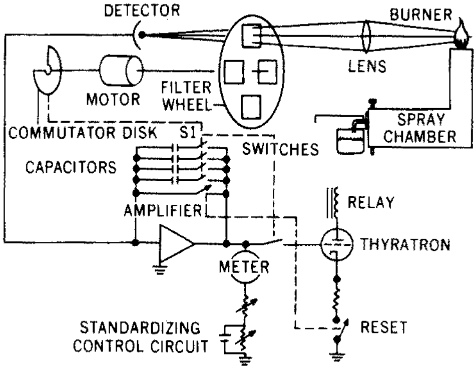

Fig. 1. Effect of fuel pressure on stability of readings. (o) sodium; (×) potassium; (△) calcium.

Fig. 2. Schematic diagram of apparatus.

Further improvement in signal-to-noise ratio may be obtained by use of the integration technique, where the output of the detector is electronically integrated over a sufficient period of time to allow random fluctuations to be averaged out. Flame photometers can be combined with integration techniques to achieve better results[2]. In general, past instruments have required a separate detector and amplifier for each element to be analyzed. Another set has been required for the internal standard, but the resulting combination of parallel channels is expensive. It must be continually and carefully maintained to minimize electronic shifts in zero and sensitivity if accurate analyses are to be obtained.

In the present assembly, the multichannel system requires only one detector and amplifier. The problems associated with drift of the amplifier and photomultiplier practically disappear in the ratioing process.

EXPERIMENTAL

Instrumentation

Figure 2 shows the schematic diagram of the instrument. The sample is atomized into a spray chamber by means of an air aspirator and then excited in a propane–air flame. The propane used is the ordinary commercial grade in 26 fl-oz. cylinders. A single detector monitors the flame through a series of optical filters whose transmission characteristics correspond to the principal emission lines of the elements to be measured. The optical filters are mounted on a motor-driven circular disk, which revolves at about 1800 rev./min. The signals are received by the detector as a series of short pulses of light energy. After conversion to electrical current, the pulses are stored by the electronic integrating amplifier.

By using a number of integrator capacitors and a series of switches to complete the integrator circuit sequentially, the combined signals for the various elements are separated and individually integrated. In practice, the switches are driven by the same motor used for rotating the optical filters. Synchronization is achieved simply by this method. Magnetically-operated reed switches are used because of demand for speed, reliability and long life.

A thyratron tube monitors the progress of the integration of the lithium standard. When the integrated lithium signal reaches a preset level, integration is terminated on all channels. To read out results, it is necessary to close individually the proper switch to connect the proper capacitor to the integrating amplifier. In practice, the switches used during the integration period are not used during readout. Functionally, the readout switches are the same, but during readout 3 separate sets of controls for adjustment of zero and span are switched along with the storage capacitors.

To restart the cycle, all that is required is to discharge the integrating capacitors and reset the thyratron. Advantages of the system are: (*a*) use of a single detector and amplifier, eliminating effects of zero and sensitivity drifts; (*b*) due to rapid interposition of the filters, there is a minimum of possible emission differences in the flame and sensitivity differences in the detector in the period of time between signals obtained at various wavelengths; (*c*) a simple and stable optical configuration is possible since only one optical path is required; (*d*) by integrating the signals over a sufficient length of time, a high signal-to-noise ratio is achieved and local or short-term flame variations are averaged out; (*e*) use of the internal standard minimizes the variation in flame emission resulting from changes in sample flow rate, fuel flow rate or air flow rate, and also compensates for amplifier or detector changes.

Operating procedure

Only 3 switches need be operated to read out results, and the results of analysis are stored in the integrator capacitors, available for readout at any time, so that automation becomes relatively simple. Only a sample, the selector switches and a reset switch are needed to initiate the next cycle.

With the automatic sample changer used, the flame photometer itself controls the operation after initial preparation by the operator. Initially, the Mode Switch on the sample changer is set to the MANUAL position and preliminary operations of standardization are done, using the front pushbuttons and standardizing controls on the inner front panel. The sample tray, holding up to 24 sample cups, is placed on the changer base and the Changer Mode Switch turned to AUTOMATIC; the sample tray tilts and presents the first sample to the atomizer. The flame photometer integrates emissions from the sample; and, when ready, the same thyratron that terminates the integration, signals the sample changer that readout may begin.

A small motor, fitted with a cam, lowers the turntable and, by means of a geneva mechanism, rotates the turntable to position the next sample under the atomizer tip. Sampling begins again and, simultaneously, the same motor carries a magnet past a series of magnetically-operated reed switches which select the required circuits. The element concentrations are displayed in sequence by the front panel meter and at the recorder terminals. Since sodium and potassium analyses are done at 1:200 dilutions and calcium at a dilution of 1:25, only 2 elements are read out at one time: Na and K or Na and Ca. The last switches reset the flame photometer and stop the sample changer motor until the next starting signal is received. Additional switches are provided for operation of a digital printer.

The 2 units continue to cycle automatically until the turntable reaches a position that contains no sample; such as position 25, so constructed that it cannot hold a sample cup. Since at that point no signals are being received by the flame photometer, the operation automatically stops. This avoids possible repetitive analysis of previous samples and accumulation of meaningless data, if no samples are present.

RESULTS AND DISCUSSION

Since the instrument is designed for determinations of Na, K, and Ca in solutions, a convenient correlation should be maintained between its physical instrumental performance and its analytical behavior, either when used for routine determinations in a number of equal or very similar samples (for instance, body fluids) or in the analysis of specific types of single samples. In other words, the physical information picked up by the instrument from the sample introduced in the flame (as a selected light signal) should be properly transformed into useful chemical information by a numerical concentration value, close to the real chemical quantitative composition of the solution examined. In order to achieve this ideal, a series of characteristics should be considered.

Good repeatability for each ion to be determined in single or multiple solutions and with short- and long-term tests. Table II shows calibration values obtained at different days trying to repeat and optimize the working settings. Table III shows values obtained by means of repeated readings taken from the same solution under the

TABLE II

REPEATABILITY IN LONG-TERM TESTS

Element	*Expected reading*[a]	*Readings (Average of several readings after optimization)*[a]	*Number of readings averaged*
Sodium (Dilution ratio 1:200)	150.0	149.6	24
	150.0	149.6	24
	145.0	145.0	24
	145.0	145.1	24
	200.0	199.8	24
	200.0	199.6	24
	200.0	200.7	24
	200.0	199.8	12
Potassium (Dilution ratio 1:200)	5.0	5.04	24
	5.0	4.94	24
	4.5	4.49	24
	4.5	4.53	24
	10.0	9.99	24
	10.0	10.01	24
	10.0	10.06	24
	10.0	10.05	12
Calcium (Dilution ratio 1:25)	10.0	10.04	24
	10.0	10.02	24
	10.0	9.98	12

[a] Expressed in meq/l of each element before dilution.

same operating conditions. Precision is expressed in terms of standard deviation from the average of percentages referred to fullscale.

Convenient analytical concentration range for each ion to be determined, covering the commonest ranges to be encountered in routine analysis at an established dilution ratio. The ranges should be such that they may be reached by single dilution at different dilution ratios (or by an easy concentration process) with samples of diverse concentration levels. These characteristics widen the applicability of the method to a variety of different samples.

Optimum concentration ranges covered by the instruments are given in Table IV; normal values of Na, K, and Ca in blood serum, for instance, after proper dilution, appear within the ranges shown in Table III. (For a complete study of analysis of biological materials, see references 1 and 3.)

TABLE III

REPEATABILITY IN SHORT-TERM TESTS

Element	*Number of readings*	*Average of readings (meq/l)*	*Standard deviation (expressed in scale divisions)*	*% Fullscale*	*Type of solution*
Sodium	24	149.6	0.264	0.13	50% Standard
(Dilution ratio	24	145.0	0.406	0.20	45% Standard
1:200)	24	199.8	0.358	0.18	100% Standard
	12	140.3	0.319	0.16	Serum
	12	141.6	0.332	0.17	Serum
	12	112.1	0.405	0.20	Serum
	12	138.5	0.341	0.17	Serum
Potassium	24	5.04	0.048	0.48	50% Standard
(Dilution ratio	24	4.49	0.049	0.44	45 %Standard
1:200)	24	9.99	0.017	0.17	100% Standard
	12	10.08	0.035	0.35	Serum
	12	6.24	0.024	0.24	Serum
	12	4.38	0.017	0.17	Serum
	12	9.57	0.028	0.28	Serum
Calcium	24	10.04	0.052	0.52	100% Standard
(Dilution ratio	24	10.02	0.057	0.57	100 %Standard
1:25)	12	9.98	0.036	0.36	100% Standard
	24	2.27	0.017	0.17	Serum
	24	2.06	0.014	0.14	Urine

TABLE IV

CONCENTRATION RANGES

Recommended dilution ratios for serum	*Scale*	*Element*	*Scale range*	
			meq/l	*p.p.m.*
1:200	Na/K	Na	0.5–1.0	11.5–23
		K	0–0.05	0–1.95
1:25	Na/Ca	Na	4–8	92–184
		Ca	0–0.4	0–8

Good linearity or a constantly reproducible curvature. Typical calibration curves are shown in Fig. 3. The curvature of the sodium curve has remained constant over a long period of instrument use.

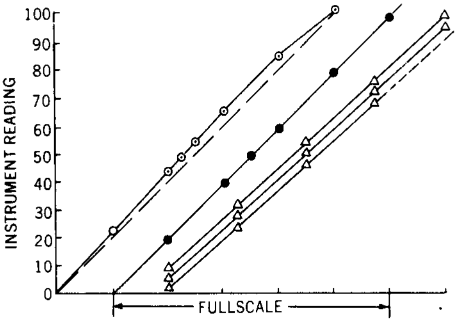

Fig. 3. Typical calibration curves. (⊙) Na, 1:200; (●) K, 1:200; (△) Ca, 1:25.

TABLE V

ACCURACY TESTS—VARIOUS Na/K RATIOS

Na/K ratios (both concns. in meq/l)[a]	*Sodium*		*Potassium*	
	Concn. found (meq/l)[a]	*% Error*	*Concn. found (meq/l)*[a]	*% Error*
120/5	122.3	+1.2	4.92	−1.6
140/5	140.9	+0.6	5.05	+1.0
160/5	159.3	−0.4	5.10	+2.0
180/5	182.2	+1.2	5.07	+1.4
140/8	140.2	+0.1	8.20	+2.4

[a] Concentrations prior to dilution at the dilution ratio 1:200.

TABLE VI

ACCURACY TESTS—PRELIMINARY DILUTION[a]

Na/K ratios before dilution[b]	*Na/K ratios after dilution*[b]	*Na concn. found*[b]	*K concn. found*[b]
200/5	160/4	159.8	3.96
200/5	142.8/3.57	142.2	3.48
200/5	111.1/2.77	111.5	2.96

[a] Dilution with various volumes of 90 p.p.m. lithium solution added to diluted solutions at 1:200 dilution ratio.

[b] Concentrations in meq/l referred to original solutions before 1:200 dilution ratio.

TABLE VII

ACCURACY TESTS—DILUTION METHOD

Na/K ratios before dilution[a]	*Diluting Na/K solution*[a]	*Na/K ratios after dilution*[a]	*Na concn. found*[a]	*K concn. found*[a]
200/5	140/2	170/3.5	170.7	3.47
140/8	120/2	130/6.5	129.6	6.52

[a] Concentrations in meq/l referred to original solutions before dilution at 1:200 dilution ratio.

TABLE VIII

ACCURACY TESTS—CLOSE STANDARD METHODS[a]

(Solutions containing sodium and potassium)

Na concn. present[b,c]	*Na concn. found*[c]	*K concn. present*[b,c]	*K concn. found*[b,c]
145·7	145·5	4·62	4.60
	146.1		4.61
	145·5		4.61
144·1	144·3	4·45	4·41
	144·2		4·43
	144.6		4·44
	144·3		4·46

[a] By comparison with single standards similar in concentration to the sample.
[b] Found by calibration method.
[c] Concentrations in meq/l referred to original solutions before dilution at 1:200 dilution ratio. Standard contained 145 meq/l Na and 4.6 meq/l K.

TABLE IX

ACCURACY TESTS—CALCIUM SOLUTIONS IN THE PRESENCE OF SODIUM

Na concn. present[a]	*Ca concn. present*[a]	*Known addition of Ca*[a]	*Calculated Ca concn.*[a]
Addition method			
100	2.50	2.50	2.45
100	2.50	5.00	2.44
100	2.50	7·50	2.48
150	2.50	2.50	2.42
150	2.50	5.00	2.49
150	2.50	7·50	2.50
200	2.50	5.00	2.46
200	2.50	7·50	2.47
200	2.50	5.00	2.48
200	2.50	7·50	2.51
Close standard method			
200	2.50	—	2.50
200	2.50	—	2.44
200	2.50	—	2.44
200	2.50	—	2.48
200	2.50	—	2.46
200	2.50	—	2.42
Two standard method			
100	5.00	—	4·99
150	5.00	—	5.06
200	5.00	—	5.07

[a] Concentrations in meq/l referred to original solutions before dilution at 1:25 dilution ratio.

Accuracy within reasonable limits for each single ion of interest, even in the presence of any of the other accompanying ions to be determined and/or components. Results of some accuracy tests are shown in Tables V–IX.

Enough sensitivity to allow determination (not simply detection) of the ions of interest at low concentrations and at low dilution ratios—if considered as relative sensitivity— and from small fractions of original sample if considered as absolute sensitivity. Because of the wide range of available control of the instrument (0% and 100%), the instrumental sensitivity itself can be adjusted to a variety of values which allows work at different relative percentage sensitivities. Maximum percentage sensitivity is reached when the fullscale is used. Sensitivities achieved for the different metal ions are summarized in Table X; relative and absolute values are included.

TABLE X

SENSITIVITY

Sensitivity criteria	*Sodium (1:200 dilution ratio scale)*	*Potassium (1:200 dilution ratio scale)*	*Calcium (1:25 dilution ratio scale)*
Relative values (meq/l)			
Sensitivity as fullscale reading	1	0.05	0.4
Sensitivity as attainable dynamic range	0.5–1	0.0005–0.05	0.004–0.4
Sensitivity as concn. attainable per 1 scale division	0.005	0.0005	0.004
Absolute values			
Sensitivity as minimum amount of sample	0.0015–0.002 ml	0.0015–0.002 ml	0.012–0.016 ml
Sensitivity as amount of analyte per 1 scale division	$1.8 \cdot 10^{-10}$ to $2.4 \cdot 10^{-10}$ g	$3 \cdot 10^{-11}$ to $4 \cdot 10^{-11}$ g	$9.6 \cdot 10^{-10}$ to $1.28 \cdot 10^{-9}$ g

The performance data shown in the preceding paragraphs clearly demonstrate the suitability of the instrument to perform a variety of Na, K, and Ca determinations with great analytical confidence, once the metal ions of interest are brought within the limits of the optimum final concentration range by dilution or concentration.

The authors wish to thank Beckman Instruments, Inc. for permission to publish this paper.

SUMMARY

A new high-speed optical chopping and demodulation system is described for use in flame photometry. Methods are described which allow integration of signal and noise over many optical pulses of flame energy. The method has been used to develop a direct-reading instrument for sodium, potassium and calcium. With this method, 4 signal channels are integrated simultaneously. With the integration technique, ordinary flame noise is significantly reduced. By using an internal standard, all signal channels are referenced to known energy levels regardless of flame variations.

RÉSUMÉ

Un nouveau système est proposé pour la photométrie de flamme. On décrit des méthodes permettant une intégration du signal et du bruit sur plusieurs pulsations optiques d'énergie de flamme. Ce procédé a été appliqué à la photométrie du sodium, du potassium et du calcium; 4 canaux sont intégrés simultanément. Grace à la technique d'intégration, le bruit de flamme ordinaire est considérablement réduit. L'utilisation d'étalon interne, permet d'éviter de tenir compte des variations de flammes.

ZUSAMMENFASSUNG

Ein neues, sehr schnelles optisches Chopping- und Demodulations-System wird für die Verwendung bei der Flammenphotometrie beschrieben. Es werden Methoden angegeben, die die Integration des Signals und Rauschens über viele optische Flammenenergiepulse erlauben. Die Methode wurde zur Entwicklung eines direkt schreibenden Instruments für Natrium, Kalium und Calcium verwendet. Mit dieser Methode werden gleichzeitig 4 Kanäle integriert. Mit der Integrationstechnik wird der gewöhnliche Flammenpegel reduziert. Bei Verwendung eines inneren Standards werden alle einzelnen Kanäle auf bekannte Energieniveaus bezogen unabhängig von Flammenvariationen.

REFERENCES

1 See, *e.g.*, F. Burriel-Martí and J. Ramírez-Muñoz, *Flame Photometry, A Manual of Methods and Applications*, Elsevier Publishing Co., Amsterdam, 1960.
2 See, *e.g.*, J. A. Ramsay, S. W. H. W. Falloon and K. E. Machin, *J. Sci. Instr.*, 28, F5 (1951).
3 H. A. Teloh, *Clinical Flame Photometry*, Charles C. Thomas Publ., Springfield, Ill., 1959.

LE DOSAGE DE TRACES D'ARGENT DANS LE ZINC EXTRA-PUR PAR ACTIVATION NEUTRONIQUE

F. MOUSTY*, J. FOUARGE* ET G. DUYCKAERTS
Laboratoire de Chimie Nucléaire, Institut de Chimie et Métallurgie, Université de Liège, Liège (Belgique)
(Reçu le 4 juillet, 1966)

Même à proximité d'un réacteur, le dosage non destructif de traces d'argent inférieures à quelques p.p.m., basé sur les courtes périodes, à savoir, ^{108}Ag ($T_{\frac{1}{2}}=2.3$ min) et ^{110}Ag ($T_{\frac{1}{2}}=24$ sec), n'est pas possible dans le zinc en raison de l'activation propre de la matrice: ^{71}Zn ($T_{\frac{1}{2}}=2.2$ min) et ^{69m}Zn ($T_{\frac{1}{2}}=13.9$ h)[1].

Par contre, l'analyse basée sur l'activation des longues périodes, à savoir, ^{110m}Ag ($T_{\frac{1}{2}}=253$ j) et ^{65}Zn ($T_{\frac{1}{2}}=245$ j), ne présente pas, en principe, de difficultés particulières sinon l'obligation de séparer ^{110m}Ag dans un très bon état de pureté radiochimique.

Etant donné la période de ^{110m}Ag, on peut, le cas échéant, attendre la décroissance des périodes courtes avant de faire la séparation.

Par ailleurs, le rapport d'activation Ag/Zn ne dépendant pratiquement pas de la durée de l'irradiation, on peut, sans accroître les activités à manipuler et sans diminuer l'activité de l'argent, compenser l'effet d'un flux moindre ou d'une durée d'irradiation plus courte par une augmentation proportionnelle du poids de l'échantillon.

La méthode de séparation proposée pour séparer l'argent chimiquement et radiochimiquement pur consiste en une double électrolyse en milieu nitrique faite dans des conditions convenables pour obtenir un dépôt adhérent et compact.

DONNÉES NUCLÉAIRES ESSENTIELLES[2]

L'activité du zinc irradié aux neutrons thermiques résulte principalement des captures suivantes:

$$\text{(a)}\quad {}^{64}\text{Zn}\ (\approx 49\%)\ \xrightarrow[\sigma=0.5\,\text{b}]{(\text{n},\gamma)}\ {}^{65}\text{Zn}:\quad T_{\frac{1}{2}}=245\ \text{j}\qquad\qquad \text{E.C. } 98.5\%$$

44% des captures électroniques (E.C.) laissent le nuclide au niveau 1.114 MeV, source du rayonnement caractéristique.

$$\text{(b)}\quad {}^{68}\text{Zn}\ (\approx 18\%)\ \xrightarrow[\sigma=0.09\,\text{b}]{(\text{n},\gamma)}\ {}^{69m}\text{Zn}:\quad T_{\frac{1}{2}}=13.8\ \text{h}\qquad\qquad \gamma = 0.438\ \text{MeV}$$

$${}^{68}\text{Zn}\ (\approx 18\%)\ \xrightarrow[\sigma=0.9\,\text{b}]{(\text{n},\gamma)}\ {}^{69}\text{Zn}:\quad T_{\frac{1}{2}}=52\ \text{m}\qquad\qquad \beta = 0.9\ \text{MeV (max)}$$

---

* Chercheurs de l'Institut Interuniversitaire des Sciences Nucléaires.

$$\text{(c)}\quad {}^{70}\text{Zn}\ (\hat{\approx}0.6\%) \xrightarrow[\sigma\,\hat{\approx}\,0.096]{(\text{n},\gamma)} {}^{71}\text{Zn}:\quad T_{\frac{1}{2}} = 2.2\ \text{min} \qquad \left\{\begin{array}{l}\beta^- = 2.4\ \text{MeV}\\ \gamma\ = 0.12;\ 0.51;\\ \qquad 0.90;\ 1.09\ \text{MeV}\end{array}\right.$$

$${}^{70}\text{Zn}\ (\hat{\approx}0.6\%) \xrightarrow{(\text{n},\gamma)} {}^{71\text{m}}\text{Zn}:\quad T_{\frac{1}{2}} = 3\ \text{h} \qquad \left\{\begin{array}{l}\beta^- = 1.5\ \text{MeV}\\ \gamma\ = 0.38;\ 0.41;\\ \qquad 0.61\ \text{MeV}\end{array}\right.$$

L'argent s'active de même en donnant surtout des nuclides à périodes très courtes.

$$\text{(a)}\quad {}^{107}\text{Ag}\ (51.4\%) \xrightarrow[\sigma=30\,\text{b}]{(\text{n},\gamma)} {}^{108}\text{Ag}:\quad T_{\frac{1}{2}} = 2.3\ \text{min} \qquad \left\{\begin{array}{l}\beta^-(98\%) = 1.8\ \text{MeV}\\ \gamma \qquad\quad\ = 0.43\ \text{MeV}\end{array}\right.$$

$$\text{(b)}\quad {}^{109}\text{Ag}\ (48.6\%) \xrightarrow[\sigma=96\,\text{b}]{(\text{n},\gamma)} {}^{110}\text{Ag}:\quad T_{\frac{1}{2}} = 24.2\ \text{sec} \quad \left\{\begin{array}{l}\beta^- = 2.84\,(40\%);\ 2.16\,(60\%)\\ \gamma\quad \text{divers}\end{array}\right.$$

$${}^{109}\text{Ag}\ (48.6\%) \xrightarrow[\sigma=2.3\,\text{b}]{(\text{n},\gamma)} {}^{110\text{m}}\text{Ag}\left|\overset{\uparrow\, 5\%}{}\right. \xrightarrow{95\%} T_{\frac{1}{2}} = 253\ \text{j}$$

Ce dernier nuclide, sur lequel se base notre analyse, présente un schéma de désintégration assez compliqué; dans les grandes lignes, on a:

$\beta^- = 0.536\ (43\%);\ 0.086\ (55\%)$ MeV

$\gamma\ = 0.656\ (100\%);\ 0.880\ (75\%);\ 0.93\ (25\%);\ 0.76\ (24\%);\ 1.38\ (20\%);$
$1.56\ (13\%)$ MeV; etc.

Dans la suite nous n'utilisons que les 2 raies γ à 656 et 880 keV.

Sous l'action de neutrons suffisamment rapides, 2 réactions parasites, qui peuvent également engendrer $^{110\text{m}}$Ag, sont à considérer ici en raison de la présence possible des éléments parents dans le zinc en général; ce sont les réactions:

$${}^{110}\text{Cd} \xrightarrow[(\text{n,p})]{} {}^{110\text{m}}\text{Ag}\ \ (Q = \text{env. } 10\ \text{MeV})\ \text{et}\ {}^{113}\text{In} \xrightarrow[(\text{n},\alpha)]{} {}^{110\text{m}}\text{Ag}$$

Toutefois, dans ce cas particulier de zinc extra-pur, avec un taux d'impureté inférieur à quelques p.p.m., leurs incidences sont tout à fait négligeables; en effet, d'un point de vue général, même en l'absence de valeurs précises, on sait que les sections de telles réactions sont assez petites (milli ou microbarns) avec les neutrons de fission où la proportion de ceux qui sont de plus en plus rapides diminue vite avec l'énergie.

Plus précisément d'ailleurs, le calcul à partir des masses isotopiques montre que la première réaction est de toute façon endoergique de 10 MeV environ, et le proton doit encore passer la barrière du potentiel nucléaire.

De même, pour la seconde, si la réaction est théoriquement exoergique (env. 3.5 MeV) et donc permise avec les neutrons thermiques, sa probabilité demeure très faible en raison de la barrière de potentiel et, de surcroît, la proportion isotopique de ^{113}In dans l'élément naturel, n'atteint que 4.2%.

RENSEIGNEMENTS EXPÉRIMENTAUX

Irradiation

Divers échantillons de zinc de pureté variant entre 99.995 et 99.9999, pesant entre 0.5 et 1.5 g, ont été irradiés soit à la pile EL3 de Saclay ($3 \cdot 10^{12}$ n/cm²/sec) soit au BR2 de Mol ($3 \cdot 10^{13}$ n/cm²/sec).

Les durées d'irradiation ont été respectivement de 7 jours et de 2 jours ce qui correspond à des flux intégrés de $1.8 \cdot 10^{18}$ et $5.2 \cdot 10^{18}$ n/cm² et donne des activités de l'ordre de 4 à 10 mc de zinc (^{65}Zn).

Les étalons utilisés ont été essentiellement préparés à partir de solutions titrées de $AgNO_3$ dont un petit volume mesuré exactement était évaporé au fond d'un tube en quartz à parois minces (0.5 mm). Ces tubes sont ensuite scellés et logés côte à côte avec les échantillons de zinc emballés dans du papier d'aluminium.

Les séparations étaient normalement effectuées de 1 à 2 semaines après la fin des irradiations.

Appareillage

La mise en solution et la première électrolyse sont effectuées dans l'appareil représenté sur la Fig. 1A. Il s'agit d'un tube en pyrex à fond plat, soigneusement recuit, terminé par un rodage B34.

Pour la mise en solution du zinc, le tube est coiffé d'un petit entonnoir à robinet qui se prolonge à l'intérieur par un capillaire recourbé vers la paroi du tube (rinçage) et d'un tube de dégagement prolongé par un tuyau plastique bourré d'ouate imbibée de glycol afin d'arrêter les aérosols actifs.

Pour l'électrolyse, on remplace la tête par le bouchon porte-électrodes (Fig. 1B);

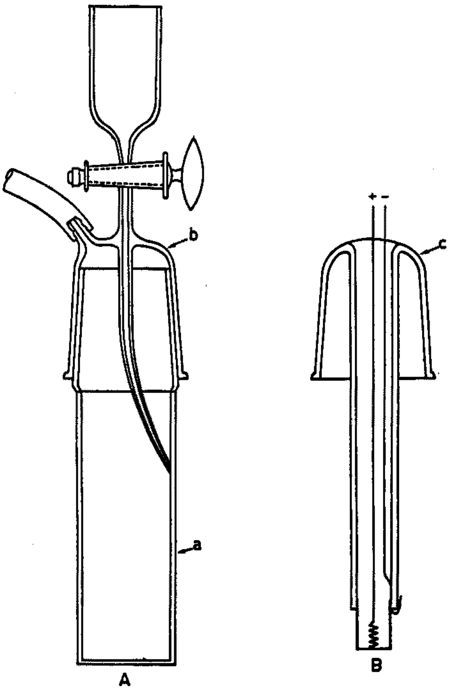

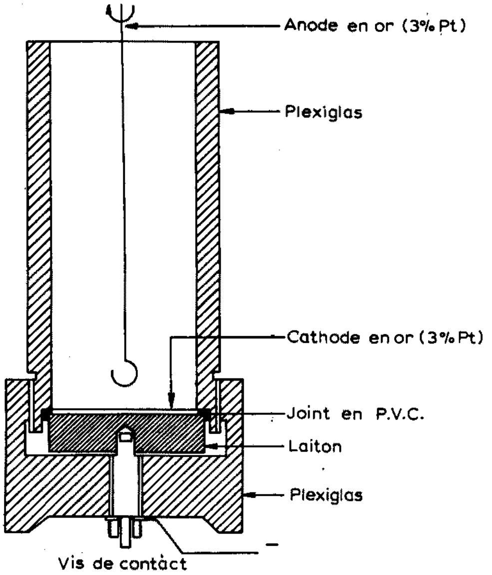

Fig. 1. (A) Appareil servant à dissoudre le zinc. (B) Appareil servant à la première électrolyse de l'argent.

Fig. 2. Appareil servant à la seconde électrolyse de l'argent.

l'anode est constituée par un fil d'or pur de 0.25 mm de diamètre; la cathode est faite d'une feuille (0.25 mm d'épaisseur) d'un alliage élastique d'or à 3% de platine qui est roulée en forme de cylindre fendu le long de la génératrice: sa hauteur est de 3 cm, son développement de 5.5 cm.

L'expérience acquise à la suite d'essais préliminaires[3,4] nous a conduit à réaliser simultanément le contact avec le fil d'or d'amenée du courant et la fixation de la cathode à la base du tube de verre en profitant de son expansion élastique naturelle.

La seconde électrolyse s'opère dans un autre appareil réalisé en plexiglas (Fig. 2): un tube d'environ 2 cm de diamètre intérieur dont le fond est la cathode en or à 3% de platine (diamètre 24 mm; épaisseur 0.25 mm). Un écrou en plexiglas la maintient fermement en écrasant un joint en polyéthylène assurant l'étanchéité.

L'anode tournante fixée à l'axe d'un petit moteur, est faite d'un bout de fil rigide du même alliage (diamètre 1.2 mm) dont l'extrémité est repliée en forme de boucle.

Mise en solution des étalons

Le bris des tubes de quartz contenant les étalons de nitrate d'argent se fait dans une solution de quelques ml d'acide nitrique 3.5 *N* contenant une quantité connue de $AgNO_3$ entraîneur (±50 mg d'Ag), après avoir au préalable rayé le tube au moyen d'un diamant.

La solution est transférée quantitativement dans un flacon jaugé de 50 ml et complétée au volume au moyen d'acide nitrique 3.5 *N*.

On prélève 5 ml pour les comptages intégraux au compteur à puits et 10 ml pour l'électrolyse sur cathode d'or.

Mise en solution du zinc et séparation de l'argent par électrolyse

On introduit, dans l'appareil représenté sur la Fig. 1A, l'échantillon de zinc (±1 g) et 1 ml de la solution connue d'entraîneur (10 à 50 mg d'Ag). Par l'entonnoir supérieur, on laisse couler en une fois la solution sulfonitrique chaude qui vient d'être préparée comme suit: 6 ml d'eau, 1.5 ml de H_2SO_4 (36 *N*) et 0.5 ml de HNO_3 (14 *N*).

Lorsque la vitesse d'attaque diminue, on ajoute petit à petit 3 ml d'acide nitrique 14 *N*; la dissolution du zinc se fait de manière régulière et dure de $\frac{1}{4}$ à $\frac{3}{4}$ d'heure; à la fin on rince les parois et on ajoute 1 à 2 g d'acide sulfamique en cristaux.

On remplace alors la tête de l'appareil par celle représentée sur la Fig. 1B et on électrolyse, en agitant, sous 1.5 V, jusqu'à courant presque nul ($\frac{1}{2}$ à $\frac{3}{4}$ h).

On retire la tête, on rince avec précaution, puis on détache la cathode en or recouverte du dépôt d'argent.

L'argent est alors redissous par 3 ml d'acide nitrique concentré; on y ajoute 2 ml d'eau, 2 g d'acide sulfamique, 2 ml d'une solution concentrée de nitrate de zinc inactif, quelques grains de sulfate ferreux... et on transvase le tout dans le second appareil d'électrolyse (Fig. 2).

Cette seconde électrolyse s'effectue encore sous 1.5 V, jusqu'au vingtième environ de l'intensité initiale (50–80 mA).

Le dépôt bien adhérent est lavé à l'eau et à l'alcool, sèché et pesé pour connaître le rendement chimique de l'électrolyse.

Les premiers essais de séparation d'argent par électrolyse en milieu nitrique ont été effectués sur cathodes en platine; les résultats furent peu satisfaisants. Deux difficultés furent observées: (*a*) un dépôt cathodique d'argent peu adhérent; (*b*) un dépôt anodique d'oxydes supérieurs d'argent[5]. Pour y remédier, nous avons remplacé la cathode en platine par une cathode en or à 3% de Pt, les dimensions réticulaires sont plus voisines de celles de l'argent. Cela a conduit immédiatement à une amélioration notable de l'adhérence du dépôt.

Par ailleurs, pour éviter le dépôt anodique, il a suffit d'introduire dans la solution un dépolarisant anodique comme le sulfate ferreux ou l'acide sulfamique.

Enfin, pour éviter la formation de dépôt cathodique en aiguilles, il faut maintenir une concentration en acide nitrique entre 3 et 6 *N*.

Le facteur de décontamination dans une électrolyse de ce genre est de l'ordre de 10^4 à 10^5.

Les mesures

Les mesures ont consisté essentiellement en comptages et en spectres "gamma"; on compare ensuite à un étalon représentatif irradié simultanément.

D'une part, le comptage gamma intégral a été réalisé avec un cristal NaI (Tl) de 5 × 5 cm, et, pour autant que la pureté radiochimique soit excellente, on en attend la meilleure précision statistique en raison du nombre total de coups enregistré qui est maximum.

D'autre part, les spectres-γ ont été relevés à l'aide d'un cristal de 7.5 × 7.5 cm, associé à un spectromètre multicanaux. Sur la Fig. 3, nous avons tracé l'histogramme du spectre de l'échantillon no. 10. C'est à partir de ces spectres que nous avons dosé l'argent; nous avons comparé des surfaces homologues de l'échantillon et de l'étalon: de 2 façons légèrement différentes.

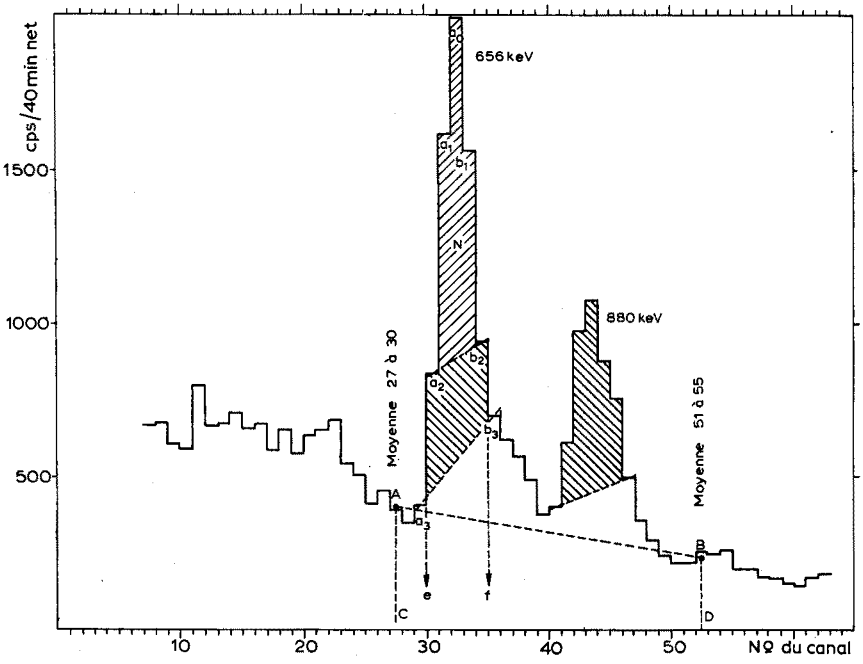

Fig. 3. Illustration graphique des méthodes d'évaluation de l'argent après spectrométrie gamma: méthode de la surface des pics caractéristiques et méthode de COVELL.

(1) Méthode de la surface des 2 pics photoélectriques principaux (656 et 880 keV). On fait la somme des activités des canaux comprenant entièrement ces 2 pics et on en soustrait l'activité comprise dans le trapèze (ABDC) qui en forme la base.

Afin de minimiser l'erreur statistique sur les hauteurs des 2 côtés du trapèze ainsi délimité, nous considérons pour chacune une valeur moyenne des activités de quelques (3 à 5) canaux situés de part et d'autre de chacune de ces limites.

(2) Méthode de Covell[6]. Cette méthode est utile notamment lorsque les spectres sont composites, et là où les bases des pics sont mal aisées à établir: on calcule l'activité nette de la partie supérieure caractéristique, N, de l'un ou de l'autre pic de ^{110m}Ag; à cet effet, de part et d'autre du canal représentant le maximum du pic (a_0 sur l'histogramme), on considère un même nombre, n, de canaux choisis de façon à englober ainsi de l'ordre de la moitié aux trois quarts du pic à déterminer. On fait la somme des activités comprises dans ces $2n+1$ canaux et on retranche la somme des activités comprise dans un trapèze inférieur, limité au sommet par une droite joignant les 2 canaux extrêmes considérés, a_n et b_n (sur l'histogramme présenté, le trapèze $a_2\ b_2\ f\ e$, par exemple).

Aux faibles activités, cette dernière méthode souffre, à notre avis, des 2 défauts résultant de l'incidence rapidement croissante des erreurs dues à la nature statistique des comptages, car: d'une part, le nombre de coups considéré pour évaluer l'élément est fortement réduit par rapport au comptage intégral (surfaces hachurées sur l'histogramme); d'autre part, l'erreur sur la valeur de la surface trapézoïdale à retrancher dépend uniquement de la précision des hauteurs des 2 seuls canaux extrêmes considérés (ici a_2 et b_2 ou a_3 et b_3).

En complément de ces mesures, et dans la première série d'analyses seulement, nous avons en outre procédé au comptage β des plaquettes portant l'argent, sans cependant introduire dans les valeurs les corrections d'autoabsorption et de rétrodiffusion.

Dans la seconde série d'analyses, où les teneurs en argent étaient de l'ordre du trentième de p.p.m., nous avons de surcroît calculé les teneurs en argent par la méthode de COVELL appliquée à trois régions du même spectre afin de confronter les valeurs obtenues: (*a*) pour le pic à 656 keV, nous avons considéré successivement et séparément 5 canaux puis 7 canaux; (*b*) pour le pic à 880 keV, nous avons considéré 7 canaux.

Les valeurs des teneurs en argent ainsi déterminées sont portées dans le Tableau III.

Calcul des erreurs

Dans l'analyse de la dispersion des résultats obtenue pour les teneurs en argent exprimées en p.p.m. (poids), nous avons essentiellement considéré:

(*a*) l'écart type des résultats obtenus par chaque méthode (comptage β, surface des 2 pics, méthode de COVELL, comptage intégral) sur différents échantillons d'un même lot.

(*b*) pour chaque échantillon considéré séparément, l'écart type caractérisant les 3 valeurs déduites des mesures γ.

De plus, pour toutes les valeurs obtenues d'après la méthode de COVELL, nous avons évalué l'erreur statistique sur le comptage proprement dit d'après la formule[6]:

$$\sigma = \sqrt{N + (n-\tfrac{1}{2})(n+\tfrac{1}{2})(a_n+b_n)}$$

TABLEAU I

DOSAGE DE L'ARGENT DANS DES GRANULÉS DE ZINC ÉLECTROLYTIQUE À 99.995%. COMPARAISON DES ÉCARTS TYPES

Echantillon		*Entraîneur*		*Rendt. chim. (%)*	*Argent en p.p.m. (poids)*							
No.	*Poids (g)*	*Mis (mg)*	*Récup. (mg)*		*Comptage β*	*Spectro γ surf. 2 photopics*	*Spectro γ Méth. Covell*	*σ théor. calc. (%)*	*Comptage γ intégral*	*Moyennes (γ)*	*Ecart type (σ_γ*) des mesures γ*	*σ_γ (%)*
1	0.815	10.9	9.5	87	1.73	1.85	1.82	0.03_4 1.5	1.84	1.84	0.01_7	0.9
2	1.398	10.9	6.8	62	1.72	1.76	1.82	0.02_7 1.5	1.78	1.79	0.03	1.7
3	1.602	10.9	6.7	61	1.81	1.87	1.90	0.02_7 1.4	1.91	1.89	0.02	1.0
4	1.375	10.9	7.9	73	1.66	1.68	1.70	0.02_7 1.6	1.68	1.69	0.01	0.6
5	1.429	10.9	0.9	8	1.61	1.61	1.69	0.05 3	1.65	1.65	0.04	2.5
6	0.493	10.9	1.5	14	1.55	1.31	1.33	0.06 4.5	1.41	—	—	—
7	1.874	10.9	5.2	48	1.87	1.93	1.93	0.02_8 1.5	1.94	1.93	0.00_7	0.4 %
Etalon		2.13	1.8	84	$\bar{M} = 1.73$ $\sigma\downarrow$** $= 0.10$ 5.8%	$\bar{M} = 1.78$ $\sigma\downarrow = 0.12$ 6.7%	$\bar{M} = 1.81$ $\sigma\downarrow = 0.10$ 5.5%		$\bar{M} = 1.80$ $\sigma\downarrow = 0.12$ 6.7%	Ecart type sur l'ensemble des mesures γ. $\sigma_{\underset{\rightarrow}{\gamma}} = 0.02_1$ (1.2%)		

Moyenne générale (mesures γ seulement): 1.80 p.p.m.
Dispersion générale des teneurs: $\sigma_\gamma\downarrow = 0.11$ (6.5%)

* σ_γ: écart type sur les valeurs γ d'une même ligne (même échantillon).
** $\sigma\downarrow$: écart type sur les valeurs d'une même colonne (ensemble des échantillons).

dans laquelle N représente le nombre de coups servant à la comparaison entre l'échantillon et l'étalon, c'est-à-dire la partie hachurée sur l'histogramme de la Fig. 3, n représente le numéro d'ordre des 2 canaux extrêmes considérés et a_n et b_n sont les nombres de coups dans chacun de ces 2 canaux extrêmes.

RÉSULTATS EXPÉRIMENTAUX

Les analyses ont porté sur 2 types de zinc:

(*a*) Zinc électrolytique de qualité courante en granulés (pureté habituelle: $\geqslant$ 99.995% en zinc).

(*b*) Un zinc extra-pur titrant 99.9999% de zinc se présentant sous forme d'un petit barreau.

Nous avons procédé à l'analyse de 7 échantillons du lot Zn 99.995 et de 4 échantillons du lot Zn 99.9999; pour ces derniers, 2 proviennent d'une même extrémité d'un premier barreau et le troisième de l'autre extrémité; le quatrième enfin a été prélevé sur un second barreau.

Zn 99.995

Les résultats relatifs aux 7 échantillons numérotés de 1 à 7 sont consignés dans le Tableau I pour chacune des méthodes de mesures expérimentées, à savoir: comptage β, surface des 2 pics, méthode COVELL, comptage γ intégral. Nous avons calculé pour chaque méthode de mesure la moyenne avec son écart type ainsi que la moyenne générale de l'ensemble des mesures pour tous les échantillons avec l'écart type correspondant.

Cela conduit à une teneur moyenne en argent de 1.80 p.p.m. (σ=0.12 p.p.m. ou 6.5%). Par ailleurs, nous avons également pour chaque échantillon comparé les différentes méthodes de comptage γ, et calculé la moyenne avec son écart type (trois dernières colonnes). On peut d'abord constater l'excellente concordance des 3 méthodes de mesures γ puisque l'écart type moyen n'est que de 1.2%.

Par contre, si l'on examine les valeurs obtenues par une même méthode de mesures pour les différents échantillons, on trouve que l'écart type, dans ce cas, est de l'ordre de 6 à 7%, quelle que soit la méthode de mesure employée.

Cette dispersion peut, en principe, résulter des causes suivantes: hétérogénéité parmi les échantillons, erreur statistique de comptage, inhomogénéité du flux dans la capsule contenant les échantillons et les étalons, erreurs chimiques et de pesée, etc.

Au sujet de l'inhomogénéité possible du flux de neutrons, on peut dire que 6 étalons placés dans le même tube d'irradiation fournissent une activité spécifique avec un écart type de 3.3% seulement dont 1% au moins revient à la pesée de la solution de nitrate d'argent introduite dans le tube en quartz (environ 60 mg).

Les erreurs de pesée du granulé de zinc sont négligeables, mais, par contre, l'erreur sur la pesée de l'entraîneur d'argent ajouté et la pesée du dépôt d'électrolyse sont estimés être de l'ordre de 2%.

Il paraît donc vraisemblable d'admettre que l'écart type relativement important trouvé pour chaque méthode est dû, en partie au moins, à un manque d'homogénéité des échantillons de ce lot.

Remarquons encore, pour finir, que la méthode par comptage β semble donner un résultat légèrement trop faible et que parmi les 3 méthodes de comptage γ, c'est

TABLEAU II

DOSAGES DE L'ARGENT DANS DEUX BARREAUX DE ZINC ULTRA-PUR À 99.9999%. COMPARAISON DES ÉCARTS TYPES

Echantillon		*Entraîneur*		*Rendt. chim. (%)*	*Argent en p.p.m. (poids)*						
No.	*Poids (g)*	*Mis (mg)*	*Récup. (mg)*		*Spectro γ surf. 2 photopics*	*Spectro γ Méth. Covell (7 canaux)*	*σ théor. calc. (%)*	*Comptage γ intégral*	*Moyennes (γ)*	*Ecart type des mesures γ*	*σ_γ (%)*
8	1.445	11.4	7.5	66	0.031_5	0.026_4	3.2	0.029_6	0.029_2	0.002_6	9
9	1.168	11.4	5.0	43	0.031	0.030_8	3.6	0.030_5	0.030_4	0.0005	1.6
10	0.987	11.4	6.8	60	0.039_5	0.040_9	2.8	0.037_3	0.039_2	0.0018	4.6
11	1.196	11.4	6.0	53	0.033	0.034	1.9	0.033_3	0.033_1	0.0007	2.2
					$\bar{M}$ = 0.034 $\sigma\downarrow$ = 0.004 (11.5%)	$\bar{M}$ = 0.033 $\sigma\downarrow$ = 0.006 (18%)		$\bar{M}$ = 0.033 $\sigma\downarrow$ = 0.0035 (11%)	Ecart type sur l'ensemble des mesures γ. $\sigma_{\underset{\rightarrow}{\gamma}}$ = 0.0015 (4.7%)		
Etalon		11.9	8.3	70	Moyenne générale: 0.033 p.p.m. Dispersion générale des teneurs: $\sigma_{\gamma\downarrow}$ = 0.005 (15%)						

TABLEAU III

TENEURS EN ARGENT DES BARREAUX ANALYSÉS AU TABLEAU II, MAIS VALEURS CALCULÉES D'APRES LA MÉTHODE DE COVELL APPLIQUÉE À TROIS RÉGIONS CARACTÉRISTIQUES DES SPECTRES GAMMA DE ^{110m}Ag. COMPARAISON DES ERREURS STATISTIQUES THÉORIQUES AVEC LES ÉCARTS EXPERIMENTAUX; CAS D'ACTIVITÉS FAIBLES

Echantillon no.	*Pic 656 keV*				*Pic 880 keV*		*Moyenne sens→ $\bar{M}$ p.p.m.*	*σ_γ sens→ (valeur)*	*% approx.*
	Ag (p.p.m.) Méth. Covell sur 7 canaux	*σ théor. (%)*	*Ag (p.p.m.) Méth. Covell sur 5 canaux*	*σ théor. (%)*	*Ag (p.p.m.) Meth. Covell sur 7 canaux*	*σ théor. (%)*			
8	0.026	3.2	0.025	4.2	0.023	6.6	0.025	0.001_8	7
9	0.031	3.6	0.023	6.0	0.034	5.9	0.029	0.005	18
10	0.041	2.8	0.042	5.4	0.044	4.3	0.042	0.001_5	4
11	0.034	1.9	0.039	5.9	0.031	6.0	0.035	0.004	11
	$\bar{M}$ = 0.033 $\sigma\downarrow$ = 0.006 (18%)		$\bar{M}$ = 0.032 $\sigma\downarrow$ = 0.009_5 (30%)		$\bar{M}$ = 0.034 $\sigma\downarrow$ = 0.009 (27%)		Ecart type réel sur l'ensemble des mesures (détermination par méthode de COVELL) σ_γ (sens→) = 0.0033 (10%)		
	Moyenne générale: 0.033 p.p.m. **Dispersion générale (COVELL):** $\sigma\downarrow$ = 0.009 (27%)								

la méthode du comptage intégral qui paraît la plus précise: de toute façon, c'est elle qui, comportant à temps de comptage égal, le plus grand nombre de coups, doit donner l'erreur statistique la plus faible. Bien entendu, pour pouvoir l'utiliser sans risque, il faut être absolument certain de la décontamination totale de l'argent séparé.

Zn 99.9999

Les résultats obtenus sur 4 échantillons de ce lot sont consignés dans le Tableau II. Le résultat moyen trouvé est de 0.033 p.p.m. d'argent ($\sigma = 0.005$ soit 15%).

On constate à nouveau que, sur un même échantillon, les 3 méthodes fournissent des valeurs consistantes ($\sigma = 4.7\%$), alors que pour une même méthode l'écart type relatif aux différents échantillons est beaucoup plus élevé (11 à 18%).

Il est à nouveau vraisemblable que cette dispersion soit en partie due à une hétérogénéité du barreau de zinc dans lequel les échantillons ont été prélevés et, à ce propos, il est utile de rappeler que l'échantillon no. 10 qui a la teneur en Ag la plus forte du second groupe provient précisément de l'extrémité opposée à celle d'où ont été prélevés les échantillons 8 et 9.

Il est également intéressant de signaler pour la méthode COVELL, un écart type nettement plus important que pour les 2 autres méthodes; cela nous a conduit à examiner de plus près cette méthode. Sa précision dépend, en effet, non seulement du nombre de canaux choisis mais encore de l'erreur statistique sur la somme des activités des 2 canaux extrêmes seulement.

Ces résultats sont consignés dans le Tableau III. On voit d'abord que le pic à 880 keV est moins indiqué que le pic à 656 keV et que, pour ce dernier, il y a intérêt à prendre 7 canaux plutôt que 5 pour réduire la dispersion; même dans ces conditions, pour les faibles teneurs en argent, la méthode de COVELL est moins précise que la méthode intégrale et que celle basée sur la surface des 2 pics. Cette dispersion dans la méthode COVELL dépasse d'ailleurs largement l'erreur statistique calculée par la formule mentionnée (voir Tableau III).

CONCLUSIONS GÉNÉRALES

La méthode proposée pour le dosage de l'argent dans le zinc par activation aux neutrons et qui consiste à séparer l'argent radiochimiquement pur par 2 électrolyses successives sur cathode en or (3% platine), en milieu nitrique contenant de l'acide sulfamique, fournit des résultats excellents.

Le facteur de décontamination est très élevé et la limite de détection obtenue avec des échantillons de l'ordre du gramme de zinc irradié quelques jours dans un flux 10^{13} n/cm^2/sec, est de l'ordre de 10 ng.

L'examen de différentes méthodes de mesure de l'activité de l'argent séparé a montré:

(*1*) que les résultats obtenus à partir de ces différentes méthodes de mesure de l'activité sont très cohérents: écart type de l'ordre de 1% pour une teneur en argent de 1.8 p.p.m. et 5% pour un échantillon à 0.033 p.p.m. d'argent.

(*2*) que les résultats d'analyses obtenus par une même méthode sur différents échantillons d'un même lot montrent une dispersion nettement plus grande (respectivement 6.5% et 15% d'écart type); cette augmentation est vraisemblablement due partiellement à une certaine hétérogénéité des échantillons examinés.

(3) que la méthode du comptage intégral fournit la meilleure précision; cette méthode exige évidemment une certitude absolue sur la pureté radiochimique.

Nous désirons remercier l'Institut des Sciences Nucléaires pour les crédits ayant permis cette recherche.

RÉSUMÉ

Le dosage non destructif de traces d'argent dans le zinc par spectrométrie-γ (^{110}Ag $T_{\frac{1}{2}} = 24$ sec) n'est plus possible en dessous de quelques p.p.m. en raison de l'activation de l'élément matriciel. Le zinc irradié est mis en solution nitrique; ^{110m}Ag ($T_{\frac{1}{2}} = 253$ j) avec son entraîneur inactif est séparé radiochimiquement pur grâce à une double électrolyse sur cathode d'or, en présence d'acide sulfamique. Dans un échantillon irradié 2 jours au BR2 de Mol ($3 \cdot 10^{13}$ n/cm^2/sec), il est possible de doser 30 ng d'argent avec une erreur relative de l'ordre de 5%. On a comparé les résultats obtenus par comptage intégral ou par spectrométrie-γ.

SUMMARY

Below the p.p.m. level, the determination of silver in zinc by non-destructive γ-spectrometry is no longer feasible due to the activation of the matrix element. The activated zinc is dissolved in nitric acid, sulfamic acid and silver carrier are added, and ^{110m}Ag (253 d) is obtained in a radiochemically pure state after two successive electrolyses on gold cathodes.

After two days of irradiation in a thermal neutron flux of the order of $3 \cdot 10^{13}$ n/cm^2/sec (BR2-Mol), 30 ng of silver can easily be evaluated with an error of 5%. Data obtained by integral γ-counting or by γ-spectrometry are compared.

ZUSAMMENFASSUNG

Der zerstörungsfreie Nachweis von Spurenmengen Silber in Zink durch Gammaspektrometrie (^{110}Ag, 24 sec) ist nicht mehr möglich für Konzentrationen unterhalb einiger p.p.m. infolge der Aktivation des Zinks selbst.

Nach der Bestrahlung wird das Zink in Salpetersäure gelöst, die Lösung mit Sulfaminsäure gesättigt und radiochemisch reines ^{110m}Ag (253 d), mit seinem inaktiven Träger, durch doppelte Elektrolyse an einer Goldkathode abgetrennt.

30 ng Silber können, mit einem Fehler von etwa 5%, in einer Probe nachgewiesen werden die zwei Tage einem Fluss von $3 \cdot 10^{13}$ n/cm^2/sec (BR2-Mol) ausgesetzt war. Die Ergebnisse von Intergralzählung und Gammaspektrometrie werden verglichen.

BIBLIOGRAPHIE

1 M. Okada, *Nature*, 187 (1960) 578.
2 R. Strominger, J. M. Hollander et G. T. Seaborg, Table of Isotopes, *Rev. Mod. Phys.*, 30 (2) (1958) 585, 904.
3 A. Giovannini, *Travail de fin d'étude*, école polytechnique, Liège, 1963.
4 L. Geladi, *Thèse de Licence*, Université de Liège, 1964.
5 L. Troost et E. Pechard, *Traité de Chimie Minérale*, Masson, Paris, 1929, p. 634.
6 D. F. Covell, *Anal. Chem.*, 31 (11) (1959) 1785.

EMISSION SPECTRA OF ORGANIC LIQUIDS IN OXY-HYDROGEN FLAMES

J. W. ROBINSON AND V. SMITH
Coates Chemical Laboratories, Louisiana State University, Baton Rouge, La. 70803 (U.S.A.)
(Received February 15th, 1966)

A preliminary study of the emission spectra of different organic solvents has been made. Previous studies, such as the extensive works of GAYDEN[1,2] indicate that organic compounds emit spectra from flames and have identified many of the species involved. In general, these species were very elementary (*e.g.*, C_2, OH, etc.) and involved mostly the terminal, or near terminal products of combustion.

Very little attention has been made to the application of these spectra to analytical chemistry. One of the principal problems is that the groups studied by GAYDEN *et al.* are present in almost all common combustion products of organic compounds such as C_2, CH, etc., and little analytical information can be achieved by observing the presence of these compounds.

COOKE *et al.*[3,4] investigated the use of flame emission spectra as a means of identifying the effluent peaks from gas chromatograms. However, they found that greater sensitivities could be achieved by using a microwave generated plasma.

The object of this study was to determine if emission spectra could be detected from whole organic molecules, or fragments of whole molecules, during the process of combustion. It was also hoped to investigate the usefulness of this process as an analytical tool. Further it was anticipated that the evaluation of such spectra would lead to a more complete understanding of combustion processes.

EXPERIMENTAL

Equipment

Spectrophotometer. DU spectrophotometer and DKI spectrophotometer.

Recorder. Photovolt model 43 Varicord.

Flame attachment. A Beckman total consumption burner was used. The flame was oxy-hydrogen. The oxygen and hydrogen rates in the flame were measured with flow meters. A metal screen was placed between the burner and the inlet-slit of the spectrophotometer. A thin horizontal slit (10 mm) in the screen allowed emission from selected parts of the flame to be examined. The mirror of the flame attachment was removed to prevent reflection of the whole flame.

Sample injection. Scanning the emission spectrum over a wide wavelength range required a significant period of time. Continuous sample injection for extended periods of time was effected by using an enclosed glass container (volume *ca.* 70 ml). This prevented flashing of the combustible solvent vapors.

The wavelength ranges examined were from 2000 Å to 7000 Å, and the oxygen–hydrogen ratio of the flame was varied to give (*a*) oxidizing, (*b*) stoichiometric, and (*c*) reducing conditions.

RESULTS

The first series of organic liquids examined were butyl chloride, butylamine, and butyl alcohol. The spectra obtained are shown in Figs. 1, 2 and 3. Identification

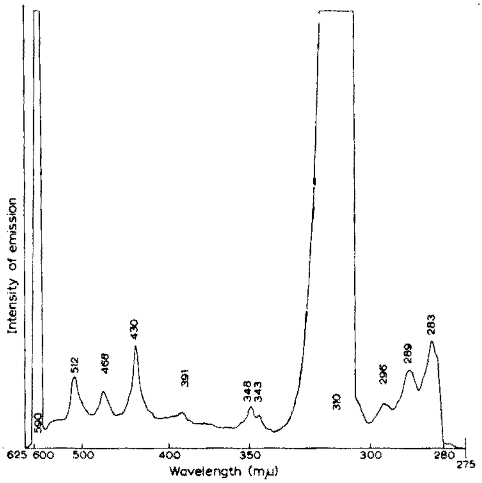

Fig. 1.

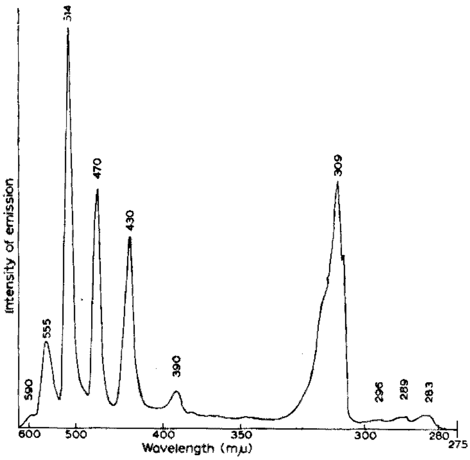

Fig. 2.

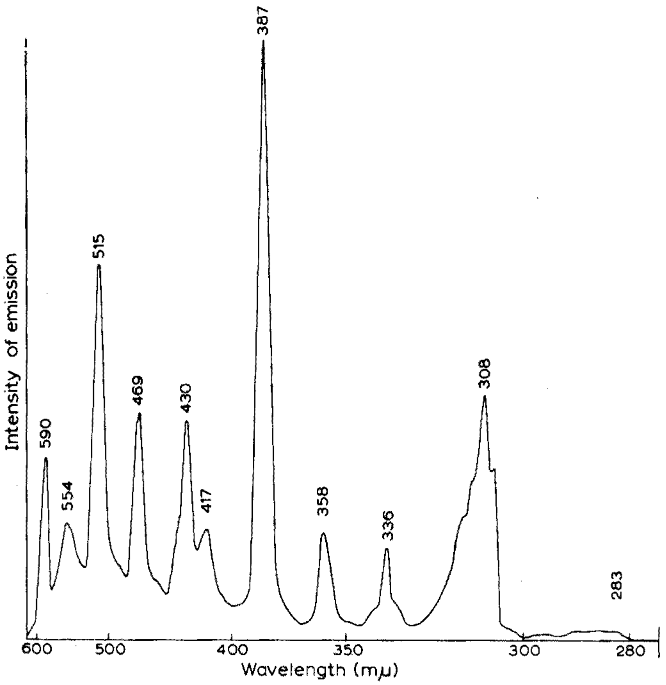

Fig. 3.

Fig. 4.

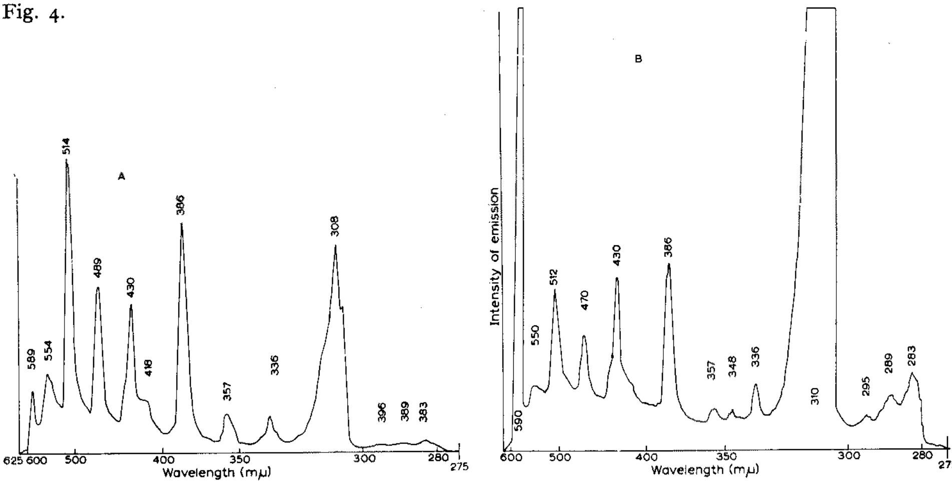

Figs. 1–4. Emission from: (1) *n*-butyl alcohol; (2) *n*-butyl chloride; (3) *n*-butylamine; (4a) equal mixture of *n*-butylamine and *n*-butyl chloride; (4b) equal mixture of *n*-butylamine and *n*-butyl alcohol. Flame conditions: oxygen 5 p.s.i.g., hydrogen 5 p.s.i.g.

of numerous bands was made by comparison with the data given in publications by GAYDEN *et al.*[1,2,5].

The spectra showed that there were similarities and differences in emission from the compounds. The peaks at 283, 289, 296, 310, 430, 468 and 512 nm were present in all spectra. By comparison with the results of GAYDEN[2,5] these can be identified as emission spectra arising from excited C_2, CH and OH species. However, Fig. 1 shows that the band at 310 nm (OH) is very intense compared to the spectra in Figs. 2 and 3. Also there is an extra sharp band at 590 nm. The peak at 310 nm is probably due to OH but the peak at 590 nm was sodium impurity. It is conceivable that it is a CO or COH band.

Figure 2 illustrates the butyl chloride spectra. All the peaks could be identified as arising from C_2, CH or OH. No effect of the chloride was noted.

Figure 3 shows the spectrum of butylamine. The peaks observed at 417, 387, and 358 nm probably arose from excited CN bands, the peak at 336 nm was from NH. Because the emission bands were well defined and intense, they could no doubt be used to identify the particular organic compound involved when simple solutions were used. This could provide the basis of a new analytical procedure. To check mutual interferences the emission spectra of mixtures of the 3 compounds were examined under the same conditions as those listed above. The spectra obtained are shown in Figs. 4a and b.

It can be seen that the spectra obtained included all the emission bands present in each individual spectrum. As a potential analytical tool, this indicated some degree of freedom of interference from other solvents present.

Aromatic compounds

Similar studies were made on benzene and cumene. The spectra are shown in Figs. 5 and 6. Again, the spectra showed distinct similarities and differences. The strong bands centered at 309, 430, 474, 514 and 555 nm were common to both spectra, but the sharp lines at 588 nm were found only in the cumene emission.

Infrared emission

The infrared emission spectra of butyl chloride and *n*-butanol had been previously recorded[6]. These are shown in Figs. 7 and 8. The positions of the major peaks seem to coincide. In particular the emission bands with heads at 800, 950, 1100, 1450, 1800, 1850, 2100, 2350, and 2700 nm should be noted. These bands seem to be similar in intensity. The shape of these bands is similar to infrared absorption bands. The breadth of these absorption bands is attributed to the numerous vibrational levels and the superimposed rotational energy levels of whole molecules. Bearing in mind the spectral range of these spectra and their similarity to infrared absorption spectra, it is reasonable to conclude that they arise from whole molecules or fragments of molecules. It will be noticed that there is an emission band at 2500 nm in the butyl chloride emission spectra, but only a weak shoulder in the *n*-butanol emission spectra.

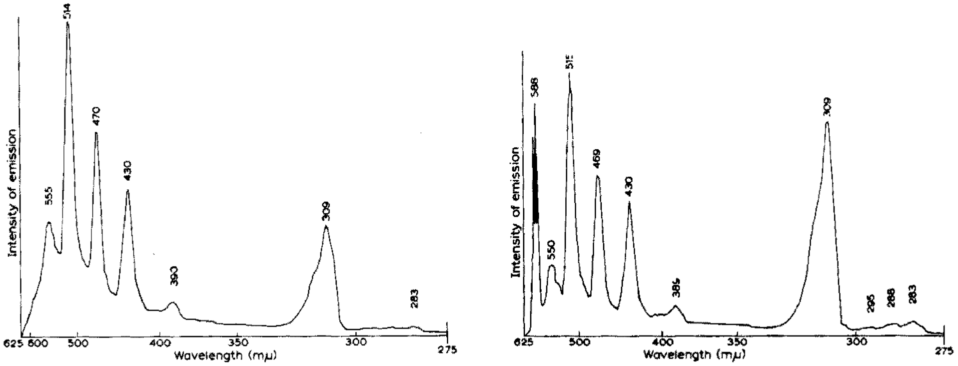

Figs. 5-6. Emission from: (5) benzene; (6) cumene. Flame conditions as before.

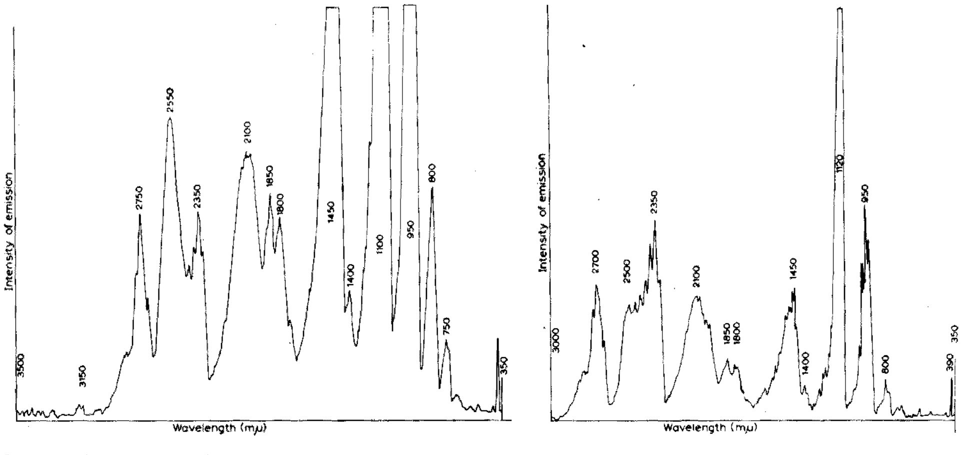

Figs. 7-8. Emission from: (7) *n*-butyl chloride; (8) *n*-butyl alcohol.

Comparison with infrared absorption spectra

It can be seen that the absorption bands and emission bands do not coincide. It was felt that the emission bands were broad enough to indicate vibrational energy levels which in turn indicates molecular-type species. However, the non-coincidence of spectra suggests that the emission was from fragments of molecules rather than complete molecules.

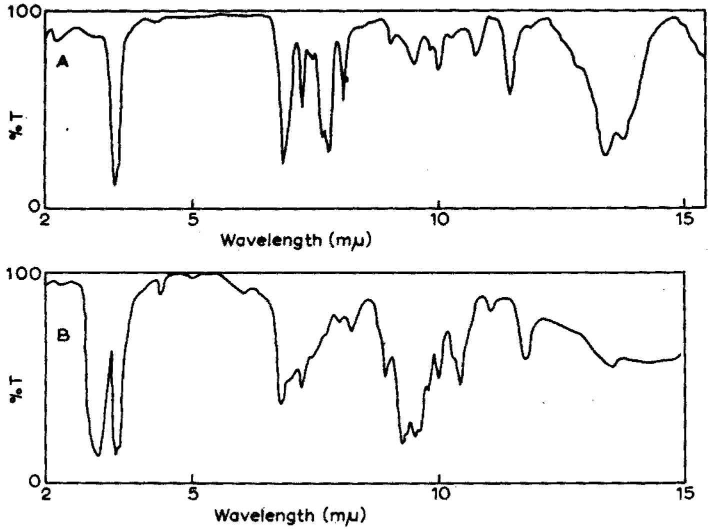

Fig. 9. Infrared absorption of: (a) 1-chlorobutane (Sadtler-4621); (b) *n*-butyl alcohol (Sadtler-75).

THE ORIGIN OF THE SPECTRA

A considerable portion of the spectrum originated from terminal or near terminal products of combustion. Examples are OH, C_2, CH bands, already identified by GAYDEN *et al.*[1,2,5]. However, numerous bands were not identified. The spectral range involved indicates that the spectra in Figs. 1 through 6 are caused by electronic transitions. The width of the bands indicate that vibrational spectra are also involved. This was confirmed by the observation of the infrared emission illustrated in Figs. 7 and 8.

The emission could originate from several sources. These include excited whole molecules, excited fragments of molecules, or excited combustion products. Previous work[1,2] proved the presence of excited combustion products.

The infrared emission and the width of the unidentified bands in Figs. 1 through 6 indicate either whole molecules, or fragments of molecules. The energy levels involved may be from excited to ground states, but it is much more likely that they are transitions from higher excited states to lower excited states of electronic excitation with vibrational and rotational energy levels superimposed.

Interaction effects

Mixtures were made up containing varying quantities of butanol, butyl chloride and butylamine. The emission spectrum of each mixture was then recorded. The change in peak height *vs.* composition is shown in Fig. 10.

It is probable that the intensity of emission depends on the concentration of emitting species (C_2, CH, etc.). For the process to be useful for direct quantitative analysis, the concentration of emitting species should be proportional to the concentration of the parent molecule in the original sample. If the intensity of line 336 nm which has been shown to arise from *n*-butylamine is examined, it can be seen that there is no linear relationship between concentration and emission intensity. Such a discrepancy could arise because of the effect of the alcohol or the chloride on the combustion pattern of the amine. This interaction effect is quite feasible since both compounds are competing for the oxygen present. It is therefore quite possible that the quantities of emitting fragments produced from the compound present, are dependent upon the other compounds competing in the combustion step. The results indicate that the process would not be useful for direct analytical determinations, but should be very useful for studying the combustion processes of organic compounds, particularly in the presence of other combustible compounds.

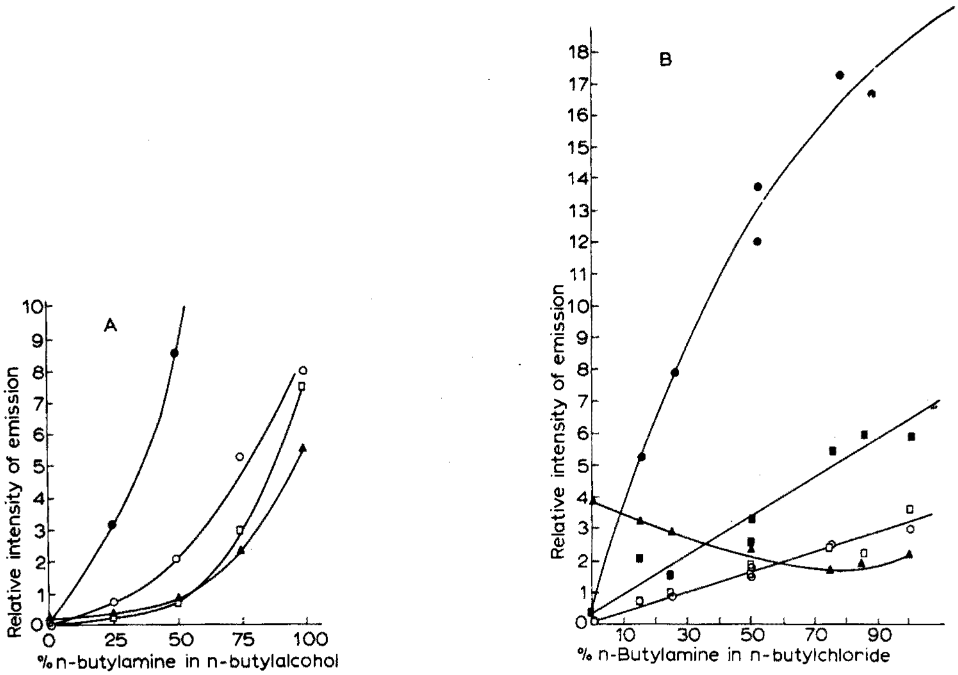

Fig. 10. *n*-Butylamine in: (a) *n*-butyl alcohol; (b) *n*-butyl chloride. (●) 387, CN; (○) 336, NH; (□) 358, CN; (▲) 555, C_2; (■) 590.

Effect of flame height

Separate samples of *n*-butylamine and isopropylbenzene were aspirated into the flame. The emission spectra from different parts of the flame were recorded. They showed variations in emission intensities at different parts of the flame. The most intense emission took place between 1 cm and 3 cm above the base of the flame. This observation clearly indicates that emission is sensitive to flame position. It also suggests that the emitting species are fragments of molecules since excited whole molecules would emit lower in the flame and excited combustion products would emit most strongly at the upper portions of the flame.

Effect of flame composition

n-Butylamine was aspirated into flames of different oxygen/hydrogen ratios. The emission spectra were recorded and are illustrated in Figs. 11a, b and c. It can be seen that as the composition varies, the relative height of the peaks varies. This is particularly noticeable with the 386 nm CN band, the 515 nm C_2 band and the unidentified band at 588 nm. The peak at 588 nm seems to distinguish the amine and the alcohol from the chloride compound. These results indicate that optimum conditions must be sought to obtain the maximum difference between spectra of different compounds.

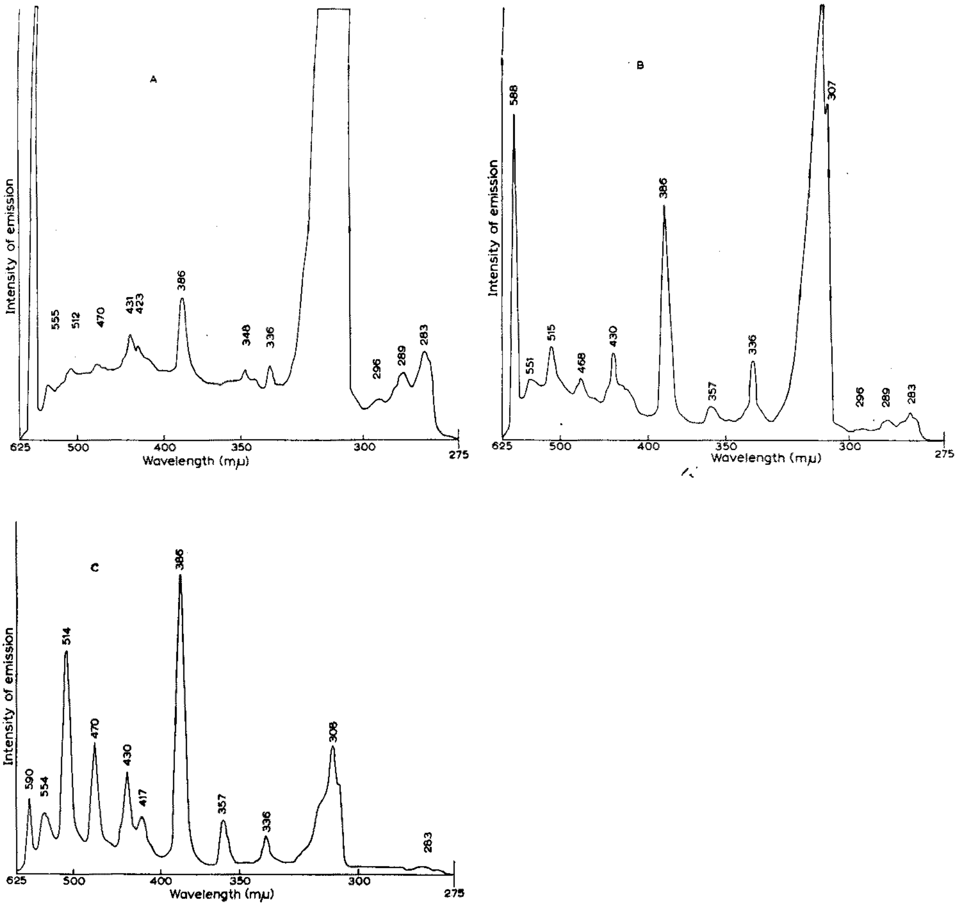

Fig. 11. Emission from *n*-butylamine. Flame conditions: oxygen, 5 p.s.i.g.; hydrogen: (a) 1 p.s.i.g., (b) 2.5 p.s.i.g., (c) 7.5 p.s.i.g.

A similar study was done with benzene. The results are shown in Fig. 12. It can be seen that there is a great difference in the emission spectra of 12a and 12c. The bands exhibited in 12c appear to coincide with the known emission bands of C_2, CH and OH. The bands shown in 12a are in the same general wavelength range but do not seem to arise from the same transitions. It should be pointed out that the 12c spectra were emitted from oxidizing flames. Partial combustion is possible in such flames and excited fragments of the benzene ring may exist for extended periods of time. Further it can be seen that the emission does not coincide with the wavelength region of the benzene absorption spectrum. This indicates that transitions between the unexcited state and upper excited states are probably not involved. It is probable therefore that the spectra arise either from transitions between higher excited states of benzene or from fragments of the benzene molecule, broken under the conditions of partial combustion.

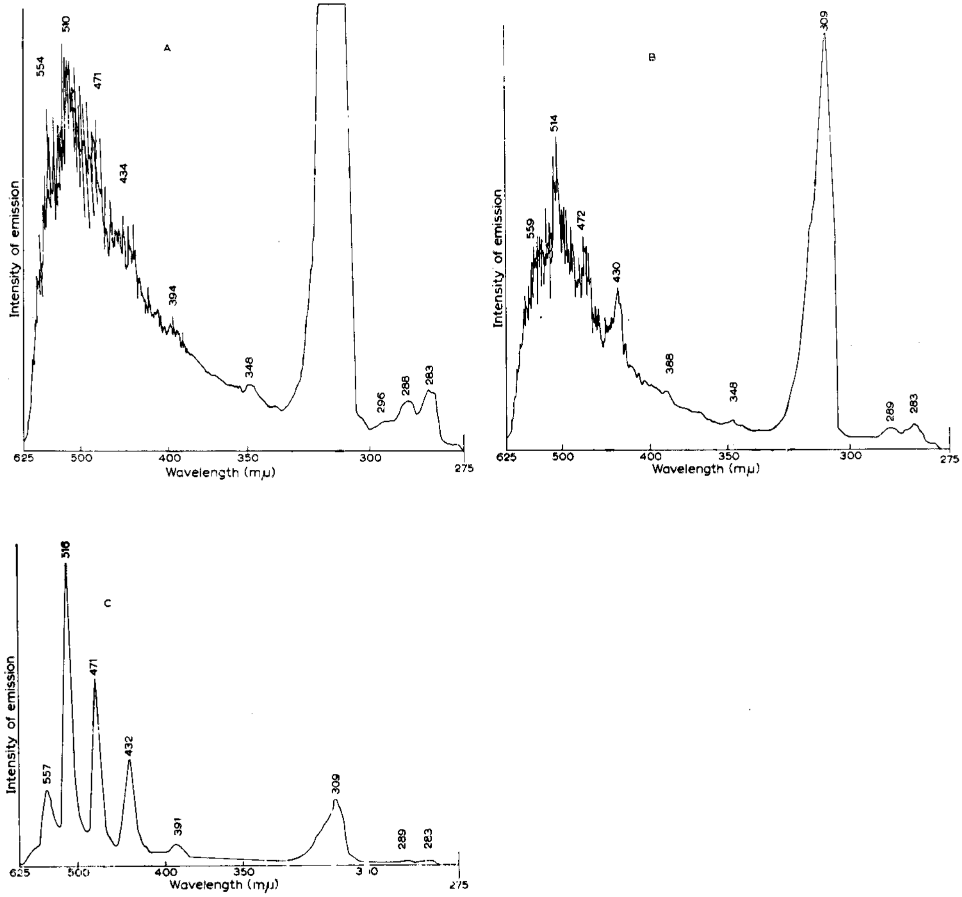

Fig. 12. Emission from benzene. Flame conditions: oxygen 5 p.s.i.g.; hydrogen: (a) 1 p.s.i.g., (b) 2.5 p.s.i.g., (c) 7.5 p.s.i.g.

CONCLUSION

In the 200–700 nm region, different emission spectra are obtained from different organic solvents in an oxy–hydrogen flame. Further work is planned to isolate and explain the differences as well as to extend the spectral region observed in an endeavor to develop a qualitative and quantitative method for the analysis of organic solvent mixtures.

It is not possible at this time to explain consistently all of the differences in the spectra obtained from the different organic solvents studied (Figs. 1–8). It is hoped, however, that further study with a more sensitive instrument and a forced feed burner[7] will help us to do so. This burner allows a fixed volume of any liquid to be sprayed into the flame in the form of uniform droplets and eliminates combustion variables such as drop size and sample feed rate.

Particularly difficult to explain are the differences in the relative intensities of emission bands at certain wavelengths, for example, the 515 nm (C_2) and 430 nm (CH) bands. Also of interest are the broad emission bands in the benzene and cumene spectra between about 390 and 600 nm, also the bands close to 590 nm found in the spectra from *n*-butanol, *n*-butylamine, and cumene. The mixtures of *n*-butylamine with *n*-butanol and *n*-butyl chloride showed the emission spectra expected from consideration of the spectra obtained from the pure solvents. Peaks due to CN and NH increased with increased amine concentration (Fig. 9).

The effects of various oxygen–hydrogen ratios on the emission spectra of benzene (Fig. 5) were striking and will be studied further.

SUMMARY

Organic compounds were aspirated into an oxy–hydrogen flame and the emission spectra studied. Spectra from terminal combustion products were observed and some emission in the infrared may be attributed to larger molecular fragments. Qualitative analysis of combustion processes may be feasible using this process, but numerous problems made quantitative analysis difficult.

RÉSUMÉ

Les auteurs ont examiné les spectres d'émission obtenus en aspirant des composés organiques dans une flamme oxy–hydrogène. Cette méthode peut être appliquée à l'analyse qualitative lors de procédés de combustion, mais de nombreux problèmes en rendent l'analyse quantitative difficile.

ZUSAMMENFASSUNG

Organische Verbindungen wurden in eine Sauerstoff–Wasserstoff-Flamme eingesprüht und die Emissionsspektren untersucht. Ein Teil der Emission der Verbrennungsprodukte im Infraroten kontte grösseren Molekülfragmenten zugeordnet werden. Für die qualitative Analyse kann dieser Verbrennungsprozess verwendet werden, zahlreiche Probleme erschweren jedoch die quantitative Analyse.

REFERENCES

1 A. G. Gayden and H. G. Wolfhand, *Flames*, Chapman and Hall, 1960.
2 A. G. Gayden, *The Spectroscopy of Flames*, John Wiley, New York, 1957.
3 A. J. McCormack, *M.S. Thesis*, Cornell University, 1963.
4 A. J. McCormack, S. C. Long and W. P. Cooke, *Anal. Chem.*, 37 (1965) 1470.
5 R. W. B. Pearse and A. G. Gayden, *The Identification of Molecular Spectra*, Chapman and Hall, London, 1963.
6 J. W. Robinson, *13th L.S.U. International Symposium on Modern Methods of Analytical Chemistry, 1960.*
7 J. W. Robinson and R. J. Harris, *Anal. Chim. Acta*, 26 (1962) 439.

L'EXTRACTION DES LANTHANIDES ET DES ACTINIDES PAR LES OXYDES D'ALKYLPHOSPHINE

TOME I. L'EXTRACTION DE L'ACIDE NITRIQUE PAR L'OXYDE DE TRI-*n*-BUTYLPHOSPHINE*

J. GOFFART** ET G. DUYCKAERTS
Laboratoire de Chimie analytique et nucléaire, 2, rue A. Stévart, Liège (Belgique)

(Reçu le 4 juillet, 1966)

HIGGINS *et al.*[1] ont montré que l'extraction des métaux par les composés organophosphorés neutres augmente avec la basicité du groupement PO, les meilleurs extractants étant les oxydes d'alkylphosphine de formule générale Alk_3PO. WHITE ET ROSS[2–4] ont proposé l'extraction par l'oxyde de tri-*n*-octylphosphine (TOPO) pour la séparation analytique du titane, du chrome, du fer, du zirconium, du niobium, du molybdène, du bismuth, du thorium et de l'uranium.

L'existence de nombreux complexes a été démontrée en phase organique: $Zr(NO_3)_4 \cdot 2$ TOPO[5], $Th(NO_3)_4 \cdot 3$ TOPO[6,7], $Pu(NO_3)_4 \cdot 2$ TOPO[8], $PuO_2(NO_3)_2 \cdot 2$ TOPO[8], $UO_2(NO_3)_2 \cdot 2$ TOPO[2], $H_2Cr_2O_7 \cdot 2$ TOPO[9], $HTcO_4 \cdot 2$ TOPO[10] et $H_2Ce(NO_3)_6 \cdot 2$ TOPO[2].

ISHIMORI *et al.*[11] ont déterminé la distribution de la plupart des nitrates métalliques entre l'acide nitrique et une solution organique de TOPO.

Notre but est une étude fondamentale de l'extraction des lanthanides et des actinides en milieu nitrique par différents oxydes d'alkylphosphine.

L'interprétation des courbes de distribution des métaux exige la connaissance préalable du partage de l'acide nitrique[6] entre les phases organique et aqueuse.

Cette première publication relate les résultats concernant l'extraction de l'acide nitrique par l'oxyde de tri-*n*-butylphosphine (TBPO).

PARTIE EXPÉRIMENTALE

Réactifs

L'oxyde de tri-*n*-butylphosphine a été synthétisé par action du bromure de *n*-butylmagnésium sur l'oxychlorure de phosphore en milieu éther anhydre[6]. Le produit obtenu a été purifié par distillation, par passage sur alumine basique et, enfin, par recristallisation dans le benzène immédiatement avant emploi. (Point de fusion: 60–61° (litt.: 62–63°[12]).)

La pureté du TBPO a été contrôlée en dosant le phosphore; à cet effet, l'organophosphoré est minéralisé dans une bombe de Parr ou de Wurzschmitt. Le phosphore est ensuite dosé avec une précision de 1 à 2% soit par pesée du phospho-

---

[*] Ce travail a été effectué dans le cadre du contrat Euratom 003–61–2 TPUB.

[**] Chercheur Agréé à l'Institut Interuniversitaire des Sciences Nucléaires.

molybdate d'ammonium[13], soit par colorimétrie différentielle au bleu de molybdène[14] (% $P_{trouvé}$: 14.1; % $P_{théor.}$: 14.19). Tous les diluants utilisés sont de qualité "pour analyse" et ont été redistillés; le benzène a été préalablement recristallisé.

Mode opératoire

Des volumes égaux (20 ml) de phase organique de TBPO et de phase aqueuse d'acidité connue (C_a^i (HNO_3)) sont équilibrés par agitation mécanique dans un bain thermostatique réglé à 25 ±0.1°. Dans tous les cas, une durée d'agitation de 15 min est suffisante pour atteindre l'équilibre de distribution.

Le TBPO, dans les différentes solutions organiques, est titré en milieu anhydride acétique par l'acide perchlorique en solution dans le dioxanne. Le titrage est suivi potentiométriquement au titriscope Metrohm équipé d'une électrode de verre conditionnée à l'anhydride acétique et d'une électrode de référence au calomel dont la solution conductrice est le perchlorate de lithium 0.1 M en solution dans l'anhydride acétique[15].

Pour déterminer le coefficient de distribution du TBPO entre les phases organique et aqueuse, il est indispensable de connaître la quantité de TBPO dissoute dans l'eau à l'équilibre; le titrage direct par l'acide perchlorique n'étant pas possible, il est nécessaire de réextraire le réactif dans le benzène après avoir rendu la phase aqueuse 2 M en $NaNO_3$ ou en $LiNO_3$.

L'acide nitrique est titré potentiométriquement par la soude; les titrages ont été effectués dans l'eau pour les solutions aqueuses, dans l'alcool éthylique[6,8] ou dans l'acétone pour les solutions organiques. L'eau a été dosée par la méthode de KARL FISCHER[16].

Conventions d'écriture

$C_a(HNO_3)$, $C_o(HNO_3)$, $C_o(TBPO)$ et $C_o(H_2O)$ représentent les concentrations (M/l) à l'équilibre respectivement dans la phase aqueuse (a) et dans la phase organique (o); $c_o^i(TBPO)$ est la représentation de la concentration initiale en réactif de la phase organique tandis que $C_o(H_2O)_c$ et $C_o(HNO_3)_c$ sont celles des concentrations corrigées pour tenir compte de la solubilité propre de l'eau et de l'acide nitrique dans la fraction de volume du diluant[17,18].

RÉSULTATS

Distribution du TBPO entre l'eau et quelques diluants organiques

Le coefficient de distribution (D o/a) du TBPO augmente avec la concentration: il est de 8 pour une solution 0.05 M dans le benzène et de 33 pour une solution 1.54 M. La présence d'acide nitrique ou de nitrate métallique ($NaNO_3$, $LiNO_3$, . . .) dans la phase aqueuse augmente également le D_{TBPO} (Tableaux I, II et III).

Distribution de l'acide nitrique et de l'eau entre une phase aqueuse et une phase organique de TBPO

La Fig. 1 illustre nos résultats concernant la distribution de l'acide nitrique entre la phase aqueuse et la phase organique de TBPO (Tableaux I et III).

Une courbe analogue est obtenue pour les solutions de réactif dans le toluène (Tableau II). Une troisième phase apparaît dans le système TBPO–H_2O–HNO_3–

TABLEAU I

DISTRIBUTION DU TBPO, DE HNO_3 ET DE H_2O ENTRE UNE PHASE AQUEUSE ET LE BENZÈNE

$C_a(HNO_3)$ *(mole/l)*	$C_o(HNO_3)$ *(mole/l)*	$C_o(H_2O)_c$ *(mole/l)*	C_o(TBPO) *(mole/l)*
c_o^i(TBPO): *0.100 M*			
0		0.081	0.092
0.057	0.0038		0.092
0.088		0.074	0.092
0.125	0.013	0.073	0.092
0.136	0.016		0.092
0.140		0.069	0.092
0.233	0.035	0.059	0.0925
0.262	0.038	0.057	0.0925
0.266	0.040	0.055	0.093
0.312	0.047	0.048	0.0935
0.396	0.058	0.039	0.0935
0.405	0.060		0.094
0.480	0.064	0.033	0.095
0.490	0.067		0.0955
0.519	0.070		0.0955
0.565	0.074		0.096
0.579	0.073		0.096
0.579	0.073		0.096
0.614	0.075	0.027	0.096
0.650	0.077		0.096
0.712	0.080		0.096
0.835	0.083		0.096
0.873	0.084		0.096
0.873	0.084		0.096
c_o^i(TBPO): *0.138 M*			
0.176	0.034		0.1285
0.201	0.035		0.129
0.211	0.042		0.129
0.250	0.048		0.1295
0.250	0.048		0.1295
0.250	0.048		0.1295
0.320	0.064		0.130
0.397	0.077		0.131
0.405	0.080		0.131
0.470	0.087		0.131
0.482	0.088		0.131
0.482	0.088		0.131
0.531	0.096		0.131
c_o^i(TBPO): *0.138 M*			
0.652	0.108		0.132
0.660	0.105		0.132
0.664	0.106		0.132
0.720	0.109		0.132
0.805	0.1135		0.132
0.874	0.116		0.133
0.907	0.118		0.133
c_o^i(TBPO): *0.150 M*			
0.139	0.023		0.139
0.176	0.035		0.1395
0.211	0.042		0.140
0.282	0.060		0.1405
0.317	0.068		0.141
0.321	0.069		0.141
0.375	0.079		0.141
0.412	0.088		0.142
0.501	0.099		0.142
0.550	0.104		0.143
0.625	0.111		0.143
0.680	0.115		0.143
0.705	0.116		0.143
0.810	0.123		0.144
0.875	0.126		0.144
c_o^i(TBPO): *0.200 M*			
0.096	0.015		0.186
0.096	0.015		0.186
0.171	0.047		0.187
0.196	0.050		0.187
0.231	0.059		0.188
0.231	0.059		0.188
0.295	0.089		0.189
0.383	0.112		0.189
0.436	0.126		0.190
0.493	0.131		0.190
0.633	0.150		0.191
0.681	0.159		0.192
0.700	0.156		0.192

n-hexane pour une concentration 0.1 *M* en TBPO et 2.5 *N* en acide nitrique (Tableau II).

Le dosage de l'eau en phase organique montre une diminution de la concentration en eau quand la concentration en acide nitrique croît (Fig. 2). On constate que la courbe passe par un minimum différent de zéro, malgré la correction appliquée pour la solubilité de l'eau dans le diluant seul[17], avant de présenter une pente positive aux fortes acidités.

TABLEAU II

DISTRIBUTION DU TBPO, HNO_3 ET H_2O ENTRE H_2O ET LE TOLUÈNE OU LE *n*-HEXANE

$C_a(HNO_3)$ *(mole/l)*	$C_o(HNO_3)$ *(mole/l)*	$C_o(TBPO)$ *(mole/l)*
$c_o^1(TBPO)$: *0.100 M dans le toluène*		
0.138	0.017	0.0875
0.180	0.024	0.088
0.271	0.0395	0.089
0.345	0.050	0.090
0.526	0.0675	0.0915
0.624	0.075	0.092
0.720	0.079	0.093
0.820	0.083	0.094

$C_a(HNO_3)$ *(mole/l)*	$C_o(HNO_3)$ *(mole/l)*	$C_o(TBPO)$ *(mole/l)*
$c_o^1(TBPO)$: *0.100 M dans le* n-*hexane*		
0	0	0.034
0.193	0.006	0.033
0.275	0.012	0.039
0.548	0.023	0.0415
0.638	0.028	0.0425
0.755	0.035	0.0435
0.935	0.038	0.044

TABLEAU III

DISTRIBUTION DE L'ACIDE NITRIQUE ET DE L'EAU ENTRE LE TBPO DANS LE BENZÈNE ET L'EAU

$C_a(HNO_3)$ *(mole/l)*	$C_o(HNO_3)_c$ *(mole/l)*	$C_o(H_2O)_c$ *(mole/l)*	$C_o(TBPO)$ *(mole/l)*
4.94	0.1105		0.099
5.04	0.1115	0.012	0.099
5.16	0.112		0.099
5.24	0.112		0.099
5.24	0.112		0.099
5.46	0.114		0.099
5.65	0.1155	0.014	0.099
5.79	0.117		0.099
4.61	0.153		0.138
4.61	0.153		0.138
5.39	0.161	0.023	0.138
5.84	0.167	0.029	0.138
3.57	0.210		0.200
4.60	0.221		0.200
5.41	0.233		0.200
5.79	0.242		0.200

DISCUSSION ET INTERPRÉTATION DES RÉSULTATS

Partage du réactif entre le diluant et l'eau

L'augmentation du coefficient de distribution du TBPO, quand la concentration en réactif croît, peut être attribuée à l'une ou l'autre des causes suivantes: augmentation de la constante diélectrique de la phase organique due à la présence de TBPO et (ou) aux associations du TBPO dans la phase organique qui croissent avec la concentration. Les mesures cryoscopiques que nous avons effectuées fournissent, en effet, pour les concentrations supérieures à 0.3 *M*, des valeurs trop élevées. La valeur du

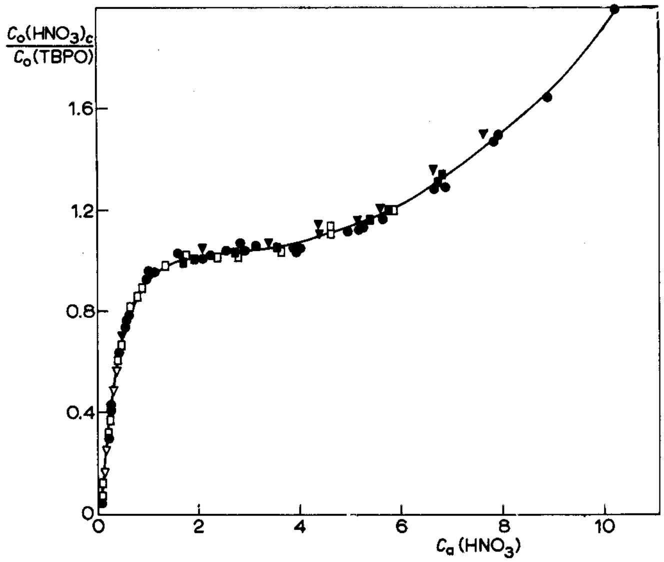

Fig. 1. Distribution de l'acide nitrique entre une phase aqueuse et une phase organique constituée de TBPO en solution dans le benzène. ● c_o^1(TBPO): 0.100 *M*; □ c_o^1(TBPO): 0.138 *M*; ▽ c_o^1 (TBPO): 0.150 *M*; ■ c_o^1(TBPO): 0.200 *M*; ▼ c_o^1(TBPO): 0.396 *M*.

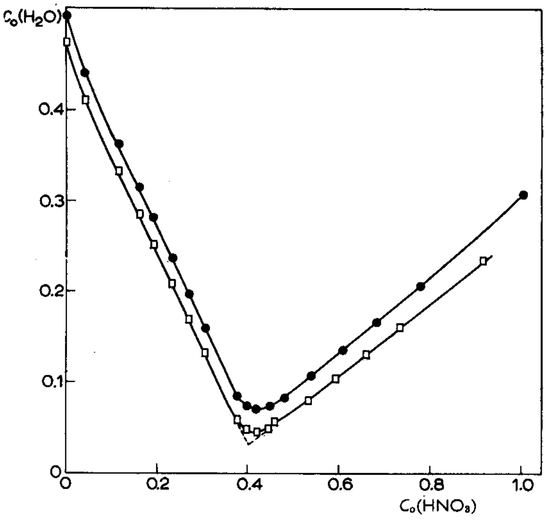

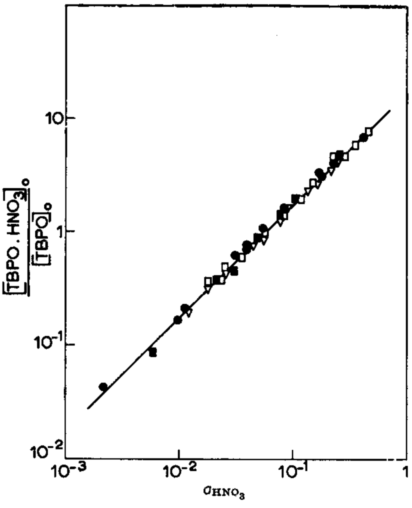

Fig. 2. Hydratation du TBPO en fonction de l'acidité. c_o^1(TBPO): 0.396 *M* dans le benzène. ● Données expérimentales; □ Valeurs corrigées.

Fig. 3. Détermination graphique de la constante apparente de stabilité K_1'. ● c_o^1(TBPO): 0.100 *M*; □ c_o^1(TBPO): 0.138 *M*; ▽ c_o^1(TBPO): 0.150 *M*; ■ c_o^1(TBPO): 0.200 *M*.

coefficient de distribution du TBPO dépend également de la nature du diluant; pour une solution 0.1 *M* en TBPO, il prend les valeurs suivantes: 11.5 pour le benzène, 6.1 pour le toluène, 0.61 pour le cyclohexane et 0.52 pour le *n*-hexane. Comme on le voit, il diminue au fur et à mesure que le pouvoir solvatant du diluant diminue.

Partage de l'acide nitrique ($C_a(\mathrm{HNO_3}) < 2\ M$)

La courbe de la Fig. 1 comprend les résultats obtenus avec des solutions benzéniques de TBPO de différentes concentrations initiales, à savoir: 0.100, 0.138, 0.150, 0.200 et 0.396 *M*; ces solutions étant présaturées en eau à 25°.

On peut constater que tous les résultats se placent pratiquement sur une même courbe si l'on représente $C_o(\mathrm{HNO_3})_c/C_o(\mathrm{TBPO})$ en fonction de $C_a(\mathrm{HNO_3})$; ce fait ne doit pas nous étonner étant donné que, dans la phase organique, nous devons avoir une neutralisation entre le réactif basique et l'acide nitrique avec formation du composé TBPO . HNO_3, c'est-à-dire la réaction

$$\mathrm{H^+}_a + (\mathrm{NO_3^-})_a + \mathrm{TBPO}_o \rightleftharpoons [\mathrm{TBPO\ .\ HNO_3}]_o \tag{1}$$

à laquelle nous pouvons appliquer la loi d'action des masses

$$\frac{[\mathrm{TBPO\ .\ HNO_3}]_o \gamma_2}{a_{\mathrm{HNO_3}}[\mathrm{TBPO}]_o \gamma_1} = K_1 \tag{2}$$

ou γ_1 et γ_2 sont les coefficients d'activité stoéchiométrique des substances présentes en phase organique et $a_{\mathrm{HNO_3}}$ l'activité de l'acide nitrique dans la phase aqueuse[19].

Pour autant que γ_2/γ_1 soit constant dans le domaine de concentrations expérimentées, comme TBPO . HNO_3 peut être considéré comme non dissocié[20] et comme la concentration en acide nitrique dans le diluant seul est négligeable pour $C_a(\mathrm{HNO_3})$ inférieure à 2 *M*, on voit que le rapport $[\mathrm{TBPO\ .\ HNO_3}]_o/[\mathrm{TBPO}]_o$ n'est plus qu'une fonction univoque de l'activité de HNO_3 dans la phase aqueuse, indépendamment de la concentration initiale en TBPO.

Si l'équilibre (1) est le seul en cause, les données expérimentales doivent nous permettre le calcul de la constante d'équilibre.

En effet, dans le domaine de concentration exploré, $C_o(\mathrm{HNO_3})$, obtenu par titrage, peut être assimilé à TBPO . HNO_3 tandis que la différence entre $C_o(\mathrm{TBPO})$ et $C_o(\mathrm{HNO_3})$ donne $[\mathrm{TBPO}]_o$, c'est-à-dire la concentration en TBPO libre à l'équilibre: nous pouvons alors porter en graphique log $[\mathrm{TBPO\ .\ HNO_3}]_o/[\mathrm{TBPO}]_o$ en fonction de log $a_{\mathrm{HNO_3}}$[19] (Fig. 3) ce qui donne, pour les concentrations initiales en TBPO allant jusqu'à 0.200 *M*, une droite unique de pente unitaire.

Ce diagramme permet la détermination de la constante apparente $K_1' \gamma_1/\gamma_2$ correspondant à l'équation d'équilibre:

$$K_1' = \frac{[\mathrm{TBPO\ .\ HNO_3}]_o}{a_{\mathrm{HNO_3}}[\mathrm{TBPO}]_o} \tag{3}$$

Nous avons trouvé pour les solutions benzéniques $K_1' = 17.5 \pm 1.3\ (M/\mathrm{l})^{-2}$.

Le Tableau II contient les résultats obtenus pour le toluène et le *n*-hexane, dans le cas d'une solution 0.100 *M* en TBPO; les considérations ci-dessus restent valables et les constantes apparentes trouvées valent respectivement $K_1' = 20.1 \pm 0.8\ (M/\mathrm{l})^{-2}$ et $11 \pm 2\ (M/\mathrm{l})^{-2}$.

Le fait que le benzène et le toluène favorisent l'extraction de l'acide nitrique comparativement au *n*-hexane, ne doit pas étonner étant donné leur pouvoir solvatant et leurs constantes diélectriques supérieurs.

Signalons ici que, dans le cas du cyclohexane et du *n*-hexane, on note l'apparition d'une troisième phase (phase organique), riche en réactif, avant la saturation du TBPO par l'acide nitrique. Ce phénomène est fréquent avec les diluants de faibles constantes diélectriques (hydrocarbures aliphatiques) non seulement avec les composés organophosphorés[21], mais encore avec les amines tertiaires[22].

Les résultats obtenus avec les solutions de TBPO dans le cyclohexane ne satisfont pas à l'équilibre (1).

Si nous réexaminons la Fig. 1, nous pouvons constater que la réaction (1) n'est pas la seule à avoir lieu puisque la courbe ne tend pas asymptotiquement vers une valeur unitaire de l'ordonnée; au contraire, même en tenant compte de la quantité d'acide nitrique dissoute par le diluant[18], c'est-à-dire en considérant $C_o(HNO_3)_c$, on peut observer un passage dans la phase organique d'acide nitrique en excès par rapport à TBPO . HNO_3. Mais, avant d'essayer de dégager l'interprétation de cette nouvelle réaction, il faut examiner l'équilibre de distribution de l'eau.

Partage de l'eau

Nous pouvons avancer, par analogie avec les résultats acquis avec le phosphate de tri-*n*-butyle[22,23] et sur la base des conclusions tirées de l'étude par spectrométrie infrarouge[24-26], que la solution benzénique de TBPO en équilibre avec l'eau contient principalement TBPO . H_2O aux faibles concentrations et qu'aux concentrations plus élevées, des dimères ou des complexes $TBPO(H_2O)_n$ existent probablement. Mais, étant donné que l'activité de l'eau dans la phase aqueuse est pratiquement constante dans le domaine de formation de TBPO . HNO_3, on peut dire que les considérations émises ci-dessus restent correctes; il ne faut cependant pas perdre de vue que le TBPO libre est partiellement hydraté et que la constante K_1' (3) contient une constante d'équilibre d'hydratation $k = [TBPO . H_2O]_o / a_{H_2O}[TBPO]_o$.

Dans ces conditions, que devient cette eau d'hydratation du TBPO lors de la neutralisation par l'acide nitrique?

Examinons la Fig. 2; celle-ci concerne les résultats d'analyse de l'eau dans une phase benzénique de TBPO de concentration initiale 0.396 *M* (Tableau IV). La courbe supérieure représente les teneurs expérimentales en eau en fonction de l'acidité dans la phase organique. Toutefois, il faut tenir compte de la solubilité non négligeable de l'eau et de l'acide nitrique[17,18] dans le diluant seul; si l'on effectue cette correction, c'est-à-dire si l'on porte en graphique $C_o(H_2O)_c$ en fonction de $C_o(HNO_3)_c$, on obtient la courbe inférieure de la Fig. 2.

On peut, en première approximation, interpréter la partie descendante de l'isotherme de la Fig. 2 par la réaction

$$H^+_a + (NO_3^-)_a + TBPO . H_2O_o \rightleftharpoons TBPO . HNO_{3o} + H_2O \qquad (4)$$

étant bien entendu que TBPO . H_2O n'est pas la seule espèce en cause et que, de plus, une faible proportion du TBPO . HNO_{3o} pourrait être hydraté, le minimum de la courbe corrigée de la Fig. 2 étant différent de zéro.

Le fait que la diminution de l'eau combinée en phase organique est proportionnelle à la concentration en HNO_{3o} montre clairement qu'il s'agit d'une réaction de substitution de l'eau du complexe par HNO_3.

Si, dès que tout le TBPO est neutralisé par l'acide nitrique, on continue à faire augmenter $C_a(HNO_3)$, on assiste à une extraction simultanée d'acide nitrique et d'eau, phénomène que nous essayerons maintenant d'expliquer.

TABLEAU IV

HYDRATATION D'UNE PHASE ORGANIQUE DE TBPO EN FONCTION DE L'ACIDITÉ

$C_o(HNO_3)_e$ *(mole/l)*	ΔV_o*(%)*	C_o(TBPO) *(mole/l)*	$C_o(H_2O)_e$ *(mole/l)*
c_o^i(TBPO): *0.396 M*			
0		0.376	0.474
0.040		0.376	0.411
0.115		0.376	0.333
0.160		0.376	0.286
0.190		0.376	0.253
0.234		0.376	0.208
0.270		0.379	0.169
0.305		0.387	0.132
0.376		0.388	0.059
0.399		0.389	0.0485
0.420		0.396	0.046
0.446		0.396	0.049
0.473		0.395	0.058
0.532	+2	0.392	0.081
0.592	+2	0.392	0.105
0.658	+3	0.380	0.130
0.733	+3	0.372	0.161
0.915	+5	0.376	0.235

Partage de HNO_3 et de H_2O ($C_a(HNO_3) > 2\ M$)

Supposons que nous ayons affaire à la réaction suivante

$$H^+_a + (NO_3^-)_a + H_2O_a + TBPO\ .\ HNO_{3o} \rightleftharpoons TBPO\ .\ 2\ HNO_3\ .\ H_2O_o \qquad (5)$$

Pour cet équilibre, nous pouvons écrire

$$K_2 = \frac{[TBPO\ .\ 2\ HNO_3\ .\ H_2O]_o \gamma_3}{a_{HNO_3}\, a_{H_2O}[TBPO\ .\ HNO_3]_o \gamma_2} \qquad (6)$$

avec γ_3 coefficient d'activité stoéchiométrique du complexe TBPO . 2 HNO_3 . H_2O_o.

Pour autant que γ_3/γ_2 puisse être considéré comme constant dans le domaine de concentration envisagé expérimentalement, la courbe log [TBPO . 2 HNO_3 . $H_2O]_o$/[TBPO . $HNO_3]_o$ en fonction de log $a_{HNO_3} \cdot a_{H_2O}$ devra être une droite de pente 1 si la réaction (5) est la seule en cause. En utilisant les valeurs de a_{HNO_3} et a_{H_2O} de DAVIS ET DE BRUIN[19] et en tenant compte de la solubilité de l'acide nitrique et de l'eau dans le benzène, on obtient effectivement une droite de pente unitaire qui nous a permis de calculer $K_2' = K_2\, \gamma_2/\gamma_3$ dans un domaine de concentration en TBPO allant jusqu'à 0.200 *M* et pour $C_a(HNO_3)$ allant de 2.5 à 6 *M*. La valeur trouvée pour K_2' vaut $(2.9 \pm 0.3)\ 10^{-3}\ (M/l)^{-2}$.

Nous tenons à remercier Euratom et spécialement le Dr. J. KOOI ainsi que l'Institut Interuniversitaire des Sciences Nucléaires pour les subsides accordés à notre laboratoire. Que Mr. F. GILNAY soit aussi remercié pour son aide technique.

RÉSUMÉ

La distribution du TBPO, de l'eau et de l'acide nitrique entre une phase aqueuse et quelques diluants inertes a été déterminée à 25°. Cette étude a permis d'établir les constantes apparentes de stabilité pour les complexes $TBPO \cdot HNO_3$ ($K_1' = 17.5 \pm 1.3$ $(M/l)^{-2}$ dans le benzène; 20.1 ± 0.8 $(M/l)^{-2}$ dans le toluène et 11 ± 2 $(M/l)^{-2}$ dans le *n*-hexane) et $TBPO \cdot 2\,HNO_3 \cdot H_2O$ ($K_2' = (2.9 \pm 0.3)\ 10^{-3}$ $(M/l)^{-2}$ dans le benzène).

SUMMARY

The distribution of TBPO, water and nitric acid has been measured between an aqueous phase and various inert diluents at 25°. This study allowed the determination of the apparent stability constants for two molecular complexes, $TBPO \cdot HNO_3$ ($K_1' = 17.5 \pm 1.3$ $(M/l)^{-2}$ (benzene); 20.1 ± 0.8 $(M/l)^{-2}$ (toluene); 11 ± 2 $(M/l)^{-2}$ (*n*-hexane)) and $TBPO \cdot 2\,HNO_3 \cdot H_2O$ ($K_2' = (2.9 \pm 0.3)\ 10^{-3}$ $(M/l)^{-2}$ (benzene)).

ZUSAMMENFASSUNG

Die Verteilung von TBPO, Wasser und Salpetersäure zwischen einer wässrigen Phase und einigen inerten organischen Lösungsmitteln wurde bei 25° untersucht und die scheinbaren Stabilitätskonstanten des Komplexes $TBPO \cdot HNO_3$ ($K_1' = 17.5 \pm 1.3$ $(M/l)^{-2}$ in Benzol, 20.1 ± 0.8 $(M/l)^{-2}$ in Toluol und 11 ± 2 $(M/l)^{-2}$ in *n*-Hexan) und des Komplexes $TBPO \cdot 2\,HNO_3 \cdot H_2O$ ($K_2' = (2.9 \pm 0.3)\ 10^{-3}$ $(M/l)^{-2}$ in Benzol) bestimmt.

BIBLIOGRAPHIE

1 C. E. Higgins, W. H. Baldwin et J. M. Ruth, *USAEC Report ORNL-1338*, 1957.
2 J. C. White et W. J. Ross, *USAEC NAS-NS 3102*, 1961.
3 J. C. White et W. J. Ross, *USAEC Report ORNL-CF-56-9-18*, 1956.
4 J. C. White, Am. Soc. Testing Materials, Special Publication no. 238, 1958.
5 J. C. White et W. J. Ross, *USAEC Report ORNL-2498*, 1958.
6 R. A. Zingaro et J. C. White, *J. Inorg. Nucl. Chem.*, 12 (1961) 315.
7 W. J. Ross et J. C. White, *USAEC Report ORNL-2627*, 1958.
8 B. Martin, D. W. Ockenden et J. K. Foreman, *J. Inorg. Nucl. Chem.*, 21 (1961) 96.
9 J. C. White et W. J. Ross, *USAEC Report ORNL-2326*, 1957.
10 G. E. Boyd et Q. V. Larson, *J. Phys. Chem.*, 64 (1960) 988.
11 T. Ishimori, K. Kimura, T. Fujino et H. Murakimi, *J. At. Energy Soc. Japan*, 4 (1962) 117.
12 C. A. Blake, K. B. Brown et G. F. Coleman, *USAEC Report ORNL-1964*, 1955.
13 D. W. Archer, R. B. Heslop et R. Kirky, *Anal. Chim. Acta*, 30 (1964) 450.
14 L. Winand, *J. Chromatog.*, 7 (1962) 400.
15 D. C. Wimer, *Anal. Chem.*, 34 (1962) 873.
16 J. Mitchell et D. M. Smith, *Aquametry*, Interscience, New York, 1948.
17 G. Duyckaerts et J. Goffart, *Rapp. Eur. 437 f*, 1964.
18 E. Hogfeldt et B. Bolander, *Arkiv Kemi*, 21 (1963) 161.
19 W. Davis et H. J. de Bruin, *J. Inorg. Nucl. Chem.*, 26 (1964) 1069.
20 K. Alcock, S. S. Grimley, T. V. Healy, J. Kennedy et H. A. C. Mac Kay, *Trans. Faraday Soc.*, 52 (1956) 39.
21 E. Foa, N. Rosintal et Y. Marcus, *J. Inorg. Nucl. Chem.*, 23 (1961) 109.
22 S. S. Choi et D. G. Tuck, *J. Phys. Chem.*, 68 (1964) 2712.
23 R. C. Axtmann, *Nucl. Sci. Eng.*, 16 (1963) 241.
24 R. Machiroux, *Thèse annexe*, Université de Liège, 1965.
25 P. Pallage, *Mémoire de Licence en Sc. Chimiques*, Université de Liège, 1962.
26 G. Duyckaerts et G. Roland, *Spectrochim. Acta*, 22 (1966) 793.

SECOND-ORDER INTERFERENCE IN THE NEUTRON ACTIVATION ANALYSIS OF ARSENIC IN A GERMANIUM MATRIX

R. DE NEVE, D. DE SOETE AND J. HOSTE
Institute for Nuclear Science, Ghent University, Ghent (Belgium)
(Received June 27th, 1966)

Activation analyses of arsenic in germanium with thermal neturons have been described by several authors[1-3]. In these methods the ^{76}As activity produced by a (n,γ) reaction on monoisotopic ^{75}As, is measured by β- or γ-spectrometry, after chemical separation of arsenic from germanium.

The sensitivity of the determination is limited by the reaction ^{74}Ge (n,γ; β^-; n,γ) ^{76}As. This interference, which gives rise to the same isotope and thus causes a positive error, was computed as a function of the irradiation time and the neutron flux by RICCI AND DYER[4] and by GROSJEAN[5]. As the computed values differ to a large extent, an experimental determination was carried out in the present work.

THEORETICAL CONSIDERATIONS

^{76}As is formed from germanium according to the reaction scheme:

$$\begin{tikzcd}
 & {}^{75m}\mathrm{Ge} \arrow[dd, "\mathrm{I.T}"] & & \\
{}^{74}\mathrm{Ge} \arrow[ur, "(n{,}\gamma)"] \arrow[dr, "(n{,}\gamma)"'] & & & \\
 & {}^{75}\mathrm{Ge} \arrow[r, "\beta^-"] & {}^{75}\mathrm{As}(n,\gamma){}^{76}\mathrm{As} \arrow[r, "\beta^-{,}\gamma"] & {}^{76}\mathrm{Ge}
\end{tikzcd} \qquad (1)$$

As the half-life of the isomeric transition of ^{75m}Ge (48 sec) is considerably lower than the half-life of ^{75}Ge (82 min), one can consider that all the ^{75}Ge is produced by direct neutron capture, with a cross-section which is the sum of both modes of formation. This simplifies the reaction scheme to:

$$N_1 \xrightarrow[\sigma_1]{\Phi} \underset{A_2}{N_2} \xrightarrow{\lambda_2} N_3 \xrightarrow[\sigma_3]{\Phi} \underset{A_4}{N_4} \xrightarrow{\lambda_4} N_5 \qquad (2)$$

where A = activity in dis./sec; N = number of atoms; λ = distintegration constant; σ = effective activation cross-section; Φ = effective thermal neutron flux (neutron density between 0 and 0.5 eV, times 2,200 m/sec).

The indices 1 to 4 indicate respectively the isotopes ^{74}Ge, ^{75}Ge, ^{75}As and ^{76}As.

The growth of the ^{76}As activity (A_4) as a function of the irradiation time t and the neutron flux, is given by the BATEMAN equation:

$$A_4 = \gamma_4 \sum_{i=1}^{4} C_i e^{-\Omega_i t} \qquad (3)$$

where

t = irradiation time;

$$C_1 = \frac{\Omega_1\Omega_2\Omega_3}{(\Omega_2-\Omega_1)(\Omega_3-\Omega_1)(\Omega_4-\Omega_1)} N_1{}^0$$
$$\vdots$$
$$C_4 = \frac{\Omega_1\Omega_2\Omega_3}{(\Omega_1-\Omega_4)(\Omega_2-\Omega_4)(\Omega_3-\Omega_4)} N_1{}^0$$

$N_1{}^0$ = number of ^{74}Ge atoms at $t=0$; $\Omega_1=\Phi\sigma_1$; $\Omega_2=\lambda_2$; $\Omega_3=\Phi\sigma_3$; $\Omega_4=\lambda_4$.

For practical purposes it is more convenient to express the activity induced by second-order interference as an apparent arsenic concentration in p.p.b.:

$$C_{\text{ppb}} = \frac{A_4 \text{ (for 1 g Ge)}}{A'_4 \text{ (for 1 m}\mu\text{ As standard)}} \tag{4}$$

or

$$C_{\text{ppb}} = \frac{A_4}{N'_4\sigma_3\phi(1-e^{-\lambda_4 t})} \tag{5}$$

If one assumes that in reaction scheme (2) the number of ^{75}As atoms undergoing neutron capture is small in comparison with the activity of ^{75}Ge, *i.e.* $N_3\Phi\sigma_3 \ll A_2$, eqn. (5) simplifies to:

$$C_{\text{ppb}} = \frac{N_1\sigma_1\phi}{N'_4(1-e^{-\lambda_4 t})}\left[t - \frac{\lambda_2+\lambda_4}{\lambda_2\lambda_4} + \frac{\lambda_2}{\lambda_4(\lambda_2-\lambda_4)} e^{-\lambda_4 t} - \frac{\lambda_4}{\lambda_2(\lambda_2-\lambda_4)} e^{-\lambda_2 t}\right] \tag{6}$$

This assumption is valid for $t \geqslant 2$ h. As appears from eqn. (6) the apparent arsenic concentration is proportional to σ_1 and to the neutron flux.

TABLE I

NUCLEAR DATA

	(1)	*(2)*
Φ_{thermal}	10^{12}	$5 \cdot 10^{13}$
$\Phi_{\text{epithermal}}$	0	0.1 Φ_{th}, 0.33 Φ_{th}
σ_1	0.60 barn	0.25 barn
σ_3	4.2 barn	5.4 barn
$(T_{\frac{1}{2}})_1$	82 min	82 min
$(T_{\frac{1}{2}})_2$	26 h	27 h
θ^{74}Ge	0.3674	0.3674

Table I shows the nuclear data, which were used by RICCI *et al.* (column 1) and GROSJEAN (column 2) for the computation of this interference, by means of the BATEMAN equation, for a given neutron flux as a function of irradiation time. As appears from Fig. 1, the apparent concentration computed by GROSJEAN (curve A) is higher by a factor of 2.4 than the values given by RICCI (curve C). This is mainly due to the higher value of σ_1, as given in Table I.

SAMPLING AND IRRADIATION CONDITIONS

Approximately 25 mg of highly pure GeO$_2$ was weighed in silica vials. The GeO$_2$ was previously analysed at a thermal neutron flux of $4 \cdot 10^{11}$ and an irradiation

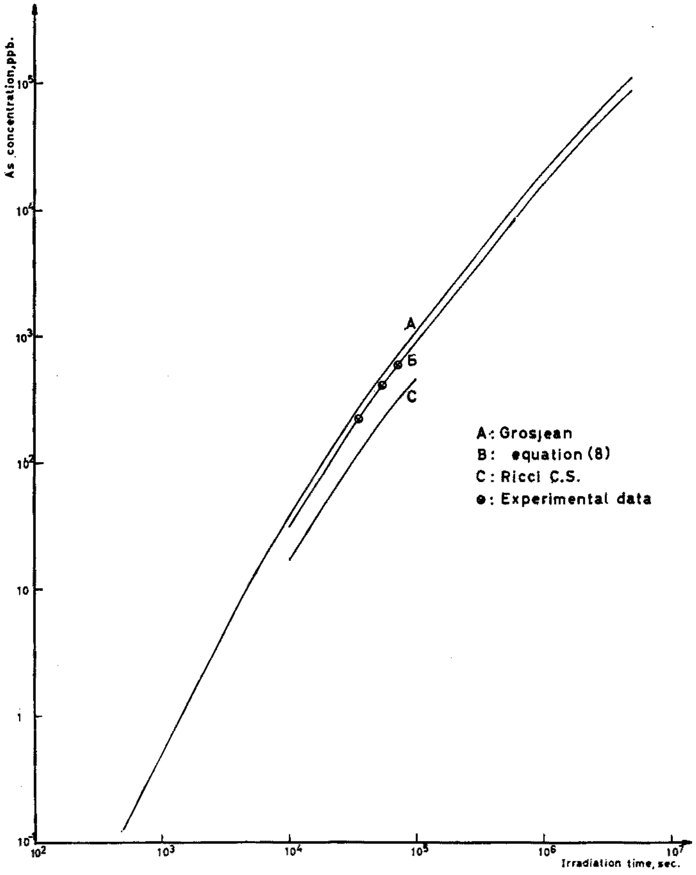

Fig. 1. Apparent As concentrations in Ge, induced by the second-order interference ^{74}Ge (n, γ; β^-; n, γ) $\rightarrow$ ^{76}As at a thermal neutron flux of 10^{14} n/cm^2/sec. (A) GROSJEAN; (B) eqn. (8); (C) RICCI; ⊗ experimental data.

time of 48 h, and showed a total arsenic concentration of 16 ± 3 p.p.b. per g of germanium.

Arsenic standards were made by evaporating 50 μl of a 6 N nitric acid solution which contained 20 μg As/ml in a silica vial. The vials were sealed after evaporation.

As the irradiation times (up to 20 h) were of the same order of magnitude of the ^{76}As half-life (26 h), cobalt flux-monitors were inserted into the irradiation containers. Each capsule contained 6 cobalt needles of 0.5 mm diameter and 9 mm length. The samples were positioned in an aluminium cylinder of 2.2 cm diameter and 1.5 cm height, with 5 large holes, for the 2 GeO_2 samples and the 3 standards and 6 smaller ones for the cobalt needles, as shown in Fig. 2.

The aluminium cylinder was introduced into a standard aluminium capsule and irradiated in the BR-2 reactor of the S.C.K. at Mol. Three capsules were irradiated for respectively 10, 15 and 20 h at an effective thermal neutron flux of approx. 10^{14} n/cm^2/sec. The analysis of the samples was carried out after a cooling period of *ca.* 20 h.

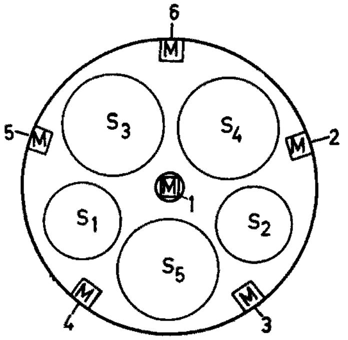

Fig. 2. Section of the Al-cylinder for sample positioning. M, Co monitors; S, samples or standards.

CHEMICAL SEPARATION

Chemical procedure for the GeO_2 samples

Transfer the GeO_2 samples to a nickel crucible, add 20 mg of As carrier as sodium arsenate and fuse with 4 g of sodium hydroxide. Dissolve the melt in 100 ml of water and filter the solution in order to remove insoluble nickel oxide particles. Add 6 g of ammonium oxalate per 1 g of germanium, dilute to 250 ml and acidify with 6 *N* hydrochloric acid to pH 1. Add 2 g of thioacetamide and *ca.* 20 mg of potassium iodide, boil the solution for 10 min, filter the arsenic trisulfide precipitate through a coarse grained filter, wash with 6 *N* hydrochloric acid containing 0.01% thioacetamide and dissolve the precipitate on the filter in 10 ml of 6 *N* ammonia solution. Add 10 ml of sodium germanate hold-back carrier solution, containing 1 mg Ge/ml and 60 mg of ammonium oxalate, dilute to 250 ml with water, acidify with 6 *N* hydrochloric acid to pH 1 and carry out a second arsenic precipitation. After filtration, dissolve the arsenic trisulfide in 10 ml of 6 *N* ammonia solution. Add 2 ml of 30% hydrogen peroxide and 5 ml of a $SbCl_5$ hold-back carrier solution containing 1 mg Sb/ml, and take the solution to dryness.

Dissolve the residue in 20 ml of Bougault's reagent (dissolve 100 g of sodium hypophosphite in 1 liter of 8 *N* hydrochloric acid and filter). Heat the solution for 30 min on a boiling water bath, filter off the elementary arsenic on a weighed glass filter plate, wash with 2 ml of 8 *N* hydrochloric acid and with acetone, and dry for 45 min at 110°. Determine the chemical yield by weighing (*ca.* 85%) and count for 5 min.

Chemical procedure for the arsenic standards

Remove any surface contamination on the sealed silica vials by boiling for 10 min in 6 *N* nitric acid. Dry and crush the vials in a 100-ml beaker containing 20 ml of 6 *N* sodium hydroxide and 20 ml of sodium arsenate carrier solution (1 mg As/ml). Boil for 30 min with vigorous stirring, filter off the silica, transfer the solution to a 1-l volumetric flask, and dilute to the mark. Withdraw a 10-ml aliquot into a 400-ml beaker containing 20 mg of As carrier and precipitate as described above. Determine the chemical yield by weighing and count for 5 min.

COUNTING TECHNIQUE

The β-spectrometric technique for the determination of arsenic in germanium has been described elsewhere[3]. A plastic scintillation detector, coupled to a 400-channel analyser was used. An aluminium absorber of 300 mg/cm^2 is required to avoid pile-up of the high activity level of the β-rays due to ^{77}As ($E_{\beta\text{max}} = 0.69$ MeV).

As relative measurements of the ^{76}As activities ($E_{\beta\text{max}} = 2.96$ MeV) were carried out, only the channels proportional to a β-energy > 0.7 MeV were taken into account. In this region the measured ^{75}As activity, extrapolated to the end of the irradiation, yielded $2.2 \cdot 10^3$ counts/min/mμ As for an irradiation time of 20 h at a thermal neutron flux of 10^{14} n/cm^2/sec, whereas the background was 15 counts/min only. In order to check the purity of the measured ^{76}As activity, the decay was followed during 6 days. Half-lives of 26.2 to 26.5 h were obtained.

DETERMINATION OF THE EFFECTIVE THERMAL NEUTRON FLUX

The effective thermal neutron flux was measured in each irradiated container by means of the 6 cobalt needles, placed as shown in Fig. 2. The flux values for the samples and the standards were calculated by linear interpolation of the values measured in the 2 adjacent monitors.

The thermal neutron fluxes were determined by the product of the neutron density between 0 and 0.5 eV and a neutron velocity of 2,200 m/sec. These measurements were carried out by DEBRUE and coworkers of the S.C.K. at Mol. The results for the 3 irradiations are given in Table II. The error on the absolute flux determinations was estimated to be *ca.* 5%. The ratio of the thermal to the epithermal neutron flux was also determined for the irradiation site and appeared to be *ca.* 75.

TABLE II

THERMAL NEUTRON FLUXES

Place of the flux monitor	$\Phi_{\text{th}} = [n]_0^{0.5\text{ eV}} \cdot V_0$ *for irradiation time =*		
	10 h	*15 h*	*20 h*
1	$0.92 \cdot 10^{14}$	$1.00 \cdot 10^{14}$	$5.48 \cdot 10^{13}$
2	$0.95 \cdot 10^{14}$	$1.00 \cdot 10^{14}$	$5.45 \cdot 10^{13}$
3	$0.93 \cdot 10^{14}$	$0.98 \cdot 10^{14}$	$5.90 \cdot 10^{13}$
4	$0.93 \cdot 10^{14}$	—	$5.72 \cdot 10^{13}$
5	$0.93 \cdot 10^{14}$	$1.06 \cdot 10^{14}$	$5.28 \cdot 10^{13}$
6	$0.95 \cdot 10^{14}$	$1.06 \cdot 10^{14}$	$5.14 \cdot 10^{13}$

$$\frac{\Phi_{\text{th}}}{\Phi_{\text{epi}}} \simeq 75 \tag{7}$$

where

$\Phi_{\text{th}} = [n]_0^{0.5\text{eV}} \cdot 2{,}200$ m/sec; Φ_{epi} = neutron flux per unit logarithmic energy interval.

Assuming in the epithermal region:

$$\Phi_{(\text{E})} = \Phi_{\text{epi}} E^{-1} \tag{8}$$

the ratio of the thermal (R_{th}) to the epithermal reaction rate (R_{epi}) is given by:

$$\frac{R_{\text{th}}}{R_{\text{epi}}} = \frac{\Phi_{\text{th}}\sigma_{2,200\text{ m/sec}}}{\Phi_{\text{epi}} \int_{0.5}^{\infty} \sigma(E)\, \frac{\text{d}E}{E}} \tag{9}$$

Accepting a $1/v$ function for σ_1, one can calculate that at the irradiation site, $R_{\mathrm{epi}} \simeq 0.007\ R_{\mathrm{th}}$.

Thus the epithermal flux contributes only to the extent of 0.7 % to the (n,γ) reaction on ^{74}Ge, and hence one can assume that the effective activation cross-section σ_1 can be replaced by $\sigma_{2,200\ \mathrm{m/sec}}$

RESULTS

The second-order arsenic interference, induced in the GeO_2 samples during the 48-h irradiation at $4 \cdot 10^{11}$ n/cm²/sec, was calculated by 2 successive approximations from the data obtained by GROSJEAN. These approximations were required as the experimental results appeared to be lower by 20% than the computed ones. They corresponded to 7 ± 1 p.p.b. of arsenic per gram of germanium. The error is the standard deviation of 4 experiments. The true arsenic content consequently was 9 p.p.b. per g of germanium.

The experimental values of the second-order interference are summarized in Table III, and are given, normalised to a flux of 10^{14} n/cm²/sec on curve B of Fig. 1.

TABLE III

EXPERIMENTAL RESULTS OF THE SECOND-ORDER INTERFERENCE

$^{74}\mathrm{Ge}\ (\mathrm{n},\gamma;\ \beta^-;\ \mathrm{n},\gamma)\ ^{76}\mathrm{As}$

Irradiation conditions		*As concn (p.p.b.)*			σ_1 *(barn)*
time (h)	Φ_{th}	*Total*	*True*	*Apparent*	
48	$4 \cdot 10^{11}$	16 ± 3	9	7	—
10	$0.93 \cdot 10^{14}$	206	9	197	0.44
10	$0.93 \cdot 10^{14}$	226	9	217	0.48
15	$0.99 \cdot 10^{14}$	402	9	393	0.48
15	$1.05 \cdot 10^{14}$	448	9	439	0.50
20	$5.7 \cdot 10^{13}$	365	9	356	0.51
20	$5.45 \cdot 10^{13}$	320	9	311	0.47

Introducing these values in eqn. (6) yielded the values of σ_1 given in the last column of Table III. In fact second-order interference provides a relatively simple way to check activation cross-sections. This technique can be useful if the product of direct activation is too complex to allow a precise measurement of the isotope of interest.

The average value of $\sigma_1 = 0.48 \pm 0.06$ barn, substituted in eqn. (6) gave curve B. The latter is parallel to the curves A and C computed by GROSJEAN and RICCI *et al.* The displacement is due to the applied experimental value of σ_1, which differs from the values used by the earlier authors, which were 0.60 barn and 0.25 barn respectively. Values reported in the literature vary from 0.25 to 0.7 barn[6-8].

The authors wish to thank the "Interuniversitair Instituut voor Kernwetenschappen" who sponsored this work, and D. DEBRUE and coworkers of the S.C.K. at Mol who carried out the flux monitoring. They also thank Mrs. J. GORLÉE-ZELS for technical assistance.

SUMMARY

The second-order interference ^{74}Ge(n, γ; β^-, n, γ)^{76}As can occur in the activation analysis of arsenic in a germanium matrix, using thermal neutrons. As the literature data show poor agreement, this interference was determined experimentally. A practical formula was derived, for irradiation times longer than 2 h, which showed that the interference, expressed as an apparent arsenic concentration, is proportional to the neutron flux. Experiments were performed for irradiation times of 10, 15 and 20 h at a neutron flux of 10^{14} n/cm^2/sec, yielding apparent arsenic concentrations in the germanium matrix of respectively 223, 408 and 597 p.p.b. From these results a value of 0.48 ± 0.06 barn could be calculated for the activation cross-section of ^{74}Ge for neutron capture.

RÉSUMÉ

Une interférence de second ordre ^{74}Ge(n, γ; β^-; n, γ) ^{76}As peut se produire lors du dosage de l'arsenic dans une matrice de germanium, par activation, avec neutrons thermiques. Une formule pratique est dérivée pour des durées d'irradiation dépassant 2 heures, montrant que l'interférence est proportionnelle au flux de neutrons. Les expériences ont été effectuées avec des temps d'irradiation de 10, 15 et 20 h avec flux de neutrons de 10^{14} n/cm^2/sec, pour des concentrations apparentes en arsenic de 223, 408 et 597 p.p.b. respectivement.

ZUSAMMENFASSUNG

Bei der neutronenaktivierungsanalytischen Bestimmung von Arsen in einer Germaniummatrix können Störungen zweiter Ordnung durch ^{74}Ge (n, γ; β^-; n, γ) ^{76}As auftreten. Da die Literaturangaben schlecht übereinstimmen, wurde diese Störung experimentell bestimmt. Dazu wurde eine Formel für Bestrahlungszeiten von mehr als 2 Stunden abgeleitet, welche zeigte, dass die Störung in Form einer scheinbaren Arsenkonzentration proportional dem Neutronenfluss ist. Bei Bestrahlungszeiten von 10, 15 und 20 Stunden bei einem Neutronenfluss von 10^{14} n/cm^2/sec ergaben scheinbare Arsenkonzentrationen in der Germaniummatrix von 223, 408 bzw. 597 p.p.b. Aus diesen Ergebnissen konnte ein Aktivierungsquerschnitt von 0.48 ± 0.06 barn für den Neutroneneinfang von ^{74}Ge berechnet werden.

REFERENCES

1 A. A. Smales and B. D. Pate, *Anal. Chem.*, 24 (1952) 717.
2 G. H. Morrison and J. F. Cosgrove, *Anal. Chem.*, 27 (1955) 810.
3 D. De Soete, R. De Neve and J. Hoste, *Modern Trends in Activation Analysis*, Texas, 1965.
4 E. Ricci and F. Dyer, *Nucleonics*, 22 (1964) 45.
5 C. C. Grosjean, private communication.
6 G. Friedlander and J. W. Kennedy, *Nuclear and Radiochemistry*, J. Wiley, New York, 1960.
7 D. J. Hughes and R. B. Schwartz, *USAEC report BNL-325*, 1954; 1958/60.
8 W. Schulze, *Neutronenaktivierung als anal. Hilfsmittel*, F. Enke Verlag, Stuttgart, 1962.

DIRECT EDTA TITRATION OF VANADIUM(V) USING VARIAMINE BLUE B BASE AS INDICATOR IN THE PRESENCE OF EXCESS IRON(II)

MOTOHARU TANAKA AND AKEMI ISHIDA

Laboratory of Analytical Chemistry, Faculty of Science, Nagoya University, Chikusa-ku, Nagoya (Japan)

(Received May 18th, 1966)

It is well known that the presence of a complexing agent modifies the potential of a system involving metallic species. On the other hand a metal generally forms a more stable complex in the tervalent state than in lower or higher oxidation states, *e.g.* with EDTA, iron(III) forms a more stable complex than iron(II), and vanadium(III) gives a more stable complex than vanadium(IV or V)[1,2]. Thus, a redox titration of a metal M(IV, V or VI) with a metal N(I or II) is favored by the presence of a suitable complexing agent. Alternatively, titration of a metal M(IV, V or VI) with a suitable complexing agent is possible in the presence of excess metal N(I or II).

In the present paper, redox titrations based on the above principle are considered theoretically and a new method of EDTA titration of vanadium(V) is developed.

THEORETICAL CONSIDERATIONS

Direct titration of vanadium(V) with iron(II) in the absence of any complexing agent seems somewhat delicate in particular in a less acid medium because of a small difference in potential of the systems VO_2^+/VO^{2+} and Fe^{3+}/Fe^{2+} (see Table I). However, since the following equilibrium (1) tends to the right, titration of vanadium(V) with iron(II) should be successful in the presence of excess EDTA.

$$(VO_2Y)' + Y' + Fe^{2+} \rightleftharpoons (VOY)' + (Fe(III)Y)' \tag{1}$$

Moreover, the titration of vanadium(V) with EDTA seems possible in the presence of excess iron(II), because equilibrium (1') also tends to the right:

$$VO_2^+ + Fe^{2+} + Y' \rightleftharpoons VO^{2+} + (Fe(III)Y)' \tag{1'}$$

These two cases can be distinguished in treating the equilibria involved.

Titration of vanadium(V) with iron(II) in the presence of excess EDTA

During the titration, the following stoichiometric relationships hold:

$$C_{Fe} = C_{Fe(III)} + C_{Fe(II)} \tag{2}$$

$$C_V = C_{V(V)} + C_{V(IV)} \tag{3}$$

The potentials of the Fe(III)/Fe(II) and V(V)/V(IV) systems are given as follows:

$$\left.\begin{aligned} E_{\mathrm{Fe}} &= E_{\mathrm{Fe'}}{}^{0} + 0.059 \log \frac{C_{\mathrm{Fe(III)}}}{C_{\mathrm{Fe(II)}}} \\ E_{\mathrm{Fe'}}{}^{0} &= E_{\mathrm{Fe}}{}^{0} + 0.059 \log \frac{\alpha_{\mathrm{Y(Fe^{II})}}}{\alpha_{\mathrm{Y(Fe^{III})}}} \end{aligned}\right\} \tag{4}$$

$$\left.\begin{aligned} E_{\mathrm{V}} &= E_{\mathrm{V'(H)}}{}^{0} + 0.059 \log \frac{C_{\mathrm{V(V)}}}{C_{\mathrm{V(IV)}}} \\ E_{\mathrm{V'(H)}}{}^{0} &= E_{\mathrm{V}}{}^{0} + 0.059 \log \frac{\alpha_{\mathrm{Y(V^{IV})}}}{\alpha_{\mathrm{Y(V^{V})}}} - 0.118\mathrm{pH} \end{aligned}\right\} \tag{5}$$

$$C_{\mathrm{Fe(III)}} = C_{\mathrm{V(IV)}} \tag{6}$$

where α's refer to the side-reaction coefficients taking into account the complex formation of the relevant metals with Y. $E_{\mathrm{Fe'}}{}^{0}$ and $E_{\mathrm{V'(H)}}{}^{0}$ are the *formal potentials*. From eqns. (4) and (5) we have

$$\log K_{\mathrm{V'(H)-Fe'}} = \frac{E_{\mathrm{V'(H)}}{}^{0} - E_{\mathrm{Fe'}}{}^{0}}{0.059} = \log \frac{C_{\mathrm{Fe(III)}} C_{\mathrm{V(IV)}}}{C_{\mathrm{Fe(II)}} C_{\mathrm{V(V)}}} \tag{7}$$

where $K_{\mathrm{V'(H)-Fe'}}$ designates the *conditional redox equilibrium constant* of equilibrium (1)[3]. Then by substitution and rearrangement of eqns. (2) through (7) we have a continuous expression for the fraction titrated a:

$$a \equiv \frac{C_{\mathrm{Fe}}}{C_{\mathrm{V}}} = (1 + X_{\mathrm{V'}})^{-1} + \frac{1}{K_{\mathrm{V'(H)-Fe'}}(1 + X_{\mathrm{V'}})X_{\mathrm{V'}}} \tag{8}$$

where

$$\log X_{\mathrm{V'}} = \log \frac{C_{\mathrm{V(V)}}}{C_{\mathrm{V(IV)}}} = \frac{E - E_{\mathrm{V'(H)}}{}^{0}}{0.059}$$

In eqn. (8) the second term is mainly concerned with the transition after the equivalence point. Thus in the second term X_{V} may be neglected. Then eqn. (8) can be rewritten as:

$$a = (1 + X_{\mathrm{V'}})^{-1} + \frac{1}{K_{\mathrm{V'(H)-Fe'}} X_{\mathrm{V'}}} \tag{8'}$$

or

$$a = \tfrac{1}{2}\{1 + \tanh 19.5(E_{\mathrm{V'(H)}}{}^{0} - E)\} + 2\{1 + \tanh 19.5(E - E_{\mathrm{Fe'}}{}^{0})\}^{-1} - 1 \tag{8''}$$

In the vicinity of the equivalence point, eqn. (8′) simplifies to:

$$a = 1 - X_{\mathrm{V'}} + \frac{1}{K_{\mathrm{V'(H)-Fe'}} X_{\mathrm{V'}}} \tag{9}$$

Equation (9) resembles the expressions for [M] during compleximetric titrations. Thus, $\log X_{\mathrm{V}}$ being linearly related to E, it is reasonable, in *a redox titration involving a one-electron transfer*, to locate the end-point at a point where $|\partial E/\partial a|$ is maximum.

Titration of vanadium(V) with EDTA in the presence of excess iron(II)

This is a new type of compleximetric titration. During the titration the following stoichiometric relationships hold:

$$C_Y = [\mathrm{Fe(III)Y}]' + [\mathrm{V(V)Y}]' + [\mathrm{V(IV)Y}]' + [\mathrm{Y}]' \qquad (10)$$

$$C_V = [\mathrm{V(V)Y}]' + [\mathrm{V(V)}]' + [\mathrm{V(IV)Y}]' + [\mathrm{V(IV)}]' \qquad (11)$$

$$C_{Fe} = [\mathrm{Fe(III)}]' + [\mathrm{Fe(II)}]' + [\mathrm{Fe(III)Y}]' \qquad (12)$$

$$[\mathrm{Fe(III)Y}]' + [\mathrm{Fe(III)}]' = [\mathrm{V(IV)Y}]' + [\mathrm{V(IV)}]' \qquad (13)$$

In eqns. (12) and (13) [Fe(III)]′ may be neglected. From eqns. (10)–(13), we have:

$$a \equiv \frac{C_Y}{C_V} = 1 - \frac{[\mathrm{V(V)}]'}{C_V} + \frac{[\mathrm{Fe(III)Y}]'\alpha_{\mathrm{H,V(IV)(Y)}}}{[\mathrm{Fe}^{3+}]K'_{\mathrm{FeY}}C_V} \qquad (14)^*$$

where $\alpha_{\mathrm{H,V(IV)(Y)}}$ denotes the side-reaction coefficient taking into account the presence of excess V(IV), *i.e.* $\alpha_{\mathrm{H,V(IV)(Y)}} = K_{\mathrm{V(IV)'Y}}[\mathrm{V(IV)}]' + \alpha_{\mathrm{H(Y)}}$.

The second term of the eqn. (14) is mainly concerned with the transition before the equivalence point, where $C_V = [\mathrm{V(V)}]' + [\mathrm{V(IV)}]'$. The third term of the same equation is mainly concerned with the transition after the equivalence point, where $C_V = [\mathrm{Fe(III)Y}]'$. If a large excess of iron(II) is used, $[\mathrm{Fe(II)}] \simeq C_{Fe}$. Then eqn. (15) results:

$$a = (1 + X_V)^{-1} + \frac{\alpha_{\mathrm{H,V(IV)(Y)}}}{K_{\mathrm{V(H)-Fe}}K'_{\mathrm{FeY}}C_{\mathrm{Fe}}X_V} \qquad (15)$$

where $X_V = [\mathrm{VO_2}^+]/[\mathrm{VO}^{2+}]$,

$$\log K_{\mathrm{V(H)-Fe}} = \frac{E_{\mathrm{V(H)}}{}^0 - E_{\mathrm{Fe}}{}^0}{0.059} = \log \frac{[\mathrm{Fe}^{3+}][\mathrm{VO}^{2+}]}{[\mathrm{Fe}^{2+}][\mathrm{VO_2}^+]}$$

and $E_{\mathrm{V(H)}}{}^0 = E_V{}^0 - 0.118\ \mathrm{pH}$**.

In the vicinity of the equivalence point, X_V being very small compared with unity, eqn. (15) approximates closely to:

$$a = 1 - X_V + \frac{\alpha_{\mathrm{H,V(IV)(Y)}}}{K_{\mathrm{V(H)-Fe}}K'_{\mathrm{FeY}}C_{\mathrm{Fe}}X_V} \qquad (16)$$

From eqn. (16) it may be said that the end-point can be reasonably located at a point where $|\partial E/\partial a|$ is a maximum. In constructing *a–E* curves, calculation is much simplified by the use of hyperbolic tangents as in the preceding case.

Potentiometric sharpness index

The potentiometric sharpness index $S_{\mathrm{pot.}}$ is defined as:

$$S_{\mathrm{pot.}} = |\partial E/\partial a|_{\mathrm{e.p.}} \qquad (17)$$

$S_{\mathrm{pot.}}$ can be easily calculated by means of eqns. (9) and (16) and serves as a measure of the sharpness of a titration. If an error of ΔE is introduced in the end-point

---

* Conditional constant $K_{\mathrm{Fe(III)Y(Fe(III)Y)'}}$ is designated as K'_{FeY}.

** Polynuclear species are neglected for simplicity. Near the equivalence point, where the concentration of V(V) is very low, the formation of polynucear species would not be considerable at pH 2, although it may be appreciable at higher concentration and higher pH[4].

location in a potentiometric titration, the theoretical titration error is given by the following:

$$\text{Titration error}(\%) = \Delta E/S_{\text{pot.}} \cdot 100 \qquad (18)$$

Calculated values for $S_{\text{pot.}}$ are tabulated in Table I.

TABLE I

POTENTIOMETRIC SHARPNESS INDEX

	$S_{\text{pot.}}$ *(V)*
Titration of V(V) with Fe(II) in the absence of any complexing agent, at pH = 0	1.1
Titration of V(V) with Fe(II) in the absence of any complexing agent, at pH = 1	0.11
Titration of V(V) with Fe(II) in presence of 10^{-2} *M* excess of EDTA at pH = 2	880
Titration of 10^{-3} *M* V(V) with EDTA in the presence of 10^{-2} *M* excess of Fe(II) at pH = 2	17

Use of a redox indicator in the EDTA titration of vanadium(V)

If a redox indicator, *e.g.* variamine blue B base, is utilized as an indicator in the EDTA titration of vanadium(V), the following equilibrium is involved:

$$2\,VO_2^+ + Red' \rightleftharpoons 2\,VO^{2+} + Ox' \qquad (19)^*$$

where Red and Ox refer to the reduced and oxidized species of the indicator. From the conditional constant of equilibrium (19), we have

$$\log K_{V(H)-I'(H)} = \frac{E_{V(H)}{}^{0} - E_{I'(H)}{}^{0}}{0.0296} = \log \frac{[VO^{2+}]^2[Ox]'}{[VO_2^+]^2[Red]'} \qquad (20)$$

Indicator transition is defined as:

$$\phi = \frac{[Ox]'}{C_I} \qquad (21)$$

And taking into account the reduction of vanadium(V) by the indicator, eqn. (13′) should be used instead of eqn. (13):

$$[Fe(III)Y]' + [Fe(III)]' + 2\,[Ox]' = [V(IV)Y]' + [V(IV)]' \qquad (13')$$

Then substituting and rearranging these equations, we get

$$a = 1 - \frac{1}{(K_{V(H)-I'(H)})^{\frac{1}{2}}}\left(\frac{\phi}{1-\phi}\right)^{\frac{1}{2}} - \frac{2C_I}{C_V}\phi + \frac{\alpha_{H,V(IV)(Y)}(K_{V(H)-I'(H)})^{\frac{1}{2}}}{K_{V(H)-Fe}K'_{FeY}C_{Fe}}\left(\frac{1-\phi}{\phi}\right)^{\frac{1}{2}} \qquad (22)$$

Equation (22) describes quantitatively the indicator transition near the equivalence point of the EDTA titration of vanadium(V) using variamine blue B base as an indicator. It may be noted that eqn. (22) is similar in form to eqn. (23) given in a previous paper[3] for the indicator transition in the EDTA titration of iron(III).

---

* Two electrons are assumed to participate in the reaction[8].

RESULTS AND DISCUSSION

Titration of vanadium(V) with iron(II) in the presence of excess EDTA

From the value of the potentiometric sharpness index given in Table I, it is expected that vanadium(V) would be successfully titrated with iron(II) in the presence of excess EDTA. It is true that a sufficient potential break is observed in the potentiometric titration. However, it was found that vanadium(V) is slowly reduced to the quadrivalent state by excess EDTA in the absence of iron(II) and that the reduction is accelerated in light. Thus this method is not suitable for the determination of vanadium(V).

Titration of vanadium(V) with EDTA in the presence of excess iron(II)

A typical titration curve is given in Fig. 1: a large potential break is observed at the equivalence point and a point with the maximum $|\partial E/\partial a|$ coincides exactly with the equivalence point ($a=1$). Thus potentiometric titration of vanadium(V) with EDTA is possible in the presence of excess iron(II). The smaller potential break than expected from the theory appears to be due to the decrease in Y′ by the air-oxidation of iron(II) after the equivalence point; expulsion of dissolved oxygen by nitrogen leads to a greater potential break.

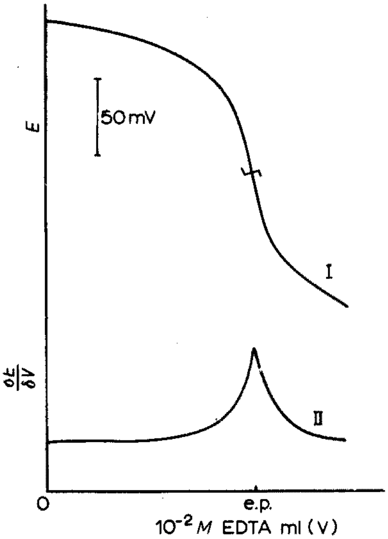

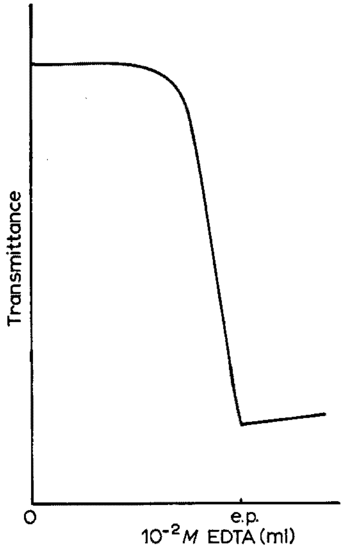

Fig. 1. Typical potentiometric titration curve. pH 1.7. $C_V = 8.16 \cdot 10^{-4}$ *M*. (I) *E versus* volume of titrant added; (II) $\partial E/\partial V$ *versus* volume of titrant added ($\partial E/\partial V$ in arbitrary units). Titration speed 0.2 ml/min.

Fig. 2. Typical photometric titration curve. pH 1.7. $C_V = 8.16 \cdot 10^{-4}$ *M*. $C_I = 2 \cdot 10^{-4}$ *M*. Titration speed 0.2 ml/min. Optical filter: 562 nm.

Photometric and visual titration of vanadium(V) with EDTA using variamine blue B base as an indicator

The satisfactory use of variamine blue B base as an indicator would be expected from eqn. (22) as in the EDTA titration of iron(III). A typical photometric titration curve is given in Fig. 2. Visual titration is also possible; the end-point should be taken as the point of complete disappearance of the blue color.

At pH 1.7–2.0 a sharp and reproducible end-point is obtainable. At higher pH the end-point tends to be sluggish and the results become too high.

Less than 10 mg of vanadium can be successfully determined with an error of ±0.01 mg by means of the visual titration (see Table II and the recommended procedure given below). When more than 10 mg of vanadium are to be titrated, the blue color of vanadium(IV) makes the visual end-point detection difficult although photometric and potentiometric titrations are successful.

TABLE II

REPRODUCIBILITY

Vanadium added (mg)	*Vanadium found (mg)*	*Error (%)*
2.04	2.03	−0.5
	2.03	−0.5
	2.04	0
4.08	4.08	0
	4.08	0
	4.07	−0.2
6.11	6.11	0
	6.11	0
	6.10	−0.2
8.15	8.14	−0.1
	8.14	−0.1
	8.15	0

The amount of iron(II) added in excess has no influence on the titration. The presence of 1 g each of such substances as KNO_3, $(NH_4)_2SO_4$, NaCl and CH_3COOH has no effect. In the visual titration of 2.04 mg of vanadium, the following elements do not interfere, at least up to the specified amounts: As(V)*(3 mg), As(III) (3 mg), Sb(III) (5 mg), Mo(VI) (1 mg), U(VI) (2 mg), W(VI) (1.5 mg) and Ti(IV) (1 mg). Elements such as zinc and cadmium which form less stable complexes with EDTA than vanadium(IV) are without effect. Copper and silver are reduced to Cu(I) and Ag(O) respectively and interfere with the titration. It may be worthwhile noting that about 1 mg of chromium(III) can be tolerated probably because of the slow rate of formation of the EDTA complex. Phosphoric, citric and tartric acids make the end-point sluggish at the 0.1 g/50 ml level, thus their use should be avoided. Iron(III) is quantitatively titrated and the sum V(V)+Fe(III) is obtained when they are present together.

EXPERIMENTAL

Reagents

$2 \cdot 10^{-2}$ M Vanadium(V) solution. Dissolve 2.34 g of NH_4VO_3 in a small amount of concentrated sodium hydroxide solution and dilute to 1 l. Standardize

---

* In the presence of As(V), heating causes high results.

the solution with a standard permanganate solution after reduction of vanadium(V) with sulfur dioxide.

10^{-1} M iron(II) solution. Dissolve 39 g of Mohr's salt in 1 l of 10^{-2} *M* sulfuric acid.

Apparatus

Automatic Recording Titrator (Hirama Rika Kenkyujo, Kawasaki, Japan).
Horiba pH Meter Model P (Horiba Instruments Inc., Kyoto, Japan).

RECOMMENDED PROCEDURE

Adjust *ca.* 50 ml of acidified sample solution to pH 1.7–2.0 with 0.5 *M* sulfuric acid. After addition of 5 ml of 10^{-1} *M* iron(II) and 1 ml of aqueous 0.1% variamine blue B indicator, titrate with 0.01 *M* EDTA solution visually or by means of an automatic titrator. Titrate slowly near the end-point. Heating makes the indicator transition faster. In the potentiometric titration the same procedure is followed except for the addition of the indicator.

SUMMARY

Continuous expressions are derived for the titration of vanadium(V) with iron(II) in the presence of excess EDTA and for the titration of vanadium(V) with EDTA in the presence of excess iron(II). A new method of EDTA titration of vanadium(V) is developed based on the theoretical consideration of these expressions. The method is simple, selective and reliable.

RÉSUMÉ

Les auteurs ont examiné le titrage du vanadium(V) au moyen de fer(II), en présence d'un excès d'EDTA; de même que le titrage du vanadium(V) avec l'EDTA, en présence d'un excès de fer(II). Une nouvelle méthode de dosage du vanadium(V) par titrage à l'EDTA est proposée; elle est simple, sélective et sûre.

ZUSAMMENFASSUNG

Mathematische Ausdrücke für die Titration von Vanadin(V) mit Eisen(II) in Gegenwart eines Überschusses von AeDTE und für die Titration von Vanadin(V) mit AeDTE in Gegenwart eines Überschusses von Eisen(II) werden abgeleitet. Aufgrund der theoretischen Betrachtungen wird eine einfache selektive und zuverlässige Methode zur massanalytischen Bestimmung von Vanadin(V) mit AeDTE entwickelt.

REFERENCES

1 L. Przyborowski, G. Schwarzenbach and Th. Zimmermann, *Helv. Chim. Acta*, 48 (1965) 1556.
2 G. Schwarzenbach, G. Gut and G. Anderegg, *Helv. Chim. Acta*, 37 (1954) 938.
3 N. Nakasuka and M. Tanaka, *Anal. Chim. Acta*, 36 (1966) 422
4 D. Dyrssen and T. Sekine, *J. Inorg. & Nucl. Chem.*, 26 (1964) 981.

SHORT COMMUNICATIONS

Effect of reagent concentration in the photometric determination of vanadium(V) with 8-quinolinol

In the course of a study on the partition of vanadium 8-quinolinolate between the aqueous and organic phases, a marked difference in the absorption spectrum was noticed when different amounts of 8-quinolinol were used. The formation of an adduct of the composition $VO(OH)(Ox)_2HOx$ was found to be responsible for the modified and enhanced absorption in the visible region. The formation constants of the adduct were determined as 1.8 ± 0.2 in chloroform and 2.6 ± 0.1 in benzene.

Reagents and apparatus

$7 \cdot 10^{-4}$ M vanadium solution. Dissolve 40.8 mg of ammonium vanadate (G.R., E. Merck) in 500 ml of 0.5 M perchloric acid solution.

Benzene. This was shaken first with dilute sodium hydroxide, then with dilute hydrochloric acid solution and finally with distilled water and stocked without dehydration.

Chloroform. This was shaken first with dilute hydrochloric acid, then with dilute sodium hydroxide solution and finally with distilled water before use.

Anhydrous sodium sulfate. G.R., Wako Pure Chemical, Ltd., Japan. Metallic impurities were removed by repeated washing with a benzene solution of 8-quinolinol. The purified reagent was stored in a well-stoppered bottle.

All other reagents were of reagent grade (Wako Pure Chemical, Ltd., Japan) and were used without further purification.

The apparatus used were: Coleman Model-14 spectrophotometer, Hitachi-Horiba Model-P pH meter, Beckman DU spectrophotometer, and Iwaki KW mechanical shaker.

Procedures

Calibration curve. 5 ml of vanadium solution and 5 ml of aqueous $1.4 \cdot 10^{-2}$ M 8-quinolinol solution were adjusted to pH 3.8–4.3 with 1 M sodium acetate solution. After dilution to 25 ml with distilled water, the solution was shaken for 5 min with 25 ml of organic solvent, which sometimes contained $2 \cdot 10^{-1}$ M of 8-quinolinol. After the phase separation and dehydration of the organic phase with purified anhydrous sodium sulfate, the absorbance of the organic phase was read at 550 nm against a blank similarly treated.

Determination of formation constant. 25 ml of $7 \cdot 10^{-4}$ M vanadium solution and 2.5 ml of aqueous $1.4 \cdot 10^{-2}$ M 8-quinolinol solution (the molar ratio of vanadium to 8-quinolinol was 1:2) were adjusted to pH 4.2 with 0.5 N sodium hydroxide solution and 1 M sodium acetate solution. This solution was extracted with 50 ml of organic solvent. After phase separation and dehydration of the organic phase, 5 ml of the organic layer were transferred to a cuvette, to which was added 5 ml of the same orga-

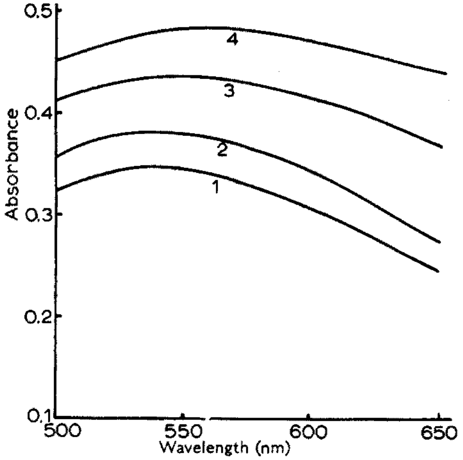

Fig. 1. Effect of the concentration of 8-quinolinol on the spectrum of vanadium 8-quinolinolate. Vanadium 8-quinolinolate in chloroform: 1.1 · 10^{-4} M. (1) No 8-quinolinol added in excess; (2) 5 · 10^{-3} M 8-quinolinol; (3) 10^{-1} M 8-quinolinol; (4) 5 · 10^{-1} M 8-quinolinol. Light path: 10 mm.

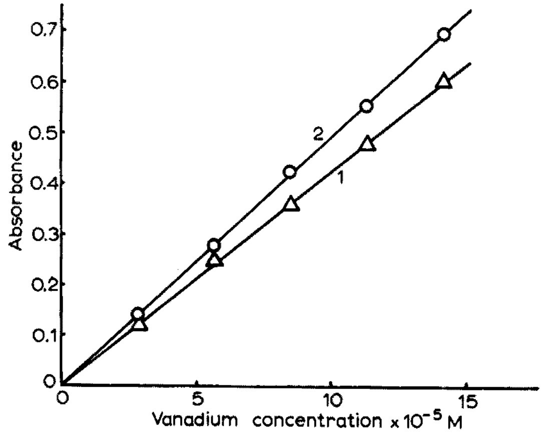

Fig. 2. Effect of the concentration of 8-quinolinol on the calibration curves for vanadium. Organic solvent: chloroform. Total concentration of 8-quinolinol: (1) 2.8 · 10^{-3} M; (2) 2.03 · 10^{-1} M. Light path: 13 mm.

nic solvent containing appropriate amounts of 8-quinolinol. After 20 min the absorbance was read at 550 nm against the same organic solvent.

Results and discussion

Spectral properties of vanadium 8-quinolinolate. When a very small excess of 8-quinolinol was used for the extraction of vanadium, the color of the organic phase was violet with a slight bluish shade. The blue shade became more intense with increasing amounts of 8-quinolinol as shown in Fig. 1*.

---

* The enhancement of absorbance observed when the excess of 8-quinolinol increases from about 10^{-3} M to 5 · 10^{-3} M seems to indicate the formation of a lower complex, probably VO_2Ox. However, results obtained under such extreme conditions are of little analytical interest. The main extracted species under ordinary conditions is not the 1:1 complex[1] but a 1:2 complex[2].

A large excess of the reagent gives rise to not only a bathochromic effect but also an enhancement of the molar absorbance on the molar basis of vanadium. Thus the more concentrated the reagent, the more sensitive the method of photometric determination of vanadium with 8-quinolinol (see Fig. 2).

Results given in Figs. 1 and 2 point to the formation of an adduct containing free 8-quinolinol.

Formation constant of the adduct. When a large excess of 8-quinolinol is used for the extraction of vanadium, vanadium is present as $VO(OH)(Ox)_2$ and $VO(OH)(Ox)_2$-HOx in the organic phase. Because of the limited solubility of 8-quinolinol in the organic solvent, it is impossible to obtain a limiting condition where the concentration of $VO(OH)(Ox)_2$ can be neglected in comparison to the other complex.

The following relationships hold in the organic phase:

$$C_V = [MR_2] + [MR_2HR] \qquad (1)$$

$$E = \varepsilon_1[MR_2] + \varepsilon_2[MR_2HR] \qquad (2)$$

where C_V refers to the total vanadium concentration, E to the observed absorbance, ε_1 and ε_2 to the molar absorbances of MR_2 and MR_2HR, respectively, MR_2 and MR_2HR to $VO(OH)(Ox)_2$ and $VO(OH)(Ox)_2HOx$, respectively. E is measured by the use of a 1-cm cuvette. The formation constant of MR_2HR, K_f, is given by:

$$K_f = \frac{[MR_2HR]}{[MR_2][HR]} \qquad (3)$$

Combining eqns. (1)–(3) and eliminating $[MR_2]$ and $[MR_2HR]$, we have

$$\frac{\varepsilon_1 C_V}{E - \varepsilon_1 C_V} = \frac{1}{(\varepsilon_2/\varepsilon_1) - 1}\left(1 + \frac{1}{K_f[HR]}\right) \qquad (4)$$

$\varepsilon_1 C_V$ being easily estimated by a simple extrapolation to $[HR] = 0$, a plot of

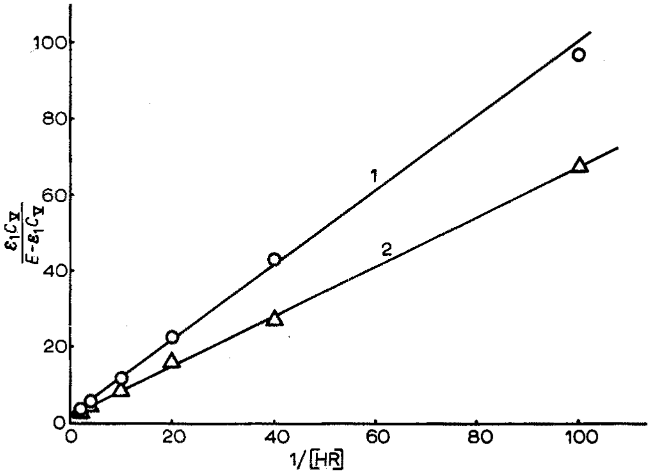

Fig. 3. Determination of K_f by means of eqn. (4). (1) $1.2 \cdot 10^{-4}$ M vanadium with chloroform as solvent; (2) $9 \cdot 10^{-5}$ M vanadium with benzene as solvent. Light path: 10 mm.

$\varepsilon_1 C_V/(E-\varepsilon_1 C_V)$ against $[HR]^{-1}$ gives $1/\left(\frac{\varepsilon_2}{\varepsilon_1}-1\right)$ and $1/\left(\left(\frac{\varepsilon_2}{\varepsilon_1}-1\right)K_f\right)$ as an intercept and a slope respectively (see Fig. 3). The results are confirmed by the curve-fitting in which a plot of log $\varepsilon_1 C_V/(E-\varepsilon_1 C_V)$ against $-\log\,[HR]$ is compared with a normalized function $y = \log\,(1+x)$. The extraction of vanadium with 8-quinolinol can be described as follows:

$$VO_2^+ + 2\,(HOx)_o \overset{K_{ex}}{\rightleftharpoons} (VO(OH)(Ox)_2)_o + H^+ \tag{5}$$

$$(VO(OH)(Ox)_2)_o + (HOx)_o \overset{K_f}{\rightleftharpoons} (VO(OH)(Ox)_2HOx)_o \tag{6}$$

$$D = K_{ex}[HOx]_o^2[H^+]^{-1}(1+K_f[HOx]_o) \tag{7}$$

At higher pH, hydrolysis of VO_2^+ should be taken into account in the aqueous phase[3,4]. The constants are given in Table I.

TABLE I

CONSTANTS OF VARIOUS EQUILIBRIA INVOLVED IN THE EXTRACTION OF VANADIUM(V) 8-QUINOLINOLATE

		Benzene	*Chloroform*
Eqn. (4)[a]	K_f	2.6 ± 0.1	1.8 ± 0.2
Curve-fitting[b]	K_f	2.5 ± 0.5	1.7 ± 0.5
Extraction constant	K_{ex}	$10^{4.2 \pm 0.1}$	$10^{4.4 \pm 0.1}$

[a] The most probable value $\pm 3\sigma$. Data weighed approximately in proportion of $(E-\varepsilon_1 C_V)$.
[b] The most probable value ± maximum deviation.

Laboratory of Analytical Chemistry,
Faculty of Science,
Nagoya University,
Chikusa-ku, Nagoya
(Japan)

MOTOHARU TANAKA
ISAO KOJIMA

1 J. STARÝ, *Anal. Chim. Acta*, 28 (1963) 132.
2 M. TANAKA AND I. KOJIMA, to be published.
3 D. DYRSSEN AND T. SEKINE, *J. Inorg. & Nucl. Chem.*, 26 (1964) 981.
4 F. J. C. ROSSOTTI AND H. ROSSOTTI, *Acta Chem. Scand.*, 10 (1956) 957.

(Received June 23rd, 1966)

Conductometric end-point detection in the titration of fluoride and fluosilicic acid with thorium nitrate

The visual end-point detection of fluoride ion can yield low results and poor reproducibility when distillates obtained by the WILLARD–WINTER method[1], containing fluosilicic acid, are titrated with thorium nitrate using sodium alizarin sulfonate as an indicator. Sodium alizarin sulfonate competes with thorium nitrate for the low fluoride-ion concentrations in the vicinity of the equivalence point resulting in early end-point detection. This is in addition to the individual's difficulty in establishing correctly the actual end-point. The use of a conductometric method for end-point detection in the titration of fluoride ion with thorium nitrate would obviate the use of the above indicator and eliminate the interference arising from its use.

DYKES *et al.*[2] described a remote-control apparatus for the titration of hydrofluoric acid, evolved by hydropyrolysis from zirconium–uranium fuel processing solutions, with thorium nitrate using conductometric end-point detection. Sample aliquots containing 0.25–1 meq of fluoride were titrated with a standard deviation of ±0.055 meq for a single determination.

The conductometric precipitation titrations of fluoride ion and fluosilicic acid with thorium nitrate were investigated in the present work in order to develop a reliable method suitable for the determination of fluoride ion in distillates of inorganic fluorides, as well as in the decomposition and distillation products of organofluorine compounds.

Chemicals and reagents

Analytical grade sodium fluoride and thorium nitrate reagents were used. A $5 \cdot 10^{-3}$ F thorium nitrate stock solution was standardized by the visual end-point detection method using sodium alizarin sulfonate. Aliquots containing 0.7–1.1 mg of fluoride in about 20 ml volume were titrated and the mean value of the results obtained was taken as the formality of thorium nitrate. For solutions of low fluoride-ion content, dilutions of thorium nitrate stock solution were made and a microburet was used.

National Bureau of Standards (N.B.S.) rock phosphate samples No. 56 *b* containing 3.4% and No. 120 *a* containing 3.92% of fluoride ion were used and solutions for titrations were prepared by distillation using the WILLARD–WINTER method[1]. An aliquot was taken, preferably corresponding to about 1 mg of fluoride ion, and the volume was made up to 10 ml with distilled water before titration.

A Teflon 6 sample (theor. 76.0% fluorine) was prepared for analysis by decomposing 30–60 mg of sample using the WICKBOLD method[3] and subsequent distillation. An identical aliquot was taken as in the case of rock phosphates.

Apparatus

Conductometric measurements were made at an ambient temperature of about 24°, using a Philips measuring bridge "Philoscop" model GM 4140, oscillator model GM 4260 provided with 50 and 1000 c/s and cell model GM 4221; 50 c/s was used throughout this work. For more accurate measurements of cell resistance an external 8-step resistance decade box (Baldwin Instruments Company) covering a range of 0.1 to 100,000 Ω, was used instead of the internal variable resistor. For phase rectification when samples of low-conductance were involved, it was necessary to use an external capacitance decade box connected in parallel to the external decade resistor. A 4-step EMT model 519 decade capacitance box was used to balance cell capacitance covering a range of 0.1–1100 μF.

The resistance, R, was expressed as conductance, $1/R$ and corrected for dilution multiplying by $(V_0+V_t)/V_0$, where V_0 is the initial volume and V_t is the volume of titrant. The value of corrected conductance was plotted against V_t and the end-point was located at the intersection of the two slopes of the lines obtained before and after the end-point.

Discussion

The titration of fluoride ion. Thorium ion reacts with fluoride to form thorium fluoride precipitate ($pK_{sp} = 28.1$)[4]. Before the end-point, the net change in conductance is due to replacing fluoride ion ($\lambda^0 = 55.4^{-1}$ cm^2/eq) by nitrate ion ($\lambda^0 = 71.4^{-1}$ cm^2/eq), therefore only a very small increase in conductance is expected. After the end-point the addition of thorium nitrate contributes more to the conductance of the solution causing a sharper increase in conductance (Fig. 1a). This titration curve is essentially similar to the one obtained by titrating fluoride ion with lanthanum acetate[5].

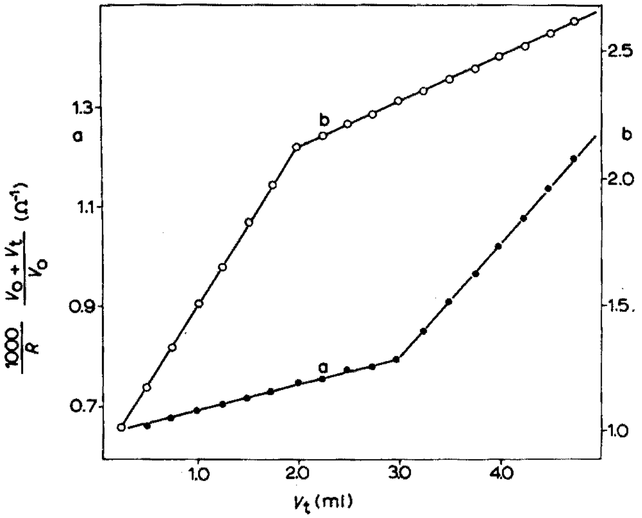

Fig. 1. Conductometric titrations of sodium fluoride and fluosilicic acid with thorium nitrate. A plot of conductance/cell constant (corrected for dilution) *vs.* volume of $5 \cdot 10^{-3}$ F thorium nitrate. (a) 10 ml of sodium fluoride solution containing 1.26 mg of fluoride. (b) An aliquot corresponding to 1.126 mg of Teflon 6 sample after WICKBOLD decomposition and subsequent WILLARD–WINTER distillation in 10 ml volume. Cell constant = 0.93/cm.

The titration of fluosilicic acid. Before the end-point the distillates containing fluosilicic acid react with thorium nitrate to precipitate thorium fluoride. The net change taking place in the system is attributed to the replacement of fluosilicic acid (a weaker acid) by nitric acid which by complete dissociation contributes more to the conductance of the solution than fluosilicic acid and thus results in a sharp increase in conductance. After the end-point only a slight increase in conductance is obtained by the addition of thorium nitrate to a solution containing nitric acid (Fig. 1b). The form of this titration curve before the end-point is very different from the one obtained by titrating fluosilicic acid with lanthanum acetate, since in the latter case the fluosilicic acid is replaced by the weaker acetic acid.

Results and conclusions

The conductometric curves obtained from the titration of fluoride ion and fluosilicic acid (Fig. 1) with thorium nitrate were suitable for end-point detection of both ionic species.

The results of determination of sodium fluoride reagent using this method are listed in Table I. Experiments 1–3 are the direct titration of sodium fluoride, while experiments 4–10 are the results of titration of distillates of sodium fluoride, actually containing fluosilicic acid. The results of determination of fluoride ion in N.B.S. rock phosphate samples and in Teflon 6 samples are listed in Table II. Excellent results were obtained in the case of Teflon 6 and satisfactory results were obtained in the case of N.B.S. No. 120 *a* rock phosphate sample. The deviation was higher in the case of N.B.S. No. 56 *b* rock phosphate sample, but in this case only one decimal figure was provided by N.B.S.

TABLE I

CONDUCTOMETRIC TITRATION OF SODIUM FLUORIDE WITH THORIUM NITRATE

Exp. no.	*F^- taken*[a] *(mg)*	*F^- found*[b] *(mg)*	*Relative mean deviation (%)*	*Remarks*
1	0.837	0.835		
2	1.05	1.03	±1.0	Direct titration
3	1.25	1.26		
4	0.634	0.634		
5	0.634	0.634		
6	0.634	0.638		Titration
7	0.760	0.770	±0.7	of distillates
8	0.887	0.900		
9	0.887	0.900		
10	1.14	1.15		

[a] Volume of titrated sample was 10 ml.

[b] Calculated for each sample using the value obtained by standardization of thorium nitrate with sodium fluoride by the visual method (see experimental).

The results in Tables I and II pertain to a concentration range of 0.3–1.25 mg in 10 ml volume. However, no difficulty was encountered in the titration of samples containing up to 5 mg in 10 ml of solution. For lower amounts, such as 0.1 mg of fluoride in 10 ml of solution, the location of the end-point was less certain. Only when these titrations were carried out in a 50% (v/v) solution ethanol–water mixture were well-defined end-points obtained. Repeated titrations of 0.1 mg of fluoride ion in 10 ml of ethanol–water medium yielded results that gave a mean relative error of —2%.

From the conductometric data for the titration of dilute samples of 0.1 mg in 10 ml in aqueous solution the equivalent conductance at 24° (in Ω^{-1} cm^2 per g.equiv.)

was calculated for nitric acid at the end-point which was 412.5, compared with that computed from the literature[6] of 417.7 at 25°. The same value in 50% (v/v) ethanol was 163.4. The data obtained after the titration end-point were utilized to calculate the equivalent conductance of thorium nitrate from increments of conductance per increments of normality and the mean values obtained were 124.9 in aqueous solution and 62.6 in 50% (v/v) ethanol (at about 24°).

TABLE II

CONDUCTOMETRIC DETERMINATION OF FLUORIDE IN ROCK PHOSPHATES AND TEFLON

Sample	*F present (%)*	*F found[a,b] (%)*	*Mean value (%) F⁻*
N.B.S. No. 56 *b*	3.4[c]	3.36 3.38 3.29	3.34 ± 0.04
N.B.S. No. 120 *a*	3.92[c]	3.98 3.86 3.98 3.95	3.94 ± 0.04
Teflon 6	76.0[d]	75.6 76.0 76.3 76.4	76.1 ± 0.3

[a] Independent sample weights were taken for determinations. See also footnote b in Table I.
[b] Volume of titrated sample was 10 ml.
[c] Certified value.
[d] Theoretical value.

The permission of the Management of Israel Mining Industries to publish this work is gratefully acknowledged. We are also indebted to Mr. B. PASCHKES for his helpful suggestions.

Israel Mining Industries,
Institute for Research and Development,
Haifa (Israel)

YECHESKEL ISRAEL
BEDRICH BERNAS
AHARON YAHALOM

1 H. H. WILLARD AND O. B. WINTER, *Ind. Eng. Chem., Anal. Ed.*, 5 (1933) 7.
2 F. W. DYKES, G. L. BOOMAN, M. C. ELLIOTT AND J. E. REIN, *U.S. At. Energy Comm.*, IDO 14405, 1957.
3 R. WICKBOLD, *Angew. Chem.*, 64 (1952) 133.
4 G. CHARLOT, *Qualitative Inorganic Analysis*, Methuen, London, 1954, p. 180.
5 C. L. GRANT AND H. M. HAENDLER, *Anal. Chem.*, 28 (1956) 415.
6 R. P. FRANKENTHAL, Conductometry, in L. MEITES, *Handbook of Analytical Chemistry*, McGraw-Hill, New York, 1963, p. 5-33.

(Received May 16th, 1966)

A comment on the mass spectrometry of materials producing sulfur trioxide

A recent publication by WENDLANDT AND SOUTHERN[1] describes the decomposition of tetramine copper(II) sulfate monohydrate as observed by a combination of effluent gas analysis and mass spectrometric analysis. The authors interpret their results as follows:

$$145°\colon Cu(NH_3)_4SO_4 \cdot H_2O(s) \rightarrow Cu(NH_3)_4SO_4(s) + H_2O(v)$$

$$175°\colon Cu(NH_3)_4SO_4(s) \rightarrow Cu(NH_3)_2SO_4(s) + 2\ NH_3(g)$$

$$290°\colon Cu(NH_3)_2SO_4(s) \rightarrow Cu(NH_3)SO_4(s) + NH_3(g)$$

$$360°\colon Cu(NH_3)SO_4(s) \rightarrow CuSO_4(s) + NH_3(g)$$

$$382° \text{ and } 486°\colon 2\ CuSO_4(s) \rightarrow CuO \cdot CuSO_4(s) + SO_2(g) + \tfrac{1}{2}\ O_2(g)$$

In order to avoid any misunderstanding by the readers of the article by WENDLANDT AND SOUTHERN, we wish to report some of our own observations on decomposition of sulfates which are not in accord with the interpretation of the results given above and to point out the difficulties involved in interpreting the mass spectra of sulfur trioxide-producing materials.

Fuming sulfuric acid (30% SO_3) or disulfuric acid ($H_2S_2O_7$) is known to release SO_3 especially on heating. A sample of this material was heated to 80–100° in a gas inlet system and the vapors allowed to pass into the ion source of a Bendix Time-of-Flight Mass Spectrometer. The mass spectrum obtained is reproduced in Table I.

TABLE I

MASS SPECTRUM OF FUMING SULFURIC ACID (30% SO_3)

(Sample temp.: 80–100°. Intensities have been corrected foı background errors and are expressed in percent of most intense peak)

m/e	*Ion*	*Intensity*
16	S^{2+}	<10 corr.
32	S^+	56 corr.
34	$^{34}S^+$	<5
48	SO^+	100
50	$^{34}SO^+$	<8
64	SO_2^+	100
66	$^{34}SO_2^+$	<8
80	SO_3^+	0
81	HSO_3^+	32
83	$H^{34}SO_3^+$	<5

A sample of copper sulfate pentahydrate was subjected to mass spectrometric thermal analysis (MTA)[2] and after an initial release of water, the mass spectrum reproduced in Table II was obtained at 650°. A differential thermogram confirmed the results reported by BORCHARD AND DANIELS[3] who report the formation of $CuSO_4 \cdot CuO$ and CuO by a two-step decomposition of anhydrous copper sulfate above 720°. After we observed an initial release of water and ammonia from the monohydrate of copper tetramine sulfate, the 2 spectra of Table III were recorded.

Any or all of the following 3 points, when considered in connection with the experimental set-up employed by Wendlandt and Southern, could be utilized to explain the lack of an observation of the $m/e = 80$ SO_3^+ ion, *but cannot justify the implication of these authors that sulfur dioxide is one of the primary reaction products of the thermal decomposition of anhydrous copper sulfate.*

TABLE II

MASS SPECTRUM OF $CuSO_4 \cdot 5H_2O$ AT 650°, 10^{-7} Torr

m/e	*Ion*	*Intensity*
32	S^+	29 corr.
48	SO^+	68
50	$^{34}SO^+$	7
64	SO_2^+	100
66	$^{34}SO^+$	5
80	SO_3^+	14

TABLE III

MASS SPECTRA OF $[Cu(NH_3)_4]SO_4 \cdot H_2O$ AT 10^{-7} Torr

m/e	*Ion*	*Intensity at 320°*	*Intensity at 550°*
30	NO^+	31	0
32	S^+	17 corr.	35 corr.
48	SO^+	83	71
50	$^{34}SO^+$	4	6
64	SO_2^+	100	100
66	$^{34}SO_2^+$	6	9
80	SO_3^+	7	11

(*1*) There is no ***a priori*** assurance that SO_3 provides an SO_3^+ ion.

(*2*) Certainly at 400°, and even at 760°, the $SO_3 \rightleftharpoons SO_2 + \frac{1}{2} O_2$ equilibrium is not unbalanced extensively toward the right. (For instance, the calculated degree of dissociation for SO_3 is 0.4% at 600°K and 1 atm and 54% at 1000°K and 1 atm[4].)

(*3*) SO_3, at 400° and above, is an oxidizing agent and hence an amount of SO_2 over and above that expected from the equilibrium reaction could be produced in the presence of oxidizable material.

It must also be pointed out that water provides ion fragments at $m/e = 17$ and 16 in sufficient abundance to prohibit a realistic analysis for NH_3 unless 18, 17, and 16 can be *monitored simultaneously* by a fast scanning instrument.

In general, a more sophisticated instrumental arrangement and data treatment procedure than was employed in the previous investigation is necessary to establish the absolute sequence of appearance and the quantity of gaseous species produced in rapidly occurring reactions.

Finally, the decomposition of anhydrous copper sulfate at the temperature reported by Wendlandt and Southern (formation of $CuO \cdot CuSO_4$ and CuO) cannot be explained. Our investigation showed this reaction to take place at about 753° and 832°, in agreement with the results reported by Borchard and Daniels.

An extensive study on thermal analysis by mass spectrometry of sulfur oxides and sulfur oxyacids and their salts is in progress in this laboratory.

The Dow Chemical Company,
Eastern Research Laboratory,
Wayland, Mass. (U.S.A.)

R. S. GOHLKE*
H. G. LANGER

1 W. W. WENDLANDT AND T. M. SOUTHERN, *Anal. Chim. Acta*, 32 (1965) 405.
2 H. G. LANGER AND R. S. GOHLKE, *Anal. Chem.*, 35 (1963) 1301.
3 H. J. BORCHARD AND F. DANIELS, *J. Phys. Chem.*, 61 (1957) 917.
4 A. SYVERUD, Thermal Research Lab., The Dow Chemical Co., Midland, Mich., private communication, March 1966.

(Received May 2nd, 1966)

---

* Present address: Dow Corning Corp., Midland, Michigan.

A coaxial NMR cell

A previous communication[1] included a description of a reasonably priced coaxial NMR cell. This paper presents complete data establishing the precision and accuracy of chemical shift and bulk susceptibility measurements taken with this cell and with a modification thereof. The modified form of the cell is especially adapted for the convenient and accurate measurement of bulk susceptibility.

Reference solute effects can be eliminated by using coaxial NMR cells. A coaxial cell is used in this laboratory in measuring chemical shifts in aqueous–electrolyte systems and in connexion with other problems requiring external references. The cell consists of a 5-mm Varian NMR tube containing the sample to be studied and a removable inner tube, containing the reference compound, made from 1.5 × 2.0 × 100 mm standard capillary tubing (Fig. 1A) or 3-mm O.D., 2.4-mm I.D. Pyrex standard wall tubing (Fig. 1B).

The construction of the capillary inner compartment involves the sealing of both ends of a piece of capillary tubing, then gently heating one end again until internal pressure causes a sphere to form. The other end is then opened, the reference compound placed inside and the tube resealed. The inner compartment made from 3-mm tubing is constructed simply by sealing one end of the tubing and then forming a "collar" near the other end by gathering a small amount of glass in a soft methane–oxygen flame. The spherical end on the capillary cell and the "collar" on the 3-mm cell are made of such size that they just fit into the NMR tube. The sphere and "collar" permit reproducible positioning of the reference compound and also prevent movement in a spinning system.

Volatilization of the reference compound becomes a problem when such common external references as benzene and cyclohexane are used in the commercially available coaxial cells (from the Wilmad Glass Company, N.J.) since the annular region cannot be stoppered by any convenient means. This is particularly disadvan-

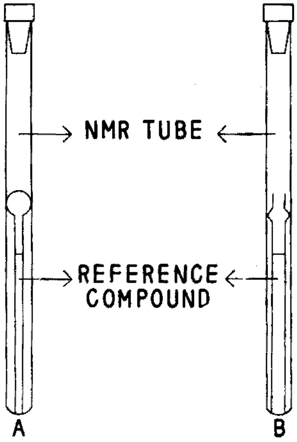

Fig. 1. Coaxial NMR cell.

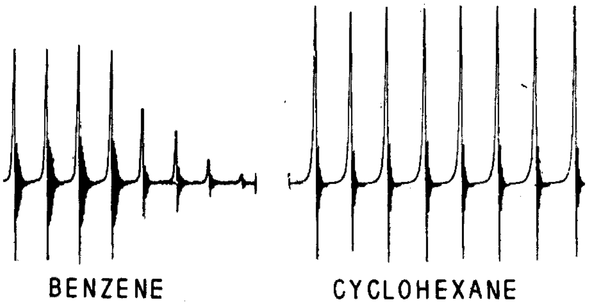

Fig. 2. Volatilization of benzene in annular region of open coaxial cell.

TABLE I

COMPARISON OF MOLAL CHEMICAL SHIFTS FOR THE TWO CELLS

Type cell	*Salt*	*Molal chemical shift (cycles/sec)*	*Type cell*	*Salt*	*Molal chemical shift (cycles/sec)*
Wilmad	$MgCl_2$(3.98 *M*)	49.2 ± 0.2	Capillary	$MgCl_2$(3.98 M)	49.1 ± 0.2
		49.2 ± 0.2			49.1 ± 0.2
		49.1 ± 0.2			49.1 ± 0.2
		49.1 ± 0.2			49.1 ± 0.2
		49.0 ± 0.2			49.2 ± 0.2
		49.2 ± 0.2			49.2 ± 0.2
		49.1 ± 0.2			49.1 ± 0.2
		49.1 ± 0.2			49.1 ± 0.2
		49.1 ± 0.2			49.0 ± 0.2
		Av. 49.1 ± 0.2			Av. 49.1 ± 0.2
			3 mm	$MgCl_2$ (3.98 *M*)	49.1 ± 0.2
					49.1 ± 0.2
					49.1 ± 0.2
					49.1 ± 0.2
					Av. 49.1 ± 0.2
Wilmad	KCl (4.5 *M*)	7.40 ± 0.20	Capillary	KCl (4.56 *M*)	7.40 ± 0.20
		7.35 ± 0.20			7.35 ± 0.20
		7.35 ± 0.20			7.35 ± 0.20
		Av. 7.36 ± 0.20			7.40 ± 0.20
					Av. 7.38 ± 0.20
			3 mm	KCl (4.56 *M*)	7.40 ± 0.20
					7.40 ± 0.20
					7.35 ± 0.20
					7.40 ± 0.20
					7.30 ± 0.20
					Av. 7.36 ± 0.20

tageous for certain studies in which the NMR cell must remain in the instrument for extended periods of time. The NMR spectra of benzene, contained in the annular region of a commercial coaxial cell, and cyclohexane, contained in the stoppered inner tube, are presented as a function of time (10-min intervals) in Fig. 2. Probe temperature for the experiment was 37°. It is evident that the benzene in the annular region of the cell begins to volatilize after about 40 min. In this respect there is some advantage in using the closed reference cell system described in this paper.

ZIMMERMAN AND FOSTER[2] have discussed the effects of tilting and glass imperfections on average field shifts and line broadening in NMR spectra using coaxial cells. It was shown that tube tilting may cause the average fields in the reference and sample compound regions to shift with respect to each other. Table I presents a comparison of chemical shift data, uncorrected for bulk susceptibilities, between 3 commercial (Wilmad) coaxial cells and those constructed in the laboratory. Molal chemical shifts, relative to pure water, in units of cycles/sec, of water protons in 3.98 M $MgCl_2$ and 4.56 M KCl solutions were determined using both types of cells. The chemical shift reported for each cell is the average of 6 NMR spectra taken at 37°. The 22 different cells constructed gave chemical shift data that were in excellent agreement with that obtained using the Wilmad cells.

Imperfections in glass tubing give rise to inhomogeneities in field strength even in spinning systems thereby causing line broadening in both reference and compound sample. NMR spectra were taken of water, as external reference, and benzene in both types of coaxial cell to compare line widths. In the Wilmad cell water was placed in the annular region and in the cell described in this paper water was sealed inside the capillary. In Fig. 3 the spectra of these compounds are shown as taken on the 500 cycles/sec and 50 cycles/sec sweep of a Varian Associates A-60 spectrometer. Spectra A and B are those obtained using the capillary-coaxial and commercial

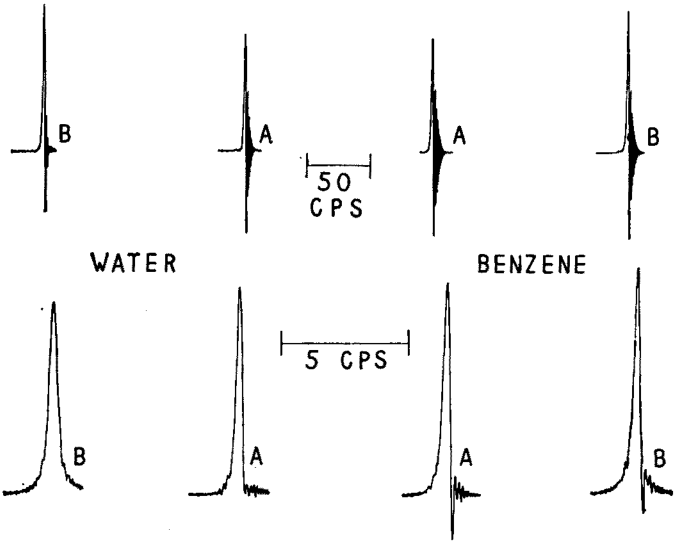

Fig. 3. Comparison of line widths of spectra obtained with both cell types. Spectra A: capillary coaxial cell; spectra B: commercial cell.

coaxial cell, respectively. No significant broadening of either the water or benzene proton resonance peak was observed in comparing the two cells.

Bulk susceptibility corrections must be made when external references are used, to obtain true chemical shift values. The true chemical shift for such systems is given by the equation[3]

$$\delta_{\mathrm{corr}} = \delta_{\mathrm{obs}} + 2\pi/3\,(X_{\mathrm{ref}} - X_{\mathrm{s}}) \qquad (1)$$

where X_{ref} and X_{s} are the volume susceptibilities of the reference compound and sample solution respectively. X_{s} can be experimentally determined rather easily using a static, non-spinning, coaxial sample tube arrangement. Under static conditions the solution in the annular region gives rise to a broad doublet resonance signal. The separation of the doublet peaks is given by[4]

$$\Delta\nu = 4\pi\nu_0[(X_1 - X_2)\,\mathrm{a}^2/\mathrm{r}^2 + (X_2 - X_3)\,\mathrm{b}^2/\mathrm{r}^2] \qquad (2)$$

where X_1, X_2 and X_3 are the volume susceptibilities of the solution in the inner tube, the glass tube itself, and the annular liquid respectively. The constants a, b and r are related to the geometry of the coaxial cell. In a spinning system, the doublet becomes a sharp single resonance peak that occurs midway between the doublet peaks observed for the static system. The spectra obtained for a spinning and static coaxial cell system (3-mm inner tube) are shown in Fig. 4. Spectrum A is that of benzene, in

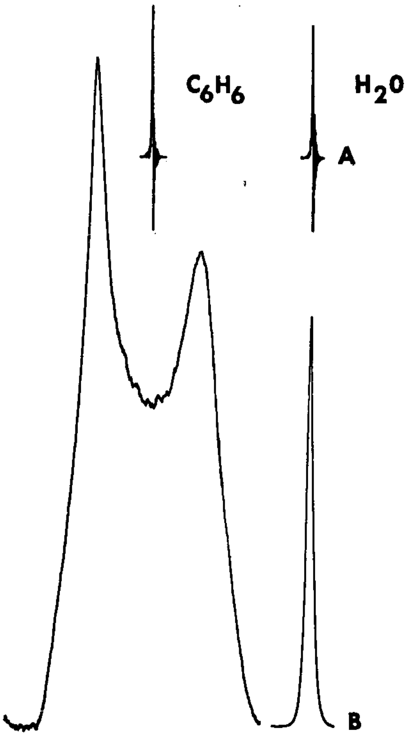

Fig. 4. Bulk susceptibility determination with 3-mm inner tube cell. Spectra A: spinning system; spectra B: static system.

the annular region, and water in the inner tube, for the spinning system. Spectrum B shows the appearance of the benzene doublet under static conditions. This type of coaxial cell has the advantage that much more solution is contained within the annular region compared with the commercial cell, and therefore the spectra can be recorded at a lower spectrum amplitude.

The coaxial cell reported here has been found to give consistently accurate bulk susceptibility measurements. The cells are easily and cheaply constructed, strong and do not impair the usefulness of standard NMR tubes in any way. Reference compounds can be sealed inside the capillary inner tube and used repeatedly or they may be placed in the open 3-mm inner tube and changed when necessary. This coaxial cell may be used with volatile reference compounds when the cell must remain inside the NMR probe for extended periods of time at normal temperatures or at elevated temperatures.

We wish to acknowledge the financial assistance provided by the National Science Foundation for the purchase of the NMR spectrometer. This work has been supported by the United States Atomic Energy Commission Contract Number AT-(40-1)-2069.

Department of Chemistry,
University of Arkansas,
Fayetteville, Ark. 72701 (U.S.A.)

J. F. HINTON
E. S. AMIS

1 J. F. HINTON AND E. S. AMIS, *J. Chem. Educ.*, in press.
2 J. R. ZIMMERMAN AND M. R. FOSTER, *J. Phys. Chem.*, 61 (1957) 282.
3 J. A. POPLE, W. G. SCHNEIDER AND H. J. BERNSTEIN, *High-Resolution Nuclear Magnetic Resonance*, McGraw-Hill, New York, 1959, p. 81.
4 C. A. REILLY, H. M. McCONNELL AND R. G. MEISENHEIMER, *Phys. Rev.*, 98 (1955) 264A.

(Received June 2nd, 1966)

Extraction and stability constants of copper complexes of 1,5-diphenylcarbazone

Recent reports by LAPIN[1-4] on 1,5-diphenylcarbazone (DCO) have demonstrated its application as a reagent for the spectrophotometric determination of micro- and submicro quantities of copper. In LAPIN's method[1] copper(II) is extracted as a Cu–DCO complex into benzene from an aqueous solution buffered at pH 4 to 5 with potassium dihydrogen phosphate. From absorption spectra, we found that the copper(II)–DCO complex has an absorption maximum in benzene at 550 nm. The molar extinction coefficients in benzene of the complex and the reagent, DCO, at this wavelength were determined to be $(75 \pm 1) \cdot 10^3$ and $(0.42 \pm 0.02) \cdot 10^3$ l cm^{-1} mol^{-1}, respectively.

The present investigation was undertaken to determine the stability constants of the complexes of DCO with copper and the partition coefficient of the extractable copper–DCO complex between the benzene and aqueous phases. The information obtained provides a basis for modifying LAPIN's method[1] to meet the needs of the individual investigator.

Experimental

Partition of copper(II)–DCO between equal volumes (5 ml) of benzene and aqueous phases was studied, using 15-ml Teflon* centrifuge tubes fitted with polyethylene stoppers. Before extraction, DCO was dissolved in benzene and copper-64 was introduced in the aqueous phase. Adjustment of pH was then made through appropriate additions of dilute hydrochloric acid and sodium hydroxide. After addition of 5 ml of benzene–DCO solution to the aqueous phase, the tubes were stoppered and shaken for 10 min; the temperature of the extractions was maintained at 28 ± 1°. No increase in the amount of copper extracted was observed after the first few minutes of shaking.

To effect a separation of phases, the tubes were centrifuged. A 2-ml aliquot was taken from each phase and counted in a well-type scintillation counter, and the pH of the remaining aqueous phase was determined.

The partition of copper(II)–DCO was studied in this manner as a function of DCO concentration and pH.

Results and discussion

The distribution ratio, D, of copper(II) between benzene and aqueous phases was related to the concentration $[L^-]$ of free DCO ligand in the aqueous phase by the relationship[5]

$$D = \frac{P_c \beta_c [L^-]^c}{\sum_0^N \beta_n [L^-]^n} \qquad (1)$$

where c, n, and N are the number of ligands in the extractable complex CuL_c, the arbitrary complex CuL_n, and the highest complex CuL_N, respectively. P_c is the par-

---

* Trade names and company names are included for the benefit of the reader and do not imply any endorsement or preferential treatment by the U.S. Department of Agriculture.

tition coefficient of the complex CuL_c. β_c and β_n are the overall stoichiometric stability constants of the respective complexes, CuL_c and CuL_n.

To relate eqn. (1) to directly measurable quantities, it is necessary to introduce the dependence of $[L^-]$ on the hydrogen ion concentration and the total DCO content of the system.

BALT AND VAN DALEN[6] have shown that DCO behaves as a weak monobasic acid having a first dissociation constant,

$$K_{a_1} = (2.9 \pm 0.3) \cdot 10^{-9}$$

at an ionic strength of 0.1. By spectrophotometric measurement of DCO in a benzene/aqueous phase system, we have estimated the partition coefficient of the acid form HL to be

$$P_a = 126 \pm 5$$

over a range of ionic strengths of $\mu = 0$ to 0.25. Therefore, at pH values less than 7.6, essentially all the DCO will be in the acid form, HL, and in the benzene phase. The free DCO ligand $[L^-]$ can then be estimated from the relationship,

$$[L^-] = \frac{[HL]_0}{[H^+]} \frac{K_a}{P_a} \qquad (2)$$

where the subscript o indicates the organic phase, and the terms without subscripts refer to the aqueous phase.

Substituting this expression for $[L^-]$ into eqn. (1), the distribution ratio D can be written as a function of $[HL]_0/[H^+]$. Extraction data from 75 separate determina-

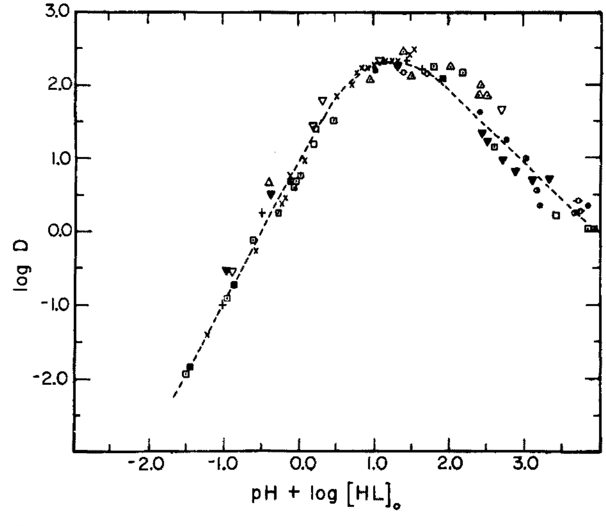

Fig. 1. Distribution of copper between benzene and aqueous phases as a function of pH and DCO concentration at $<\mu> = (1 \pm 3) \cdot 10^{-3}$ and $T = 28 \pm 1°$.
□ 80 and ■ 160 p.p.b. Cu, $1.5 \cdot 10^{-5}$ M DCO, pH 3.3–7.0.
▽ 10 and ▼ 100 p.p.b. Cu, $6.0 \cdot 10^{-5}$ M DCO, pH 3.3–7.3.
○ 2 and ● 1000 p.p.b. Cu, $7.6 \cdot 10^{-4}$ M DCO, pH 4.2–7.0.
△ 10 and -○- 200 p.p.b. Cu, $7.6 \cdot 10^{-5}$–$9.3 \cdot 10^{-4}$ M DCO, pH 4.8–5.7.
+ 2 and × 200 p.p.b. Cu, $2.0 \cdot 10^{-6}$–$1.0 \cdot 10^{-3}$ M DCO, pH 4.4–4.7, $1 \cdot 10^{-4}$ M KH_2PO_4.

tions could, therefore, be conveniently represented by plotting the logarithm of the ratio D against pH + log $[HL]_o$, as shown in Fig. 1. The principal variables in these determinations were pH (3.3 to 7.3) and DCO concentration in benzene ($2.0 \cdot 10^{-6}$ to $1.0 \cdot 10^{-3}\,M$). The average ionic strength of the aqueous phases was $<\mu> = (1 \pm 3) \cdot 10^{-3}$.

To evaluate c and N from the data in Fig. 1, the limiting forms of eqn. (1) were examined. At sufficiently low, free ligand concentrations, where copper in the aqueous phase is predominately uncomplexed, the limiting slope is c. At high concentrations of free ligand, the copper in the aqueous phase is primarily in the form of the highest complex and the limiting slope[5] is $-N$.

From the data in Fig. 1, c and N are found to be equal to 2 and 3, respectively. It is, therefore, evident that the extractable complex that forms between copper and DCO is CuL_2, and the highest complex that forms between copper and DCO under the conditions used is CuL_3.

The stability constants, β_1, β_2, β_3, and the partition coefficient P_2 were estimated by applying DYRSSEN AND SILLEN's two-parameter approximation procedure[5] to the data in Fig. 1. The calculated parameters are given in Table I and used in eqn. (1) to construct the curve represented by the dashed line in Fig. 1.

TABLE I

PARTITION COEFFICIENT AND STABILITY CONSTANTS OF DCO AND Cu–CARBAZONE COMPLEXES AT $<\mu> = (1 \pm 3) \cdot 10^{-3}$, $T = 28 \pm 1°$ AND pH = 3.3–7.3

DCO complex	*Partition coefficient benzene/water*	*Stability constant*
HL	$\log P_a = 1.10$	$(\log K_2^H = 8.54)^a$
CuL^+	—	$\log \beta_1 = 9.8$
CuL_2	$\log P_2 = 2.82$	$\log \beta_2 = 19.5$
CuL_3^-	—	$\log \beta_3 = 29$

[a] Value calculated from the dissociation constant reported by BALT AND VAN DALEN[6] to comply with the notation used by ROSSOTTI[5].

According to Fig. 1, a ratio $[HL]_o$: $[H^+]$ between 10 and 30 would be necessary to attain maximum extraction ($D = 200$) of the CuL_2 complex and also maximum sensitivity in a spectrophotometric method. A ratio of 30 was found to achieve maximum sensitivity in the method proposed by LAPIN[1].

Application of the above investigation has been successful in the development of methods for the determination of the concentration of copper present as the free ion[7], as well as the total concentration of copper[8] in aqueous solutions.

*U.S. Plant, Soil and Nutrition Laboratory**,
Soil and Water Conservation Research Division,
Agricultural Research Service,
U.S. Department of Agriculture,
Ithaca, N.Y. (U.S.A.)

H. R. GEERING
J. F. HODGSON

---

[*] In cooperation with the Department of Agronomy, New York State College of Agriculture, Ithaca, N.Y.

1 L. N. LAPIN, *Biochemistry (USSR) (Engl. Transl.)*, 22 (1957) 773.
2 L. N. LAPIN AND I. G. PRIEV, *Vopr. Pitaniya*, 17 (1958) 68; *C. A.*, 52 (1958) 14881d.
3 L. N. LAPIN AND N. V. REIS, *Zh. Analit. Khim.*, 13 (1958) 426.
4 L. N. LAPIN AND M. A. RISH, *Tr. Tadzhiksk. Uchitelsk. Inst.*, 4 (1957) 71; *C. A.*, 52 (1958) 18610g.
5 F. J. C. ROSSOTTI AND H. ROSSOTTI, *The Determination of Stability Constants and Other Equilibrium Constants in Solution*, McGraw-Hill, New York–Toronto–London, 1961, Chapter 10.
6 S. BALT AND E. VAN DALEN, *Anal. Chim. Acta*, 27 (1962) 188.
7 J. F. HODGSON, H. R. GEERING AND W. A. NORVELL, *Soil Sci. Soc. Am. Proc.*, 29 (1965) 665.
8 H. R. GEERING AND J. F. HODGSON, *J. Assoc. Offic. Agr. Chemists*, in press.

(Received June 23rd, 1966)

BOOK REVIEW

N. D. CHERONIS, J. D. ENTRIKIN AND E. M. HODNETT, *Semimicro Qualitative Organic Analysis, The Systematic Identification of Organic Compounds*, 3rd Edn., Interscience Publishers–J. Wiley and Sons, Inc., New York, 1965, xi+1060 pp., price 222 s.

This third edition of CHERONIS AND ENTRIKIN's comprehensive work on semimicro qualitative organic analysis reinforces its position as the premier text on the subject. The new edition has been thoroughly brought up to date by extensive revision and expansion of the second edition.

Presented in 4 main parts, the text deals successively with the techniques of organic analysis, procedures for the tentative identification of unknown substances, procedures for their final characterization and, finally, tables of physical constants of organic compounds and their derivatives. About 7,100 compounds are considered in these tables (an increase of about 3,000 over the second edition), and all the data have been checked against the recent literature. The emphasis is still essentially on chemical methods of examination, but instrumental techniques are by no means ignored and some of the more widely used methods are given prominence in the technique section of the text. Very many new chemical tests have been incorporated into the existing pattern of the analytical scheme to make the detection or identification of an unknown substance that much easier and quicker.

Now that an attenuated text (of the second edition) is available for student use, the authors have obviously set out to make this new edition an even more useful and complete reference volume than the previous editions. The book is without doubt the best account of qualitative organic analysis now available and can be thoroughly recommended to all interested in this subject.

W. I. STEPHEN (Birmingham)

ANNOUNCEMENT

INTERNATIONAL SYMPOSIUM ON PHYSICAL SEPARATION METHODS IN CHEMICAL ANALYSIS, AMSTERDAM, 10–14 APRIL 1967

(Organized under the auspices of the Koninklijke Nederlandse Chemische Vereniging)

GENERAL PROGRAMME (provisional)

Sunday, 9 April	
4.00–7.00 p.m.	Registration of participants at the Congrescentrum RAI
5.00–7.00 p.m.	Informal get-together at the RAI
Monday, 10 April	
9.00–10.00 a.m.	Registration of participants (continued)
10.00–10.30 a.m.	Opening of the symposium by E. A. M. F. Dahmen (Technische Hogeschool Twente, Enschede)
11.00–12.00 a.m.	Band broadening in packed chromatographic columns; S. T. Sie and G. W. A. Rijnders (Koninklijke/Shell Laboratorium, Amsterdam)
Gas chromatography	
2.00–2.30 p.m.	Herstellung und Erprobung flüssig-kristalliner Phasen für den Einsatz bei Temperaturen oberhalb 200° als stationäre Phasen in der Gaschromatographie; H. Kelker und B. Scheurle (Farbwerke Hoechst AG, Frankfurt)
2.30–3.00 p.m.	Chromatography with supercritical fluids; S. T. Sie and G. W. A. Rijnders
3.00–3.30 p.m.	Struktur und Retentionsverhalten von offenkettigen und cyclischen Kohlenwasserstoffen und deren einfacher Substitutionsprodukte; G. Schomburg (Max-Planck-Institut für Kohleforschung, Mülheim)
4.00–4.30 p.m.	Two-stage capillary gas chromatography; P. A. Schenck and C. H. Hall (Shell Development Cy, Houston)
4.30–5.00 p.m.	La chromatographie en phase gazeuse. Modification de la structure interne des colonnes préparatives; M. B. Dixmier, B. Roz et G. Guiochon (Ecole polytechnique, Paris)
evening	Cold buffet at the Krasnapolski Hotel
Tuesday, 11 April	
9.30–10.30 a.m.	Gel permeation and molecular sieve effects in chromatography; P. Flodin (Perstorp AB, Perstorp)
11.00–12.00 a.m.	Utilisation de l'ultracentrifugation pour la mesure des masses et pour l'étude de la polydispersité des polymères de synthèse; H. Benoit (Centre de recherches sur les macromolécules, Strassbourg)
Section I: Liquid chromatography	
2.00–2.30 p.m.	Chromato–polarographic analysis of the mixtures of mononitro-ethylbenzenes; W. Kemula and D. Sybilska (University of Warszawa)
2.30–3.00 p.m.	Performance of liquid columns; T. E. Young (W. G. Pye and Co. Ltd., Cambridge)
3.00–3.30 p.m.	Optimizing liquid-chromatography time of separation; J. F. H. Huber and J. A. R. Hulsman (University of Amsterdam)
4.00–4.30 p.m.	Heats of preferential adsorption of chelates; M. P. T. Bradley and D. A. Pantony (Imperial College, London)
4.30–5.00 p.m.	The determination of normal paraffins in petroleum products; J. V. Mortimer and L. A. Luke (B. P. Research Centre, Sunbury-on-Thames)
5.00–5.30 p.m.	Correlations in the partition thin-layer chromatography of alkali ions; G. E. Janauer and R. C. Johnston (State University of New York)
Section II: Sedimentation analysis	
2.00–2.30 p.m.	The processing of ultracentrifuge data by "on line" digital computer; S. P. Spragg (University of Birmingham)
2.30–3.00 p.m.	The measurement of the particle size of dispersions and emulsions; T. R. Manley (Rutherford College, Newcastle-upon-Tyne)
3.00–3.30 p.m.	The determination of molecular weights, sedimentation coefficients and specific densities, using the absorption optics of an analytical ultracentrifuge equipped with an electronic scanning system; W. S. Bont and W. L. van Es (Netherlands Cancer Institute, Amsterdam)
4.00–4.30 p.m.	Continuous preparative thin-layer chromatography; R. Visser (Technische Hogeschool Twente, Enschede)

Wednesday, 12 April
Excursions

Thursday, 13 April

9.30–10.30 a.m.	Ion exchange chromatography; O. Samuelson (Chalmers Tekniska Högskola, Göteborg)
11.00–12.00 a.m.	Electrophoresis: dependence on the medium; H. Bloemendal (University of Nijmegen)

Section I: Ion exchange chromatography

2.00–2.30 p.m.	Separation of noble-metal ions from base metals by means of a new chelating resin; G. Schmuckler and G. Koster (Israel Institute of Technology, Haifa)
2.30–3.00 p.m.	Adsorption of the rare earth elements on an anion exchange resin from nitric acid–acetone mixtures; J. Alstad and A. O. Brunfelt (University of Oslo)
3.00–3.30 p.m.	Macroreticular ion exchange resins, some analytical applications to petroleum products; P. V. Webster, J. N. Wilson and M. C. Franks (B. P. Research Centre, Sunbury-on-Thames)
4.00–4.30 p.m.	Die Ausnutzung der Ionexeigenschaften des Silikagels für die Trennung von Metallen; F. Vydra (J. Heyrovsky Polarographic Institute, Prague)
4.30–5.00 p.m.	Anwendung der Ionenaustauschchromatographie zur aktivierungsanalytischen Bestimmung von Natrium und Kalium in Molybdän und Wolfram; H. G. Döge (Institut für Metallphysik und Reinstmetalle, Dresden)
5.00–5.30 p.m.	Separations of traces of metals by column chromatography on natural and substituted celluloses; R. A. A. Muzzarelli (University of Sherbrooke)

Section II: Electrophoresis

2.00–2.30 p.m.	Criteria for successful separation by continuous electrophoresis and electrochromatography in blocks and columns; E. Ravoo, P. J. Gellings and T. Vermeulen (Technische Hogeschool Twente, Enschede)
2.30–3.00 p.m.	Displacement electrophoresis; A. J. P. Martin and F. M. Everaerts (Technische Hogeschool, Eindhoven)
3.00–3.30 p.m.	Mobilitätsbestimmungen bei der Elektrophorese in Agargelen; H. J. Hoenders und W. de Boer (University of Nijmegen)
4.00–4.30 p.m.	Electrophoretic separation of inorganic cations on cellulose acetate; K. Aitzetmüller, F. Gras and K. Buchtela (Atominstitut der Oesterreichischen Hochschulen, Wien)
4.30–5.00 p.m.	Apparative Anordnung zur kontinuierlichen ionophoretischen Trennung nach dem Gegenstromprinzip; W. Preetz und H. L. Pfeifer (Universität des Saarlandes)
evening	Reception in the Rijksmuseum by the Ministry of Education and Sciences and the Municipal Executive of Amsterdam.

Friday, 14 April

9.30–10.30 a.m.	Zone melting as an analytical tool; H. Schildknecht (University of Heidelberg)
11.00–12.00 a.m.	Some effects of macromolecular interaction in gel permeation, electrophoresis and ultracentrifugation; G. A. Gilbert (University of Birmingham)

Zone melting

2.00–2.30 p.m.	A fast method of zone melting as an aid in analytical chemistry; N. J. G. Bollen and M. J. van Essen (Institute for Physical Chemistry TNO, Utrecht)
2.30–3.00 p.m.	Zone melting, an aid in (im)purity determination by thermal analysis; H. F. van Wijk and P. F. J. van der Most (Institute for Physical Chemistry TNO, Utrecht)
3.00–3.30 p.m.	Comparaison de la purification par fusion de zones et par cristallisation en colonne dans le cas d'amines aromatiques liquides à température ordinaire; B. Pouyet (Université de Lyon)
4.00–4.30 p.m.	Ultra-micro zone melting; K. Maas and H. Schildknecht (University of Heidelberg)
4.30–5.00 p.m.	Summary and integration; J. F. K. Huber (University of Amsterdam)
5.00 p.m.	Closing of the symposium by E. A. M. F. Dahmen (Technische Hogeschool Twente, Enschede)

Further information may be obtained from: Dr. C. L. de Ligny (Secretary), Congress Bureau, St. Agnietenstraat 4, Amsterdam-C, The Netherlands.

ANALYTICA CHIMICA ACTA VOL. 36 (1966)

AUTHOR INDEX

ANALYTICA CHIMICA ACTA, VOL. 36 (1966)

SUBJECT INDEX

Where in the world are EASTMAN Organic Chemicals and EASTMAN CHROMAGRAM System available?

Here:

EASTMAN Organic Chemicals and CHROMAGRAM products are sold in the U.S.A. by Distillation Products Industries and local laboratory supply houses, and throughout the world by the following:

AUSTRALIA
H. B. Selby & Co. Pty. Ltd.
Brisbane
Melbourne
Sydney

BELGIUM
s. a. Belgolabo
Overijse

BRAZIL
Atlantida Representacoes e Importacoes Ltda.
Rio de Janeiro

CANADA
Fisher Scientific Co. Ltd.

COSTA RICA
Costa Rica Dental and Medical Supply Co.
San Jose

DENMARK
H. Struers Chemiske Laboratorium
Copenhagen

FINLAND
Havulinna Oy
Helsinki

FRANCE
*Kodak-Pathé
Paris
**Touzart & Matignon
Paris

GERMANY
Serva-Entwicklungslabor
Heidelberg

INDIA
Andhra Scientific Co. Ltd.
Madras
Raj-Der-Kar and Co.
Bombay

ISRAEL
Landseas Israel
Tel Aviv

ITALY
Prodotti Gianni s.r.l.
Milan

JAPAN
Muromachi Kagaku Kogyo Kaisha, Ltd.
Tokyo
Totsu Co., Ltd.
Tokyo

MEXICO
Hoffman Pinther and Bosworth, S. A.
Mexico 1, D. F.

NETHERLANDS
N. V. Holland-Indie Agenturen Mij. HIAM
Amsterdam

NEW ZEALAND
Kempthorne, Prosser and Co's
Wellington
Dunedin

NORWAY
Nerliens Kemisk Tekniske Aktieselskap
Oslo

****PHILIPPINES**
Botica de Santa Cruz
Manila

PORTUGAL
Soquimica Sociedade de Representacoes de Quimica, Lda.
Lisbon

SPAIN
CEPA Sociedad Anonima
Barcelona

SWEDEN
Rudolph Grave A/B
Solna

SWITZERLAND
Dr. Bender & Dr. Hobein AG
Zurich

UNITED KINGDOM
Kodak Limited
Liverpool

* For CHROMAGRAM products only

** For EASTMAN Organic Chemicals only

Of the thousands of EASTMAN Organic Chemicals distributed by these firms, some are uncommon and some are uncommonly pure. You will probably find it more economical to buy them than to make them yourself.

The EASTMAN CHROMAGRAM System for thin-layer chromatography consists of flexible EASTMAN CHROMAGRAM Sheet and the simple EASTMAN CHROMAGRAM Developing Apparatus. The advantages of TLC are preserved without the nuisance of coating one's own plates. The distributors listed here can supply detailed information, including separation procedures. Get in touch with the firm best located to serve you.

DPI
Distillation Products Industries
Rochester, N.Y. 14603, U.S.A.

Distillation Products Industries is a division of Eastman Kodak Company

Toyo

FRACTION COLLECTORS

Model SF-200A
SF-400E

new and classic type

SF-200A

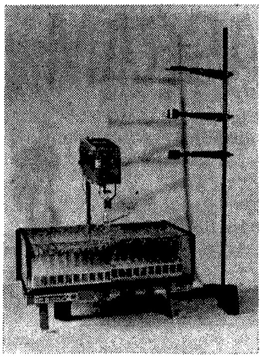

RECTANGULAR PLATFORM BASE only requires such small spaces as 58 cm x 32 cm and 60 cm x 60 cm for the 200 tube type and 400 tube type respectively.

BALANCE SYSTEM in the fractionation is entirely carried out without consuming electric power, so that it can not be affected by fluctuation of voltage, temperature, humidity or chemical vapor, and is consistently stable and powerful.

OPERATION is extremely simple. Fraction is predetermined merely by addition and reduction of balance weight.

and provided with Drop Counter and Timer as accessories.

Toyo Roshi Kaisha, LTD.

HEAD OFFICE: 7.3 - chome, Nihonbashi-Honcho, Chuo-ku, Tokyo.

554

METHODS IN CHEMICAL AND MINERAL MICROSCOPY

by E. E. EL-HINNAWI

Mineralogisches Institut, Hannover, Germany

6 x 9"
xi + 240 pages + index
103 illustrations
16 tables
266 lit.refs.
1966
approx. Dfl. 45.00

In preparing this book the author has incorporated the most recent and rapid methods from English, German, French, Italian and Russian literature, as well as techniques developed by himself and his colleagues. It will serve as a complete manual covering these methods and will be of use not only to research workers, but also to post-graduate students.

Contents: 1. Preparation of materials for microscopic examination. 2. Morphological measurements. 3. Determination of refractive index. 4. Absorption and pleochroism. 5. Extinction and birefringence. 6. Quantitative conoscopy and the determination of the optic axial angle. 7. Dispersion. 8. Spindle stage methods. 9. Universal stage methods. 10. Hot stage microscopy. 11. Phase contrast microscopy. Index.

ELSEVIER PUBLISHING COMPANY
AMSTERDAM LONDON NEW YORK

562E

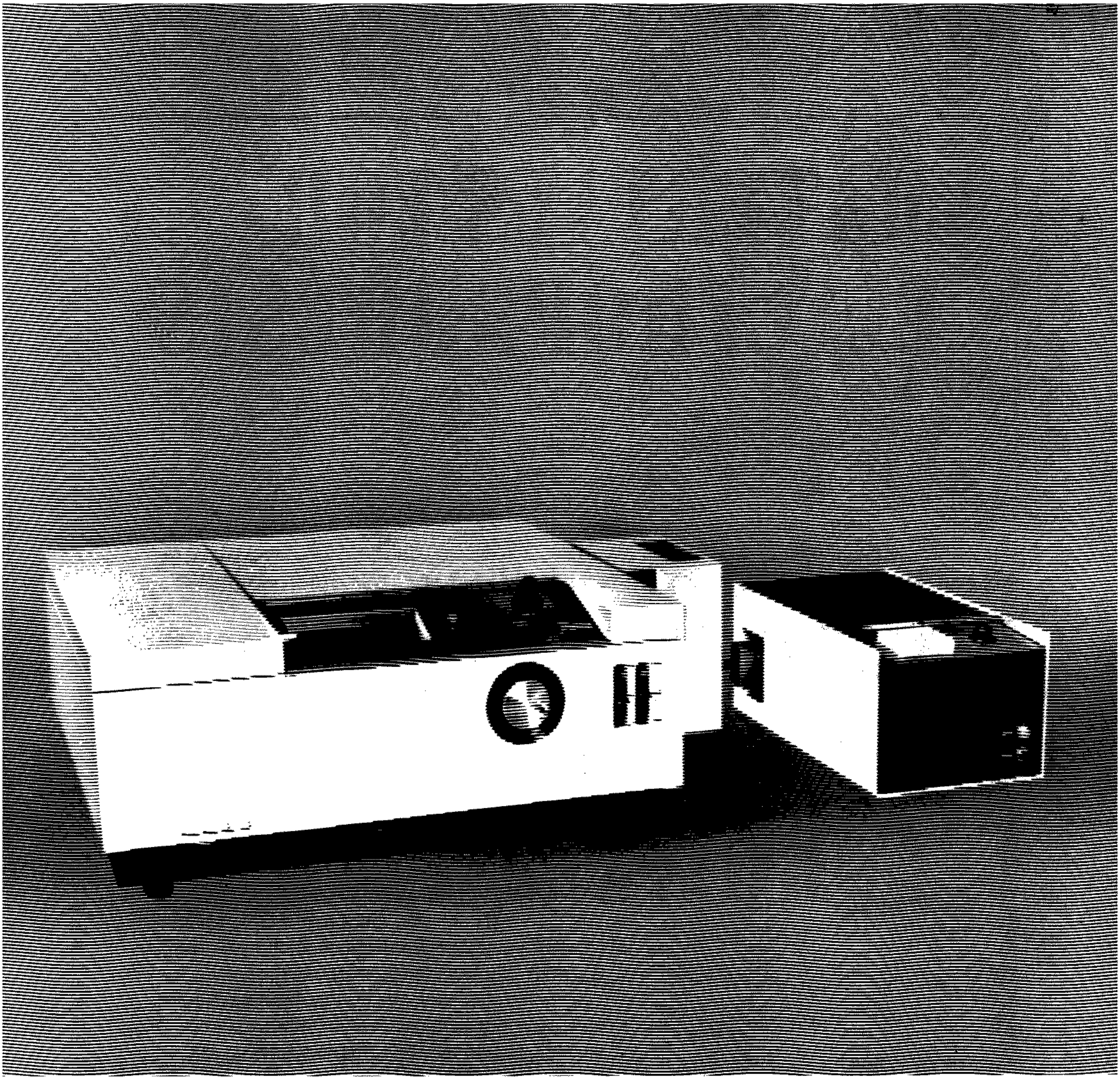

VOL. 36 NO. 4 ANALYTICA CHIMICA ACTA DECEMBER 1966

CONTENTS

Short Communications

PRINTED IN THE NETHERLANDS

ANNOUNCEMENT
concerning the
JOURNAL OF ELECTROANALYTICAL CHEMISTRY

The boundaries between what are regarded as electroanalytical chemistry, electrochemistry and colloid chemistry are becoming increasingly diffuse. This has been reflected in the pages of the journal, where many of the papers published are of interest to chemists who consider themselves as falling under any of these three broad divisions.

The linking phenomena are those associated with the electrical double layer, and it is felt that it would be both useful and appropriate to acknowledge these broader interests by extending the scope of the journal to include all phenomena in which the electrical double layer plays an essential role.

These extend from applications in analytical chemistry through the fundamentals of electrode reactions, which are already the staple part of the journal, to studies of the double layer around colloidal particles, the stability of dispersions and electrokinetic phenomena as well as other surface chemical problems such as monolayers and soap films.

Since this broadening of the scope does not involve any change in the basic interests of the journal, the title will be only slightly modified. From January 1967 it will become:

JOURNAL OF ELECTROANALYTICAL CHEMISTRY AND INTERFACIAL ELECTROCHEMISTRY

An International Journal Devoted to All Aspects of Electroanalytical Chemistry, Double Layer Studies, Electrokinetics, Colloid Stability and Electrode Kinetics

Since the aim of a journal must be to publish papers rapidly, it has been decided that three volumes will be published in 1967 instead of the present two. The delay in publication will thereby be reduced to a minimum level.

Dr. R. H. OTTEWILL of the University of Bristol has agreed to join the board of Editors, and will have special responsibility for the papers which fall within his field of interest.

Papers for publication should be sent to one of the following addresses:

Professor J. O'M. BOCKRIS, John Harrison Laboratory of Chemistry, University of Pennsylvania, Philadelphia 4, Pa. 19104, U.S.A.;

Dr. R. H. OTTEWILL, Department of Chemistry, The University, Bristol 8, England;

Dr. R. PARSONS, Department of Chemistry, The University, Bristol 8, England;
(Until July, 1967: Gates and Crellin Laboratories of Chemistry, California Institute of Technology, Pasadena, Calif. 91109, U.S.A.)

Professor C. N. REILLEY, Department of Chemistry, University of North Carolina, Chapel Hill, N.C. 27515, U.S.A.

A printed pamphlet "hints to authors" is available free of charge from the publishers, who will be glad to supply any further information to intending authors.

Subscription price for 1967: £18.18.0; US$52.50, Dfl. 189.00 plus postage 13 s. US$1.80, Dfl. 6.50.

Orders may be placed with subscription agencies, booksellers or with

ELSEVIER PUBLISHING COMPANY
P.O. BOX 211 — AMSTERDAM — THE NETHERLANDS